Overcoming barriers to T cell activation, infiltration and function in tumors

Melssen, M.M.

Overcoming barriers to T cell activation, infiltration and function in tumors

Marit Melssen

Overcoming barriers to T cell activation, infiltration and function in tumors

Marit Melssen

Overcoming barriers to T cell activation, infiltration and function in tumors

The research presented in this thesis was performed at the Department of Microbiology, Immunology and Cancer Biology and the Department of Surgery at the University of Virginia.

Financial support for the research and publication of the work in this thesis was kindly provided by: National Institutes of Health, Cancer Research Institute, GlaxoSmithKline, Alice and Bill Goodwin, Rebecca C. Harris Fellowship and the Commonwealth Foundation for Cancer Research.

Cover design	Sydna Mundy
Layout by	Loes Kema
Printed by	GVO drukkers & vormgevers B.V.
ISBN	978-94-6332-721-3

Overcoming barriers to T cell activation, infiltration and function in tumors

Proefschrift

Ter verkrijging van
de graad van Doctor
aan de Universiteit Leiden,
op gezag van de Rector Magnificus prof. Mr. C.J.J.M. Stolker,
volgens besluit van het College voor Promoties
te verdedigen op dinsdag 26 januari,
klokke 15:00 uur

door

Marit Melssen

Geboren te Helmond, Nederland
in 1990

Promotor:	Prof. Dr. S.H. van der Burg
Co-promotoren:	Prof. Dr. C.J.M. Melief Prof. Dr. V.H. Engelhard (University of Virginia, USA)
Leden promotiecommissie:	Prof. Dr. J.B.A.G. Haanen Prof. Dr. T.D. de Gruijl (Vrije Universiteit, Amsterdam) Prof. Dr. J.E.M.A. Debets (Erasmus Universiteit, Rotterdam)

I shot an arrow into the air,
It fell to earth, I knew not where;
For, so swiftly it flew, the sight
Could not follow it in its flight.

I breathed a song into the air,
It fell to earth, I knew not where;
For who has sight so keen and strong,
That it can follow the flight of song?

Long, long afterward, in an oak
I found the arrow, still unbroke;
And the song, from beginning to end,
I found again in the heart of a friend.

Henry Wadsworth Longfellow
The arrow and the song (1845)

CONTENTS

Chapter 1

General Introduction

1. THE IMMUNE SYSTEM

The immune system consists of two components: the innate and adaptive immune system. Innate immune cells are the first-line responders; they guard tissues from damage or invasion of foreign elements such as viruses and bacteria, in a non-specific manner. Among innate immune cells are the myeloid-derived cells, including monocytes, macrophages, dendritic cells (DCs) and granulocytes, as well as lymphoid-derived innate lymphoid cells (ILCs) including natural killer (NK) cells. Each cell type has its own mechanism of action, though in general innate cells recognize commonly shared receptors or secreted molecules by pathogens. Subsequently they respond by engulfing the pathogen or infected cells and/or secreting inflammatory signals in the form of cytokines and chemokines to recruit more immune cells. After engulfment, professional antigen-presenting cells (APCs), such as DCs, further process the pathogen or infected cells. This mechanism functions as a bridge between the innate and adaptive immune systems, where these APCs present processed, foreign antigens from the engulfed pathogens to adaptive immune cells in order to generate a very specialized, targeted response.

The adaptive immune compartment consists of B and T cells, which have somatically re-arranged B- or T-cell receptors, each recognizing a specific antigen sequence at low frequency. When activated by their cognate antigen, the adaptive immune cells rapidly divide to generate effector and memory cells meant to clear pathogens or infected cells and create long-lasting memory against the specific antigen that is encountered. Activated B cells engulf pathogens and produce antigen-specific antibodies, facilitating targeted engulfment by professional phagocytes and destruction through the complement system.

The T cell compartment is comprised of CD8 and CD4 T cell subsets. CD8 T cells are considered cytotoxic effector cells, designed to eradicate virus-infected or tumor cells. CD8 T cells recognize antigen sequences presented on MHC class I molecules. In lymph nodes, professional antigen-presenting cells (APCs) present antigen-MHC complexes to naïve CD8 T cells and upon recognition these naïve CD8 T cell become activated. Once activated, or "primed", the CD8 T cells rapidly proliferate and differentiate into cytotoxic effector CD8 T cells[1]. At the same time, CD8 T cells lose the S1P1 receptor, which they require to leave the lymphoid tissue. Effectively this traps the expanding T cells within the lymph node and allows them to fully utilize the activation signals for optimal expansion and differentiation. After expansion and differentiation, S1P1 is recovered and the T cell are able to leave the lymphoid tissue and travel to peripheral target tissues. In order to "find" the infected or tumor tissue, the T cell expresses a plethora of homing and chemokine receptors, which recognize ligands expressed by inflamed endothelial cells[2,3]. Once they have entered the tissue successfully, the T cell recognizes antigen-MHC class I complexes on target cells which triggers production and release of granzymes and cytotoxins. These molecules are specifically designed to force apoptosis of virus-infected cells or tumor cells. In this manner, one cytotoxic T cell is capable of efficiently killing multiple target cells in a row, a

concept described as T cell serial killing[1,4]. The frequency and efficiency of serial killing *in vivo* is not very well understood, but appears to be slower than *in vitro* and affected by external factors[5,6]. Then lastly, cytotoxic CD8 T cells produce effector cytokines to further increase inflammation and recruitment of immune cells. CD4 T cells recognize antigens presented on MHC class II molecules by APCs. A wide variety of distinct CD4 T cell lineages exists and each of them has a different role in guiding, inducing or dampening immune responses in different contexts, such as infections, allergy or autoimmunity. In viral infections and tumors specifically, the Th1 CD4 T cell lineage offers crucial support during naïve CD8 T cell activation and differentiation, through co-stimulation and expression of inflammatory cytokines[7]. Th1 CD4 cells can furthermore support effector function within the target tissue through co-stimulatory receptor interactions and generation of an inflammatory cytokine milieu[8–10]. In some instances, CD4 T cells can also directly induce apoptosis or senescence of target cells through FASL, TRAIL, granzyme B, perforin and IFNγ[11–13]. IFNγ from CD4 Th1 cells also helps to polarize monocytes/macrophages towards a pro-inflammatory and anti-tumorigenic M1 phenotype[14]. Through these mechanisms, effector CD8 and Th1 CD4 cells are the basis of a type I immune response, which is deemed crucial for the eradication of both virally-infected and tumor cells.

2. IMMUNE MEMORY FORMATION

An important aspect of adaptive immunity is the formation of immune memory. This is established by the generation of memory cells alongside terminal effector cells, during the acute phase of the immune response. Memory T cells are self-renewing and can often remain in the body for years after the initial antigen encounter. Three different memory T cell subsets have been described: the circulatory central memory and effector memory cells and a third, non-circulatory tissue-resident memory subset[15]. Central memory T cells remain in the circulation and secondary lymphoid organs only, with great self-renewal capacity and plasticity. Upon re-encounter with antigen they rapidly proliferate and generate new terminal effector T cells[16]. Effector memory T (TEM) cells can be found in the circulation and peripheral tissues, and though they are self-renewing, their main purpose is to rapidly localize to inflamed sites and provide immediate effector function upon antigen recognition[16,17]. Then lastly, non-circulatory tissue resident memory (TRM) T cells remain in peripheral tissues long-term, predominantly at barriers such as skin, intestines and lungs[15]. Though TRM T cells are antigen-specific and rapidly induce inflammation upon encounter with antigen, they are also capable of responding in an innate fashion by producing inflammatory cytokines in an antigen-independent way[18,19]. Immune memory formation is most optimally generated during acute infections, with long-lived memory cells staying behind after the infection is cleared and terminal effectors have dissipated[20]. Whether the fate decision of effector T cells to become memory precursor cells for the different lineages occurs early or late during the acute response is still controversial[15,21]. What is clear is that transcription factor repertoire and metabolic

regulation are important in the eventual differentiation path of memory cells[15], and it is envisioned that these can be skewed by TCR signal strength and environmental cues[22,23]. When antigen persists in chronic infections or cancer, memory cell formation is often distorted and the generation of the different memory subsets can be skewed or non-existent[20,24,25]. Chronic restimulation by their antigen renders T cells functionally exhausted, a phenomenon thoroughly described in both chronic infection and cancer. Instead of gaining memory cell properties, T cells obtain a specific epigenetic chromatin state which is accompanied by the upregulation of inhibitory receptors, loss of stem-like markers and suppression of effector function[26,27]. These cells are largely dysfunctional, even during re-encounter with their cognate antigen and often eventually undergo apoptosis.

3. CANCER-SPECIFIC IMMUNE RESPONSE AND IMMUNE EVASION

It has been long understood that the immune system plays an important role in the eradication of cancer. Because the "non-self" antigen is intrinsic to the tumor cell, a type I immune response comparable to an anti-viral response, is crucial for tumor rejection[28]. In a very comprehensive study across 33 different cancer types, the nature of immune responses against the tumor were mapped and indeed, those with a predominant type I signature were correlated with the best patient survival[29]. A type I immune response involves activation of both effector CD8 T cells and CD4 Th1 cells. These T cell subsets produce type I inflammatory cytokines and cytotoxins in response to antigen stimulation and these induce target cell apoptosis. Thus, in order to survive, tumors often utilize mechanisms to divert or silence the type I immune response.

The development of cancer is a multistep process driven by the acquisition of somatic mutations in critical genes for cell division, replicative immortality and protection against apoptosis, that together lead to uncontrolled division of cells[30]. Accumulation of "driver" mutation is generally accompanied by other "passenger" mutations that are not directly involved in driving cancer development, but still change the genome of the (pre)cancerous cell[31]. Due to the accumulation of both types of mutations, peptide sequences arise that are unknown to the immune system, thereby classifying them as "non-self" antigens or neo-antigens[32]. The multistep process of cancer development leads to overexpression or induction of proteins normally not expressed in the cell type that is transforming, which can lead to recognition of these proteins as antigens, named shared antigens[32]. When neo- or shared- antigens get processed and presented on MHC molecules, they can induce an immune response against the cancerous cells and initiate a process called immunoediting. The extent of the immune response and immunoediting thus varies between cancer types and likely depends on the mutational burden. Immunoediting consists of three phases: elimination, equilibrium and evasion. During the early phase of cancer development, the immune system can successfully recognize and eliminate the cancerous cells through immunosurveillance. It is

thought that the human body continuously eradicates precancerous cells through this process. However, some cells will survive, continue to evolve and gain new driver mutations, leading to the equilibrium phase of cancer immunoediting. During this phase the immune system is able to eradicate mutated tumor cells, while they continuously divide at a balanced rate. Subsequently the cancer cells further evolve, until immune evasion mechanisms arise, initiating the escape phase of cancer development. At this stage, the tumor successfully evades immune destruction in one way or another and is able to grow without supervision of the immune system. To evade immune destruction, cancers utilize a plethora of mechanisms at different steps of the cancer-specific immune response (Figure 1), as will be outlined in greater detail in this chapter. Targeting these immune evasion mechanisms through therapeutic strategies can successfully prolong survival of cancer patients. However, there are still a lot of gaps in our knowledge with regards to the exact mechanisms and how to most successfully target them in individual patients.

Antigen uptake and DC maturation

To start a successful adaptive immune response, professional APCs, such as DCs have to engulf foreign antigen and get properly activated. When activated the APC will traffic to the lymph node to present the antigens to the adaptive immune subsets. Immunogenic DC activation is most commonly driven through pattern recognition receptors (PRRs), which respond to pathogen-associated molecular patterns (PAMPs)[33]. DC activation can also be induced by inflammatory cytokine signals[34,35]. In the context of a tumor, PAMPs normally present during pathogenic infections are absent. In such an environment, whether a dying cell creates an immune response or instead induces tolerance depends on a variety of factors[36]. When a sufficient amount of damage-associated molecular patterns (DAMPs) and cytokines are released, they can replace PAMPs and induce proper DC activation[36] (Figure 1, Step 1). However, when these DAMPs are absent during engulfment of antigens, the DCs can become tolerogenic, activating regulatory T cell subsets to dampen further response against these antigens[37]. DAMPs capable of inducing immunogenic DC activation include HMGB1, uric acid, ATP, cytosolic DNA and heat shock proteins[38–40]. Each of these molecules can activate DCs through a different mechanism, for example, ATP or HGMB1 release leads to inflammasome or TLR4 mediated DCs activation. Contrastingly, uptake of cytosolic DNA by APCs leads to the activation through the STING pathway and expression of type I IFNs[40]. All of these mechanisms activate APCs to generate a tumor-specific T cell mediated immune response. If these signals are abundant enough to successfully induce mature DCs during engulfment they become immunogenic, though there is some evidence that mature DCs can be tolerogenic in some circumstances[37]. During maturation DCs upregulate CCR7, MHC class II and CD40[41,42]. CCR7 allows the cells to exit peripheral tissues and traffic to the lymph node for antigen presentation. CD40 is important for the interaction of CD4 helper T cells with DCs during antigen-presentation and the further upregulation of costimulatory, signal 2 receptors CD80, CD86 and CD70[7], which will be discussed in more detail below.

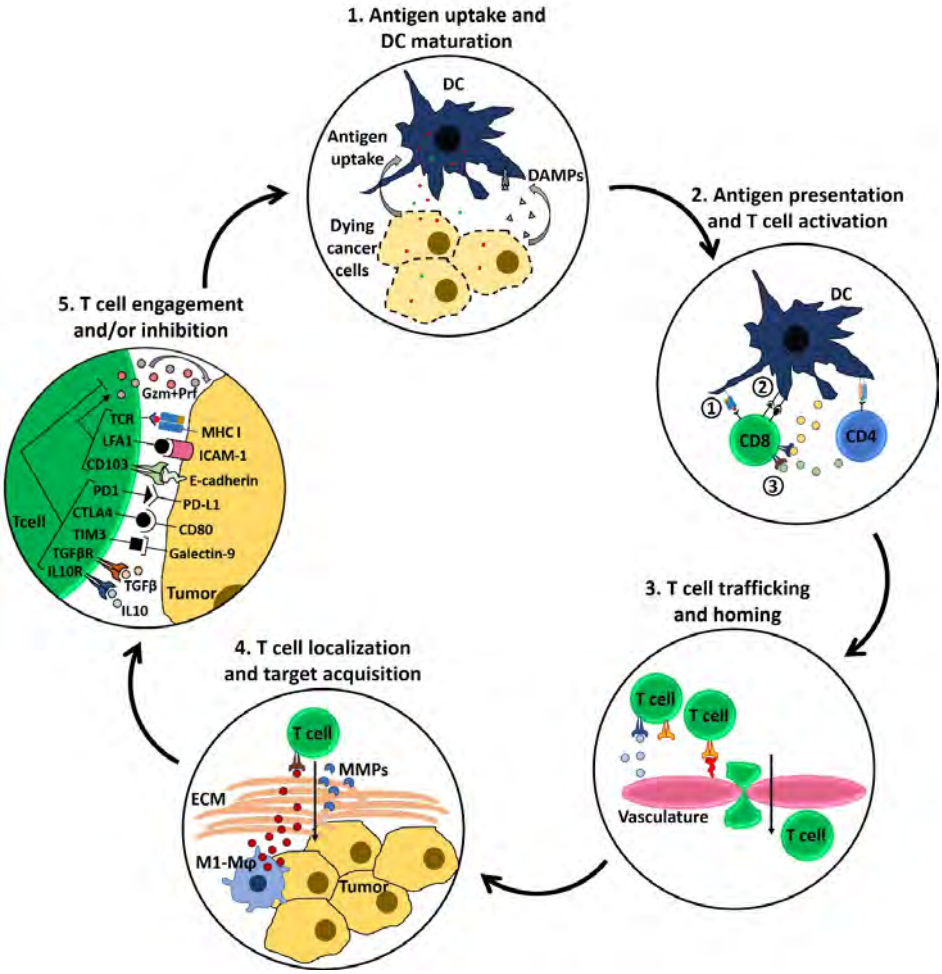

Figure 1. Cancer-specific Immune response. The cytotoxic, effector T cell driven anti-tumor immune response consists of several steps. Step 1. DCs take up antigen from dying cancer cells in the presence of DAMPs. These signals mature the DC and initiate migration to the lymph node. Step 2. The mature DC presents the antigen to CD4 and CD8 T cells (signal 1). CD4 helper T cells further mature the DC, leading to increased expression of MHC molecules (signal 1) and the expression of co-stimulatory molecules (signal 2). Furthermore, expression of cytokines by both mature DCs and helper CD4 T cells contribute to the activation and differentiation of CD8 T cells (signal 3). Step 3. Activated CD8 T cells traffic through the circulation to the tumor site. Inflammatory signals have upregulated chemokines and homing receptor ligands on the tumor vasculature, leading to a cascade or rolling, adherence and extravasation through the endothelial cells. Step 4. In order to localize among tumor cells and target them, T cells require chemokine gradients, often provided by macrophages and monocytes (M1-Mφ). Furthermore, expression of MMPs allows for migration through dense ECM molecules often surrounding tumor cells. Step 5. In addition to TCR-mediated MHC class I-antigen complex recognition, T

cells utilize integrins LFA1 and CD103 to generate long-term adhesion to tumor cells. This long-term adherence is required for the proper induction of the immunologic synapse. A mix of stimulatory and inhibitory receptors in the synapse will determine expression of granzymes (Gzm) and perforins (Prf) in the immunologic synapse; and thus, whether tumor cell apoptosis is induced. In case of apoptosis, tumor cells release more antigens in the tumor microenvironment, possibly eliciting T cell response.

Thus, to induce a proper immune response against tumor-antigen, cancer cells have to release DAMPs during apoptosis. Normal apoptotic processes are caspase-driven, which eventually causes pore formation and efficient removal of dead cell corpses in an immunologically silent manner[43–45]. Cancer cells often follow these same pathways, because they face many cell intrinsic stressors, and often undergo apoptosis without the release of DAMPs. However, in some tumors, caspase is actively blocked, while cell death still occurs. In such situations, cell death is accompanied by type I IFN response and NF-kb signaling[45]. Extrinsic stressors, such as FASL and TRAIL, can also induce NF-kb signaling in tumor cells[46]. Both these mechanisms can lead to a more immunogenic cell death (ICD) and the release of DC-activating factors in the microenvironment.

In addition to the potential release of DAMPs, tumor cells produce or induce the production of factors that have been shown to directly reduce the differentiation into DCs from progenitors. Progenitors are instead pushed to differentiate into suppressive monocyte populations, such as myeloid-derived suppressor cells (MDSCs) and tumor-associated macrophages (TAMs)[47–49]. Involved factors include retinoic acid (RA), VEGF, TGFβ, IL1β, IL13, GM-CSF, CCL2 and prostaglandins. Interestingly, the increased activity of the PI3K-AKT oncogenic pathway has been linked to the enhanced expression of VEGF and CCL2 in a melanoma mouse model[50]. Additionally, decreased recruitment and activation of DCs has also been linked to the activation of oncogenic WNT-βcatenin pathway in melanoma models[51]. Through secretion of βcatenin, this pathway can inhibit DC recruitment through suppression of chemokines, such as CCL4. These findings suggest that specific oncogenic mutations in tumor cells can directly affect the tumor microenvironment and thereby actively prevent the recruitment and/or generation of functional DCs that can take up antigen. These tumors then lack functional, fully mature DCs and will fail to activate T cells in the draining lymph node.

Both suppression of ICD and DC recruitment/differentiation, can lead to a decreased population of mature DCs in tumors. Either mechanism results in decreased uptake of tumor antigen and subsequent presentation to tumor-specific CD4 and CD8 T cells in the tumor-draining lymph node. Even more so, when T cells get activated by immature or tolerogenic DCs they become anergic or suppressive, thereby not only decreasing the tumor-specific cytotoxic T cell pool, but also creating active immunosuppression[37].

Antigen presentation and T cell activation

Once DC's successfully capture antigen and gain a mature phenotype, CCR7 allows them to traffic to the draining lymph node where the DC presents antigen to T cells. At this point, the activation state of the DC is again important for the directionality and magnitude of the response. Fully matured DCs express high levels of MHC molecules and co-stimulatory receptors such as CD40, CD80 and CD86. Classically, the mature DC activates T cells through 3 independent signals (Figure 1, Step 2). Signal 1 is delivered by engaging the TCR of the specific naïve CD8 T cells through cross-presentation of antigen on MHC class I molecules, a specialized function of APCs[52]. At the same time, the DC presents antigen to helper CD4 T cells on MHC class II, which, mainly through additional CD40-CD40L interactions leads to the upregulation of co-stimulatory molecules CD80, CD86 and CD70 as well as MHC class I molecules on the surface of the DC[7]. The upregulation of MHC molecules strengthens signal 1 and the co-stimulatory receptors interact with receptors on CD8 T cells to induce signal 2. Thirdly, DCs and helper CD4 T cells secrete cytokines, including IL-12, IL-2, IL-15 and type I IFN, that promote further effector differentiation and proliferation[7]. The integration and strength of these three signals determine the eventual effector capacity and clonal expansion of the T cell. If part of the signal is missing, cells can become regulatory or anergic instead of full effectors, or the generation of memory cells can be suboptimal[33,53]. As described earlier, tumors often lack the proper immunogenic cues to mature DCs and fail to upregulate CD40. Loss of CD40 on APCs impairs the interaction with helper CD4 T cells, which is required for proper signal 2 support during CD8 activation[7]. Additionally, suppressive molecules, including TGFβ have been suggested to drain from the tumor microenvironment to the lymph node and directly impact the strength of the T cell activation signals[54–56]. Together, these mechanisms, resulting in diminished DC maturation, illuminate the role of tumor microenvironment composition in the initiation of the anti-tumor immune response. Additionally, they highlight the importance of finding alternative ways to generate tumor-specific effector T cells in tumors without adequate levels of mature DCs.

T cell trafficking and homing

After effector T cells are primed in the lymph node, they traffic through the circulation to the tumor. Subsequent entry of these T cells into specific peripheral tissues requires a multistep process, which involves sequential interactions between ligands or chemokines expressed by the vasculature and homing receptors on T cells (Figure 1, Step 3). Initial interactions lead to T cell rolling on the endothelial cells making up the vasculature wall[2]. Then subsequently chemokine receptors on the T cell are activated to bind to chemokine ligands expressed by the tissue. This results in T cell arrest and final transmigration through the endothelium[2]. The specific repertoire of homing receptors and homing receptor ligands required for T cell entry depends on anatomical location of the target tissue[2,3]. Each peripheral tissue expresses its own set of homing receptor ligands on the vasculature, which is further influenced by presence or absence of inflammation. In subcutaneous

tumors, ligand-receptor interactions VCAM1-α4β1, ICAM1-LFA1, ESL-E-selectin and HA-CD44, as well as chemokine signaling through CXCR3 are required for T cell infiltration[3]. In these tumors, VCAM1, ICAM1 and CXCL9 expression on endothelium are regulated by inflammatory cytokines and chemokines, TNFα, IFNγ and CCL5[57]. Tumors can thus influence the capacity of T cell homing by directly suppressing the production of these cytokines and chemokines, or indirectly by recruiting suppressive cell types.

Besides downregulation of homing receptor ligands, distorted organization of the vasculature can impair T cell infiltration in tumors. Because tumors often grow so rapidly, the vasculature is unable to generate new blood vessels fast enough to provide sufficient nutrients and oxygen, leading to massive hypoxia[58]. Hypoxia induces HIF-1α expression in both tumor cells and endothelial cells, which upregulates expression of pro-angiogenic genes including VEGF and other growth factors. The rapid neovascularization that occurs due to large amounts of these growth factors results in irregularly shaped, dilated and tortuous vessels, which are leaky and poorly covered by pericytes[59]. These structural defects in tumor vasculature alone are suggested to represent significant hurdles for T cell infiltration. In addition, the endothelial cells generated in rapid neovascularization often respond inefficiently to inflammatory signals, failing to upregulate sufficient levels of homing receptor ligands even when proper inflammatory cytokines and chemokines are present. VEGF furthermore has been shown to directly interfere with TNF-induced adhesion molecule expression on endothelial cells and other molecules expressed in the TME such as nitric oxide and epidermal growth factor like domain multiple 7 (egfl7) can also directly suppress endothelial cell activation[60–62].

T cell localization and target acquisition

To efficiently target tumor cells, infiltrating T cells have to be retained in the tissue overall, but also be able to traffic among and interact with tumor cells. For example, patients with diffuse immune cell infiltration amongst tumor cells have a better prognosis than patients who have limited immune cell infiltration in perivascular spaces[63]. Therefore, induction of barriers to diffuse immune cell infiltration and motility among tumor cell could provide immune evasion for tumors (Figure 1, Step 4).

When a cytotoxic T cell reaches its target organ after activation its main function is to eradicate infected or tumor cells. To optimize the serial killing capacity of T cells, they require rapid movement between cells to sample for antigen, then durable arrest once the target has been acquired[64,65]. In subcutaneous tumor rejection models, a large proportion of T cells indeed physically interacts with tumor cells leading to long-term arrest and display rapid motility between cells[64,66]. This efficient scanning and tumor cell engagement may be absent in non-rejected tumors, making serial killing more difficult. However, how tumors can evade T cell motility followed by long-term arrest is complex and can involve both direct cues

to change T cell motility and arrest as well as physical barriers in the environment. T cell movement is driven by both intrinsic motile capacity and extrinsic environmental organization and cues, such as matrix proteins and chemokines[67]. This makes T cell motility highly dependent on activation status, density of antigen, secretion of chemokines and target tissue type. In infection models and solid tumors it has been shown that myeloid-derived CXCL9 expression recruits effector T cells to target cells, through CXCR3[57,68,69]. Downregulating CXCL9 expression in myeloid cells thus provides an opportunity for immune evasion. Separately, in tissues with dense extracellular matrix (ECM), inflammatory signals such as TNFα, IFNγ and TGFβ can induce secretion of proteases to loosen the ECM matrix and allow integrin-mediated T cell motility within the tissue[70–72]. In viral infections, T cell motility along ECM molecules is driven by integrins α1β1 (or CD49a) and α2β1 (or CD49b)[73–75]. Thus, integrin expression on T cells and induction of proteases by inflammatory signals are both crucial to T cell motility and localization within tissues and provide targets for immune evasion for the tumor. The regulation and function of integrins on T cells, including CD49a and CD49b, under these circumstances is largely unexplored and gaining more understanding is crucial to find novel ways to tackle this barrier to T cell function in tumors.

Irrespective of whether T cells display proper integrins to traffic through ECM matrix, the organization of ECM itself determines the direction and efficiency of T cell movement. Most normal epithelial tissues are in a tensional homeostatic state, which leads to a relaxed meshwork of collagens and other ECM components, likely allowing for optimal lymphocyte motility. In tumors, however, activated cancer associated fibroblasts (CAFs), inflammation, high interstitial pressure and increased expression of collagen-processing lysyl oxidases can lead to increased collagen deposition, cross-linking and distorted organization[76,77]. Additionally, tumors often express higher levels of matrix metalloproteinases (MMPs) than normal epithelial tissue, leading to increased remodeling of ECM fibers[78]. In various solid tumor types, collagen alignment, length, width, density and straightness is altered compared to adjacent normal tissue[79]. As each of these components are dependent on all components highlighted above, collagen organization in tumors is highly variable, and the specifics affect T cell motility and function differently. For example, when tumors have dense stromal regions, T cells are confined within these regions, unable to move towards and engage with tumor cells[80–82]. Altering ECM organization could be an effective way for tumors to evade T cell motility and efficient “serial killing” of tumor cells. However, the exact effects of different tumor ECM structures on T cell motility have not been comprehensively studied in different tumor types beyond anecdotal observations.

3.5 T cell engagement and/or inhibition

Part of efficient T cell-mediated serial killing of tumor cells requires efficient motility through the interstitial spaces. Once a target cell has been acquired, the T cell needs to arrest motility and interact with the tumor cell long enough to create

the immunologic synapse[64,65] (Figure 1, Step 5). T cell arrest can be mediated by TCR signaling itself. Arrest and adhesion is further strengthened by integrins LFA-1 and CD103 on the T cell, interacting with ICAM-1 and E-cadherin, respectively, on the tumor cells[83–85]. In addition to adhesion, both of these integrins also support TCR-mediated killing itself[84,86,87]. One obvious way to evade T cell recognition and adhesion tumor often employ is the downregulation of MHC class I molecules on their surface[88]. In doing so, tumor cells actively make themselves "invisible" to the TCR on a T cell. Separately, tumor cells often lose E-cadherin expression as a part of epithelial-to-mesenchymal transition (EMT), which occurs as tumors progress and become metastatic. By driving the downregulation of E-cadherin, tumor cells not only become more invasive, they may also evade CD103 mediated engagement of T cells, possibly leading to decreased recognition and eradication[83,84]. However, direct evidence to support the relation between loss of E-cadherin and T cell recognition of tumor cells *in vivo* remains to be elucidated. Contrastingly, ICAM-1 is not often decreased as tumor progress, likely due to a possible role in metastatic capacity of tumor cells[85]. Instead, tumors secrete galectins, which bind to glycosylated receptors on tumor infiltrating T cells, including LFA1. This directly impairs the interaction between ICAM-1 and LFA-1 and synapse formation[89]. Through these mechanisms, tumors inhibit T cell adhesion to individual tumor cells and immunologic synapse formation.

As described above, appropriately activated antigen-specific T cells recognize peptides expressed on tumor cells through their TCR. Similar to the recognition of virus infected cells, TCR binding to antigen-MHC class I complexes on tumor cells leads to the formation of an immunologic synapse[90]. At the same time, T cell increase the expression of inflammatory cytokines, such as IFNγ and TNFα[91]. At the interface of the immunologic synapse, granzymes and perforins are expressed and directly targeted to kill the tumor cell[90,92]. During this process, tumor intrinsic and stromal aspects of the tumor can exert suppression mechanisms to dampen the direct eradication of tumor cells (Figure 1, Step 5). First of all, tumor cells express inhibitory ligands, such as PD-L1, which bind to inhibitory receptors on the T cell surface during the formation of the immunologic synapse. Because T cells have often become exhausted in the chronic antigen context of cancer, these inhibitory receptors are highly upregulated on tumor infiltrating T cells and engaging these receptors leads to suppressed release of cytokines and cytotoxins. The tumor microenvironment also contributes to the generation of exhausted cells, independent from chronic antigen stimulation, through high abundance of VEGF-A[93].

In addition to the evasion mechanisms tumor cells utilize to dampen T cell-mediated eradication directly, there are also several indirect mechanisms involving stromal cells or suppressive immune cell subsets. Among these are myeloid-derived suppressor cells (MDSCs), regulatory T cells (Treg) and cancer-associated fibroblasts (CAFs). MDSCs contain a collection of myeloid-derived cells that suppress the immune response in tumors. MDSCs are recruited through chemokines produced by tumor cells. Predominant chemokines include CCL2

and CCL5, though others have been shown capable of recruiting MDSCs and monocytes depending on the tumor type[94–96]. MDSCs suppress T cell homing, proliferation and function through secretion of Arginase-1, nitric oxide and ROS, as well as surface expression of IDO and PD-L1[61,96,97]. MDSCs also express suppressive cytokines IL-10 and TGFβ, induce Treg recruitment or differentiation and alter NK cell function[96,98]. Tregs are suppressive T cells, often found in tumors. They can be recruited from the circulation or differentiated from non-regulatory T cells in the TME. Tregs utilize a wide variety of suppression mechanisms to induce tolerance in mice and humans, though a few key mechanisms impact tumor immunity most predominantly. Among these are: sequestration of survival cytokine IL-2, limiting availability for other T cell subsets; the constitutive expression of inhibitory receptor CTLA-4; and expression of suppressive cytokines IL-10 and TGFβ[99]. Finally, tumors contain fibroblast-like cells, CAFs, representing the most abundant stromal cell population. In normal tissue, fibroblasts are quiescent stromal cells that only activate upon hypoxia, oxidative stress and growth factor signals, which are present during wound healing and inflammation[100]. Because tumors are essentially wounds that never heal, fibroblasts are constitutively activated and promote tumor growth by expressing growth factors, angiogenic factors and by inducing fibrosis. Fibroblasts are a multipotent cell type; thus, CAFs consist of a heterogeneous population of cells with different phenotypic markers and tumor-promoting mechanisms[100]. The phenotype and function of CAFs depend on fibroblast origin, recruitment and specific environmental signals[101]. For example, α-smooth muscle actin (αSMA)-expressing CAFs resemble activated myofibroblasts. These CAFs are involved in ECM remodeling, but also express chemokines and cytokines to recruit monocytes and drive their differentiation into tumor-promoting M2 macrophages[102]. CAFs subpopulations can also express TGFβ, IDO and PD-L1/2 to directly suppress effector function of lymphocytes and recruit MDSCs and Tregs[100,101]. Overall CAF function is dependent on tumor type and specific environment, though similarities exist, providing opportunities for CAFs targeted therapies.

4. THERAPIES TO TARGET IMMUNE EVASION

4.1 Current approved immune therapies

The majority of recently approved immune therapies to treat cancer are targeting immune checkpoint pathways, such as PD-1 and CTLA-4[103]. PD-1 and CTLA-4, among others, are inhibitory receptors expressed by T cells and engaging ligands effectively suppresses activation or effector function. Tumor often drive expression of ligands for these inhibitory receptors as an immune evasion strategy. Blocking the interaction has proven to be successful in boosting T cell mediated tumor eradication in patients and improve their survival[104,105]. It is clear that factors such as pre-existing T cell infiltration are strongly associated with successful checkpoint blockade treatment[106], and it has thus been most effective in melanoma and lung cancer, which generally have a high mutational burden. In patients without pre-existing T cell infiltrates, these therapies are often not

sufficient or effective at all. Other immune evasion mechanisms may be involved, especially those creating barriers for T cell priming and T cell infiltration, causing low to negligible T cell infiltrates. Therefore, it is important to study other potential strategies to overcome these barriers in particular, either alone or in combination with checkpoint inhibitor therapies. In this thesis we have therefore aimed to answer two broad research questions: 1). How can we overcome barriers to T cell priming?; and 2). What are the barriers to T cell infiltration and trafficking within the tumor microenvironment, and how can we overcome these?.

4.2 Overcoming barriers to T cell priming

The barriers to T cell priming are two-fold: First, the recruitment and differentiation of professional APCs in tumors can be impaired, leading to diminished opportunities of antigen-presentation to adaptive immune cells. Secondly, the availability of DAMPs and inflammatory cytokines to mature APCs can be low or negligible, thereby limiting the magnitude and quality of adaptive immune cell activation. Both can be targeted individually, for example, therapies aimed to drive monocyte differentiation into mature antigen-presenting DCs are being established[39]. Currently used chemotherapies and radiation can induce ICD and improve antigen-presentation and T cell priming. Optimization trials of these existing therapies and trials with new chemotherapies designed to induce ICD are underway[107]. Also, therapies designed to enhance DC maturation by inhibiting ATP degradation are investigated in *in vivo* tumor models[108].

An interesting strategy to simultaneously overcome both barriers to T cell priming involves cancer-targeted vaccination. The optimal vaccine would encompass all three activation signals required for proper induction of a type I immune response: antigen presentation, co-stimulation and stimulatory cytokine release. Current strategies to accomplish this range from injecting matured and antigen-pulsed DCs to injecting immunogenic peptides with immune-activating adjuvants[32]. Preclinical and clinical research has shown great potential of these strategies in generating a systemic immune response, especially in high-mutational cancers such as melanoma. Aspects that impact the capacity of vaccines to induce a systemic immune response include adjuvant choice, injection site and antigen delivery method, as each of these play a role in inducing immunogenic APCs. Current adjuvants that are being tested in clinical trials are, among others, the emulsion forming Incomplete Freund's Adjuvant (IFA), several toll-like receptor (TLR) agonists or DC activating cytokines such as GM-CSF. IFA is an oil-based emulsion, which in contrast to water-soluble compounds, protects antigen from dilution, degradation and elimination. In doing so it creates an antigen depot at the vaccine site, allowing for continued antigen exposure[109]. TLR agonists bind to PRR on DCs to mimic DAMP signals and induce maturation. In addition to adjuvant of choice, several antigen delivery methods are currently tested in clinical trials. Methods include injection of mature, peptide-pulsed DCs, tumor protein or (a cocktail of) tumor-specific peptides, whole tumor cells, tumor lysate or tumor RNA/DNA[32]. These methods are mostly being tested independently,

however one study in human melanoma elucidated that vaccines with peptides in IFA induced better systemic immunity than injection of cytokine-matured and peptide-pulsed APCs[110]. More comparative clinical and preclinical studies are required to understand how vaccine components influence the local immune response at the vaccine site as well as whether the local response supports a systemic anti-tumor immune response. Additionally, for cancer vaccines to induce fully functional T cell responses at the tumor site, barriers to T cell infiltration and function should be addressed in parallel, likely through combination therapies.

Adoptive transfer therapy is another approach to overcome T cell priming evasion. With adoptive transfer, the goal is to infuse patients with *ex vivo* expanded or generated effector T cells[111,112]. Either, tumor-specific T cells from tumor mass excisions are isolated and expanded, or, blood-derived T cells are manipulated to express a tumor-specific cloned TCR or a chimeric antigen receptor (CAR). Both methods aim to infuse a large army of activated, patient- and tumor-specific T cells into a cancer patient, thereby overriding the need for antigen presentation by mature DCs and *in vivo* activation of new T cells. However, the infused T cells have to be capable of infiltrating tumors and fully function in the tumor microenvironment. So far these strategies have therefore yielded limited success in solid cancers, with low actual infiltration of infused T cells into tumors[112]. Adoptive transfer approaches would greatly benefit from gaining more insight into how *ex vivo* activation methods affect homing and infiltration mechanisms.

4.3 Overcoming barriers to T cell infiltration

One major hurdle to T cell infiltration is the nature of tumor vasculature. The leaky structure and often lack of homing receptor ligands can severely diminish T cell extravasation from the circulation into the tumor tissue. Preclinical and clinical studies involving anti-angiogenic drugs, such as anti-VEGF antibodies, showed that they induce vessel pruning, maturation and improved perfusion[113]. By normalizing the vasculature, the expression of adhesion receptors and chemokines was also enhanced as well as the number of infiltrating T cells. Preclinical models have shown great potential in combining anti-angiogenic therapy with checkpoint blockade and current ongoing clinical trials are studying the efficacy of these combined immune therapies in human cancers[58,114].

Another hurdle is the localization of T cells in the tumor microenvironment. Physical and chemical barriers are able to prevent T cell engagement with T cells in some tumors. Breaking down ECM matrix barriers through matrix metalloprotease (MMP) regulation, could provide a therapeutic angle to improve T cell engagement and function in tumors. For example, blocking MMP9 and thereby ECM remodeling, in murine tumor models showed increased immune activation and reduced tumor outgrowth[115]. However, the exact mechanism of action with this kind of therapy remains to be elucidated, mainly because the interactions between ECM and T cells, as well as the resulting effects on T cell localization and function in different tumor types, is largely unclear at this point.

Interestingly, MMP9 also cleaves chemokines CXCL9 and CXCL10, suggesting MMP9 inhibitors may affect T cell infiltration and localization by breaking chemical barriers as well[115,116].

The function of infiltrating T cells can be directly inhibited by tumor cells, suppressive immune and stromal cells and/or cytokines in the microenvironment. In addition to the already approved checkpoint inhibitor blockade therapies, numerous therapeutic strategies tackling each of these issues are currently being investigated in preclinical and clinical settings. These include blocking the recruitment, generation and function of MDSCs and Tregs through various mechanisms, inhibiting TGFβ signaling and others[108,117].

5. BRIEF OUTLINE OF THE THESIS CHAPTERS

Despite advances in utilizing immunotherapies for cancer treatment, many gaps remain in our knowledge regarding immune evasion mechanism and how to overcome barriers to successful immune mediated cancer eradication in different cancer types. One hurdle is the lack of tumor-specific T cell activation, which can be tackled by cancer vaccines. In **Chapter 2** it is described where the field stands and why it is important to target CD4 helper T cells with cancer vaccines as a method to support CD8 T cell responses. Furthermore, to analyze which adjuvant combination allows for the most optimal systemic tumor-specific T cell activation, two different TLR agonists, LPS and polyICLC were tested as adjuvants, with or without emulsion-forming Incomplete Freund's adjuvant (IFA) in a peptide-based vaccine for metastatic melanoma patients (**Chapter 3**). In this study, the capacity of tumor-specific circulating T cells to produce IFNγ was assessed at different time points post vaccination, thereby unraveling the importance of each component (LPS, polyICLC and IFA) in the durability and magnitude of a vaccine-induced tumor-specific CD8 T cell response. Importantly, it revealed the role of the vaccine site in generating a systemic immune response. The vaccine sites from patients vaccinated with melanoma-specific antigens either in presence of IFA or TLR agonist cocktail AS15 were assessed for innate and adaptive immune cell subsets, as well as expression of tertiary lymphoid structure (TLS) genes and immune cell homing/retention genes **(Chapter 4)**.

A second hurdle is formed by barriers to T cell infiltration and motility in the tumor microenvironment. The role of integrins on T cells and the resulting effects of integrin-mediated interactions with ECM and E-cadherin on T cell localization and motility, are particularly poorly understood. From work in murine models of infection and autoimmunity, it is clear that collagen-binding integrins CD49a and CD49b are both upregulated during the course TCR-mediated activation of CD8 T cells. E-cadherin-binding integrin CD103 on the other hand, is only expressed on tissue resident memory cells and tumor infiltrating T cells. Beyond this, not much is known about the expression dynamics of these integrins on tumor infiltrating T cells, or how expression correlates with differentiation state and functional

capacity in tumors. Therefore, in **Chapter 5,** CD8 T cells from human metastatic melanoma lesions were categorized based on expression of these 3 integrins, and subsequently placed in a framework of memory and effector cell markers. Here we found that CD49a, CD49b and CD103 expression characterizes five phenotypically and functionally distinct intratumoral CD8 T cell subpopulations. Additionally, cytokines regulating the expression of CD49a and CD103 on human CD8 T cells in addition to TCR-mediated activation were illuminated. In **Chapter 6,** we delve deeper into the expression dynamics and specific cues driving collagen-binding integrins CD49a and CD49b in *in vivo* models for melanoma and breast carcinoma. Interestingly, we found that CD49b is induced on a fraction of antigen-specific cells fairly quickly after TCR-mediated activation. CD49a on the other hand, requires additional environmental cues specific to the tumor for its upregulation. CD49a signaling in these tumor-infiltrating T cells then drives rapid motility, which renders them unable to engage with and respond to tumor cells. Environment-driven expression of CD49a in the context of these tumors may thus be a novel Immune escape mechanism that can be therapeutically targeted.

Finally, in **Chapter 7,** the major findings on how to improve T cell activation, localization and function in tumors are summarized and implications for new therapeutic approaches to target barriers to T cell function in cancer are discussed. Furthermore, new and important scientific questions that arose from the work in this thesis are highlighted.

REFERENCES

1. Halle, S., Halle, O. & Förster, R. Mechanisms and Dynamics of T Cell-Mediated Cytotoxicity In Vivo. *Trends Immunol.* **38**, 432–443 (2017).
2. Ley, K., Laudanna, C., Cybulsky, M. I. & Nourshargh, S. Getting to the site of inflammation: the leukocyte adhesion cascade updated. *Nat. Rev. Immunol.* **7**, 678–689 (2007).
3. Woods, A. N. *et al.* Differential Expression of Homing Receptor Ligands on Tumor-Associated Vasculature that Control CD8 Effector T-cell Entry. *Cancer Immunol. Res.* **5**, 1062 LP – 1073 (2017).
4. Isaaz, S., Baetz, K., Olsen, K., Podack, E. & Griffiths, G. M. Serial killing by cytotoxic T lymphocytes: T cell receptor triggers degranulation, re-filling of the lytic granules and secretion of lytic proteins via a non-granule pathway. *Eur. J. Immunol.* **25**, 1071–1079 (1995).
5. Deguine, J., Breart, B., Lemaître, F., Di Santo, J. P. & Bousso, P. Intravital imaging reveals distinct dynamics for natural killer and CD8(+) T cells during tumor regression. *Immunity* **33**, 632–644 (2010).
6. Coppieters, K., Amirian, N. & von Herrath, M. Intravital imaging of CTLs killing islet cells in diabetic mice. *J. Clin. Invest.* **122**, 119–131 (2012).
7. Borst, J., Ahrends, T., Bąbała, N., Melief, C. J. M. & Kastenmüller, W. CD4(+) T cell help in cancer immunology and immunotherapy. *Nat. Rev. Immunol.* **18**, 635–647 (2018).
8. Giuntoli, R. L. 2nd, Lu, J., Kobayashi, H., Kennedy, R. & Celis, E. Direct costimulation of tumor-reactive CTL by helper T cells potentiate their proliferation, survival, and effector function. *Clin. cancer Res. an Off. J. Am. Assoc. Cancer Res.* **8**, 922–931 (2002).
9. Kennedy, R. & Celis, E. Multiple roles for CD4+ T cells in anti-tumor immune responses. *Immunol. Rev.* **222**, 129–144 (2008).
10. Bos, R. & Sherman, L. A. CD4+ T-cell help in the tumor milieu is required for recruitment and cytolytic function of CD8+ T lymphocytes. *Cancer Res.* **70**, 8368–8377 (2010).
11. Malyshkina, A. *et al.* Fas Ligand-mediated cytotoxicity of CD4+ T cells during chronic retrovirus infection. *Sci. Rep.* **7**, 7785 (2017).
12. Quezada, S. A. *et al.* Tumor-reactive CD4(+) T cells develop cytotoxic activity and eradicate large established melanoma after transfer into lymphopenic hosts. *J. Exp. Med.* **207**, 637–650 (2010).
13. Castro, F., Cardoso, A. P., Gonçalves, R. M., Serre, K. & Oliveira, M. J. Interferon-Gamma at the Crossroads of Tumor Immune Surveillance or Evasion. *Front. Immunol.* **9**, 847 (2018).
14. Eisel, D. *et al.* Cognate Interaction With CD4+ T Cells Instructs Tumor-Associated Macrophages to Acquire M1-Like Phenotype. *Front. Immunol.* **10**, 219 (2019).
15. Jameson, S. C. & Masopust, D. Understanding Subset Diversity in T Cell Memory. *Immunity* **48**, 214–226 (2018).
16. Mueller, S. N., Gebhardt, T., Carbone, F. R. & Heath, W. R. Memory T Cell Subsets, Migration Patterns, and Tissue Residence. *Annu. Rev. Immunol.* **31**, 137–161 (2013).
17. Martin, M. D. & Badovinac, V. P. Defining Memory CD8 T Cell. *Front. Immunol.* **9**, 2692 (2018).
18. Ariotti, S. *et al.* Skin-resident memory CD8⁺ T cells trigger a state of tissue-wide pathogen alert. *Science (80-.).* **346**, 101 LP – 105 (2014).

19. Schenkel, J. M. *et al.* Resident memory CD8 T cells trigger protective innate and adaptive immune responses. *Science (80-.).* **346**, 98 LP – 101 (2014).
20. McLane, L. M., Abdel-Hakeem, M. S. & Wherry, E. J. CD8 T Cell Exhaustion During Chronic Viral Infection and Cancer. *Annu. Rev. Immunol.* **37**, 457–495 (2015).
21. Rosato, P. C., Wijeyesinghe, S., Stolley, J. M. & Masopust, D. Integrating resident memory into T cell differentiation models. *Curr. Opin. Immunol.* **63**, 35–42 (2020).
22. Fiege, J. K. *et al.* The Impact of TCR Signal Strength on Resident Memory T Cell Formation during Influenza Virus Infection. *J. Immunol.* **203**, 936–945 (2019).
23. Slütter, B. *et al.* Dynamics of influenza-induced lung-resident memory T cells underlie waning heterosubtypic immunity. *Sci. Immunol.* **2**, (2017).
24. Newell, E. W., Sigal, N., Bendall, S. C., Nolan, G. P. & Davis, M. M. Cytometry by time-of-flight shows combinatorial cytokine expression and virus-specific cell niches within a continuum of CD8+ T cell phenotypes. *Immunity* **36**, 142–152 (2012).
25. van Aalderen, M. C. *et al.* Infection history determines the differentiation state of human CD8+ T cells. *J. Virol.* **89**, 5110–5123 (2015).
26. Sen, D. R. *et al.* The epigenetic landscape of T cell exhaustion. *Science (80-.).* **354**, 1165 LP – 1169 (2016).
27. Miller, B. C. *et al.* Subsets of exhausted CD8(+) T cells differentially mediate tumor control and respond to checkpoint blockade. *Nat. Immunol.* **20**, 326–336 (2019).
28. Galon, J. *et al.* Type, Density, and Location of Immune Cells Within Human Colorectal Tumors Predict Clinical Outcome. *Science (80-.).* **313**, 1960 LP – 1964 (2006).
29. Thorsson, V. *et al.* The Immune Landscape of Cancer. *Immunity* **48**, 812-830.e14 (2018).
30. Hanahan, D. & Weinberg, R. A. Hallmarks of Cancer: The Next Generation. *Cell* **144**, 646–674 (2011).
31. Stratton, M. R., Campbell, P. J. & Futreal, P. A. The cancer genome. *Nature* **458**, 719–724 (2009).
32. Kwak, M., Leick, K. M., Melssen, M. M. & Slingluff, C. L. Vaccine Strategy in Melanoma. *Surg. Oncol. Clin. N. Am.* **28**, 337–351 (2019).
33. Joffre, O., Nolte, M. A., Spörri, R. & Reis e Sousa, C. Inflammatory signals in dendritic cell activation and the induction of adaptive immunity. *Immunol. Rev.* **227**, 234–247 (2009).
34. Chen, G. Y. & Nuñez, G. Sterile inflammation: sensing and reacting to damage. *Nat. Rev. Immunol.* **10**, 826–837 (2010).
35. Blanco, P., Palucka, A. K., Pascual, V. & Banchereau, J. Dendritic cells and cytokines in human inflammatory and autoimmune diseases. *Cytokine Growth Factor Rev.* **19**, 41–52 (2008).
36. Galluzzi, L., Buqué, A., Kepp, O., Zitvogel, L. & Kroemer, G. Immunogenic cell death in cancer and infectious disease. *Nat. Rev. Immunol.* **17**, 97–111 (2017).
37. Ferguson, T. A., Choi, J. & Green, D. R. Armed response: how dying cells influence T-cell functions. *Immunol. Rev.* **241**, 77–88 (2011).
38. Green, D. R., Ferguson, T., Zitvogel, L. & Kroemer, G. Immunogenic and tolerogenic cell death. *Nat. Rev. Immunol.* **9**, 353–363 (2009).
39. Ma, Y. *et al.* Anticancer Chemotherapy-Induced Intratumoral Recruitment and Differentiation of Antigen-Presenting Cells. *Immunity* **38**, 729–741 (2013).
40. Woo, S.-R. *et al.* STING-dependent cytosolic DNA sensing mediates innate immune

recognition of immunogenic tumors. *Immunity* **41**, 830–842 (2014).
41. Cella, M. *et al.* Maturation, activation, and protection of dendritic cells induced by double-stranded RNA. *J. Exp. Med.* **189**, 821–829 (1999).
42. Ohl, L. *et al.* CCR7 Governs Skin Dendritic Cell Migration under Inflammatory and Steady-State Conditions. *Immunity* **21**, 279–288 (2004).
43. Garg, A. D. & Agostinis, P. Cell death and immunity in cancer: From danger signals to mimicry of pathogen defense responses. *Immunol. Rev.* **280**, 126–148 (2017).
44. Kalkavan, H. & Green, D. R. MOMP, cell suicide as a BCL-2 family business. *Cell Death Differ.* **25**, 46–55 (2018).
45. Legrand, A. J., Konstantinou, M., Goode, E. F. & Meier, P. The Diversification of Cell Death and Immunity: Memento Mori. *Mol. Cell* **76**, 232–242 (2019).
46. Annibaldi, A. & Meier, P. Checkpoints in TNF-Induced Cell Death: Implications in Inflammation and Cancer. *Trends Mol. Med.* **24**, 49–65 (2018).
47. Hargadon, K. M. Tumor-altered dendritic cell function: implications for anti-tumor immunity. *Front. Immunol.* **4**, 192 (2013).
48. Hargadon, K. M. The extent to which melanoma alters tissue-resident dendritic cell function correlates with tumorigenicity. *Oncoimmunology* **5**, e1069462 (2016).
49. Devalaraja, S. *et al.* Tumor-Derived Retinoic Acid Regulates Intratumoral Monocyte Differentiation to Promote Immune Suppression. *Cell* **180**, 1098-1114.e16 (2020).
50. Peng, W. *et al.* Loss of PTEN Promotes Resistance to T Cell–Mediated Immunotherapy. *Cancer Discov.* **6**, 202 LP – 216 (2016).
51. Spranger, S., Bao, R. & Gajewski, T. F. Melanoma-intrinsic β-catenin signalling prevents anti-tumour immunity. *Nature* **523**, 231–235 (2015).
52. Jakubzick, C. V, Randolph, G. J. & Henson, P. M. Monocyte differentiation and antigen-presenting functions. *Nat. Rev. Immunol.* **17**, 349–362 (2017).
53. Schwartz, R. H. T cell anergy. *Annu. Rev. Immunol.* **21**, 305–334 (2003).
54. Wei, H. *et al.* Cancer Immunotherapy Using In vitro Genetically Modified Targeted Dendritic Cells. *Cancer Res.* **68**, 3854 LP – 3862 (2008).
55. Quatromoni, J. G. *et al.* The timing of TGF-β inhibition affects the generation of antigen-specific CD8+ T cells. *BMC Immunol.* **14**, 30 (2013).
56. Rotman, J., Koster, B. D., Jordanova, E. S., Heeren, A. M. & de Gruijl, T. D. Unlocking the therapeutic potential of primary tumor-draining lymph nodes. *Cancer Immunol. Immunother.* **68**, 1681–1688 (2019).
57. Dangaj, D. *et al.* Cooperation between Constitutive and Inducible Chemokines Enables T Cell Engraftment and Immune Attack in Solid Tumors. *Cancer Cell* **35**, 885-900.e10 (2019).
58. Georganaki, M., van Hooren, L. & Dimberg, A. Vascular Targeting to Increase the Efficiency of Immune Checkpoint Blockade in Cancer. *Front. Immunol.* **9**, 3081 (2018).
59. Bergers, G. & Benjamin, L. E. Tumorigenesis and the angiogenic switch. *Nat. Rev. Cancer* **3**, 401–410 (2003).
60. Delfortrie, S. *et al.* Egfl7 Promotes Tumor Escape from Immunity by Repressing Endothelial Cell Activation. *Cancer Res.* **71**, 7176 LP – 7186 (2011).
61. Gehad, A. E. *et al.* Nitric Oxide–Producing Myeloid-Derived Suppressor Cells Inhibit Vascular E-Selectin Expression in Human Squamous Cell Carcinomas. *J. Invest. Dermatol.* **132**, 2642–2651 (2012).
62. Huang, H. *et al.* VEGF suppresses T-lymphocyte infiltration in the tumor

microenvironment through inhibition of NF-κB-induced endothelial activation. *FASEB J.* **29**, 227–238 (2014).
63. Erdag, G. *et al.* Immunotype and Immunohistologic Characteristics of Tumor-Infiltrating Immune Cells Are Associated with Clinical Outcome in Metastatic Melanoma. *Cancer Res.* **72**, 1070 LP – 1080 (2012).
64. Mrass, P. *et al.* Random migration precedes stable target cell interactions of tumor-infiltrating T cells. *J. Exp. Med.* **203**, 2749–2761 (2006).
65. Weninger, W., Biro, M. & Jain, R. Leukocyte migration in the interstitial space of non-lymphoid organs. *Nat. Rev. Immunol.* **14**, 232–246 (2014).
66. Boissonnas, A., Fetler, L., Zeelenberg, I. S., Hugues, S. & Amigorena, S. In vivo imaging of cytotoxic T cell infiltration and elimination of a solid tumor. *J. Exp. Med.* **204**, 345–356 (2007).
67. Krummel, M. F., Bartumeus, F. & Gérard, A. T cell migration, search strategies and mechanisms. *Nature reviews. Immunology* vol. 16 193–201 (2016).
68. Ariotti, S. *et al.* Subtle CXCR3-Dependent Chemotaxis of CTLs within Infected Tissue Allows Efficient Target Localization. *J. Immunol.* **195**, 5285 LP – 5295 (2015).
69. Hickman, H. D. *et al.* CXCR3 Chemokine Receptor Enables Local CD8+ T Cell Migration for the Destruction of Virus-Infected Cells. *Immunity* **42**, 524–537 (2015).
70. Sorokin, L. The impact of the extracellular matrix on inflammation. *Nat. Rev. Immunol.* **10**, 712–723 (2010).
71. Overstreet, M. G. *et al.* Inflammation-induced interstitial migration of effector $CD4^+$ T cells is dependent on integrin αV. *Nat. Immunol.* **14**, 949–958 (2013).
72. Espinosa-Carrasco, G. *et al.* Integrin β1 Optimizes Diabetogenic T Cell Migration and Function in the Pancreas. *Front. Immunol.* **9**, 1156 (2018).
73. Ray, S. J. *et al.* The collagen binding alpha1beta1 integrin VLA-1 regulates CD8 T cell-mediated immune protection against heterologous influenza infection. *Immunity* **20**, 167–179 (2004).
74. Richter, M. *et al.* Collagen distribution and expression of collagen-binding alpha1beta1 (VLA-1) and alpha2beta1 (VLA-2) integrins on CD4 and CD8 T cells during influenza infection. *J. Immunol.* **178**, 4506–4516 (2007).
75. Reilly, E. C. *et al.* T(RM) integrins CD103 and CD49a differentially support adherence and motility after resolution of influenza virus infection. *Proc. Natl. Acad. Sci. U. S. A.* (2020) doi:10.1073/pnas.1915681117.
76. Egeblad, M., Rasch, M. G. & Weaver, V. M. Dynamic interplay between the collagen scaffold and tumor evolution. *Curr. Opin. Cell Biol.* **22**, 697–706 (2010).
77. Henke, E., Nandigama, R. & Ergün, S. Extracellular Matrix in the Tumor Microenvironment and Its Impact on Cancer Therapy. *Front. Mol. Biosci.* **6**, 160 (2020).
78. Nissen, N. I., Karsdal, M. & Willumsen, N. Collagens and Cancer associated fibroblasts in the reactive stroma and its relation to Cancer biology. *J. Exp. Clin. Cancer Res.* **38**, 115 (2019).
79. Zunder, S. M., Gelderblom, H., Tollenaar, R. A. & Mesker, W. E. The significance of stromal collagen organization in cancer tissue: An in-depth discussion of literature. *Crit. Rev. Oncol. Hematol.* **151**, 102907 (2020).
80. Salmon, H. *et al.* Matrix architecture defines the preferential localization and migration of T cells into the stroma of human lung tumors. *J. Clin. Invest.* **122**, 899–910 (2012).
81. Bougherara, H. *et al.* Real-Time Imaging of Resident T Cells in Human Lung and

Ovarian Carcinomas Reveals How Different Tumor Microenvironments Control T Lymphocyte Migration. *Front. Immunol.* **6**, 500 (2015).
82. Li, X. *et al.* Infiltration of CD8⁺ T cells into tumor cell clusters in triple-negative breast cancer. *Proc. Natl. Acad. Sci.* **116**, 3678 LP – 3687 (2019).
83. Franciszkiewicz, K. *et al.* Intratumoral induction of CD103 triggers tumor-specific CTL function and CCR5-dependent T-cell retention. *Cancer Res.* **69**, 6249–6255 (2009).
84. Le Floc'h, A. *et al.* Minimal engagement of CD103 on cytotoxic T lymphocytes with an E-cadherin-Fc molecule triggers lytic granule polarization via a phospholipase Cgamma-dependent pathway. *Cancer Res.* **71**, 328–338 (2011).
85. Reina, M. & Espel, E. Role of LFA-1 and ICAM-1 in Cancer. *Cancers (Basel).* **9**, 153 (2017).
86. Franciszkiewicz, K. *et al.* CD103 or LFA-1 engagement at the immune synapse between cytotoxic T cells and tumor cells promotes maturation and regulates T-cell effector functions. *Cancer Res.* **73**, 617–628 (2013).
87. Anikeeva, N. *et al.* Distinct role of lymphocyte function-associated antigen-1 in mediating effective cytolytic activity by cytotoxic T lymphocytes. *Proc. Natl. Acad. Sci. U. S. A.* **102**, 6437–6442 (2005).
88. Garrido, F., Aptsiauri, N., Doorduijn, E. M., Garcia Lora, A. M. & van Hall, T. The urgent need to recover MHC class I in cancers for effective immunotherapy. *Curr. Opin. Immunol.* **39**, 44–51 (2016).
89. Petit, A.-E. *et al.* A major secretory defect of tumour-infiltrating T lymphocytes due to galectin impairing LFA-1-mediated synapse completion. *Nat. Commun.* **7**, 12242 (2016).
90. Dieckmann, N. M. G., Frazer, G. L., Asano, Y., Stinchcombe, J. C. & Griffiths, G. M. The cytotoxic T lymphocyte immune synapse at a glance. *J. Cell Sci.* **129**, 2881–2886 (2016).
91. Kristensen, N. N., Madsen, A. N., Thomsen, A. R. & Christensen, J. P. Cytokine production by virus-specific CD8(+) T cells varies with activation state and localization, but not with TCR avidity. *J. Gen. Virol.* **85**, 1703–1712 (2004).
92. Ritter, A. T. *et al.* Actin depletion initiates events leading to granule secretion at the immunological synapse. *Immunity* **42**, 864–876 (2015).
93. Kim, C. G. *et al.* VEGF-A drives TOX-dependent T cell exhaustion in anti-PD-1-resistant microsatellite stable colorectal cancers. *Sci. Immunol.* **4**, (2019).
94. Murdoch, C., Giannoudis, A. & Lewis, C. E. Mechanisms regulating the recruitment of macrophages into hypoxic areas of tumors and other ischemic tissues. *Blood* **104**, 2224–2234 (2004).
95. Huang, B. *et al.* CCL2/CCR2 pathway mediates recruitment of myeloid suppressor cells to cancers. *Cancer Lett.* **252**, 86–92 (2007).
96. Kumar, V., Patel, S., Tcyganov, E. & Gabrilovich, D. I. The Nature of Myeloid-Derived Suppressor Cells in the Tumor Microenvironment. *Trends Immunol.* **37**, 208–220 (2016).
97. Raber, P. L. *et al.* Subpopulations of myeloid-derived suppressor cells impair T cell responses through independent nitric oxide-related pathways. *Int. J. cancer* **134**, 2853–2864 (2014).
98. Mao, Y. *et al.* Inhibition of tumor-derived prostaglandin-e2 blocks the induction of myeloid-derived suppressor cells and recovers natural killer cell activity. *Clin. cancer*

Res. an Off. J. Am. Assoc. Cancer Res. **20**, 4096–4106 (2014).
99. Tanaka, A. & Sakaguchi, S. Regulatory T cells in cancer immunotherapy. *Cell Res.* **27**, 109–118 (2017).
100. Kalluri, R. The biology and function of fibroblasts in cancer. *Nat. Rev. Cancer* **16**, 582–598 (2016).
101. Liu, T. *et al.* Cancer-associated fibroblasts: an emerging target of anti-cancer immunotherapy. *J. Hematol. Oncol.* **12**, 86 (2019).
102. Zhang, R. *et al.* Cancer-associated fibroblasts enhance tumor-associated macrophages enrichment and suppress NK cells function in colorectal cancer. *Cell Death Dis.* **10**, 273 (2019).
103. Alsaab, H. O. *et al.* PD-1 and PD-L1 Checkpoint Signaling Inhibition for Cancer Immunotherapy: Mechanism, Combinations, and Clinical Outcome. *Front. Pharmacol.* **8**, 561 (2017).
104. Hodi, F. S. *et al.* Improved survival with ipilimumab in patients with metastatic melanoma. *N. Engl. J. Med.* **363**, 711–723 (2010).
105. Larkin, J. *et al.* Combined Nivolumab and Ipilimumab or Monotherapy in Untreated Melanoma. *N. Engl. J. Med.* **373**, 23–34 (2015).
106. Havel, J. J., Chowell, D. & Chan, T. A. The evolving landscape of biomarkers for checkpoint inhibitor immunotherapy. *Nat. Rev. Cancer* **19**, 133–150 (2019).
107. Vanmeerbeek, I. *et al.* Trial watch: chemotherapy-induced immunogenic cell death in immuno-oncology. *Oncoimmunology* **9**, 1703449 (2020).
108. Buqué, A. *et al.* Trial Watch—Small molecules targeting the immunological tumor microenvironment for cancer therapy. *Oncoimmunology* **5**, e1149674 (2016).
109. AWATE, S., Babiuk, L. & Mutwiri, G. Mechanisms of Action of Adjuvants. *Front. Immunol.* **4**, 114 (2013).
110. O'Neill, D. W. *et al.* Comparison of the immunogenicity of Montanide ISA 51 adjuvant and cytokine-matured dendritic cells in a randomized controlled clinical trial of melanoma vaccines. *J. Clin. Oncol.* **27**, 3002 (2009).
111. Dzhandzhugazyan, K. N., Guldberg, P. & Kirkin, A. F. Adoptive T cell cancer therapy. *Nat. Mater.* **17**, 475–477 (2018).
112. Met, Ö., Jensen, K. M., Chamberlain, C. A., Donia, M. & Svane, I. M. Principles of adoptive T cell therapy in cancer. *Semin. Immunopathol.* **41**, 49–58 (2019).
113. Jain, R. K. Antiangiogenesis Strategies Revisited: From Starving Tumors to Alleviating Hypoxia. *Cancer Cell* **26**, 605–622 (2014).
114. Cabo, M. *et al.* Trial Watch: Immunostimulatory monoclonal antibodies for oncological indications. *Oncoimmunology* **6**, e1371896 (2017).
115. Juric, V. *et al.* MMP-9 inhibition promotes anti-tumor immunity through disruption of biochemical and physical barriers to T-cell trafficking to tumors. *PLoS One* **13**, e0207255 (2018).
116. Fields, G. B. The Rebirth of Matrix Metalloproteinase Inhibitors: Moving Beyond the Dogma. *Cells* **8**, (2019).
117. Murciano-Goroff, Y. R., Warner, A. B. & Wolchok, J. D. The future of cancer immunotherapy: microenvironment-targeting combinations. *Cell Res.* **30**, 507–519 (2020).

Chapter 2

Vaccines targeting helper T cells for cancer immunotherapy

Marit M. Melssen and Craig L. Slingluff, Jr.

Curr Opin Immunol. 2017 Aug;47:85-92.

ABSTRACT

There are compelling arguments for designing cancer vaccines specifically to induce $CD4^+$ helper T cell responses. Recent studies highlight the crucial role of proliferating, activated effector memory Th1 $CD4^+$ T cells in effective antitumor immunity and reveal that $CD4^+$ T cells induce more durable immune-mediated tumor control than $CD8^+$ T cells. $CD4^+$ T cells promote antitumor immunity by numerous mechanisms including enhancing antigen presentation, co-stimulation, T cell homing, T cell activation, and effector function. These effects are mediated at sites of T cell priming and at the tumor microenvironment. Several cancer vaccine approaches induce durable $CD4^+$ T cell responses and have promising clinical activity. Future work should further optimize vaccine adjuvants and combination therapies incorporating helper peptide vaccines.

The goal of cancer therapies is to destroy malignant cells, without damage to healthy tissues. Thus, many immune therapies are designed to take advantage of the specificity and cytotoxic capacity of $CD8^+$ T cells (T_{CD8}). However, clinical outcomes with cancer vaccines targeting T_{CD8} has been disappointing [1]. On the other hand, there are compelling arguments for designing vaccines specifically to induce $CD4^+$ helper T cell (T_{CD4}) responses instead. This review will summarize preclinical data supporting the critical role of T_{CD4} in antitumor immunity, and both preclinical and clinical data for the immunogenicity and clinical activity of cancer vaccines targeting induction of T_{CD4}.

KEY ROLES OF T_{CD4} LYMPHOCYTES IN ANTI-TUMOR IMMUNE RESPONSES

Murine studies show that T_{CD4} are required for induction of CD8 antitumor T cell responses [2,3]. Recent very comprehensive analysis of cellular subsets in cancer immunity highlight the crucial role of proliferating, activated effector memory Th1 T_{CD4} ($CD69^+$ T-bet^+ $CD44^+$ $CD62L^{neg}$ $CD27^{low}$ $CD90^{hi}$) in effective antitumor immunity [4] and showed that T_{CD4} induce more durable immune-mediated tumor control than T_{CD8}. Depletion of T_{CD4} can abrogate all or part of protective immune responses to cell-based vaccines [5]. Furthermore, adoptive therapy with T_{CD4} has induced tumor protection in some model systems and in humans [6,7]. Thus, protective immunity induced by tumor cell vaccines and other immune therapies appears to depend on T_{CD4}. The mechanisms by which T_{CD4} may promote antitumor immunity include numerous direct and indirect effects of those cells, impacting antigen presentation, co-stimulation, T cell homing, T cell activation, and effector function, both systemically and in the tumor microenvironment (TME), which are detailed below:

Antigen presentation

When Th1 T_{CD4} encounter their cognate antigen, whether expressed by tumor cells or by professional antigen presenting cells (APCs), they can produce IFNγ. Within the TME, effects of IFNγ include the induction of Class I and Class II MHC molecules and upregulation of antigen processing machinery (Figures 1 and 2). Increased expression of these molecules enhances recognition of tumor-associated antigens by T_{CD8} in a class I restricted manner, or by T_{CD4} in a class II restricted manner [8–10].

Co-stimulation

Activated T_{CD4} cells express CD40L [11–13] by which they can activate dendritic cells (DC) through ligation of CD40, for heightened antigen presentation and expression of costimulatory molecules (Figure 1). They also provide help by enabling DC to secrete IL-12 and other cytokines to direct the immune response. Additionally, this interaction triggers release of chemokines CCL3 and CCL4 by

the APCs, which guide naïve CD8 T cells to APC within the lymph node, to improve efficacy of T cell priming [14,15]. Mimicking T cell help in the priming phase, with agonistic antibodies to CD40 or CD27, can improve efficacy of vaccines and other immune therapies [16,17]. Furthermore, strong Th1 help produces the proper cytokine milieu to induce immune-mediated tumor destruction [18–20]. Within the TME, T_{CD4} can directly bind to T_{CD8} through co-stimulatory molecules, such as CD27, CD137 and 4-1BB, thus potentiating T_{CD8} proliferation, survival and effector function [21].

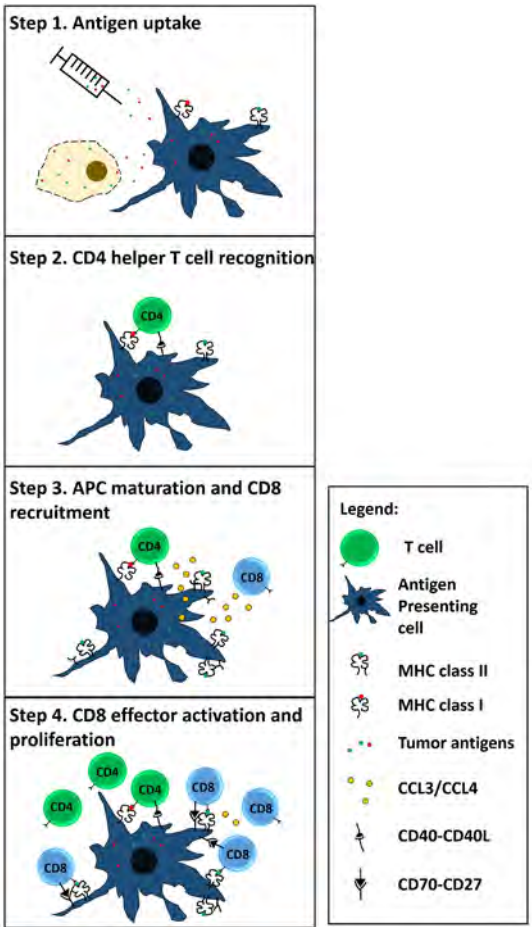

Figure 1. Role of helper T cells in priming of tumor specific effector T cells. Step 1. Vaccination with helper peptides allows antigen presenting cells (APCs) to take up tumor specific helper peptides in addition to tumor antigen directly from dying tumor cells. Step 2. APCs migrate to the lymph node where they interact with CD4 T cells through MHC class II molecules. Step 3. CD40 on the CD4 T cells ligates CD40L to mature the APC, which leads to enhanced MHC class I expression as well as costimulatory molecules CD70 and CCL3 and CCL4. Step 4 The chemokines recruit CD8 T cells to the complex, and binding the MHC molecules with costimulation induces optimal effector priming. The primed effectors proliferate and are capable of trafficking to the tumor site.

T cell homing

As mentioned above, effector Th1 T_{CD4} are a source of IFNγ if they recognize their cognate antigen in the TME (Figure 2). In addition to enhancing antigen presentation, IFNγ also supports homing of T cells to the TME: it induces expression of the IFN-responsive chemokines CXCL9, CXCL10, and CXCL11 [22,23], and also induces expression, by tumor-associated endothelium, of VCAM-

1 and other critical ligands for T cell homing receptors [24]. The receptor for these chemokines is CXCR3, which is expressed by activated T_{CD4} and T_{CD8}, including T cells induced by cancer vaccines [25]. Thus, CXCL9-11 recruit CXCR3+ T cells into the TME [26–28]. Overall, Th1 T_{CD4} have a net effect of enhancing infiltration of tumor by T_{CD8} [26,29,30]. It is relevant to acknowledge that IFNγ in the TME also induces immunosuppressive and immunoregulatory processes, including indoleamine-2,3-dioxygenase (IDO), regulatory T cells, and PD-L1 expression [31] and may limit effectiveness of cancer vaccines [32]. Interestingly, analysis of TCGA data reveal that increased IFNγ expression in the TME is associated with improved overall survival [33,34] (Figure 3), which supports the favorable association of IFNγ in the TME with melanoma control.

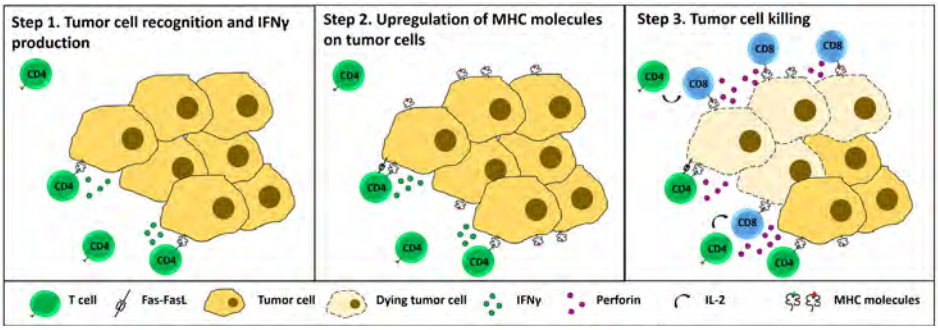

Figure 2. Role of CD4 T cells in the tumor microenvironment. Step 1. CD4 T cells can home to the tumor where they can interact with tumor cells when they express MHC class II. When activated Th1 CD4+ cells produce IFNg. Step 2. IFNg enhances MHC expression by tumor cells. Additionally, it induces CXCL9 and CXCL10 expression by the vasculature, to optimally recruit CD8 effector T cells to the tumor site. Step 3. Some CD4 T cells also are capable of direct tumor cell killing through FasL and TRAIL interactions as well as T cell receptor mediated cytotoxicity. Additionally, the T cells produce IL-2, which supports CD8 effector T cells in survival, proliferation and cytotoxic activity

Effector function

T_{CD4} are not classically cytotoxic effector cells; however, some T_{CD4} do have direct antitumor effector function [9,35,36] mediated by expression of granzymes, perforin, TRAIL or FasL [2,37,38] (Figure 2). In addition to direct tumor cell killing, T_{CD4} can also promote antitumor immunity by inhibiting angiogenesis through IFNγ signaling on non-hematopoietic cells [39]. Thus, T_{CD4} cells may support tumor control in some cases by direct lytic effector function, in addition to their more typical role in providing help to T_{CD8} and B cells. Interestingly, they can also provide help to other T_{CD4}; this helper function has supported activation of T_{CD4} to an epitope that otherwise is poorly immunogenic [40].

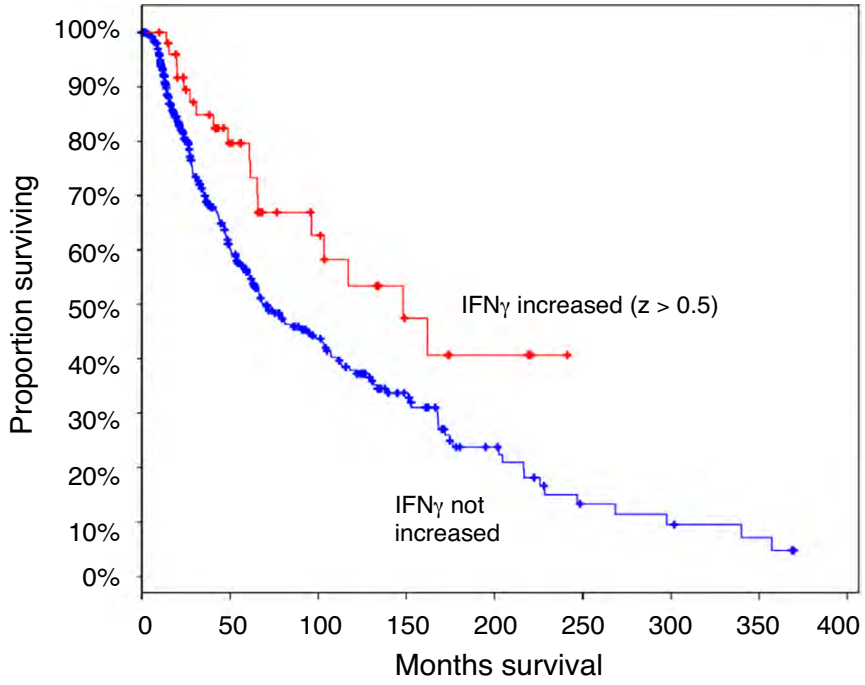

Figure 3. Association of IFNγ expression with survival in melanoma. Data from the Cancer Genome Atlas (TCGA) were interrogated through cbioportal.org for 459 patients. Overexpression of IFNγ in the tumor microenvironment (z > 0.5, 11% of patients), was associated with enhanced overall survival (148 versus 69 months median survival, P = 0.011). Similar significant differences were evident with z scores of 0.8, 1, 1.2, 1.5 (P < 0.006 to P = 0.02, data not shown).

Memory formation

Classically, CD4 help has been thought to be required for priming T_{CD8} responses only in situations in the absence of a strong primary immune response. A strong danger signal can induce a primary immune response in the presence of toll-like receptor (TLR) ligands or proinflammatory cytokines, which can activate APCs independent of T_{CD4}, thereby circumventing the necessity of T_{CD4} help for proper effector function [41–43]. However, more recent research has shown that, regardless of the strength of the primary T_{CD8} response, CD4 help is always required for optimal CD8 memory cell formation and secondary recall response [44]. Without CD4 help, signaling through receptors important for formation and survival of specific memory T_{CD8} subsets (CD25, CD127 and CD103) is diminished [13,45]. Furthermore, T_{CD8} activated in the absence of CD4 help are more prone to apoptosis when restimulated [46]. Regardless, as the TME is not considered pro-inflammatory, the primary anti-tumor immune response will most likely be weak. Thus, we suggest that to elicit optimal effector as well as memory T_{CD8} responses against tumor antigens, vaccines will require a mechanism to activate T_{CD4}. However,

most studies of the role of T_{CD4} in memory have been done in murine models of viral infection. Thus, there is a need for more studies in cancer models and in humans to understand the role of T_{CD4} in optimal immune memory for cancer control.

Summary of preclinical data

Thus, activation of a T_{CD4} response supports cytotoxic T_{CD8} priming, memory formation, recruitment to the tumor, and tumor cell recognition. Additionally, some T_{CD4} have the capacity to contribute directly to tumor cell killing. It is thus not surprising that immune therapies solely focusing on T_{CD8} do not offer optimal results for anti-tumor immunity. Activation of tumor specific T_{CD4} through helper peptide vaccines or other methods offer promise to enhance anti-tumor T_{CD8} responses and optimal tumor control. Furthermore, the impact of T_{CD4} goes well beyond the effects of cytokines alone or DC licensing alone so that simply mimicking CD4 help through administration of IFNs, IL-2, or anti-CD40 antibodies will not reconstitute the breadth of the beneficial effects of anti-tumor T_{CD4} responses.

CLINICAL EXPERIENCE WITH HELPER PEPTIDE VACCINES

Several cancer vaccine approaches have targeted T_{CD4} responses and offer promise. Representative examples are summarized briefly here and in Table 1.

Helper peptides from Her2/neu

Patients with breast cancer have decreased Her2-reactive T_{CD4} responses compared to patients without cancer, providing justification for enhancing Th1 responses to Her2 as therapy [47]. Vaccines with these Her2/neu helper peptides have been administered as peptide pulsed type 1 DC administered intranodally: this regimen has induced durable T_{CD4} responses to those peptides in patients with breast cancer [48] and has induced complete regressions of DCIS [49,50]. The immune responses and clinical activity have been comparable regardless of the route of vaccination (intranodal versus intralesional) [50]. These findings are important because they show evidence for clinical activity of a low toxicity vaccine regimen, at least for early stage disease (DCIS). They are also important because they show activity with a vaccine designed to induce T_{CD4} and that uses an overexpressed antigen, despite presumed pre-existing tolerance.

Telomerase helper peptides

Telomerase (hTERT) is an appealing target for cancer vaccines because it is overexpressed in a wide range of cancers. Several hTERT vaccines have incorporated helper peptides and have induced Th1 T_{CD4} responses [51–53], as well as epitope spreading to Ras peptides [51]. One hTERT vaccine enhanced DC activation in preclinical models, including IL-12 production [54]. A phase III clinical trial of the

GV1001 vaccine showed no impact on outcome when added to chemotherapy for pancreatic cancer [55], but others remain in trials. Currently, a clinical trial is testing the safety and effectivity of a vaccine incorporating UCP2 and UCP4 in Incomplete Freund's Adjuvant (IFA) in NSCLC patients (NCT02818426).

Melanoma peptide vaccines administered with dendritic cells

A dendritic cell vaccine includes DC pulsed with multiple peptides including 3 short peptides restricted by HLA-A2, with or without 2 helper peptides restricted by class II MHC. Patients vaccinated with the helper peptides developed helper T cell responses in circulation and in skin infiltrating lymphocytes, and had higher responses to CD8 T cells than those vaccinated only with the T_{CD8} epitopes [56]. There was also a trend to better clinical outcome in those who also received helper peptides [56].

Table 1. Helper peptide vaccines with favorable immunologic and/or clinical outcomes

Cancer target	Source proteins: Peptides in vaccines	Adjuvant/ delivery	Immunologic outcome	Clinical outcomes
Invasive breast cancer, DCIS	[**Her2/neu**]: Her2 (42-56), (98-114), (328-345), (776-790), (927-941), (1166-1180) +/− HLA-A2 peptides Her2 (369-377), (689-697)	Peptide-pulsed type 1 DC (matured in IFNγ and LPS), intranodal. Also evaluated intralesional vaccines.	Durable T_{CD4} responses in about 80% of patients [48].	Complete regressions of DCIS in 19%–29%; decreased Her2 expression [49] [50].
NSCLC and pancreatic cancer	[**hTERT**]: **GV1001 vaccine**: hTERT (611-626)	Administered to patients with NSCLC and also with gemcitabine for patients with pancreatic cancer.	Polyfunctional Th1 cells induced to hTERT (59%); epitope spreading to Ras (29%), but transient and weak responses. [51]	Survival for NSCLC enhanced in immune responders (54 vs. 13 mos, p<0.001) [52]. Failed to impact survival in randomized phase III trial [55].
Prostate cancer, renal cell cancer	[**hTERT**]: **GX301 vaccine**: hTERT (611-626), (672-686), (766-780); plus HLA-A2 restricted hTERT (540-548)	Each peptide administered with IFA and topical imiquimod in the skin of the abdomen: each peptide in a different site. Each vaccine administration in the same sites.	Immune response in all patients.	SD in 4 patients

table continues

Cancer target	Source proteins: Peptides in vaccines	Adjuvant/ delivery	Immunologic outcome	Clinical outcomes
Melanoma	[**gp100, tyrosinase**]: HLA-A2 restricted: gp100 (154–162); tyros (369– 377); +/– MHC-II– restricted gp100 (44–59); tyros (448–462).	Monocyte-derived DC prepared in IL4, GM-CSF and matured PGE2 and TNFa. Also pulsed with KLH. Intranodal injection.	IFNγ response of SKIL to melanoma cells 29% vs 7%; Tetramer+ in blood 17% vs 0% for T_{CD8}, 23% for T_{CD4}.	PFS enhanced for addition of helper peptides (5 vs 2.8 mos, p < 0.01)
Melanoma	[**gp100, tyrosinase, MelanA, MAGE-A] 6MHP vaccine**: gp100 (44-59); tyros (56-70); tyros (386-406); Melan-A (51-73); MAGE-A3 (281-295); MAGE-A1-3,6 (121-134);	Peptides + IFA +/– GM-CSF, administered half SC, half ID.	T_{CD4} response in 81% (blood or node); epitope spreading to T_{CD8} responses (different antigens) in 45% tested; induction of Ab responses.	ORR 7–12% (duration up to 7 years). Survival associated with T_{CD4} response. Survival exceeds matched controls. 5 year survival 74% for resected stage IV.

Abbreviations: AdenoCA = adenocarcinoma; tyros = tyrosinase; SKIL = skin test infiltrating lymphocytes; LPS = lipopolysaccharide; IN = intranodal; SC = subcutaneous; ID = intradermally; ORR = objective response rate (PR + CR); NSCLC: non small cell lung cancer.

Amino acid sequences of selected peptides are: $gp100_{154–162}$(KTWGQYWQV); $gp100_{280–288}$(YLEPGPVTA); $tyros_{369–377}$(YMDGTMSQV); $gp100_{44–59}$(WNRQLYPEWTEAQRLD); $tyros_{448–462}$(DYSYLQDSDPDSFQD); $tyros_{56-70}$(AQNILLSNAPLGPQFP); $tyros_{386-406}$(FLLHHAFVDSIFEQWLQRHRP); Melan-A_{51-73}(RNGYRALMDKSLHVGTQCALTRR); MAGE-$3_{281-295}$(TSYVKVLHHMVKISG); MAGE-1,2,3,$6_{121-134}$(LLKYRAREPVTKAE); hTERT$_{611-626}$(EARPALLTSRLRFIPK)

Melanoma peptide vaccines administered in adjuvant emulsion

Our group has evaluated a multipeptide melanoma vaccine containing 6 peptides from melanocytic proteins and cancer-testis antigens, restricted by HLA-DR molecules (6MHP vaccine) in an emulsion with IFA, with or without GM-CSF [57–59]. This vaccine has induced high rates of Th1 T_{CD4} immune responses [57,60] as well as promising clinical outcomes, with durable clinical responses and durable stable disease lasting up to 7 years in 7-12% of patients, plus stable disease in another 12–29% [57,59]. Overall survival for stage IV melanoma patients who received 6MHP vaccines significantly exceeded that of matched pair controls (5-year survival 57% versus 16%; P < 0.001) [61]. Epitope spreading to T_{CD8} was induced in 45% of patients evaluated [62]. Also, antibody (IgG) responses to the peptides were induced. Patient survival was significantly associated with T_{CD4} responses and especially to the combination of antibody plus T_{CD4} responses [59,63], supporting the clinical relevance of immune responses induced to the

6MHP vaccine. Ongoing trials are testing the 6MHP vaccine in combination therapy with checkpoint blockade and with BRAF/MEK inhibition.

NEW DIRECTIONS

Long peptide vaccines to include both T_{CD4} and T_{CD8} specific presented peptides

Preclinical and clinical studies with long (approximately 30-mer) peptides suggest that they may be more effective immunogens than the minimal peptides representing individual CD8 epitopes and that they may also induce T_{CD4} responses. The extra length contributes to a tertiary structure that may protect from peptidases, and they are too long to be presented directly on MHC; so, intracellular processing by professional APCs is required. A vaccine using long peptides for squamous vulvar neoplasia has been associated with high rates of clinical regressions[64], and a vaccine using overlapping long peptides from the cancer-testis antigen NY-ESO-1 has induced T_{CD4}, T_{CD8} and antibody responses [65]. Thus, long peptides offer promise as a form of helper peptide vaccine that may also induce broad integrated immune responses.

Vaccines targeting mutated neoantigens

Melanomas, lung cancers, and other solid tumors have high rates of somatic mutations, and T cells infiltrating melanoma metastases often recognize peptides encompassing these mutations [66]. Furthermore, peptide vaccines have been developed to test whether mutated neoantigens can be predicted and vaccinated against. Personalized vaccines using minimal peptides restricted by HLA-A2-restricted putative neoantigens were successful at inducing T cell responses to 3 peptides per patient in a small study [67]. Ongoing clinical trials are testing long peptide vaccines encompassing cancer-associated somatic point mutations (e.g.: NCT02950766, NCT02427581, NCT01970358, NCT02287428).

Challenges of vaccines targeting mutated neoantigens

Current efforts to develop neoantigen vaccines are hindered by imprecision of algorithms to predict those epitopes, especially for T_{CD4} cells; the heterogeneity of mutation profiles among different metastases in the same patient [67], plus the time and cost required to develop vaccines on a per-patient basis. Another critical challenge is that optimal strategies to induce T cell responses to peptides remain unclear. Among the recent and current clinical trials of neoantigen vaccines, the vaccine adjuvants vary widely, reflecting the lack of consensus. Substantial effort is being directed toward addressing these challenges.

Adjuvants for cancer vaccines

The ability of vaccines to induce effective and durable immunity depends on inclusion of local or systemic vaccine adjuvants, to activate DCs and to provide

danger signals. Options are numerous and include pulsing DCs with peptide, administering nanoparticles containing peptides plus adjuvant, or administering peptides with incomplete Freund's adjuvant (IFA), TLR agonists, or other agents that may activate innate immunity. Vaccines using DNA, RNA or viral constructs are also options and are in trials. There has been debate about using IFA with a peptide vaccine. In murine studies, vaccines using short peptides in IFA induce chronic inflammation at the site of vaccination that recruits and retains antigen-specific T cells at the vaccine site (rather than supporting T cell homing to tumor) and may deplete antigen-reactive T cells [68]. Similarly, vaccination with short peptides plus TLR agonist and agonistic CD40 antibody has been much more effective than subcutaneous administration in IFA at inducing strong circulating T_{CD8} responses in murine models [69]: that approach holds promise but has not yet been explored in humans, but deserves study when CD40 antibodies are available for that purpose. For induction of T_{CD4} in mice, antigen-reactive T_{CD4} cells may also accumulate preferentially at sites of vaccination with IFA [70]; however, use of IFA with a long peptide (20-mer) did not have the same negative effects that were observed with a short 9-mer peptide [68]. In humans, on the other hand, vaccines incorporating IFA, with or without a TLR agonist, can induce strong and durable Th1 dominant T cell responses, especially with intermediate length peptides (14–23 mers) or long peptides (30 mers) [60,71], and addition of a TLR agonist further enhances T_{CD4} responses, as well as antibody and T_{CD8} cell responses[71]. There is no consensus about the optimal strategy to induce durable responses. There is a need to optimize adjuvants further and to reach some consensus on optimal adjuvant. Mutated neoantigen vaccines present a challenge for testing adjuvants: because each vaccine is different, it is not possible to interpret differences in outcome to choice of adjuvant when the peptides are not controlled. Thus, there is rationale for using defined antigen vaccines to identify optimal adjuvants, which subsequently may be selected for use with neoantigen vaccines.

SUMMARY

Immune therapy with checkpoint blockade antibodies can induce dramatic and durable cancer control if there is already an immune response to the cancer. However, active induction of immune responses may be required to enable tumor control by these immune therapies in tumor without an active immune response present. T_{CD4} have myriad roles in enhancing tumor control both during priming of effector T cells as well as in the tumor microenvironment. More importantly, in a suppressive environment such as the tumor, effector T cell responses are often suboptimal without T_{CD4} help. Despite this, the role of CD4 T cells has not been addressed sufficiently in current approaches to cancer immunotherapy. Vaccines designed to induce Th1 T_{CD4} responses are showing significant promise both for induction of durable T cell responses and also for induction of clinical activity in a subset of patients with melanoma and breast cancer. Helper peptide vaccines can induce circulating T_{CD4} responses that enable recognition of tumor antigen in the

tumor microenvironment, and should be able to enhance homing and expansion of T cells to the tumor. Helper peptide vaccines have induced epitope spreading to epitopes in the same or different proteins, and presented by Class I or II MHC. Thus, it is possible that helper peptides, even without incorporating somatic mutations, may also enhance reactivity to mutated neoantigens by epitope spreading or by enhancing responses that are otherwise suboptimal. Definitive testing of these hypotheses is warranted. Other questions remain about how to optimize vaccine adjuvants and combination strategies. Many promising trials are underway with helper peptide vaccines and combinations, and these should advance this field over the next few years.

ACKNOWLEDGEMENTS

This work was supported by the National Institutes of Health [grant numbers R01 CA178846, P30 CA044579] and a Cancer Research Institute Clinical Laboratory Integration Project (CLIP) award.

REFERENCES

1. Rosenberg SA, Yang JC, Restifo NP: Cancer immunotherapy: moving beyond current vaccines. Nat Med 2004, 10:909-915.
2. Kim HJ, Cantor H: CD4 T-cell subsets and tumor immunity: the helpful and the not-so-helpful. Cancer Immunol Res 2014, 2:91- 98.
3. Kumai T, Lee S, Cho HI, Sultan H, Kobayashi H, Harabuchi Y, Celis E: Optimization of peptide vaccines to induce robust antitumor CD4 T-cell responses. Cancer Immunol Res 2017, 5:72-83.
4. Spitzer MH, Carmi Y, Reticker-Flynn NE, Kwek SS, Madhireddy D, Martins MM, Gherardini PF, Prestwood TR, Chabon J, Bendall SC et al.: Systemic immunity is required for effective cancer immunotherapy. Cell 2017.
5. Kayaga J, Souberbielle BE, Sheikh N, Morrow WJ, Scott-Taylor T, Vile R, Chong H, Dalgleish AG: Anti-tumour activity against B16- F10 melanoma with a GM-CSF secreting allogeneic tumour cell vaccine. Gene Therapy 1999, 6:1475-1481.
6. Hunder NN, Wallen H, Cao J, Hendricks DW, Reilly JZ, Rodmyre R, Jungbluth A, Gnjatic S, Thompson JA, Yee C: Treatment of metastatic melanoma with autologous CD4+ T cells against NY-ESO-1. N Engl J Med 2008, 358:2698-2703.
7. Kahn M, Sugawara H, McGowan P, Okuno K, Nagoya S, Hellstrom KE, Greenberg P: CD4+ T cell clones specific for the human p97 melanoma-associated antigen can eradicate pulmonary metastases from a murine tumor expressing the p97 antigen. J Immunol 1991, 146:3235-3241.
8. Xie Y, Akpinarli A, Maris C, Hipkiss EL, Lane M, Kwon EK, Muranski P, Restifo NP, Antony PA: Naive tumor-specific CD4(+) T cells differentiated in vivo eradicate established melanoma. J Exp Med 2010, 207:651-667.
9. Quezada SA, Simpson TR, Peggs KS, Merghoub T, Vider J, Fan X, Blasberg R, Yagita H, Muranski P, Antony PA et al.: Tumorreactive CD4(+) T cells develop cytotoxic activity and eradicate large established melanoma after transfer into lymphopenic hosts. J Exp Med 2010, 207:637-650.
10. Redondo M, Ruiz-Cabello F, Concha A, Hortas ML, Serrano A, Morell M, Garrido F: Differential expression of MHC class II genes in lung tumour cell lines. Eur J Immunogenet 1998, 25:385-391.
11. Ridge JP, Di RF, Matzinger P: A conditioned dendritic cell can be a temporal bridge between a CD4+ T-helper and a T-killer cell. Nature 1998, 393:474-478.
12. Bennett SR, Carbone FR, Karamalis F, Flavell RA, Miller JF, Heath WR: Help for cytotoxic-T-cell responses is mediated by CD40 signalling. Nature 1998, 393:478-480.
13. Smith CM, Wilson NS, Waithman J, Villadangos JA, Carbone FR, Heath WR, Belz GT: Cognate CD4(+) T cell licensing of dendritic cells in CD8(+) T cell immunity. Nat Immunol 2004, 5:1143-1148.
14. Castellino F, Huang AY, Altan-Bonnet G, Stoll S, Scheinecker C, Germain RN: Chemokines enhance immunity by guiding naive CD8+ T cells to sites of CD4+ T cell-dendritic cell interaction. Nature 2006, 440:890-895.
15. Kumamoto Y, Mattei LM, Sellers S, Payne GW, Iwasaki A: CD4+ T cells support cytotoxic T lymphocyte priming by controlling lymph node input. Proc Natl Acad Sci U S A 2011, 108:8749- 8754.

16. Ahrends T, Babala N, Xiao Y, Yagita H, van Eenennaam H, Borst J: CD27 agonism plus PD-1 blockade recapitulates CD4+ T-cell help in therapeutic anticancer vaccination. Cancer Res 2016, 76:2921-2931.
17. Hassan SB, Sorensen JF, Olsen BN, Pedersen AE: Anti-CD40- mediated cancer immunotherapy: an update of recent and ongoing clinical trials. Immunopharmacol Immunotoxicol 2014, 36:96-104.
18. Hung K, Hayashi R, Lafond-Walker A, Lowenstein C, Pardoll D, Levitsky H: The central role of CD4+ T-cells in the antitumor immune response. J Exp Med 1998, 188:2357-2368.
19. Matsui S, Ahlers JD, Vortmeyer AO, Terabe M, Tsukui T, Carbone DP, Liotta LA, Berzofsky JA: A model for CD8+ CTL tumor immunosurveillance and regulation of tumor escape by CD4 T cells through an effect on quality of CTL. J Immunol 1999, 163:184-193.
20. Schoenberger SP, Toes RE, van der Voort EI, Offringa R, Melief CJ: T-cell help for cytotoxic T lymphocytes is mediated by CD40– CD40L interactions. Nature 1998, 393:480-483.
21. Giuntoli RL 2nd, Lu J, Kobayashi H, Kennedy R, Celis E: Direct costimulation of tumor-reactive CTL by helper T cells potentiate their proliferation, survival, and effector function. Clin Cancer Res 2002, 8:922-931.
22. Dengel LT, Norrod AG, Gregory BL, Clancy-Thompson E, Burdick MD, Strieter RM, Slingluff CL Jr, Mullins DW: Interferons induce CXCR3-cognate chemokine production by human metastatic melanoma. J Immunother 2010, 33:965-974.
23. Peng W, Liu C, Xu C, Lou Y, Chen J, Yang Y, Yagita H, Overwijk WW, Lizee G, Radvanyi L et al.: PD-1 blockade enhances T-cell migration to tumors by elevating IFN-gamma inducible chemokines. Cancer Res 2012, 72:5209-5218.
24. Wang X, Michie SA, Xu B, Suzuki Y: Importance of IFN-gammamediated expression of endothelial VCAM-1 on recruitment of CD8+ T cells into the brain during chronic infection with Toxoplasma gondii. J Interferon Cytokine Res 2007, 27:329-338.
25. Clancy-Thompson E, King LK, Nunnley LD, Mullins IM, Slingluff CL Jr, Mullins DW: Peptide vaccination in Montanide adjuvant induces and GM-CSF increases CXCR3 and cutaneous lymphocyte antigen expression by tumor antigen-specific CD8 T cells. Cancer Immunol Res 2013, 1:332-339.
26. Bos R, Sherman LA: CD4+ T-cell help in the tumor milieu is required for recruitment and cytolytic function of CD8+ T lymphocytes. Cancer Res 2010, 70:8368-8377.
27. Nakanishi Y, Lu B, Gerard C, Iwasaki A: CD8(+) T lymphocyte mobilization to virus-infected tissue requires CD4(+) T-cell help. Nature 2009, 462:510-513.
28. Harlin H, Meng Y, Peterson AC, Zha Y, Tretiakova M, Slingluff C, McKee M, Gajewski TF: Chemokine expression in melanoma metastases associated with CD8+ T-cell recruitment. Cancer Res 2009, 69:3077-3085.
29. Dosset M, Vauchy C, Beziaud L, Adotevi O, Godet Y: Universal tumor-reactive helper peptides from telomerase as new tools for anticancer vaccination. Oncoimmunology 2013, 2:e23430.
30. Wong SB, Bos R, Sherman LA: Tumor-specific CD4+ T cells render the tumor environment permissive for infiltration by low-avidity CD8+ T cells. J Immunol 2008, 180:3122-3131.
31. Spranger S, Spaapen RM, Zha Y, Williams J, Meng Y, Ha TT, Gajewski TF: Up-regulation

of PD-L1, IDO, and T(regs) in the melanoma tumor microenvironment is driven by CD8(+) T cells. Sci Transl Med 2013, 5:200ra116.
32. Cho HI, Lee YR, Celis E: Interferon gamma limits the effectiveness of melanoma peptide vaccines. Blood 2011, 117:135-144.
33. Gao J, Aksoy BA, Dogrusoz U, Dresdner G, Gross B, Sumer SO, Sun Y, Jacobsen A, Sinha R, Larsson E et al.: Integrative analysis of complex cancer genomics and clinical profiles using the cBioPortal. Sci Signal 2013, 6:pl1.
34. Cerami E, Gao J, Dogrusoz U, Gross BE, Sumer SO, Aksoy BA, Jacobsen A, Byrne CJ, Heuer ML, Larsson E et al.: The cBio cancer genomics portal: an open platform for exploring multidimensional cancer genomics data. Cancer Discov 2012, 2:401-404.
35. Matsuzaki J, Tsuji T, Luescher I, Old LJ, Shrikant P, Gnjatic S, Odunsi K: Nonclassical antigen-processing pathways are required for MHC class II-restricted direct tumor recognition by NY-ESO-1-specific CD4(+) T cells. Cancer Immunol Res 2014, 2:341-350.
36. Matsuzaki J, Tsuji T, Luescher IF, Shiku H, Mineno J, Okamoto S, Old LJ, Shrikant P, Gnjatic S, Odunsi K: Direct tumor recognition by a human CD4(+) T-cell subset potently mediates tumor growth inhibition and orchestrates anti-tumor immune responses. Sci Rep 2015, 5:14896.
37. Kennedy R, Celis E: Multiple roles for CD4+ T cells in anti-tumor immune responses. Immunol Rev 2008, 222:129-144.
38. Tateyama M, Oyaizu N, McCloskey TW, Than S, Pahwa S: CD4 T lymphocytes are primed to express Fas ligand by CD4 crosslinking and to contribute to CD8 T-cell apoptosis via Fas/FasL death signaling pathway. Blood 2000, 96:195-202.
39. Qin Z, Blankenstein T: CD4+ T cell – mediated tumor rejection involves inhibition of angiogenesis that is dependent on IFN gamma receptor expression by nonhematopoietic cells. Immunity 2000, 12:677-686.
40. Zanetti M: Tapping CD4 T cells for cancer immunotherapy: the choice of personalized genomics. J Immunol 2015, 194:2049- 2056.
41. Buller RM, Holmes KL, Hugin A, Frederickson TN, Morse HC 3rd: Induction of cytotoxic T-cell responses in vivo in the absence of CD4 helper cells. Nature 1987, 328:77-79.
42. Wu Y, Liu Y: Viral induction of co-stimulatory activity on antigen-presenting cells bypasses the need for CD4+ T-cell help in CD8+ T-cell responses. Curr Biol 1994, 4:499-505.
43. Bevan MJ: Helping the CD8(+) T-cell response. Nat Rev Immunol 2004, 4:595-602.
44. Sun JC, Bevan MJ: Cutting edge: long-lived CD8 memory and protective immunity in the absence of CD40 expression on CD8 T cells. J Immunol 2004, 172:3385-3389.
45. Laidlaw BJ, Zhang N, Marshall HD, Staron MM, Guan T, Hu Y, Cauley LS, Craft J, Kaech SM: CD4+ T cell help guides formation of CD103+ lung-resident memory CD8+ T cells during influenza viral infection. Immunity 2014, 41:633-645.
46. Janssen EM, Droin NM, Lemmens EE, Pinkoski MJ, Bensinger SJ, Ehst BD, Griffith TS, Green DR, Schoenberger SP: CD4+ T-cell help controls CD8+ T-cell memory via TRAIL-mediated activation-induced cell death. Nature 2005, 434:88-93.
47. Datta J, Fracol M, McMillan MT, Berk E, Xu S, Goodman N, Lewis DA, DeMichele A, Czerniecki BJ: Association of depressed anti-HER2 T-helper type 1 response with recurrence in patients with completely treated HER2-positive breast cancer: role for

immune monitoring. JAMA Oncol 2016, 2:242-246.
48. Koski GK, Koldovsky U, Xu S, Mick R, Sharma A, Fitzpatrick E, Weinstein S, Nisenbaum H, Levine BL, Fox K et al.: A novel dendritic cell-based immunization approach for the induction of durable Th1-polarized anti-HER-2/neu responses in women with early breast cancer. J Immunother 2012, 35:54-65.
49. Sharma A, Koldovsky U, Xu S, Mick R, Roses R, Fitzpatrick E, Weinstein S, Nisenbaum H, Levine BL, Fox K et al.: HER-2 pulsed dendritic cell vaccine can eliminate HER-2 expression and impact ductal carcinoma in situ. Cancer 2012, 118:4354-4362.
50. Lowenfeld L, Mick R, Datta J, Xu S, Fitzpatrick E, Fisher CS, Fox KR, DeMichele A, Zhang P, Weinstein S et al.: Dendritic cell vaccination enhances immune responses and induces regression of HER2pos DCIS independent of route: results of randomized selection design trial. Clin Cancer Res 2016.
51. Staff C, Mozaffari F, Frodin JE, Mellstedt H, Liljefors M: Telomerase (GV1001) vaccination together with gemcitabine in advanced pancreatic cancer patients. Int J Oncol 2014, 45:1293-1303.
52. Hansen GL, Gaudernack G, Brunsvig PF, Cvancarova M, Kyte JA: Immunological factors influencing clinical outcome in lung cancer patients after telomerase peptide vaccination. Cancer Immunol Immunother 2015, 64:1609-1621.
53. Fenoglio D, Traverso P, Parodi A, Tomasello L, Negrini S, Kalli F, Battaglia F, Ferrera F, Sciallero S, Murdaca G et al.: A multipeptide, dual-adjuvant telomerase vaccine (GX301) is highly immunogenic in patients with prostate and renal cancer. Cancer Immunol Immunother 2013, 62:1041-1052.
54. Dosset M, Godet Y, Vauchy C, Beziaud L, Lone YC, Sedlik C, Liard C, Levionnois E, Clerc B, Sandoval F et al.: Universal cancer peptide-based therapeutic vaccine breaks tolerance against telomerase and eradicates established tumor. Clin Cancer Res 2012, 18:6284-6295.
55. Middleton G, Silcocks P, Cox T, Valle J, Wadsley J, Propper D, Coxon F, Ross P, Madhusudan S, Roques T et al.: Gemcitabine and capecitabine with or without telomerase peptide vaccine GV1001 in patients with locally advanced or metastatic pancreatic cancer (TeloVac): an open-label, randomised, phase 3 trial. Lancet Oncol 2014, 15:829-840.
56. Aarntzen EH, De Vries IJ, Lesterhuis WJ, Schuurhuis D, Jacobs JF, Bol K, Schreibelt G, Mus R, De Wilt JH, Haanen JB et al.: Targeting CD4(+) T-helper cells improves the induction of antitumor responses in dendritic cell-based vaccination. Cancer Res 2013, 73:19-29.
57. Slingluff CL Jr, Petroni GR, Olson W, Czarkowski AR, Grosh WW, Smolkin M, Chianese-Bullock KA, Neese PY, Deacon DH, Nail CJ et al.: Helper T cell responses and clinical activity of a melanoma vaccine with multiple peptides from MAGE and melanocytic differentiation antigens. J Clin Oncol 2008, 26:4973-4980.
58. Slingluff CL Jr, Petroni GR, Chianese-Bullock KA, Smolkin ME, Ross MI, Haas NB, von Mehren M, Grosh WW: Randomized multicenter trial of the effects of melanoma-associated helper peptides and cyclophosphamide on the immunogenicity of a multipeptide melanoma vaccine. J Clin Oncol 2011, 29:2924- 2932.
59. Slingluff CL Jr, Lee S, Zhao F, Chianese-Bullock KA, Olson WC, Butterfield LH, Whiteside TL, Leming PD, Kirkwood JM: A randomized phase II trial of multiepitope vaccination with melanoma peptides for cytotoxic T cells and helper T cells for

patients with metastatic melanoma (E1602). Clin Cancer Res 2013, 19:4228-4238.
60. Dillon PM, Olson WC, Czarkowski A, Petroni GR, Smolkin M, Grosh WW, Chianese-Bullock KA, Deacon DH, Slingluff CL Jr: A melanoma helper peptide vaccine increases Th1 cytokine production by leukocytes in peripheral blood and immunized lymph nodes. J Immunother Cancer 2014, 2:23.
61. Hu Y, Kim H, Blackwell CM, Slingluff CL Jr: Long-term outcomes of helper peptide vaccination for metastatic melanoma. Ann Surg 2015, 262:456-464 (discussion 462-454).
62. Hu Y, Petroni GR, Olson WC, Czarkowski A, Smolkin ME, Grosh WW, Chianese-Bullock KA, Slingluff CL Jr: Immunologic hierarchy, class II MHC promiscuity, and epitope spreading of a melanoma helper peptide vaccine. Cancer Immunol Immunother 2014, 63:779-786.
63. Reed CM, Cresce ND, Mauldin IS, Slingluff CL Jr, Olson WC: Vaccination with melanoma helper peptides induces antibody responses associated with improved overall survival. Clin Cancer Res 2015, 21:3879-3887.
64. Kenter GG, Welters MJ, Valentijn AR, Lowik MJ, B-vdM DM, Vloon AP, Essahsah F, Fathers LM, Offringa R, Drijfhout JW et al.: Vaccination against HPV-16 oncoproteins for vulvar intraepithelial neoplasia. N Engl J Med 2009, 361:1838-1847.
65. Tsuji T, Sabbatini P, Jungbluth AA, Ritter E, Pan L, Ritter G, Ferran L, Spriggs D, Salazar AM, Gnjatic S: Effect of Montanide and poly-ICLC adjuvant on human self/tumor antigen-specific CD4+ T cells in phase I overlapping long peptide vaccine trial. Cancer Immunol Res 2013, 1:340-350.
66. Cohen CJ, Gartner JJ, Horovitz-Fried M, Shamalov K, TrebskaMcGowan K, Bliskovsky VV, Parkhurst MR, Ankri C, Prickett TD, Crystal JS et al.: Isolation of neoantigen-specific T cells from tumor and peripheral lymphocytes. J Clin Invest 2015, 125:3981-3991.
67. Carreno BM, Magrini V, Becker-Hapak M, Kaabinejadian S, Hundal J, Petti AA, Ly A, Lie WR, Hildebrand WH, Mardis ER et al.: Cancer immunotherapy. A dendritic cell vaccine increases the breadth and diversity of melanoma neoantigen-specific T cells. Science 2015, 348:803-808.
68. Hailemichael Y, Dai Z, Jaffarzad N, Ye Y, Medina MA, Huang XF, Dorta-Estremera SM, Greeley NR, Nitti G, Peng W et al.: Persistent antigen at vaccination sites induces tumor-specific CD8(+) T cell sequestration, dysfunction and deletion. Nat Med 2013, 19:465-472.
69. Cho HI, Celis E: Optimized peptide vaccines eliciting extensive CD8 T-cell responses with therapeutic antitumor effects. Cancer Res 2009, 69:9012-9019.
70. Reinhardt RL, Bullard DC, Weaver CT, Jenkins MK: Preferential accumulation of antigen-specific effector CD4 T cells at an antigen injection site involves CD62E-dependent migration but not local proliferation. J Exp Med 2003, 197:751-762.
71. Diefenbach CS, Gnjatic S, Sabbatini P, Aghajanian C, Hensley ML, Spriggs DR, Iasonos A, Lee H, Dupont B, Pezzulli S et al.: Safety and immunogenicity study of NY-ESO-1b peptide and montanide ISA-51 vaccination of patients with epithelial ovarian cancer in high-risk first remission. Clin Cancer Res 2008, 14:2740-2748.

Chapter 3

A multipeptide vaccine plus toll-like receptor agonists LPS or polyICLC in combination with incomplete Freund's adjuvant in melanoma patients

Marit M. Melssen, Gina R. Petroni, Kimberly A. Chianese-Bullock, Nolan A. Wages, William W. Grosh, Nikole Varhegyi, Mark E. Smolkin, Kelly T. Smith, Nadejda V. Galeassi, Donna H. Deacon, Elizabeth M. Gaughan, Craig L. Slingluff Jr

J Immunother Cancer. 2019 Jun 27;7(1):163.

ABSTRACT

Background

Cancer vaccines require adjuvants to induce effective immune responses; however, there is no consensus on optimal adjuvants. We hypothesized that toll-like receptor (TLR)3 agonist polyICLC or TLR4 agonist lipopolysaccharide (LPS), combined with CD4 T cell activation, would support strong and durable CD8+ T cell responses, whereas addition of an incomplete Freund's adjuvant (IFA) would reduce magnitude and persistence of immune responses.

Patients and methods: Participants with resected stage IIB-IV melanoma received a vaccine comprised of 12 melanoma peptides restricted by Class I MHC (12MP), plus a tetanus helper peptide (Tet). Participants were randomly assigned 2:1 to cohort 1 (LPS dose-escalation) or cohort 2 (polyICLC). Each cohort included 3 subgroups (a-c), receiving 12MP + Tet + TLR agonist without IFA (0), or with IFA in vaccine one (V1), or all six vaccines (V6). Toxicities were recorded (CTCAE v4). T cell responses were measured with IFNγ ELIspot assay ex vivo or after one in vitro stimulation (IVS).

Results

Fifty-three eligible patients were enrolled, of which fifty-one were treated. Treatment-related dose-limiting toxicities (DLTs) were observed in 0/33 patients in cohort 1 and in 2/18 patients in cohort 2 (11%). CD8 T cell responses to 12MP were detected ex vivo in cohort 1 (42%) and in cohort 2 (56%) and in 18, 50, and 72% for subgroups V0, V1, and V6, respectively. T cell responses to melanoma peptides were more durable and of highest magnitude for IFA V6.

Conclusions

LPS and polyICLC are safe and effective vaccine adjuvants when combined with IFA. Contrary to the central hypothesis, IFA enhanced T cell responses to peptide vaccines when added to TLR agonists. Future studies will aim to understand mechanisms underlying the favorable effects with IFA.

Trial registration

The clinical trial Mel58 was performed with IRB (#15781) and FDA approval and is registered with Clinicaltrials.gov on April 25, 2012 (NCT01585350). Patients provided written informed consent to participate. Enrollment started on June 24, 2012.

INTRODUCTION

Resistance to checkpoint blockade immunotherapy is commonly attributed to a lack of pre-existing T cell responses to cancer antigens. Thus, there is compelling need for methods to induce antitumor immunity. Cancer vaccines targeting either mutated neo-antigens or shared tumor antigens may accomplish this; however, a critical limitation of cancer vaccine technology is lack of consensus on optimal vaccine adjuvants, which are required to induce functional immune responses. Clinical trials to test adjuvants are more feasible with shared antigen vaccines than with mutated neo-antigens because neo-antigen vaccine composition varies for each patient, whereas the composition of a shared antigen vaccine is consistent across the study population. The most common adjuvant for peptide vaccines in melanoma has been an incomplete Freund's adjuvant (IFA). Peptide vaccines incorporating IFA have induced circulating T cell responses [1–3], but some are weak and transient [4]. Recent studies in mice have shown negative effects of IFA as a vaccine adjuvant [5, 6] and have suggested instead that an optimal adjuvant for short peptide vaccines is a TLR agonist plus an agonistic CD40 antibody, which induced strong and durable T cell responses and tumor control [5]. A goal of the present trial was to evaluate a similar approach in patients with melanoma. A multipeptide vaccine (12MP) has previously been found to be both safe and immunogenic [7, 8]. When this trial was initiated, agonistic CD40 antibodies were not available for clinical use. Instead, we used an alternative approach to support licensing of antigen presenting cells (APC) through CD40. Activated CD4 T cells upregulate CD40L; so, we included a peptide from tetanus toxoid known to activate CD4 T cells at the vaccine site and draining node [9–11]. We have shown that a modified form of the p2 peptide of tetanus toxoid residues 830–844 (AQYIKANSKFIGITEL, Tet) induces strong CD4 T cell responses in patients [8, 12]; so, inclusion of this peptide may offer an alternative to CD40 antibodies. Thus, the present study was designed to evaluate the safety and immunogenicity of vaccinating with a mixture of 12 short melanoma peptides (12MP) plus a tetanus helper peptide, combined with TLR agonists. To assess whether IFA interferes with vaccine activity, the study also included treatment arms with IFA. The central hypotheses were that the TLR agonists may be safe and effective vaccine adjuvants and that decreasing use of IFA may further enhance the magnitude and persistence of the immune responses. Specific goals were: a) to determine the safety of intradermal and subcutaneous injection of the TLR4 agonist lipopolysaccharide (LPS) as a vaccine adjuvant with a multipeptide vaccine, b) to obtain preliminary data on whether administration of a multipeptide vaccine plus each of 2 TLR agonists is immunogenic with or without IFA, c) to obtain preliminary data on whether addition of either of two TLR agonists improves the persistence of circulating CD8 T cell responses to vaccination with a multipeptide vaccine, and d) to determine the local and systemic toxicities of administration of a multipeptide vaccine with each of 2 TLR agonists, and with or without IFA.

MATERIALS AND METHODS

Patient eligibility

Patients at least 18 years of age, expressing HLA-A1, −A2, −A3, −A11 or -A31 were eligible if they had biopsy-proven Stage IIB-IV melanoma rendered clinically free of disease by surgery, other therapy or spontaneous remission. Patients with Stage III-IV melanoma with definite or equivocal findings of persistent metastatic disease could be eligible if they did not meet RECIST criteria for measurable disease. Also required were ECOG performance status (PS) 0–1, and adequate organ function.

Vaccine components and treatment regimen

All participants were vaccinated with MELITAC 12.1 (100mcg of each of 12 Class I MHC restricted melanoma peptides (12MP) [7] and 200mcg of a tetanus helper peptide [12] (Additional file 1: Table S1)). Vaccines were administered with either of two TLR agonists and with or without IFA (Fig. 1a). The IFA used was Montanide ISA-51VG adjuvant (Seppic, Inc., Puteaux, France). PolyICLC (lot PJ2515-1-10, 2.0 mg/ml dry weight) was provided by the Cancer Research Institute/Ludwig Institute for Cancer Research (New York), who purchased it from Oncovir (Washington, DC). LPS was provided by Dr. Anthony Suffredini (Drug Master File Number BB-MF7294) at the National Cancer Institute (NCI) and was vialed and tested by Cambrex BioScience (Walkersville, MD) under oversight of the Biopharmaceutical Development Program, SAICFrederick, Inc., NCI-Frederick, Frederick, MD. Each vial contained lyophilized solid representing 10,000 endotoxin units (EU) of E. coli O:113 Reference Endotoxin Lot CC-RE-LOT 3 (1mcg endotoxin). Upon reconstitution in 5 mL water, it contained 2000 EU/mL in 1% Lactose, 0.1% PEG-6000. Regimens were administered half-subcutaneously and half-intradermally in one skin location that is rotated to different extremity sites on days 1, 8, 15, 36, 57 and 78.

Study design

This was an early phase trial designed to determine the maximum tolerated dose combination (MTDC) of LPS and IFA from among twelve possible combinations in cohort 1 and the MTDC of polyICLC and IFA from among three possible combinations in cohort 2, and to obtain preliminary data on immune response for all the combinations under study. Eligible patients were randomly assigned 2:1 to cohort 1 or cohort 2 (Fig. 1). The 12 combinations in cohort 1 included 4 dose levels of endotoxin (25, 100, 400, 1600EU) administered in three vaccine regimens (12MP + Tet + LPS) and i) without IFA (V0), ii) plus IFA in the first vaccine only (V1), or iii) plus IFA in all six vaccines (V6); (Fig. 1b, Additional file 1: Table S2). The 3 combinations in cohort 2 included 1 dose level of polyICLC (1 mg) administered similarly for each of the three adjuvant regimens and, V0 or V1 or V6; (Fig. 1b, Additional file 1: Table S2). Toxicities were recorded (CTCAE v4). Blood was collected weeks 0, 1, 4, 5, 8, 13, and 26 (Fig. 1a). One week after

the first vaccine, a vaccine site-draining lymph node was harvested under local anesthesia, using techniques reported [13], and 4 mm punch biopsies of that vaccine site were obtained (Fig. 1a). In cohort 1, dose escalation was conducted using a two-stage method for dose-finding for combinations of agents [14]. The first stage was designed such that participants were treated in groups of size 2 until a participant experienced a dose-limiting toxicity (DLT), after which a model-based allocation (stage 2) began. The escalation plan for the first stage was based on grouping dose combinations into "zones," which are shown in Fig. 1b and detailed in Additional file 2: Supplemental Text. With this dose escalation design, participants were accrued and assigned to other open combinations within a zone, but escalation did not occur outside the zone until a minimum 3-week follow-up period was observed for the first 2 participants accrued to a combination. The second stage modeling strategy using the continual reassessment model (CRM) [15] was planned but not realized since no participants in cohort 1 experienced a DLT. Additional design details are provided in Additional file 1: Supplemental Text. For cohort 2, with only 3 possible combinations of interest, the goal was to accrue 3 patients per combination in increasing magnitude conditional on 1 or fewer DLTs being observed and then to randomly accrue up to 3 additional patients per combination (Fig. 1b). A DLT was defined as any unexpected adverse event that was possibly, probably, or definitely related to treatment and (1) ≥ Grade 1 selected ocular adverse events, (2) ≥ Grade 2 allergic reactions, (3) ≥ Grade 3 nonhematologic/non-metabolic toxicities, and (4) ≥ Grade 3 hematologic/metabolic toxicities. Grade 2 nausea and Grade 3 fatigue lasting ≤3 days after vaccination were expected toxicities, and injection site ulceration was expected in a subset of patients but vaccine site ulceration of 2 cm diameter or greater was considered a DLT.

Expansion

To assess the impact of including IFA (or not) on the immunologic parameters, the goal was to accrue up to 6 patients at the highest levels of LPS considered safe for each level of IFA. The choice of 6 patients per final combination was chosen to provide improved estimates of variability

ELIspot assays

T cell responses were measured with IFNγ ELIspot either directly ex vivo, after cryopreservation (direct) or after in vitro sensitization (IVS). Responses to the 12 class I MHC-restricted melanoma peptides are mediated by CD8 T cells specifically [16–26], and responses to the tetanus peptide are mediated by CD4 T cells [12, 27]. Therefore, total PBMC were used for ELIspot assays, and responses per CD8 and CD4 counts were calculated based on their proportion of total PBMC as determined by flow cytometry as previously reported [8, 28, 29]. Methods for the IVS ELIspot assay have been reported [28]. For direct ELIspot assays, 200,000 PBMC were plated per well, and pulsed with synthetic peptide (10mcg/ml), in quadruplicate. Controls included irrelevant peptides, a mixture of viral peptides

(CEF peptide pool), PMA/ionomycin and PHA. Evaluation of T-cell responses was based on the following definitions: Nvax = number T-cells responding to vaccine peptide; Nneg = number T-cells responding to maximum negative control; Rvax = Nvax/Nneg. For evaluations of PBMC, a patient was considered to have a T-cell response to vaccination (binary yes/no), by direct ELIspot assay only if all the following criteria were met: (1) Nvax exceeded Nneg by at least 20/100,000 CD4 or CD8 cells (0.02%), where CD8 and CD4 counts were based on flow cytometry of PBMC. (2) Rvax ≥ 2, (3) (Nvax–1SD) ≥ (Nneg + 1SD), and (4) Rvax after vaccination ≥2xRvax pre-vaccine, as described in our prior analyses [8, 28]. The same criteria applied for IVS ELIspot assays except that the threshold for criterion (1) was higher at 30/100,000 CD8 cells. Fold-increases less than one were set to one to indicate no response and to prevent overinflating adjusted fold-increases. Continuous measures of immune response denoted as fold-increase must satisfy conditions (1)–(3) and were defined as the amount of Rvax. Interassay coefficients of variation (CVs) were calculated for the response of 2 normal donors to the CEF peptide pool: for the high responder, mean number of spots per 100,000 cells was 250, and CV was 30%, and for the low responder, mean was 40 and CV was 44%.

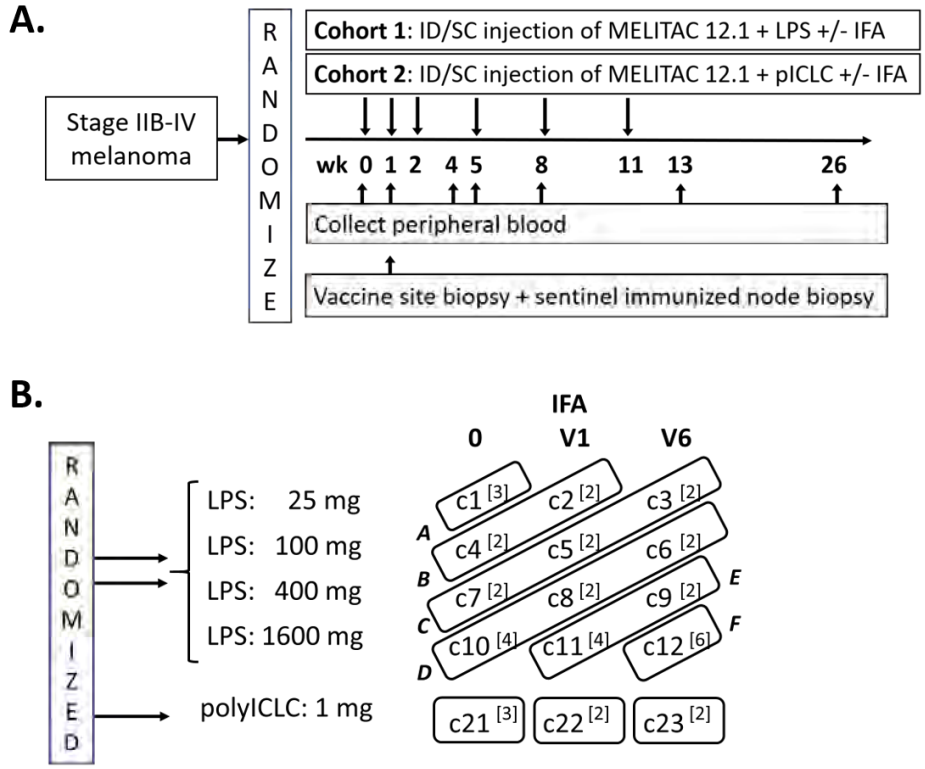

Figure 1. Clinical trial design. The schema for the clinical trial is shown in a. The zones for dose escalation of LPS in cohort 1 (A-F) are shown in b. The study combinations are numbered c1 - c12 for cohort 1 and c21-c23 for cohort 2 as shown.

Statistical analysis of immunologic analyses

Primary immunologic analyses were based upon eligible patients, and maximal immune response was based upon responses in the blood through week 26. For hypothesis testing, patients who discontinued protocol therapy prior to collection of all blood samples for allergic reactions or adverse events, disease progression, or noncompliance were considered immune response failures if no response was observed in evaluable samples. Immune response was a binary indicator of whether or not the criteria listed above were met, and immune response rates were calculated as the proportion of participants with an immune response. Point estimates and 90% confidence intervals were calculated for all summary parameters. Permutation tests [30] were used to assess differences in number of T-cells responding to vaccine peptide adjusting for negative control (i.e., Nvax-Nneg) over the first 12 weeks across groups defined by combinations of LPS dose, inclusion of IFA and inclusion of polyICLC. P-values were based upon 2000 randomly generated permutations and a p-value cutoff of 10% was used to indicate statistically significant results. Negative binomial regression was used to assess count data and contrasts were used to test specific hypotheses with p-values computed from the likelihood ratio chi-square test statistic (LR).

RESULTS

Clinical characteristics

Total enrollment was 53 participants; however, 2 participants did not receive study treatment. Thus, demographic, safety, and immunologic summary data are reported for 51 patients who were enrolled and treated. These included 33 males (65%) and 18 females (35%). Most patients had ECOG PS of 0 (90%) and stage III disease at registration (78%). Additional details are provided in Additional file 1: Table S3.

Toxicities and adverse events

Treatment related adverse events (AE) were limited to grades 1–3, with only one grade 3 (Additional file 1: Table S4). Two participants experienced DLTs, both in cohort 2 (polyICLC). One treated on the V1 sub-arm had grade 3 skin ulceration and was taken off study after 3 vaccines. One on the V6 sub-arm experienced several grade 2 toxicities, none of which individually met predefined criteria for a DLT, but which in aggregate were felt to be dose-limiting. This patient was taken off treatment after 4 vaccines. Overall, no study combinations were estimated to be too toxic for patient accrual.

CD8 T cell response to 12MP

T cell responses to 12 peptide epitopes were evaluated both against the pool of 12 peptides (12MP pool), as well as each peptide individually, using IFNγ ELIspot assays. As described in the methods section, pre-existing immune responses

were not considered responses to vaccination: in the uncommon cases with pre-existing immune responses, response to vaccination required at least a 2-fold increase over pre-existing response. The primary comparisons among study groups were made for weeks 0–12, as these data were consistently available (Fig. 2a). Responses to 12MP were detected ex vivo for 47% of patients overall, with the magnitude exceeding 600 spots/105 CD8 T cells for some patients (Fig. 2a). Responses per study cohort and sub-arm are summarized in Additional file 1: Table S5 and per patient in Additional file 1: Table S6. Ex vivo T cell responses to 12MP were detected in 14 of 33 patients (42%) in cohort 1 (LPS) and in 10 of 18 patients (56%) for cohort 2 (polyICLC). Overall, for study arms with no IFA; IFA V1, and IFA V6, CD8 T cell responses to 12MP were detected ex vivo in 18, 50, and 72% of patients, respectively. Similarly, the sum of CD8 T cell responses to each of the 12 peptides was assessed after IVS, and these plots are shown in Fig. 2b. Patterns of immune response over time were compared across study groups by modeling the data in PBMC across all time points through week 12. This method is a statistically robust assessment of differences in response patterns between groups over time (Table 1). In cohort 2 (polyICLC), direct ELIspot responses to 12MP were higher if IFA was given for all vaccines compared to no IFA (V6 vs V0, $p = 0.036$). This was evident also for cohort 1 ($p = 0.065$) and for analysis across both cohorts ($p = 0.036$). The CD8 response to 12MP also was higher with polyICLC than with the highest dose of LPS, among patients receiving IFA with all 6 vaccines ($p = 0.031$). Similarly, the ex vivo and IVS CD8 responses to the sum of individual peptides in 12MP were higher for polyICLC than for LPS1600 and for V6 than V0 in multiple comparisons (Table 1). Thus, for both direct and IVS ELIspot assessments, polyICLC was a more effective adjuvant than LPS, and inclusion of IFA in all vaccines significantly enhanced CD8 T cell response rates to defined melanoma antigens. We also evaluated immune responses in the sentinel immunized nodes (SINs), but the SINs were harvested early (week 1), and responses were not detected ex vivo. However, among 34 patients evaluated for immune response in the SIN after in vitro stimulation, 11 (32%) had an immune response. These included 18% (4/18) after vaccines with LPS, and 58% (7/12) after vaccines with pICLC. Immune responses in the SIN were observed in 27% (3/11) without IFA, and in 35% (8/23) with IFA (V1 or V6). These SIN responses are shown for all patients in Additional file 1: Table S6. A pre-existing T cell response to 12MP was detected ex vivo in only 1 patient (#53), who did not develop a vaccine-induced T cell response. In IVS ELIspot assays, 3 (6%) had small pre-existing responses (patients 1, 14, 28), of whom 2 developed vaccine induced responses to 12MP ex vivo, and 2 had responses to 12MP after in vitro stimulation. As specified in the methods, a vaccine-induced T cell response was reported only if there was additional response of at least 2x any pre-existing response. For the two patients in cohort 2 who came off early for DLTs, immune response data are shown in Additional file 1: Figure S1, where T cell responses to multiple peptides were evident in both.

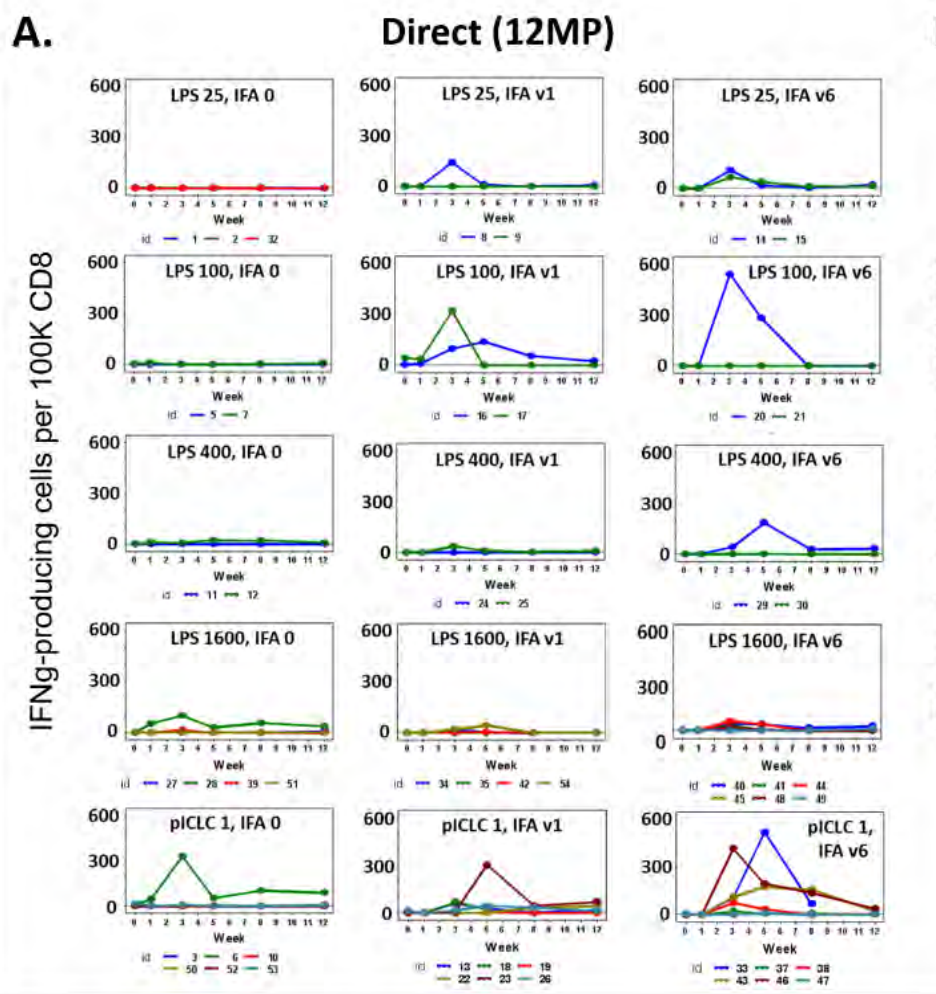
A.
Direct (12MP)
IFNg-producing cells per 100K CD8
LPS 25, IFA 0
LPS 25, IFA v1
LPS 25, IFA v6
LPS 100, IFA 0
LPS 100, IFA v1
LPS 100, IFA v6
LPS 400, IFA 0
LPS 400, IFA v1
LPS 400, IFA v6
LPS 1600, IFA 0
LPS 1600, IFA v1
LPS 1600, IFA v6
pICLC 1, IFA 0
pICLC 1, IFA v1
pICLC 1, IFA v6
600
300
0
Week
Weeks 0 - 12

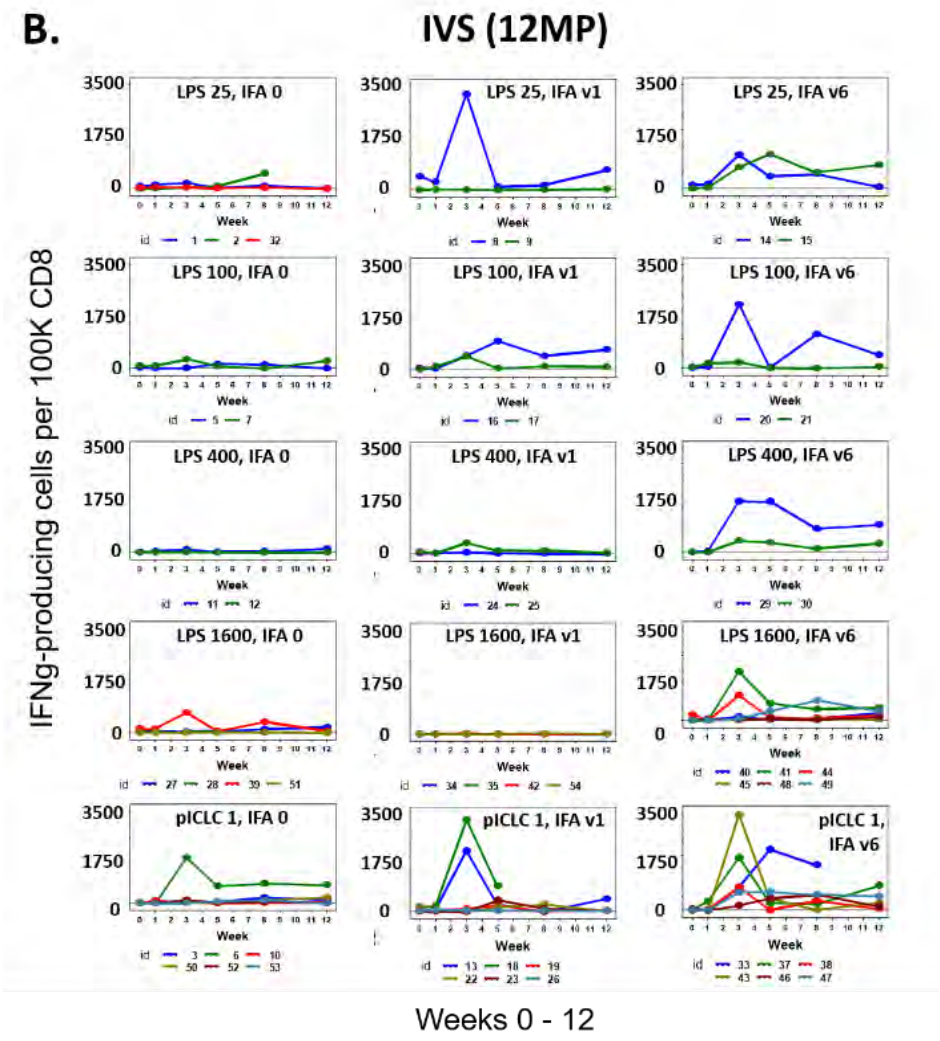

Figure 2. T cell responses over time (weeks 0–12). CD8 T cell responses to 12MP are shown for each patient from direct ELIspot assays (a), and from IVS ELIspot assays (b). Direct assay data represent response to pooled 12MP; IVS ELIspot data represent sum of responses to each of the 12 individual peptides. Response magnitude is shown as the number of IFNγ-secreting cells, less negative controls, per 100,000 CD8 cells. Values are shown as zero if they did not meet criteria for positivity.

Table 1. MEL58 ELIspot data comparisons across time (weeks 0-12)

Comparison table				Permutation Test p-value (based upon 2000 permutations)		
	IFA 0	IFA V1	IFA V6	**12MelPool Direct**	**Sum Individual Direct**	**Sum Individual Stimulated**
LPS 25	C1	C2	C3			
LPS 100	C4	C5	C6			
LPS 400	C7	C8	C9			
LPS 1600	C10	C11	C12			
PolyICLC	C21	C22	C23			
LPS dose comparison						
LPS100 vs LPS25, Average across all IFA doses (C4 vs C1, C5 vs C2, C6 vs C3)				0.150	0.243	0.833
LPS400 vs LPS25, Average across all IFA doses (C7 vs C1, C8 vs C2, C9 vs C3)				0.693	0.194	0.615
LPS1600 vs LPS25, Average across all IFA doses (C10 vs C1, C11 vs C2, C12 vs C3)				0.749	0.362	0.336
PolyICLC vs LPS comparison						
PolyICLC vs LPS1600, Average across all IFA doses (C21 vs C10, C22 vs C11, C23 vs C12)				0.101	**0.035**	**0.050**
PolyICLC vs LPS1600, IFA=0 (C21 vs C10)				0.755	0.696	0.766
PolyICLC vs LPS1600, IFA=V1 (C22 vs C11)				0.545	0.807	0.216
PolyICLC vs LPS1600, IFA=V6 (C23 vs C12)				**0.031**	0.710	**0.089**
IFA V0 – V6 comparison						
IFA V6 vs IFA 0, Average All (C3 vs C1, C6 vs C4, C9 vs C7, C12 vs C10, C23 vs C21)				**0.016**	**0.078**	**0.005**
IFA V6 vs IFA 0, Average across LPS doses (C3 vs C1, C6 vs C4, C9 vs C7, C12 vs C10)				**0.065**	0.324	**0.017**
IFAV6 vs IFA 0, PolyICLC (C23 vs C21)				**0.036**	**0.009**	**0.039**

Bolded numbers represent *P*-values less than 0.1

CD4+ T cell responses to tetanus peptide

T cell responses to the tetanus helper peptide were assessed in direct ELIspot assays. Overall, the permutation tests found no significant differences in response patterns to tetanus peptide among cohorts or study arms. Individual plots of these data for all patients are shown in Additional file 1: Figure S2. T cell responses to the tetanus peptide for any time point were observed in 58% (90% CI:[42, 72]) of patients on cohort 1 and 72% (90% CI:[50, 88]) on cohort 2, and in 24% (90% CI:[8, 46]), 75% (90% CI:[52, 91]), and 89% (90% CI:[69, 98]) of patients in subgroups V0, V1, and V6, respectively (Additional file 1: Table S5).

Magnitude and breadth of CD8 T cell responses

In addition to modeling the immune response across the study population, the fractions of patients with CD8 T cell responses were assessed directly. Immune response rates to 12MP increased with increasing IFA use, both in direct and IVS ELIspot assays (Fig. 3a, b). Similar findings were evident with direct ELIspot based on the sum of responses to the individual peptides (Additional file 1: Table S5), with higher responses for cohort 2 than cohort 1. When IFA was included, the maximum number of IFNγ-secreting cells was higher in direct (Fig. 3c) and in IVS ELIspot assays (Fig. 3d). Similarly, the fold increase in the T cell responses to 12MP was also higher with inclusion of IFA (data not shown). Immune responses were detected to a broader range of peptides when IFA was included in ex vivo assays (Fig. 3e) or in IVS assays (Fig. 3f).

Persistence and durability of the CD8 immune responses

Durability of CD8 T cell responses was assessed by number of time points with positive responses to 12MP after start of vaccine treatment (weeks 1 or later) and by the percent of participants evaluated who had T cell responses at week 26 (wk26). Median numbers of time points with ex vivo responses to 12MP, for V0, V1, V6, respectively, were 0, 0, and 1.5 for LPS and 0, 1.5, and 2.5 for polyICLC. For IVS assays, those values were 0, 0.5, and 4, for LPS, and 1.5, 2, and 4 for polyICLC (Fig. 4a, b), representing significant increases overall from V0 to V6 (LR $p = 0.022$ and $p < 0.001$ for ex vivo and IVS, respectively) but not for V0 to V1 (LR $p = 0.4$ and $p = 0.3$ for ex vivo and IVS, respectively). Persistence of T cell responses in PBMC at wk26 was evaluable by ex vivo ELIspot (n = 30) and in IVS ELIspot (n = 40) assays. At this late time point, CD8 T cell responses to 12MP were detected ex vivo in 13%, and after IVS in 48%. Ex vivo responses at wk26 were detected only in cohort 2 patients who had IFA included (V1 and V6) (Fig. 4c). After IVS, responses were detected wk26 in 14, 42, and 86% of patients in V0, V1, and V6 subgroups, respectively (n = 14, 12, 14, respectively) (Fig. 4d). The increase for V6 versus V1 versus V0 overall was significant for IVS assay results only (LR $p < 0.001$) Thus, persistent responses were significantly enhanced with inclusion of IFA in all 6 vaccines, compared to use of TLR agonists alone, and were similar with either TLR agonist, though they may be slightly more common with polyICLC than with LPS.

Immune response rates summarized by HLA type

Patients expressing HLA-A1, A2, A3, or other A3 supertype alleles (A11, A31), were represented in each cohort, and CD8+ T cell responses were identified among patients expressing each HLA subtype (Additional file 1: Tables S6 and S7). There were differences in immunogenicity among the individual peptides, as previously observed [7, 8, 28]. By IVS ELIspot, the highest response rates were to the HLA-A2 peptide IMD (gp100209–217 (2M)) (68%), HLA-A1 peptide DAE (tyrosinase240-251S) (59%), HLA-A3 peptide SLF (MAGE-A196–104) (43%), and the HLA-A2 peptide GLY (MAGE-A10254–262) (52%) (Additional file 1: Table

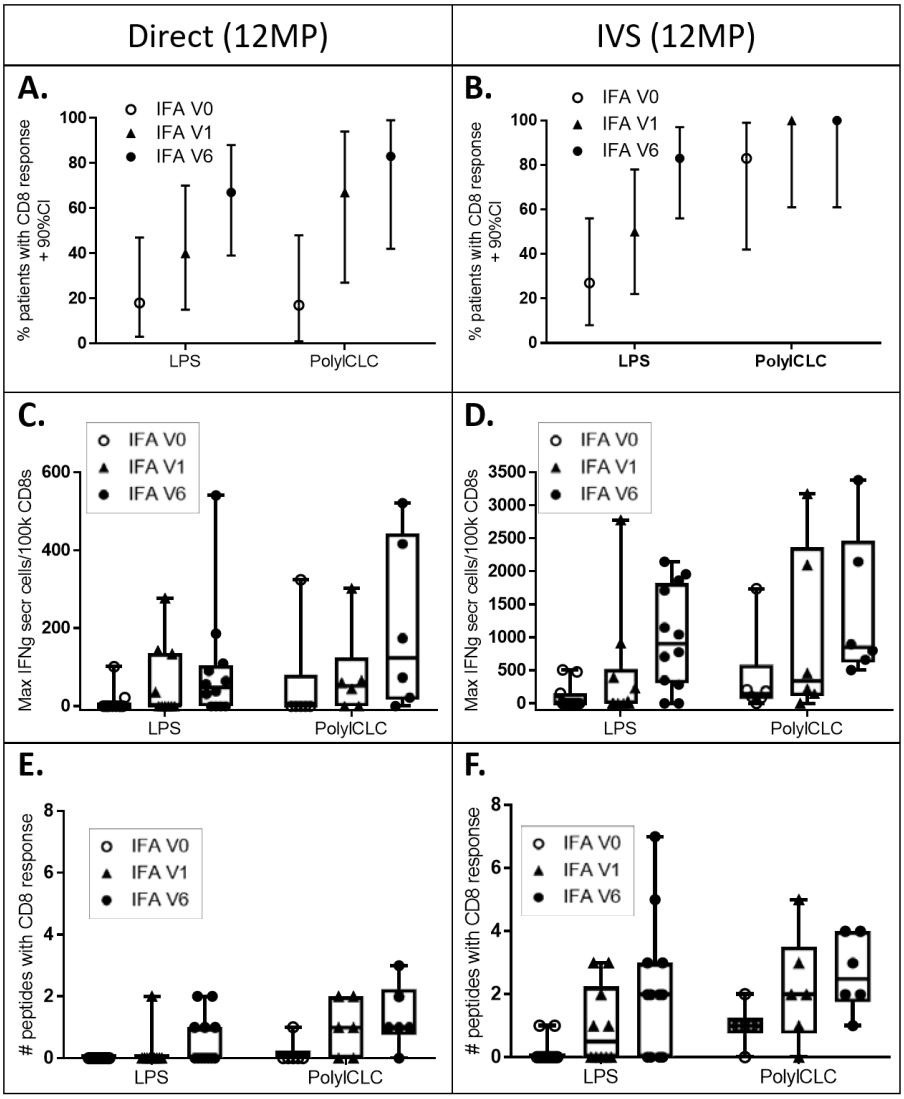

Figure 3. Frequency and Magnitude of T cell responses to 12MP by ELIspot assay ex vivo (a, c, e), and after IVS (b, d, f). The proportion and 90% confidence interval (CI) of patients with a response to 12MP pool are shown in panels A and B, for each cohort and subgroup. The magnitude of these responses (maximum number of spots per 1×105 CD8 T cells) is shown in (c) and (d), where each symbol represents the maximum response for a patient. If the values did not meet criteria for a response, they are shown as zero. Boxplots represent 25th to 75th percentiles, with tails showing the full range, except outliers. The number of peptides to which a response was detected is shown for each patient with a response ex vivo (e) and after IVS (f).

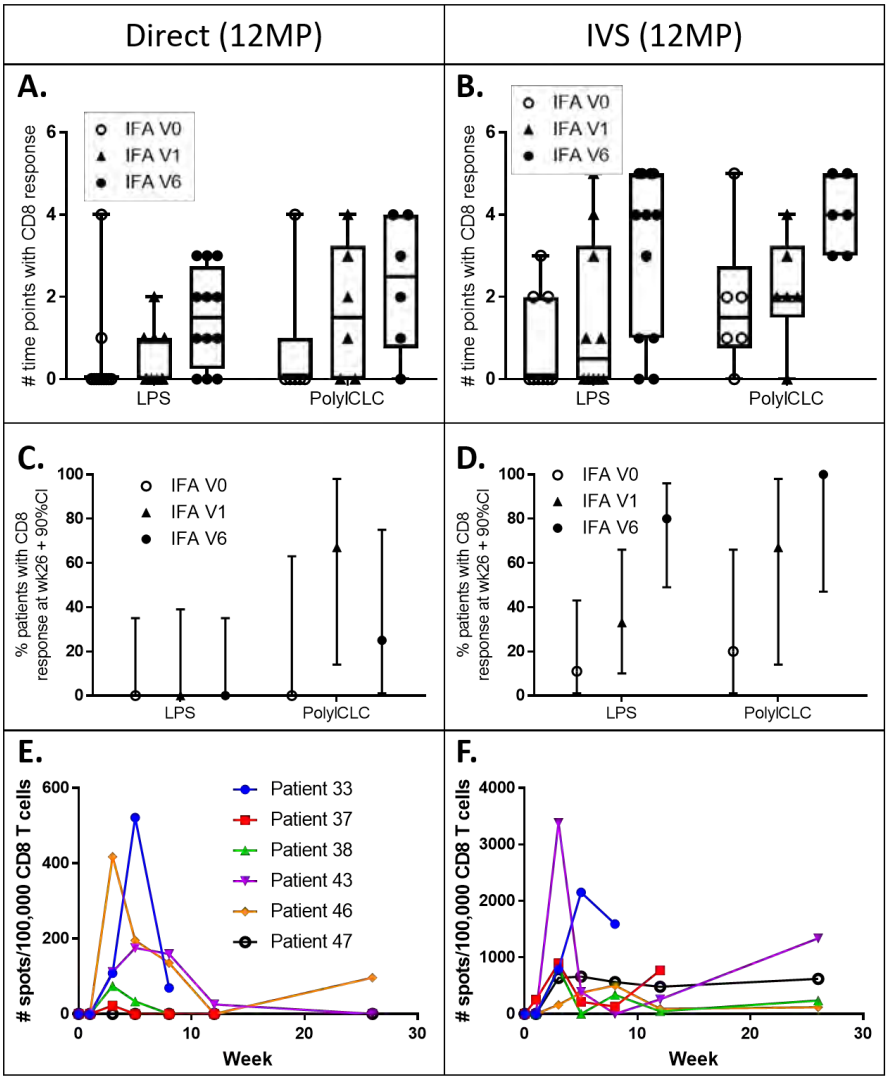

Figure 4. Persistence and durability of the CD8 T cell responses to 12MP. Persistence of the T cell responses to 12MP are shown in a (ex vivo) and b (IVS) as the number of PBMC dates in which a response was detected (after week 0). The maximum possible is 6 (after baseline). Durability of the T cell response for 3months after the last vaccine is shown as the proportion of patients with 90% confidence interval (CI) with response detected at d183 (of those evaluated ex vivo (c) and after IVS (d)). Also, for group 23 (pICLC, V6), the measured immune response magnitudes are shown through week 26 ex vivo (e) and IVS (f).

S8). For 9/12 peptides, the immune response rates were higher in Cohort 2 than in Cohort 1, and for 2 of them the immune response rates were 0 in both; only one peptide (YMD) had an immune response rate marginally higher in Cohort 1

(29% vs 25%). No apparent differences in durability of immune response were observed among different HLA alleles (Additional file 1: Table S9).

Clinical outcome

Overall survival and disease-free survival were high for the entire study population. The study was not powered to investigate changes in overall and disease-free survival among study groups, but they appear similar thus far. (Additional file 1: Figure S3).

DISCUSSION

There is no consensus on best adjuvants to support strong and durable T cell responses to cancer antigens. Our prior work has demonstrated that vaccines using peptides emulsified in IFA can induce CD8 T cell responses in 70–80% of patients based on ex vivo IVS ELIspot assays, and can also induce CD4 T cell responses in most patients, while also supporting induction of peptide-specific antibody responses [31]. The immune responses can exceed 5% of circulating CD8 T cells after vaccination with peptides in IFA alone [1, 28]. However, some T cell responses with IFA are transient and not all patients develop strong responses [4]. Thus, there is interest in enhancing T cell responses to vaccines. Concerns about use of IFA have been raised by murine studies, which showed that peptide vaccination in IFA induced inflammation at vaccine sites that selectively recruited and depleted peptide-specific T cells, thereby negatively impacting tumor control [5, 6]. Multiple investigators have induced strong and durable CD8 T cell responses to short peptides in mice using adjuvants combining a TLR agonist and an agonistic CD40 Ab [5, 32, 33]; however, this approach has not yet been evaluated in humans. The Mel58 clinical trial was designed to test whether vaccination with minimal epitope melanoma peptides in a TLR agonist, combined with helper T cell activation, would be more effective at inducing durable T cell responses than use of the same adjuvant preparation combined with IFA. However, in contrast to our underlying hypothesis, we found that circulating CD8 T cell responses to minimal epitopes were greater in magnitude and durability when IFA was included, especially when IFA was included in all 6 vaccines. The trial tested agonists for both TLR3 and TLR4. TLR4 agonists have also been studied as vaccine adjuvants, but the classic TLR4 agonist, LPS, has long been considered too toxic for human use. However, the present formulation of GMP grade endotoxin has a strong safety profile [34–38]. Human experience with it, administered systemically, either by intravenous injection or by inhalation, is that it causes systemic inflammatory responses that are transient and very well-tolerated up to 2500 EU per dose [34, 35, 39]. LPS is known to activate innate immunity, however; to our knowledge, it has not been previously been used as a vaccine adjuvant. In the present study, we escalated from 25 EU to 1600 EU, with and without IFA, and there were no DLTs. Thus, these data support the safety of bacterial LPS as a vaccine adjuvant. Interestingly, one patient had skin hypopigmentation (patient

27, LPS 1600, V0) though no T cell response to 12MP or tetanus peptide ex vivo, but positive to tyrosinase (DAEK) with in vitro stimulated ELIspot assay in PBMC and SIN (Additional file 1: Table S4). The goal of the rapid dose escalation was to define safety at the maximal tolerated dose, up to 1600 EU. Since that dose was found safe, most patients in Cohort 1 were enrolled at 1600 EU dose, limiting the ability to determine which of the 4 LPS doses is most immunogenic. Within this constraint, no significant difference in immunogenicity was observed among the LPS doses. The TLR3 agonist polyICLC has been studied in preclinical models and in clinical trials [40–42], with favorable safety and immunogenicity profiles, and, when combined with IFA, it has been shown to enhance CD4, CD8, and antibody responses to long NYESO-1 peptides compared to IFA alone [3]. Sabbatini et al. did observe marked injection site reactions in 2 patients treated with NYESO1 long peptides plus IFA and 1.4 mg polyICLC, and discontinued treatment early for 4 of 11 patients. Considering this, we employed a lower dose (1 mg) in our study [3]. We observed injection site reactions that met stopping criteria for 1 of 6 patients in arm 22 (polyICLC, V1) and that contributed to the overall DLT for one of 6 patients in arm 23 (polyICLC, V6). However, these were not serious adverse events, which resolved after stopping treatment. These DLTs did not meet stopping criteria for any sub-arm of cohort 2. Thus, the regimen is considered safe; however, prominent local injection site reactions can be expected. Overall, the data support polyICLC as an effective vaccine adjuvant when combined with IFA, for inducing CD8 T cell responses to minimal peptides, with an acceptable safety profile. This regimen appears marginally better than LPS plus IFA, which was very well-tolerated, but also supported immune responses. Other TLR agonists have been shown to enhance T cell responses to peptides in vaccines, in particular TLR9 agonist CpG-B (7909, PF3512676) [43, 44]. Thus, a range of TLR agonists have value in combination with IFA as vaccine adjuvants. For an adjuvant to have maximum benefit, it has to generate an antigen depot, to activate APC, and to provide co-stimulation through CD4 T cell help [45]. The present study provided an antigen depot with the water-in-oil emulsion with IFA, TLR agonists to activate APC, and a tetanus peptide that is very effective at inducing CD4 helper T cell responses. Activation of CD4 helper T cells will induce CD40L expression, which in turn can license APC and enhance their antigen presentation. We have not formally tested the impact of CD40L expression by tetanus-reactive CD4 T cells but have found in this trial that T cell responses to the tetanus helper peptide was greater with inclusion of IFA (V1 or V6) than without it (V0). Thus, the impact of IFA may include both a direct effect on the CD8 T cell response and an indirect effect, through activation of CD4 T cells, and subsequent APC activation. In the murine studies that have shown negative effects of IFA on CD8 T cell responses to short peptides, an alternative vaccination approach using a water-soluble adjuvant preparation, including TLR7 agonist imiquimod and CD40 antibody induced more durable immune responses and better tumor control [5]. Also, strong CD8 responses have been induced in mice by co-administration of peptides, CD40 Ab, and PolyIC [46]. Clinical grade human agonistic antibodies to CD40 were not available at the time of the present clinical trial. Thus, the vaccine regimen included the tetanus helper peptide to enhance CD4 help via CD40L

expression. It will be valuable to reconcile the favorable findings from this trial in light of the unfavorable findings with use of IFA in murine models. There are several differences in the experimental setting for the murine studies and that of the present clinical trial. These include dose and volume differences in the vaccine, differences in T cell frequency, inclusion of helper peptide in the human trial, as well as potential differences between human and mouse. In the murine studies, 100 mcg of peptide was given in a 100 mcl emulsion with IFA [5, 6]. In the human trial, 100 mcg of each peptide was given in a 1 ml emulsion with IFA. Considering the impact of the large depot in the mouse, volume of that depot is likely relevant to the observed findings. A mouse typically weighs about 25 g; thus, 100 mcl represents 1/250th of the mass of the mouse. For a 70 kg human, the 1 ml emulsion used in the clinical trial represents 1/70,000th of the mass of the patient. This 280-fold v/v difference is dramatic: If the patients had been administered a 280 ml emulsion, a much more dramatic vaccine site effect might be anticipated. Also, the murine studies used adoptive transfer of 1 × 106 activated antigen-reactive T cells which represents about 50% of circulating CD8 T cells [47]. This exceeds the pre-treatment frequency of antigen-specific T cells in humans, probably by at least 2 logs, and also exceeds what is induced over time with vaccination. Thus, the administration of a high dose of antigen-reactive T cells into a massive IFA depot may explain in part the difference between the experimental findings in the mouse and what is observed in this clinical trial. Also, this trial included T cell help, in the form of a tetanus helper peptide, which was not included in the murine studies. We have found that vaccination with IFA plus TLR agonist and inclusion of CD4 help induced a high rate of T cell responses ex vivo, durable in most patients for at least 6 months. In prior work, we observed transient responses by circulating T cells [4, 28] and that T cells accumulate at sites of vaccination with peptides in IFA [48, 49]. These observations, in light of murine data on IFA as an adjuvant [5], suggested a decline of responsive circulating T cells due to accumulation at vaccine sites. Alternatively, the transient responses observed with direct ELIspots may be explained by reversion of effector T cells to memory, especially after the vaccine sequence is completed. As such, they may not be detected as effectors ex vivo but are functional after restimulation. In support of this, we observed stimulated responses out to wk. 26 in 85% of the evaluable patients with V6 IFA (Fig. 2b), compared to 50 and 14% respectively with V1 and V0. Therefore, repeated doses of IFA may support durable memory responses rather than accumulation and depletion at vaccine sites. New strategies for vaccination against mutated neoantigens have promise for enhancing immune repertoires; however, the clinical trials of neoantigen vaccines published to date have all used different vaccine adjuvant strategies, and most of the T cell responses induced were detectable only after in vitro stimulation [50–52]. Thus, enhanced strategies for vaccination remain a high priority for the field. The present study suggests that a TLR agonist alone may not be sufficient for induction of a strong T cell response to a peptide vaccine, and that inclusion of IFA with a helper peptide remains an effective strategy. Future trials should test whether addition of a CD40 antibody plus TLR agonist at the vaccine site can further enhance T cell responses in patients, with or without IFA.

CONCLUSIONS

This clinical trial was designed to test whether vaccination with 12 short melanoma peptides in combination with TLR agonists polyICLC or LPS with IFA was safe and immunogenic in melanoma patients. Only 2 DLTs were observed, in different sub-arms of cohort 2 (polyICLC): no treatment combination met stopping criteria. A driving hypothesis was that inclusion of IFA with TLR agonists would be less effective in generating a durable T cell response. However, in contrast to our hypothesis, peptide-specific CD8 T cell responses were more durable and of greater magnitude when IFA was included as an adjuvant, regardless of whether it was combined with polyICLC or LPS. Furthermore, our study suggests that, overall, polyICLC may induce marginally better CD8 T cell responses than LPS. Future studies will aim to understand mechanisms underlying the favorable effects with IFA.

ABBREVIATIONS

12MP: 12 melanoma peptides; APC: Antigen-presenting cell; CV: Coefficient of variation; DLT: Dose-limiting toxicity; EU: Endotoxin Unit; IFA: Incomplete Freund's Adjuvant; IVS: In vitro stimulation; LPS: Lipopolysaccharide; LR: Likelihood of chi-square test statistic; MTDC: Maximum tolerated dose combination; PS: Performance status; SIN: Sentinel immunized node; Tet: Tetanus helper peptide; TLR: Toll-like receptor; V0: No IFA; V1: IFA with first vaccine; V6: IFA with all six vaccines

ACKNOWLEDGEMENTS

We thank the NIH Clinical Center (Anthony Suffredini) and the Cancer Research Institute/ Ludwig Institute for Cancer Research for kindly providing the LPS and polyICLC, respectively.

REFERENCES

1. Rosenberg SA, Sherry RM, Morton KE, Scharfman WJ, Yang JC, Topalian SL, Royal RE, Kammula U, Restifo NP, Hughes MS, et al. Tumor progression can occur despite the induction of very high levels of self/tumor antigenspecific CD8+ T cells in patients with melanoma. J Immunol. 2005;175:6169–76.
2. Obeid J, Hu Y, Slingluff CL Jr. Vaccines, adjuvants, and dendritic cell activators--current status and future challenges. Semin Oncol. 2015;42:549–61.
3. abbatini P, Tsuji T, Ferran L, Ritter E, Sedrak C, Tuballes K, Jungbluth AA, Ritter G, Aghajanian C, Bell-McGuinn K, et al. Phase I trial of overlapping long peptides from a tumor self-antigen and poly-ICLC shows rapid induction of integrated immune response in ovarian cancer patients. Clin Cancer Res. 2012;18:6497–508.
4. Slingluff CL Jr, Petroni GR, Yamshchikov GV, Hibbitts S, Grosh WW, ChianeseBullock KA, Bissonette EA, Barnd DL, Deacon DH, Patterson JW, et al. Immunologic and clinical outcomes of vaccination with a multiepitope melanoma peptide vaccine plus low-dose interleukin-2 administered either concurrently or on a delayed schedule. J Clin Oncol. 2004;22:4474–85.
5. Hailemichael Y, Dai Z, Jaffarzad N, Ye Y, Medina MA, Huang XF, DortaEstremera SM, Greeley NR, Nitti G, Peng W, et al. Persistent antigen at vaccination sites induces tumor-specific CD8(+) T cell sequestration, dysfunction and deletion. Nat Med. 2013;19:465–72.
6. Hailemichael Y, Woods A, Fu T, He Q, Nielsen MC, Hasan F, Roszik J, Xiao Z, Vianden C, Khong H, et al. Cancer vaccine formulation dictates synergy with CTLA-4 and PD-L1 checkpoint blockade therapy. J Clin Invest. 2018;128(4): 1338-54.
7. Slingluff CL Jr, Petroni GR, Chianese-Bullock KA, Smolkin ME, Hibbitts S, Murphy C, Johansen N, Grosh WW, Yamshchikov GV, Neese PY, et al. Immunologic and clinical outcomes of a randomized phase II trial of two multipeptide vaccines for melanoma in the adjuvant setting. Clin Cancer Res. 2007;13:6386–95.
8. Slingluff CL Jr, Petroni GR, Chianese-Bullock KA, Smolkin ME, Ross MI, Haas NB, von Mehren M, Grosh WW. Randomized multicenter trial of the effects of melanomaassociated helper peptides and cyclophosphamide on the immunogenicity of a multipeptide melanoma vaccine. J Clin Oncol. 2011;29:2924–32.
9. van Mierlo GJ, den Boer AT, Medema JP, van der Voort EI, Fransen MF, Offringa R, Melief CJ, Toes RE. CD40 stimulation leads to effective therapy of CD40(−) tumors through induction of strong systemic cytotoxic T lymphocyte immunity. Proc Natl Acad Sci U S A. 2002;99:5561–6.
10. Schoenberger SP, Toes RE, van der Voort EI, Offringa R, Melief CJ. T-cell help for cytotoxic T lymphocytes is mediated by CD40-CD40L interactions. Nature. 1998;393:480–3.
11. Melssen M, Slingluff CL Jr. Vaccines targeting helper T cells for cancer immunotherapy. Curr Opin Immunol. 2017;47:85–92.
12. Slingluff CL Jr, Yamshchikov G, Neese P, Galavotti H, Eastham S, Engelhard VH, Kittlesen D, Deacon D, Hibbitts S, Grosh WW, et al. Phase I trial of a melanoma vaccine with gp100(280-288) peptide and tetanus helper peptide in adjuvant: immunologic and clinical outcomes. Clin Cancer Res. 2001;7:3012–24.
13. Slingluff CL Jr, Yamshchikov GV, Hogan KT, Hibbitts SC, Petroni GR, Bissonette EA,

Patterson JW, Neese PY, Grosh WW, Chianese-Bullock KA, et al. Evaluation of the sentinel immunized node for immune monitoring of cancer vaccines. Ann Surg Oncol. 2008;15:3538–49.
14. Wages NA, Conaway MR, O'Quigley J. Dose-finding design for multi-drug combinations. Clin Trials. 2011;8:380–9.
15. O'Quigley J, Pepe M, Fisher L. Continual reassessment method: a practical design for phase 1 clinical trials in cancer. Biometrics. 1990;46:33–48.
16. Cox AL, Skipper J, Chen Y, Henderson RA, Darrow TL, Shabanowitz J, Engelhard VH, Hunt DF, Slingluff CL Jr. Identification of a peptide recognized by five melanoma-specific human cytotoxic T cell lines. Science. 1994;264:716–9.
17. Kittlesen DJ, Thompson LW, Gulden PH, Skipper JC, Colella TA, Shabanowitz J, Hunt DF, Engelhard VH, Slingluff CL Jr. Human melanoma patients recognize an HLA-A1-restricted CTL epitope from tyrosinase containing two cysteine residues: implications for tumor vaccine development [published erratum appears in J Immunol 1999 Mar 1;162(5):3106]. J Immunol. 1998;160:2099–106.
18. Skipper JC, Hendrickson RC, Gulden PH, Brichard V, Van Pel A, Chen Y, Shabanowitz J, Wolfel T, Slingluff CL Jr, Boon T, et al. An HLA-A2-restricted tyrosinase antigen on melanoma cells results from posttranslational modification and suggests a novel pathway for processing of membrane proteins. J Exp Med. 1996;183:527–34.
19. Skipper JC, Kittlesen DJ, Hendrickson RC, Deacon DD, Harthun NL, Wagner SN, Hunt DF, Engelhard VH, Slingluff CL Jr. Shared epitopes for HLA-A3- restricted melanoma-reactive human CTL include a naturally processed epitope from Pmel-17/gp100. J Immunol. 1996;157:5027–33.
20. Chaux P, Luiten R, Demotte N, Vantomme V, Stroobant V, Traversari C, Russo V, Schultz E, Cornelis GR, Boon T, van der Bruggen P. Identification of five MAGE-A1 epitopes recognized by cytolytic T lymphocytes obtained by in vitro stimulation with dendritic cells transduced with MAGE-A1. J Immunol. 1999;163:2928–36.
21. Kawakami Y, Robbins PF, Wang X, Tupesis JP, Parkhurst MR, Kang X, Sakaguchi K, Appella E, Rosenberg SA. Identification of new melanoma epitopes on melanosomal proteins recognized by tumor infiltrating T lymphocytes restricted by HLA-A1, –A2, and -A3 alleles. J Immunol. 1998;161:6985–92.
22. Wang RF, Johnston SL, Zeng G, Topalian SL, Schwartzentruber DJ, Rosenberg SA. A breast and melanoma-shared tumor antigen: T cell responses to antigenic peptides translated from different open reading frames. J Immunol. 1998;161:3598–606.
23. Huang LQ, Brasseur F, Serrano A, De Plaen E, van der Bruggen P, Boon T, Van Pel A. Cytolytic T lymphocytes recognize an antigen encoded by MAGE-A10 on a human melanoma. J Immunol. 1999;162:6849–54.
24. Traversari C, van der Bruggen P, Luescher IF, Lurquin C, Chomez P, Van Pel A, De Plaen E, Amar-Costesec A, Boon T. A nonapeptide encoded by human gene MAGE-1 is recognized on HLA-A1 by cytolytic T lymphocytes directed against tumor antigen MZ2-E. J Exp Med. 1992;176:1453–7.
25. Kawakami Y, Eliyahu S, Jennings C, Sakaguchi K, Kang X, Southwood S, Robbins PF, Sette A, Appella E, Rosenberg SA. Recognition of multiple epitopes in the human melanoma antigen gp100 by tumor-infiltrating T lymphocytes associated with in vivo tumor regression. J Immunol. 1995;154:3961–8.
26. Gaugler B, Van den Eynde B, van der Bruggen P, Romero P, Gaforio JJ, De Plaen E,

Lethe B, Brasseur F, Boon T. Human gene MAGE-3 codes for an antigen recognized on a melanoma by autologous cytolytic T lymphocytes. J Exp Med. 1994;179:921–30.
27. Panina-Bordignon P, Tan A, Termijtelen A, Demotz S, Corradin G, Lanzavecchia A. Universally immunogenic T cell epitopes: promiscuous binding to human MHC class II and promiscuous recognition by T cells. Eur J Immunol. 1989;19:2237–42.
28. Slingluff CL Jr, Petroni GR, Olson WC, Smolkin ME, Ross MI, Haas NB, Grosh WW, Boisvert ME, Kirkwood JM, Chianese-Bullock KA. Effect of granulocyte/ macrophage colony-stimulating factor on circulating CD8+ and CD4+ T-cell responses to a multipeptide melanoma vaccine: outcome of a multicenter randomized trial. Clin Cancer Res. 2009;15:7036–44.
29. Slingluff CL Jr, Lee S, Zhao F, Chianese-Bullock KA, Olson WC, Butterfield LH, Whiteside TL, Leming PD, Kirkwood JM. A randomized phase II trial of multiepitope vaccination with melanoma peptides for cytotoxic T cells and helper T cells for patients with metastatic melanoma (E1602). Clin Cancer Res. 2013;19:4228–38.
30. Good PI. Permutation, parametric, and bootstrap tests of hypotheses. 3rd ed. New York: Springer-Verlag New York; 2005.
31. Reed CM, Cresce ND, Mauldin IS, Slingluff CL Jr, Olson WC. Vaccination with melanoma helper peptides induces antibody responses associated with improved overall survival. Clin Cancer Res. 2015;21:3879–87.
32. Cho HI, Jung SH, Sohn HJ, Celis E, Kim TG. An optimized peptide vaccine strategy capable of inducing multivalent CD8(+) T cell responses with potent antitumor effects. Oncoimmunology. 2015;4:e1043504.
33. Sanchez PJ, McWilliams JA, Haluszczak C, Yagita H, Kedl RM. Combined TLR/ CD40 stimulation mediates potent cellular immunity by regulating dendritic cell expression of CD70 in vivo. J Immunol. 2007;178:1564–72.
34. Talwar S, Munson PJ, Barb J, Fiuza C, Cintron AP, Logun C, Tropea M, Khan S, Reda D, Shelhamer JH, et al. Gene expression profiles of peripheral blood leukocytes after endotoxin challenge in humans. Physiol Genomics. 2006;25:203–15.
35. Preas HL, Jubran A, Vandivier RW, Reda D, Godin PJ, Banks SM, Tobin MJ, Suffredini AF. Effect of endotoxin on ventilation and breath variability: role of cyclooxygenase pathway. Am J Respir Crit Care Med. 2001;164:620–6.
36. O'Grady NP, Preas HL, Pugin J, Fiuza C, Tropea M, Reda D, Banks SM, Suffredini AF. Local inflammatory responses following bronchial endotoxin instillation in humans. Am J Respir Crit Care Med. 2001;163:1591–8.
37. Bornstein SR, Wolkersdorfer GW, Tauchnitz R, Preas HL, Chrousos GP, Suffredini AF. Plasma dehydroepiandrosterone levels during experimental endotoxemia and anti-inflammatory therapy in humans. Crit Care Med. 2000;28:2103–6.
38. Suffredini AF, Hochstein HD, McMahon FG. Dose-related inflammatory effects of intravenous endotoxin in humans: evaluation of a new clinical lot of Escherichia coli O:113 endotoxin. J Infect Dis. 1999;179:1278–82.
39. Preas HL, Nylen ES, Snider RH, Becker KL, White JC, Agosti JM, Suffredini AF. Effects of anti-inflammatory agents on serum levels of calcitonin precursors during human experimental endotoxemia. J Infect Dis. 2001;184:373–6.
40. Mehrotra S, Britten CD, Chin S, Garrett-Mayer E, Cloud CA, Li M, Scurti G, Salem ML, Nelson MH, Thomas MB, et al. Vaccination with poly (IC:LC) and peptide-pulsed

autologous dendritic cells in patients with pancreatic cancer. J Hematol Oncol. 2017;10:82.
41. Tewari K, Flynn BJ, Boscardin SB, Kastenmueller K, Salazar AM, Anderson CA, Soundarapandian V, Ahumada A, Keler T, Hoffman SL, et al. Poly(I:C) is an effective adjuvant for antibody and multi-functional CD4+ T cell responses to plasmodium falciparum circumsporozoite protein (CSP) and alphaDEC-CSP in non human primates. Vaccine. 2010;28(45):7256-66.
42. Zhu X, Nishimura F, Sasaki K, Fujita M, Dusak JE, Eguchi J, FellowsMayle W, Storkus WJ, Walker PR, Salazar AM, Okada H. Toll like receptor-3 ligand poly-ICLC promotes the efficacy of peripheral vaccinations with tumor antigen-derived peptide epitopes in murine CNS tumor models. J Transl Med. 2007;5(10):10.
43. Baumgaertner P, Costa Nunes C, Cachot A, Maby-El Hajjami H, Cagnon L, Braun M, Derre L, Rivals JP, Rimoldi D, Gnjatic S, et al. Vaccination of stage III/IV melanoma patients with long NY-ESO-1 peptide and CpG-B elicits robust CD8+ and CD4+ T-cell responses with multiple specificities including a novel DR7-restricted epitope. Oncoimmunology. 2016;5:e1216290.
44. Speiser DE, Lienard D, Rufer N, Rubio-Godoy V, Rimoldi D, Lejeune F, Krieg AM, Cerottini JC, Romero P. Rapid and strong human CD8+ T cell responses to vaccination with peptide, IFA, and CpG oligodeoxynucleotide 7909. J Clin Investig. 2005;115:739 –46.
45. Overwijk WW. Cancer vaccines in the era of checkpoint blockade: the magic is in the adjuvant. Curr Opin Immunol. 2017;47:103 –9.
46. Cho HI, Celis E. Optimized peptide vaccines eliciting extensive CD8 T-cell responses with therapeutic antitumor effects. Cancer Res. 2009;69:9012 –9.
47. Pinchuk LM, Filipov NM. Differential effects of age on circulating and splenic leukocyte populations in C57BL/6 and BALB/c male mice. Immun Ageing. 2008;5:1.
48. Salerno EP, Shea SM, Olson WC, Petroni GR, Smolkin ME, McSkimming C, Chianese-Bullock KA, Slingluff CL Jr. Activation, dysfunction and retention of T cells in vaccine sites after injection of incomplete Freund's adjuvant, with or without peptide. Cancer Immunol Immunother. 2013;62:1149 –59.
49. Schaefer JT, Patterson JW, Deacon DH, Smolkin ME, Petroni GR, Jackson EM, Slingluff CL Jr. Dynamic changes in cellular infiltrates with repeated cutaneous vaccination: a histologic and immunophenotypic analysis. J Transl Med. 2010;8:79.
50. Ott PA, Hu Z, Keskin DB, Shukla SA, Sun J, Bozym DJ, Zhang W, Luoma A, Giobbie-Hurder A, Peter L, et al. An immunogenic personal neoantigen vaccine for patients with melanoma. Nature. 2017;547(7662):217-21.
51. Sahin U, Derhovanessian E, Miller M, Kloke BP, Simon P, Lower M, Bukur V, Tadmor AD, Luxemburger U, Schrors B, et al. Personalized RNA mutanome vaccines mobilize poly-specific therapeutic immunity against cancer. Nature. 2017;547(7662):222-6.
52. Carreno BM, Magrini V, Becker-Hapak M, Kaabinejadian S, Hundal J, Petti AA, Ly A, Lie WR, Hildebrand WH, Mardis ER, Linette GP. Cancer immunotherapy. A dendritic cell vaccine increases the breadth and diversity of melanoma neoantigen-specific T cells. Science. 2015;348:803 –8.

Supplemental Table 1. Peptides used in vaccines

Prep	Allele	Sequence	Epitope
12MP	HLA-A1	DAEKSDICTDEY	Tyrosinase $_{240\text{-}251}$ *
		SSDYVIPIGTY	Tyrosinase $_{146\text{-}156}$
		EADPTGHSY	MAGE-A1 $_{161\text{-}169}$
		EVDPIGHLY	MAGE-A3 $_{168\text{-}176}$
	HLA-A2	YMDGTMSQV	Tyrosinase $_{369\text{-}377}$ ¨
		IMDQVPFSV	gp100 $_{209\text{-}217}$ #
		YLEPGPVTA	gp100 $_{280\text{-}288}$
		GLYDGMEHL	MAGE-A10 $_{254\text{-}262}$
	HLA-A3/A11/A31	ALLAVGATK	gp100 $_{17\text{-}25}$
		LIYRRRLMK	gp100 $_{614\text{-}622}$
		SLFRAVITK	MAGE-A1 $_{96\text{-}104}$
		ASGPGGGAPR	NY-ESO-1 $_{53\text{-}62}$
Tet	HLA-DR (multiple)	AQYIKANSKFIGITEL	Tetanus toxoid p2$_{830\text{-}844}$ **

* substitution of S for C, at residue 244.
¨(post-translational change of N to D at residue 371)
#(209-2M, substitution of M for T at residue 210)
**An alanine residue was added to the N-terminus to prevent cyclization.

Supplemental Table 2. Target Study Groups and Subgroups

Study cohort	Peptide vaccine	TLR agonist	Dose of TLR agonist	IFA	Route peptide + TLR agonist
1	MELITAC 12.1 (12MP + Tet)	LPS*	Escalation 25, 100, 400, 1600 EU	None (0)	Id/sq
				Vaccine 1 (V1)	Id/sq
				All vaccines (V6)	Id/sq
2	MELITAC 12.1 (12MP + Tet)	polyICLC	1 mg	None (0)	Id/sq
				Vaccine 1 (V1)	Id/sq
				c) All vaccines (V6)	Id/sq

* LPS = lipopolysaccharide (endotoxin)

Supplemental Table 3. Patient demographics

	Arm 1. LPS	Arm 2. pICLC	Overall
N	33	18	51
Race			
White	33	17	50
Asian	0	1	1
Gender			
F	7	12	19
M	26	6	32
Ethnicity			
Hispanic	2	0	2
ECOG PS at registration			
0	28	18	46
1	5	0	5
HLA*			
A1+	15	7	22
A2+	17	8	25
A3+	8	6	14
A11/31	5	4	9
Primary site			
Skin, non-acral	26	17	43
Unknown	4	0	4
Acral	2	1	3
Ocular	1	0	1
Stage at Registration**			
IIB-IIC	4	1	5
III	25	15	40
IIIA	6	2	8
IIIB/C	19	13	32
IV	4	2	6
LDH			
<=ULN	31	17	48
>ULN	1	1	2
Missing	1	0	1

Supplemental Table 4. Treatment-related adverse events

MEL 58 Maximum Grade Toxicities (Related)

		Cohort Totals								
		LPS			PolyICLC			Total		
Toxicity Category	Toxicity Description	G1	G2	G3	G1	G2	G3	G1	G2	G3
BLOOD AND LYMPHATIC SYSTEM DISORDERS	ANEMIA	1			1			2		
EAR AND LABYRINTH DISORDERS	TINNITUS	1						1		
EYE DISORDERS	OTHER	1						1		
GASTROINTESTINAL DISORDERS	DIARRHEA	2				1		2	1	
	DRY MOUTH				1			1		
	MUCOSITIS ORAL	1				1		1	1	
	NAUSEA	3			3			6		
	VOMITING				1			1		
GENERAL DISORDERS AND ADMINISTRATION SITE CONDITIONS	CHILLS	5			2	2		7	2	
	EDEMA LIMBS					1			1	
	FATIGUE	14	3		12	2		26	5	
	FEVER	4			3			7		
	FLU LIKE SYMPTOMS	4	2		3	1		7	3	
	INJECTION SITE REACTION	16	15		2	16		18	31	
	PAIN	2						2		
IMMUNE SYSTEM DISORDERS	AUTOIMMUNE DISORDER	2			2			4		
	CYTOKINE RELEASE SYNDROME					1			1	
INJURY, POISONING AND PROCEDURAL COMPLICATIONS	SEROMA	2						2		
	WOUND DEHISCENCE	2						2		
INVESTIGATIONS	LYMPHOCYTE COUNT DECREASED					2			2	
	WEIGHT GAIN				1			1		
	WHITE BLOOD CELL DECREASED	1			1	1		2	1	

table continues

MEL 58 Maximum Grade Toxicities (Related)

		Cohort Totals								
		LPS			PolyICLC			Total		
Toxicity Category	Toxicity Description	G1	G2	G3	G1	G2	G3	G1	G2	G3
METABOLISM AND NUTRITION DISORDERS	ANOREXIA	2			1			3		
	DEHYDRATION				1			1		
MUSCULOSKELETAL AND CONNECTIVE TISSUE DISORDERS	ARTHRALGIA	10	1		5			15	1	
	MYALGIA	5			5			10		
	PAIN IN EXTREMITY	1						1		
NERVOUS SYSTEM DISORDERS	CONCENTRATION IMPAIRMENT	1						1		
	DIZZINESS	2						2		
	HEADACHE	4			5	1		9	1	
PSYCHIATRIC DISORDERS	AGITATION				1			1		
	ANXIETY	1						1		
RESPIRATORY, THORACIC AND MEDIASTINAL DISORDERS	ALLERGIC RHINITIS	2						2		
	COUGH				1			1		
	DYSPNEA	1						1		
	NASAL CONGESTION	1						1		
	SORE THROAT	1			1			2		
SKIN AND SUBCUTANEOUS TISSUE DISORDERS	ALOPECIA				1			1		
	PAIN OF SKIN	2			3	1		5	1	
	PRURITUS	1			2			3		
	RASH ACNEIFORM				1			1		
	RASH MACULO-PAPULAR	1			2	1		3	1	
	SKIN HYPERPIGMENTATION	1						1		
	SKIN HYPOPIGMENTATION	1						1		
	SKIN INDURATION	9	4			3		9	7	
	SKIN ULCERATION		1			1	1		2	1
VASCULAR DISORDERS	FLUSHING	3			2			5		
	HOT FLASHES	3			2			5		

Supplemental Table 5: Direct ELIspot: number of patients in each study group with T cell response through week 26.

T cell response to:	Cohort	Vaccine adjuvant	IFA V0	IFA V1	IFA V6	IFA 0-V6
N evaluable patients	1	LPS 25	3	2	2	7
		LPS 100	2	2	2	6
		LPS 400	2	2	2	6
		LPS 1600	4	4	6	14
		LPS (all)	*11*	*10*	*12*	*33*
	2	pICLC	6	6	6	18
	1+2	*All*	*17*	*16*	*18*	*51*
12MP pool	1	LPS 25	0%	50%	100%	43%
		LPS 100	0%	100%	100%	67%
		LPS 400	50%	50%	50%	50%
		LPS 1600	25%	0%	50%	29%
		LPS (all)	*18%*	*40%*	*67%*	*42%*
	2	pICLC	17%	67%	83%	56%
	1+2	*All*	*18%*	*50%*	*72%*	*47%*
any of 12 individual peptides	1	LPS 25	0%	50%	100%	43%
		LPS 100	0%	0%	0%	0%
		LPS 400	0%	0%	50%	17%
		LPS 1600	0%	0%	33%	14%
		LPS (all)	*0%*	*10%*	*42%*	*18%*
	2	pICLC	17%	67%	83%	56%
	1+2	*All*	*6%*	*31%*	*56%*	*31%*
tetanus helper peptide	1	LPS 25	0%	50%	100%	43%
		LPS 100	0%	100%	100%	67%
		LPS 400	0%	50%	100%	50%
		LPS 1600	25%	75%	83%	64%
		LPS (all)	*9%*	*70%*	*92%*	*58%*
	2	pICLC	50%	83%	83%	72%
	1+2	*All*	*24%*	*75%*	*89%*	*63%*

Supplemental Table 6: Patient information, treatment regimen and ELIspot responses summarized per patient. Yes/no response based on positive response for one or more time points post start of vaccine.

Patient information				Vaccine adjuvants			Direct ELIspot response		Stimulated ELIspot response	
ID	Age	Sex	HLA type	IFA group	TLR agonist	Dose	12MP	Tetanus	PBMC	SIN
1	28	M	A3	V0	LPS	25 EU	no	no	yes	no
2	62	**F**	A1, A2	V0	LPS	25 EU	no	no	yes	no
3	61	M	A2	V0	pICLC	1 mg	no	no	yes	no
5	45	M	A2, A11	V0	LPS	100 EU	no	no	no	ND
6	77	F	A1, A31	V0	pICLC	1 mg	yes	yes	yes	yes
7	78	M	A2	V0	LPS	100 EU	no	no	no	no
8	53	M	A2	V1	LPS	25 EU	yes	yes	yes	ND
9	79	M	A3, A26	V1	LPS	25 EU	no	no	no	no
10	63	M	A3	V0	pICLC	1 mg	no	yes	yes	ND
11	63	M	A2, A3	V0	LPS	400 EU	no	no	no	no
12	65	M	A1, A2	V0	LPS	400 EU	yes	no	no	ND
13	42	F	A2	V1	pICLC	1 mg	yes	yes	yes	yes
14	78	**F**	A2, A3	V6	LPS	25 EU	yes	yes	yes	yes
15	59	M	A2	V6	LPS	25 EU	yes	yes	yes	yes
16	50	**F**	A2	V1	LPS	100 EU	yes	yes	yes	yes
17	64	M	A1	V1	LPS	100 EU	yes	yes	yes	no
18	61	F	A1, A3	V1	pICLC	1 mg	yes	yes	yes	yes
19	52	F	A1, A33	V1	pICLC	1 mg	no	no	yes	yes
20	73	M	A2, A11	V6	LPS	100 EU	yes	yes	yes	no
21	77	M	A31, A33	V6	LPS	100 EU	yes	yes	yes	no
22	66	F	A1, A3	V1	pICLC	1 mg	yes	yes	yes	yes
23	52	M	A2, A11	V1	pICLC	1 mg	yes	yes	yes	no
24	67	**F**	A11, A23	V1	LPS	400 EU	no	no	yes	no
25	58	M	A2, A24	V1	LPS	400 EU	yes	yes	yes	no
26	66	F	A11, A24	V1	pICLC	1 mg	no	yes	yes	no
27	53	M	A1	V0	LPS	1600 EU	no	no	yes	yes
28	55	M	A1, A3	V0	LPS	1600 EU	yes	no	no	no
29	31	M	A1	V6	LPS	400 EU	yes	yes	yes	no
30	51	**F**	A1, A3	V6	LPS	400 EU	no	yes	yes	no
32	55	M	A1, A68	V0	LPS	25 EU	no	no	no	no
33	55	M	A3	V6	pICLC	1 mg	yes	yes	yes	no
34	70	M	A1, A25	V1	LPS	1600 EU	no	yes	no	ND
35	63	**F**	A1, A29	V1	LPS	1600 EU	no	no	no	ND
37	42	F	A1, A2	V6	pICLC	1 mg	yes	yes	yes	ND

table continues

Patient information				Vaccine adjuvants			Direct ELIspot response		Stimulated ELIspot response	
ID	Age	Sex	HLA type	IFA group	TLR agonist	Dose	12MP	Tetanus	PBMC	SIN
38	44	F	A2	V6	pICLC	1 mg	yes	yes	yes	no
39	37	M	A1, A2	V0	LPS	1600 EU	no	yes	yes	no
40	64	M	A2, A23	V6	LPS	1600 EU	yes	yes	yes	ND
41	61	M	A1, A36	V6	LPS	1600 EU	yes	yes	yes	no
42	67	M	A2, A24	V1	LPS	1600 EU	no	yes	no	no
43	51	F	A2	V6	pICLC	1 mg	yes	yes	yes	yes
44	61	M	A1, A3	V6	LPS	1600 EU	yes	yes	yes	ND
45	59	M	A11, A30	V6	LPS	1600 EU	no	yes	no	no
46	64	M	A11, A24	V6	pICLC	1 mg	yes	yes	yes	ND
47	63	F	A1, A24	V6	pICLC	1 mg	no	no	yes	ND
48	71	M	A2, A33	V6	LPS	1600 EU	yes?	yes	no	ND
49	62	M	A2, A24	V6	LPS	1600 EU	no	no	yes	ND
50	75	F	A2	V0	pICLC	1 mg	no	yes	yes	yes
51	63	M	A1, A3	V0	LPS	1600 EU	no	no	no	ND
52	72	M	A2, A3	V0	pICLC	1 mg	no	no	yes	ND
53	76	F	A1, A3	V0	pICLC	1 mg	no	no	no	ND
54	67	**F**	A1, A2	V1	LPS	1600 EU	no	yes	no	ND

ND = not done. Participants 4, 31, 36 not evaluable and not listed.

Supplemental Table 7. HLA expression by study group and subgroup, and associated immune response rates through week 26.

Distribution of HLA by study group and subgroup*					
N	Cohort (adjuvant)	HLA-A1	HLA-A2	HLA-A3	A11,31
33	1a-c (LPS)	15 (45%)	17 (52%)	8 (24%)	5 (15%)
18	2a-c (polyICLC)	7 (39%)	8 (44%)	6 (33%)	4 (22%)
17	1a + 2a: IFA V0	9 (53%)	9 (53%)	7 (41%)	2 (12%)
16	1b + 2b: IFA V1	7 (44%)	7 (44%)	3 (19%)	3 (19%)
18	1c + 2c : IFA V6	6 (33%)	9 (50%)	4 (22%)	4 (22%)
Immune response rates, ex vivo	12MP (CD8)	45%	52%	43%	56%
	HLA specific 12MP (CD8)	14%	36%	29%	33%
	Any of 12MP (CD8)	23%	40%	29%	33%
	Tetanus (CD4)	55%	68%	50%	78%

* Totals can exceed 100% because there are two HLA-A alleles each.

Supplemental Table 8. Stimulated ELIspot response rate by cohort (N and %) through week 26

Groups		DAEK	EVD	EAD	SSD	YMD	GLY	IMD	YLE	ALLA	SLF	LIY	ASG
	Relevant HLA	**A1**				**A2**				**A3, A11, A31**			
All patients N = 51	N (relevant HLA)	22	22	22	22	25	25	25	25	23	23	23	23
	# positive	13	6	1	0	7	13	17	0	4	10	6	4
	% positive	59%	27%	5%	0%	28%	52%	68%	0%	17%	43%	26%	17%
Cohort 1 (LPS) N = 33	N (relevant HLA)	15	15	15	15	17	17	17	17	13	13	13	13
	# positive	7	3	0	0	5	8	9	0	2	5	3	2
	% positive	47%	20%	0%	0%	29%	47%	53%	0%	15%	38%	27%	15%
Cohort 2 (pICLC) N = 18	N (relevant HLA)	7	7	7	7	8	8	8	8	10	10	10	10
	# positive	6	3	1	0	2	5	8	0	2	5	3	2
	% positive	86%	42%	14%	0%	25%	63%	100%	0%	20%	50%	30%	20%

The 12MP, listed in this table, are abbreviated with the first 3-4 letters of the single-letter abbreviation codes.

Supplemental Table 9. T cell response by IVS ELIspot to 12MP at day 183, among evaluable patients, by HLA type

IFA use In vaccines	HLA-A1+	HLA-A2+	HLA-A3 superfamily+	All*
V0	2/8 (25%)	1/7 (14%)	1/7 (14%)	2/14 (14%)
V1	3/6 (50%)	3/5 (60%)	3/5 (60%)	6/12 (50%)
V6	4/4 (100%)	6/7 (86%)	5/7 (71%)	12/14 (86%)
All	9/18 (50%)	10/19 (53%)	9/19 (47%)	20/40 (50%)

* values for “All” are less than the sum across all HLA types because some patients expressed 2 different HLA alleles in these categories.

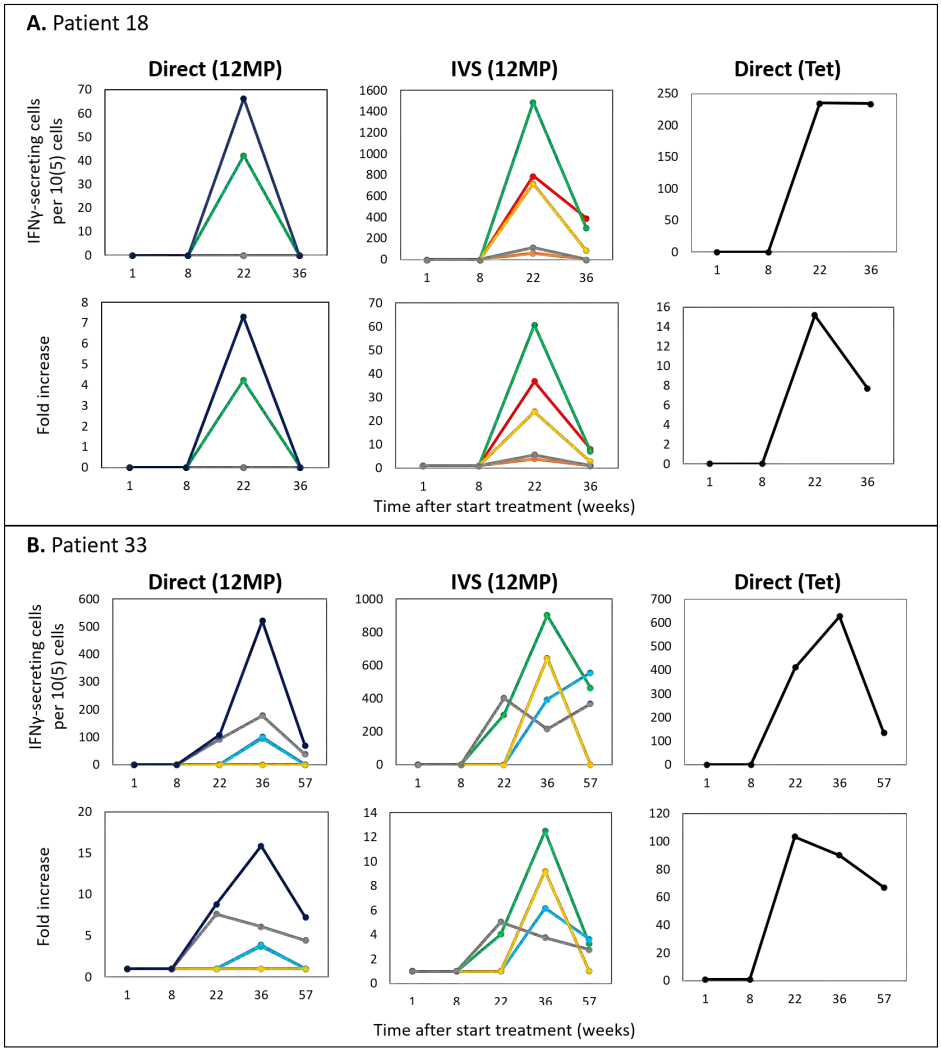

Supplemental Figure 1. Immune responses in patients with DLTs. T cell responses to 12MP peptides and to tetanus helper peptide were observed in both patients who discontinued early for DLTs, as shown for patient 18 (A,B,E,F,I,J) and 33 (C,D,G,H,K,L), with the increase response magnitudes shown as number of IFN-gamma secreting cells per 10^5 CD8 (A-H) for the short peptides, or per 10^5 CD4 (I-L) for the tetanus helper peptide. Data are shown both for Direct (ex vivo) ELISpot assays (A-D) for 12MP and Tetanus (I-L) and for IVS (stimulated) ELIspot assays (E-H) for 12MP. Peptide data are color coded: DAEK (red), EVD (orange), ALLA (green), LIY (yellow), SLF (gray), ASG (light blue), 12MP pool (dark blue), Tet (black).

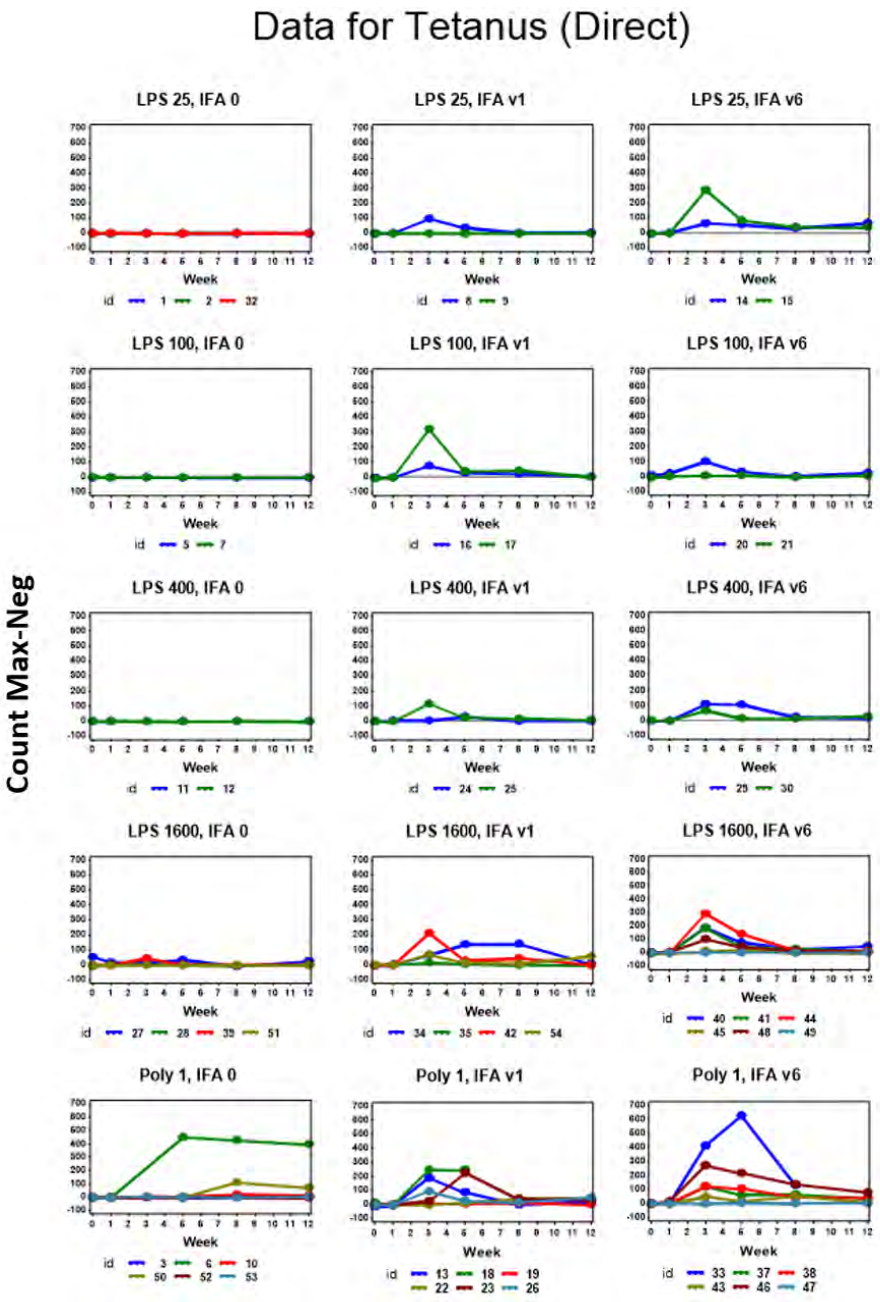

Supplemental Figure 2. T cell responses to tetanus peptide are shown from Direct ELIspot assay, with counts shown as IFN-gamma secreting cells per 10^5 CD4 T cells, for each patient group, through week 12.

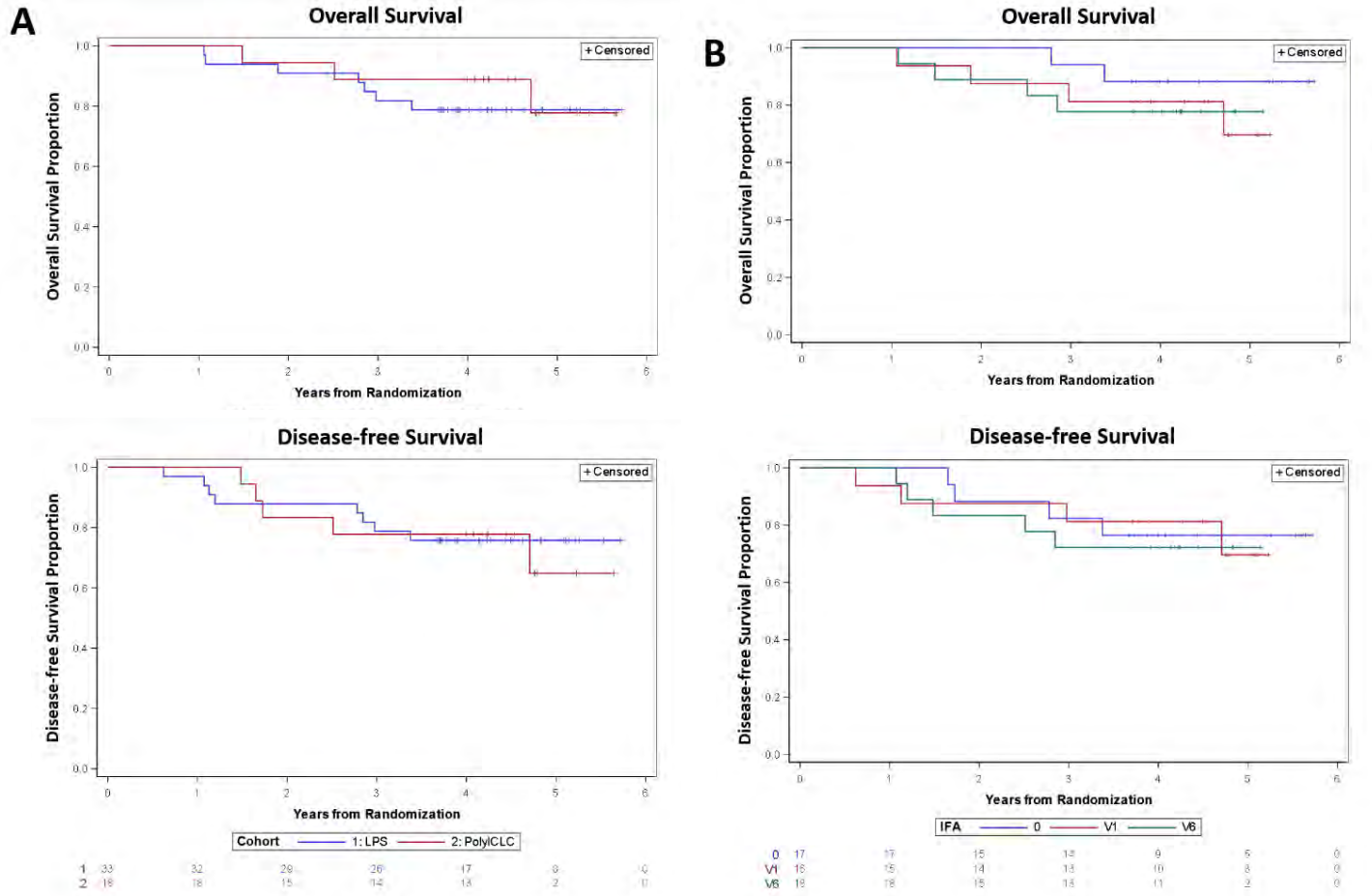

Supplemental Figure 3. Survival and progression free survival curves, comparing cohort 1 and 2 (A) and IFA groups V0, V1 and V6 (B).

Chapter 4

Characterization and comparison of innate and adaptive immune responses at vaccine sites in melanoma vaccine clinical trials

Marit M. Melssen, Karlyn E. Pollack, Max O. Meneveau, Mark E. Smolkin, Joel Pinczewski, Alexander F. Koeppel, Stephen D. Turner, Katia Sol-Church, Alexandra Hickman, Donna H. Deacon, Gina R. Petroni, Craig L. Slingluff, Jr.

Submitted

ABSTRACT

The strength and durability of systemic anti-tumor immune responses induced by cancer vaccines depends on vaccine adjuvants to support an immunogenic vaccine site microenvironment (VSME). Adjuvant formulations include water-in-oil emulsions with incomplete Freund's adjuvant (IFA) and combinations of toll-like receptor (TLR) agonists, such as an aqueous preparation containing TLR4 and TLR9 agonists with QS-21 (AS15). IFA-containing vaccines can induce immune cell accumulation at the VSME, whereas effects of AS15 are largely unexplored. Therefore, we aimed to assess innate and adaptive immune cell accumulation at the VSME after vaccination with AS15 and also to compare to known accumulation with IFA. We hypothesized that AS15 would promote less accumulation of innate and adaptive immune cells at the VSME than IFA vaccines. In separate studies, patients with resected stage IIB-IV melanoma received either a multipeptide vaccine with IFA (NCT00705640) or a recombinant MAGE-A3 protein vaccine combined with AS15 (NCT01425749). Vaccine site biopsies were obtained after 1 vaccine (week 1) or multiple vaccines (weeks 3 and/or 7). Early accumulation of CD4 and CD8 T cells was observed after vaccination with AS15, though this was not durable or of the same magnitude as vaccination in IFA. Additionally, innate immune cell subsets did not accumulate at either time point after AS15 vaccination when compared to IFA. However, AS15 increased durable expression of DC- and T cell-related genes compared to normal skin, pointing to presence of innate and adaptive immune accumulation with AS15, though to a lesser extent than with IFA. Evidence of tertiary lymphoid structure (TLS) formation was observed with both adjuvants, though more durable with IFA. Our findings highlight adjuvant-dependent differences in the immune features at the VSME and suggests the need for future studies investigating the role of VSME inflammation and composition in a systemic T-cell response and clinical benefit.

INTRODUCTION

New immune therapies have demonstrated the therapeutic value of harnessing an immune response for cancer treatment. These findings fuel renewed interest in developing effective cancer vaccines. In murine models, cancer vaccines can induce anti-tumor immune responses that mediate durable cancer control. In human clinical trials, cancer vaccines can induce anti-tumor T-cell responses; however, durable clinical responses have been rare(3-5). Cancer vaccines often use purified antigens, which require an effective vaccine adjuvant, yet there is no consensus on the most effective adjuvant strategy. Adjuvants may support immune responses to vaccine antigens by activation of dendritic cells (DC) and other components of innate immunity, and by creating a local depot of antigen at the site of immune activation. TLR agonists have emerged as effective adjuvants for inducing cellular and humoral immune responses(6). and a recently-approved vaccine for hepatitis B has enhanced activity because it includes a TLR9 agonist as an adjuvant(7). For experimental cancer vaccines, agonists for TLRs 3, 4, 7, and 9 have induced favorable cellular and/or humoral responses and may either be more effective than using incomplete Freund's adjuvant (IFA), or may enhance the activity of IFA(8-12). However, remarkably little is known about the cellular and molecular effects of adjuvants containing TLR agonists at the vaccine site microenvironment (VSME), and few studies have evaluated the effects of any adjuvants over time at the VSME.

AS15 is a combination of a TLR4 agonist [3-O-desacyl-4'- monophosphoryl lipid A (MPL, produced by GSK)], a TLR9 agonist [CpG 7909 synthetic oligodeoxynucleotides containing unmethylated CpG motifs], and *Quillaja saponaria* Molina, fraction 21 (QS-21, Licensed by GSK from Antigenics LLC, a wholly owned subsidiary of Agenus Inc., a Delaware, USA corporation) in a liposomal formulation (13, 14). AS15 has been shown to support T cell and antibody responses to protein vaccines in several phase II and phase III clinical trials in melanoma and NSCLC(13-17), and those TLR4 and TLR9 agonists are employed in other experimental vaccines. We have previously reported immune response data from a clinical trial of vaccination with a MAGE-A3 protein plus AS15(18). Secondary endpoints of that study included evaluation of the VSME for immune cell infiltrates and immune signaling, and biopsies were obtained to enable those analyses. A primary goal of the present manuscript is to assess changes over time at the VSME induced by this regimen.

Prior work in a mouse model has shown that peptide vaccination with a TLR agonist in an aqueous adjuvant induced more durable immune responses than vaccination in IFA, and that IFA induced chronic inflammation at the VSME that recruited and retained T cells there(12). However, we have also previously found that inflammatory adverse events at the vaccine site correlate with prolonged disease-free survival, suggesting that accumulation of immune cells and inflammation at the VSME may in fact be associated with improved clinical outcome in patients receiving these vaccines (19). Additionally, in a separate clinical trial, we observed that adding IFA to a melanoma peptide vaccine led to

higher and more durable T cell responses than using a TLR agonist alone(9). These findings warrant further investigation into the local effects of vaccine adjuvants in human tissues and comparison between vaccine adjuvants. In the present study, we report changes over time in cellular infiltrates and gene expression in the VSME from each of the two clinical trials. We quantified innate and adaptive immune cell infiltration in the VSME and compared early responses (after one vaccine, at one week) and late responses (after multiple vaccine replicates, at weeks 3 and 7) of either AS15 or IFA. By quantifying the immune subsets accumulating in the VSME and associated immune signaling at those sites, we have generated more insight in the importance of adjuvant choice in creating vaccine site inflammation and ultimately systemic antitumor immune responses. We hypothesized that AS15 would promote less chronic inflammation and, thus, less accumulation of innate and adaptive immune cells at the VSME than IFA, and that AS15 would induce less T-cell retention, a stronger Th1-biased microenvironment, and reduced regulatory T-cell accumulation.

MATERIALS AND METHODS

Patients and Trials

Tissue samples were obtained from patients enrolled in the Mel48 (NCT00705640) and Mel55 (NCT01425749) clinical trials at the University of Virginia, which have been reported (20-22). For Mel48, 36 evaluable patients with resected stage IIB-IV melanoma were randomly assigned to 2 study groups based on vaccine regimen, each with 5 subgroups based on date of vaccine site biopsy (Figure 1). Each patient received a 12-melanoma peptide (12MP) vaccine + tetanus helper peptide with incomplete Freund's adjuvant (Montanide ISA-51, Seppic, Inc, Paris, France) in one extremity, administered intradermal/subcutaneously. The majority of patients also received replicate immunizations of adjuvant only (group 1) or peptide vaccine + adjuvant (group 2), administered at a site distant from the original vaccination. Patients underwent biopsy of the replicate vaccine site on days 1, 8, 22, 50, or 85 (subgroups A-E, respectively), after 0, 1, 3, 6 and 6, replicate vaccines, respectively. For the present research project, patients who had biopsies at week 0 (day 1, groups 1A, 2A), week 1 (day 8, groups 1B, 2B), week 3 (day 22, groups 1C, 2C) or week 7 (day 50, groups 1D, 2D) were analyzed (See Supplemental Table 1 for characterization of sample analysis).

In Mel55, 25 eligible patients with resected stage IIB-IV melanoma were randomly assigned to 2 study groups. Each patient received a recombinant MAGE-A3 protein vaccine combined with AS15 Adjuvant System, either intramuscularly (group 1) or intradermal/subcutaneously (group 2), five times at alternating sides in 3-week intervals. Vaccine site biopsies were taken at two time points, on week 1 (day 8) and week 7 (day 50) for patients in group 2.

All patients were studied following informed consent, and with Institutional Review Board (IRB) approval (HSR-IRB 13498 and 15398, respectively) and FDA

approval (BB-IND #12191, 14654). At week 1, both Mel48 and Mel55 patients had received one vaccine. At week 3, Mel48 patients had received 3 vaccines at the same site. By week 7, Mel48 patients had received 6 vaccines at the same site and Mel55 patients had received 3 vaccines, two of which were at the same site.

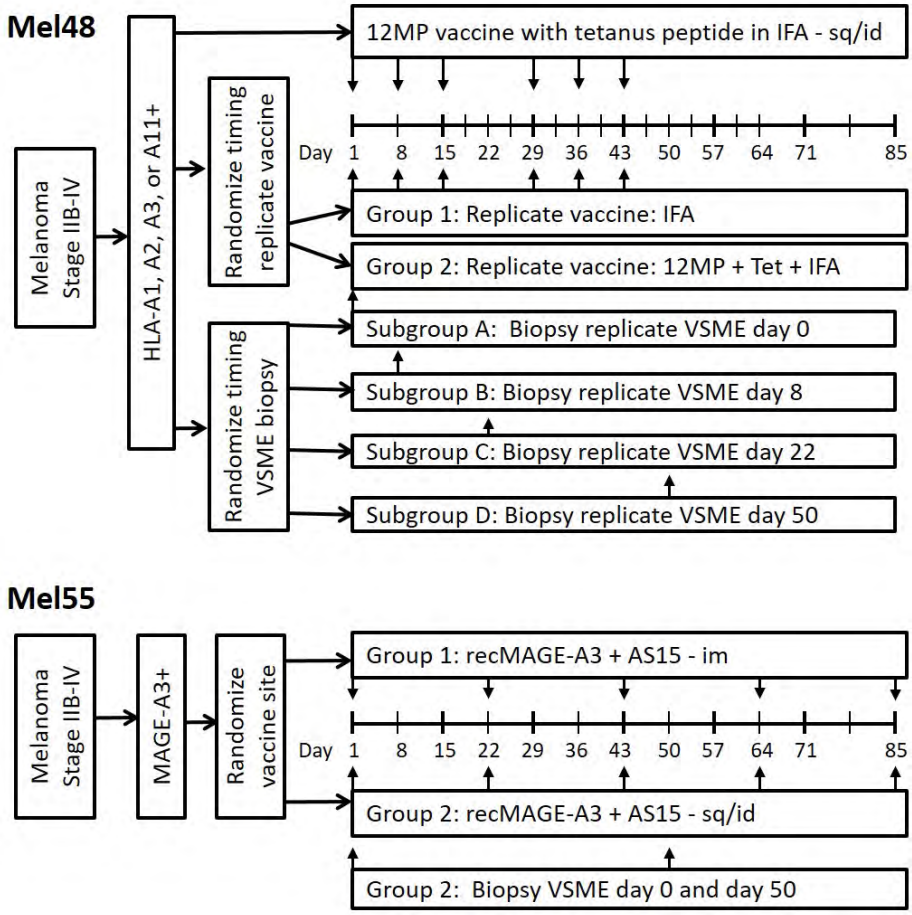

Figure 1. Clinical study designs for MEL48 and MEL55.

Immunohistochemistry and quantification

Vaccine site biopsies were formalin-fixed and paraffin embedded by the Biorepository and Tissue Research Facility (BTRF) at the University of Virginia. Tissues were stained by immunohistochemistry (IHC) with antibodies to CD1a, CD8 and CD20 (DakoCytomation, Denmark), CD4 (Vector, California), CD83 (Novocastra, Maryland), FoxP3 (eBioscience, California), peripheral node addressin (PNAd) and GATA3 (BD Pharmingen, California) and Tbet (Santa Cruz, Texas). The staining protocols used have been reported(21, 23). Cell counts were

enumerated with an automated approach (for CD4, CD8, CD45) or manually by a trained pathologist (for the remainder) and are reported as cells per millimeter squared. Automated cell counts were calculated by the Nikon Elements Software (Nikon, Melville NY) after scanning the slides with Aperio CS slide scanner (Leica Biosystems, Buffalo Grove IL). The algorithm used was first tested by comparing automated and manual counts for selected regions from 10 slides. Resulting counts demonstrated a close correlation (R^2 = 0.939, data not shown). Eosinophils were enumerated manually by a trained pathologist (JP) on Hematoxylin & Eosin (H&E) stained slides. Cells were enumerated separately in deep, mid and superficial layers of the dermis. For final analysis, average cell counts/mm^2 for only the mid and superficial dermis layers were used to compare between trials. Where cell ratio was analyzed and compared, the values were converted to natural log transformed values prior to analysis. The two sample T test was used to test for differences between Mel48 and Mel55 results for each of the two time points, and for differences in time within Mel48. To guide interpretation and adjust for multiple comparisons, a p-value ≤0.005 is considered indicative of a potentially important difference.

RNA extraction and library preparation

Total RNA was isolated from cells collected at the VSME of patients from Mel48 (weeks 0, 1, and 3) and Mel55 (weeks 1 and 7). RNA extraction was performed using the RNeasy Lipid Tissue MiniKit (Qiagen), according to manufacturer instructions. RNA samples were processed for library preparation using the NEBNext Ultra II Directional RNA Library Prep Kit (Illumina), according to validated standard operating procedures established by the UVA School of Medicine's Genome Analysis and Technology Core. Briefly, total RNA was used to isolate mRNA, using NEBNext Poly(A) mRNA Magnetic Isolation Module (New England Biolabs, Inc), followed by fragmentation and first & second-strand cDNA synthesis and fragmentation, following manufacturer recommendations. The resulting cDNA was end-repaired, adenylated, and then subjected to sequence adapter ligation. The final purified libraries were quantified and sized using the Invitrogen Qubit 3 Fluorometer (ThermoFisher Scientific) and Agilent Technologies 4200 TapeStation (Agilent).

Next-Generation sequencing run and QC

RNA sequencing was performed using the Illumina NextSeq 75bp High Output sequencing kit reagent cartridge in conjunction with the Illumina NextSeq 500 (Illumina, San Diego, California; 75 cycles, single read sequencing), according to the standard manufacturer- recommended procedure. Samples were randomized into 4 groups and run sequentially on the Illumina NextSeq 500 for single-end sequencing. After transfer to the Illumina Base Space interface, the quality of the runs was assessed by the numbers of reads in millions passing filter and the % of indexed reads.

RNA sequencing analysis

RNAseq reads were assessed for quality using FastQC. Transcript abundances and were quantified against the human reference genome, (Gencode v28 Transcripts, Ensembl GRCh38) using Salmon(24) and read into the R statistical computing environment as gene-level counts using the tximport package. The DESeq2 Bioconductor package (25) was used to normalize for differences in sequencing depth between samples (using the default median-of-ratios method), estimate dispersion and fit a negative binomial model for each gene. The Benjamini Hochberg False Discovery Rate procedure (26) was then used to re-estimate the adjusted p-values. All statistical analyses and data visualization, including GAGE (27), were done using the R statistical computing environment and GraphPad Prism 8 (GraphPad Software, San Diego, California, USA).

RESULTS

Human subjects

Both trials included patients without clinical evidence of disease, after resection of melanoma (at original diagnosis or restaged at recurrence). The 10 participants of the Mel55 trial whose vaccine site biopsies were evaluated in this study included 40% females, median age 53, stages IIIB-IV based on staging at recurrence, with 70% stage III (70% IIIB/C). The 23 participants of the Mel48 trial evaluated in this study included 30% females, median age 56, stages IIB-IV based on staging at recurrence, with 78% stage III (65% IIIB/C). Details are shown in Supplemental Table 1. All patients on both trials had been rendered clinically free of disease by surgery; so, they were also similar in having no measurable melanoma at the time of study entry.

Accumulation of innate immune cells at the VSME with AS15, compared to IFA

To assess immune cell accumulation over time in the VSME, vaccine site biopsies were assessed by IHC for patients treated with melanoma vaccines using AS15 (Mel55 trial) or IFA (Mel48 trial), at weeks 1 and 7. Histology images from Mel48 patients have been published(21). Representative sections from the Mel55 trial are shown in Figure 2, demonstrating cell aggregates through the dermis that vary among patients. At week 1, numbers of mature DC's (CD83) were higher after IFA compared to AS15 (Figure 3A, $p<0.001$, and numbers of immature DC's (CD1a) trended higher after IFA (Figure 3B, $p=0.007$). Eosinophils were rare in both patient subsets at week 1 (Figure 3C). At week 7, the VSME induced with IFA had increased numbers of all three innate immune cell subsets, compared to the VSME induced with AS15 as adjuvant; however, when adjusted for multiple testing, none are significant ($p> 0.005$, Figure 3A/B/C).

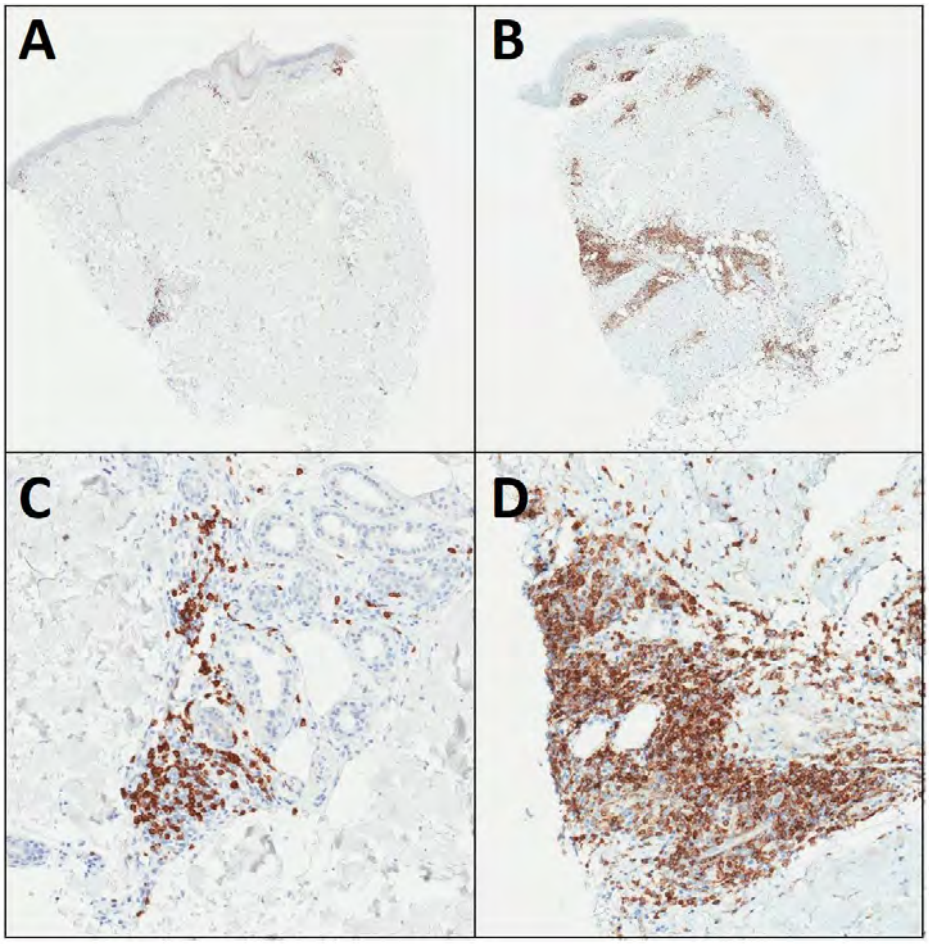

Figure 2. Example IHC stains for CD4 on MEL55 VSME biopsies for patients 15341 **(A)** and 16578 **(B)** one week after vaccination, with high power images in panels **(C)** and **(D)**, respectively. Deep and superficial perivascular dermal lymphoid aggregates are evident in both cases.

Accumulation of adaptive immune cells at the VSME with AS15, compared to IFA

We also evaluated the accumulation of adaptive immune cells: $CD4^+$, $CD8^+$ and $CD20^+$ lymphocytes in the dermis at the VSME. At week 1 (1 week after the first vaccine), $CD8^+$ T cell density trended lower with IFA (Mel48) than with AS15 (Mel55) (Figure 3D, p=0.029). There were no significant differences between the two trials at week 1 in accumulation of $CD4^+$ T cells (p=0.079) or $CD20^+$ B cells (p=0.081, Figure 3E/F). However, after 7 weeks, Mel48 VSMEs had increased accumulation of $CD4^+$ T cells, $CD8^+$ T cells, and B cells compared to week 1, whereas patients in Mel55 did not (Figure 3D/E/F). VSME densities of CD8 T cells

and B cells were significantly greater at week 7 for Mel48 patients than Mel55 patients (p = 0.003, p<0.0001, respectively) and there was a trend for more CD4 T cells (p=0.015). These data suggest that repeat vaccination with IFA at the same site enhances inflammation and durable accumulation of T and B lymphocytes, whereas AS15 only induced short-term accumulation of T cells.

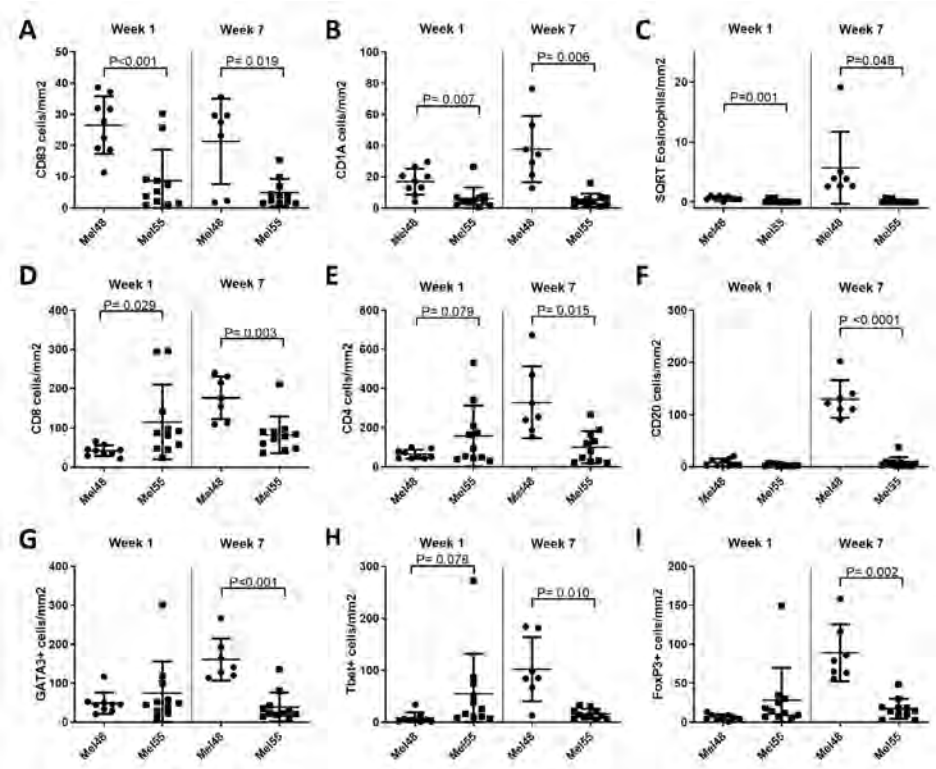

Figure 3. Number of immune cells per mm2 of vaccine site biopsies in both the superficial and mid deep layers of the skin. Displayed are number of CD83+ cells **(A),** CD1A+ cells **(B),** and square root of Eosinophils **(C),** $CD8^+$ cells **(D),** $CD4^+$ cells **(E),** $CD20^+$ cells **(F),** $GATA3^+$ cells **(G),** $Tbet^+$ cells **(H)** or $FoxP3^+$ cells **(I)** week 1 and week 7 after the first vaccine in MEL48 (with IFA) and MEL55 (with AS15). All p values have been corrected for false-discovery rate as stated in the methods and statistical significance was determined at p<0.005.

Vaccines sites that received IFA had higher expression of retention integrin subunits alpha1 and beta1 and homing receptor subunits alpha4 and beta7

We have previously observed that T cells accumulating at vaccine sites have high expression of retention integrins α1β1, α2β1, αEβ7(20). Therefore, we hypothesized that expression of these retention integrins, as well as the homing integrin α4β7, would be induced in highly inflamed vaccine sites induced by

IFA in Mel48. To evaluate expression of these molecules, we compared VSME-derived gene expression data from Mel48 and Mel55 trials. For these studies, VSME biopsies were evaluated by RNAseq from weeks 1 and 7 from the Mel55 trial and from weeks 1 and 3 from the Mel48 trial. The alpha chains α1 and α2 only dimerize with β1, and αE only dimerizes with β7; thus, expression of α1β1, α2β1, αEβ7 can be evaluated by expression of the genes corresponding to the alpha chains (ITGA1, ITGA2, and ITGAE, respectively). ITGA4 and ITGB7 encode α4 and β7, respectively. Expression of ITGA1, ITGB1, ITGA4, and ITGB7 were significantly enhanced at week 3 post vaccination with IFA (Mel48 W3) compared to normal skin, Mel48 week 1 and Mel55 (Supplemental Figure 1). In contrast, ITGA2 (α2) and ITGAE (αE) did not increase in either trial, suggesting that cells accumulating at the vaccine sites treated with IFA may use alpha4beta7 to home and alpha1beta1 to be retained at the site.

Th2/Th1 and CD8/FoxP3 ratios at the VSME

To assess the Th1 and Th2 phenotype of T lymphocytes in the VSME, biopsies were evaluated by IHC for transcription factors Tbet, GATA3, and FoxP3, which mediate Th1, Th2, and Treg programming, respectively. There were more $CD4^+$ and $CD8^+$ T cells in the VSME of Mel48 at week 7 compared to Mel55 (Figure 3) (21); thus, it is not surprising that more $Tbet^+$, $GATA3^+$ and $FoxP3^+$ cells were evident at this time point (Figure 3G/H/I); however, proportions of those cells are likely more informative about the VSME. At week 1, the GATA3/Tbet ratio was significantly lower in Mel55 than for Mel48 p=0.004, Figure 4A). However, by week 7, the GATA3/Tbet ratio was similarly low for both trials. This was explained by a significant decrease in the ratio in the Mel48 samples, as previously reported(21) and as evident in Figure 4A (p=0.005), but no change was evident in that ratio over time for Mel55 samples. However, the Th2/Th1 ratio remains above 1, indicating that, regardless of the adjuvant, the VSME appears to be Th2-dominant by this measure (Figure 4A/C).

Also evaluated was the accumulation of $FoxP3^+$ cells, which likely represent regulatory T cells. At week 1, the proportions of $FoxP3^+$ cells were similar in patients from both trials (Figure 4C), and the CD8/FoxP3 ratios were similarly high (Figure 4B). On the other hand, proportional density of $FoxP3^+$ cells increased by week 7 in the IFA samples (Mel48, Figure 4C), accompanied by a decrease in CD8/FoxP3 ratio (Figure 4B, p=0.003). The same change was not seen with vaccines containing AS15 (Mel55), so that the CD8/FoxP3 ratios at week 7 were significantly lower for Mel48 than for Mel55 ($p<0.001$, Figure 4B).

Peripheral node addressin is expressed in vaccine sites of patients treated with AS15 as adjuvant

Peripheral node addressin (PNAd) is the classic ligand for L-selectin, enabling naïve T cells to recognize high endothelial venules in lymph nodes as a critical first step enabling transmigration into the node(29). We have previously reported

that PNAd⁺ HEV-like vessels can be induced, in association with lymph node like structures, in the VSME of some patients after repeated injection of vaccines in IFA(23). Staining the VSME for PNAd after AS15 injections identified PNAd⁺ vasculature, surrounded by immune cells in VSME biopsies of 3 out of 12 patients (4/22 specimens: 2/11 at week 1 and 2/11 at week 7, Figure 5). This suggests that AS15 may be capable of generating tertiary lymphoid structures (TLS) containing high-endothelial venues in some patients.

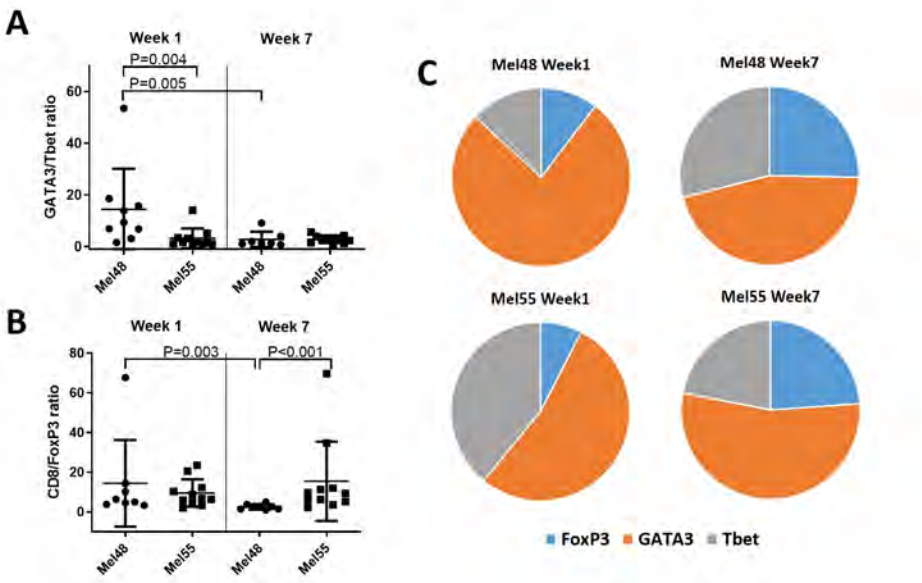

Figure 4. (A) Ratio of GATA3⁺ cells to Tbet⁺ cells in the VSME in MEL48 and MEL55 both week 1 and week 7 after the first vaccine. **(B)** Ratio of CD8⁺ cells to FoxP3⁺ cells in the VSME in MEL48 and MEL55 both week 1 and week 7 after the first vaccine. For panels A and B, means and standard deviations are shown in addition to values for each sample. **(C)** Relative proportions of FoxP3⁺, Tbet⁺, and GATA3⁺ cells in the VSME dermis are shown for both trials and both time points. All p values have been corrected for false-discovery rate as stated in the methods and statistical significance was determined at $p<0.005$.

AS15 and IFA induce expression of TLS –associated genes

To evaluate factors that may contribute to TLS formation in AS15- and IFA-treated VSME, we compared VSME-derived gene expression data from both trials. A list of target genes was developed based upon a previously defined 12- chemokine TLS-associated gene signature(30), plus 6 additional genes (BAFF, APRIL, LIGHT, lymphotoxin alpha [LTA], lymphotoxin beta [LTB], CD20), which have been shown in other work to be correlated with TLS formation(31-38).

Compared to control normal skin, there were significant ($p<0.05$) increases in expression of 16 of these 18 genes in the VSME skin 1 week after AS15 injection

(Mel55 week 1, Figure 6 & Supplemental Table 2). By week 7, mean expression had dropped in 5/18 of the TLS-associated genes, compared to the week 1 time point, with only 8 genes significantly increased at week 7 compared to normal skin ($p<0.05$). These findings are consistent with the reduced immune cell accumulation upon repeat vaccination with AS15.

In contrast, in IFA-treated samples, there were no significant increases in TLS-associated gene expression over control at week 1 (Mel48 week 1, Figure 6). Compared to the AS15 treated samples, mean expression at week 1 was significantly lower in the IFA-treated samples for 4 of the genes. However, expression of these TLS-associated genes increased significantly upon repeat vaccination with IFA. By week 3, 16/18 genes were more highly expressed in IFA treated patients over control normal tissue ($p<0.05$), with 16 of them significantly higher in IFA-treated samples than in AS15 treated samples after the 3rd vaccine.

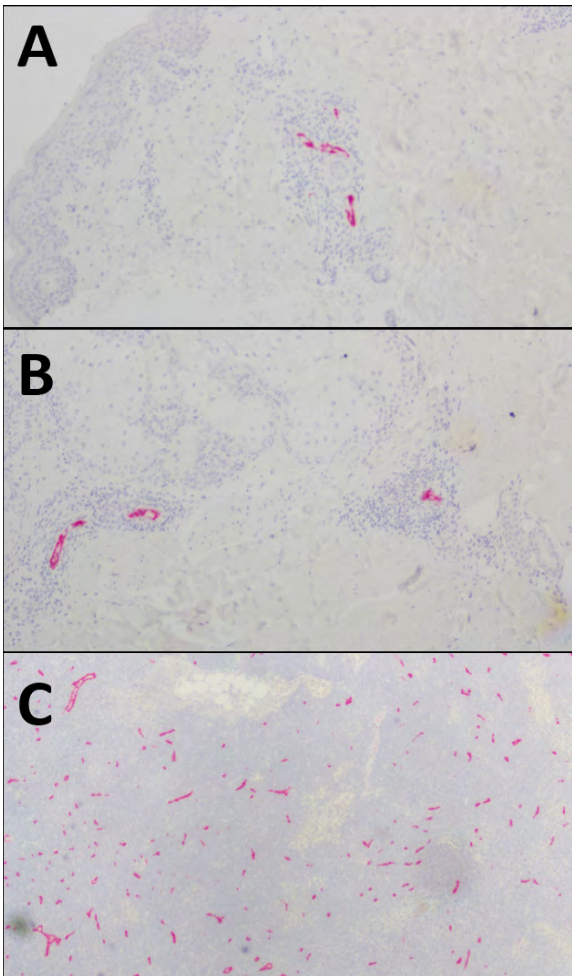

Figure 5. Examples of PNAd staining in vaccine sites of MEL55 in superficial dermis **(A)** and deep dermis/subcutaneous **(B).** Normal lymph node was used as control **(C).** Small hematoxylin-staining nuclei clustered around PNAd+ vessels in **A** and **B** are consistent with lymphocytes and other immune cells.

Comprehensive analysis of changes at vaccine site after AS15 adjuvant

In addition to the TLS-associated gene signature, we aimed to more comprehensively analyze changes in gene expression at the VSME post AS15 injection and to compare these to known gene expression changes by IFA(39). Differential gene expression was determined as >5-fold change over normal skin with and adjusted P-value of <0.05 (40). Overall, AS15-containing vaccines induced a total of 657 genes that were differentially expressed for both time points combined, with 554 upregulated and 103 downregulated genes (Supplemental Figure 2A/B). The vast majority of differentially expressed genes were only present at day 8 post vaccination, though 149 (up) and 58 (down) were differentially expressed at both time points (Supplemental Figure 2A/B). Genes upregulated at both time points included T cell markers, DC markers and granzymes. Similarly, pathways for T cell receptor signaling, antigen processing and presentation and leukocyte trafficking were upregulated in both time points, compared to normal skin (Supplemental Table 3). This suggests that, despite the lower and less durable accumulation of T cells and DCs at the VSME of AS15 vaccinated patients when compared to Mel48, they are significantly more present and durable when compared to normal skin. Therefore, AS15 does induce durable immune accumulation at the vaccine site, though not to the same extent as IFA.

AS15 and IFA induced components of FAS-mediated apoptosis pathway

Our data showed that despite a larger and more durable accumulation of DC and T cells at the VSME with IFA compared to AS15, there was significant and sustained increased T cell gene expression and other immune-related pathways with AS15 compared to normal skin. Murine studies have shown that IFA actually induced high accumulation at the VSME, but at the same time induced T cell deletion and immune suppression mediated by myeloid-derived suppressor cells (MDSCs) and FAS-FASL driven T cell killing (12). Thus, we hypothesized that MDSC-related genes and genes involved in FAS signaling were induced after IFA but not AS15. Interestingly, MDSC-specific genes were not upregulated by either IFA or AS15 besides generic myeloid marker CD14 (Figure 7A-D). In fact, in addition to previously reported Arginase-1(39), GITR and Syndecan-4 were downregulated after IFA. All three MDSC-related genes were unchanged after AS15 compared to control skin (Figure 7B-E). Other suppressive molecules PD-L1 and IDO were increased significantly after IFA and AS15, though to a lesser extent and not durably with AS15 compared to IFA (Figure 7F/G). This suggests there are suppressive mechanisms at play at the VSME of patients vaccinated with IFA or AS15. Similarly, components of the FAS-mediated apoptosis pathway were induced with both AS15 and IFA, though this was only extended to the later time point with IFA (Figure 7H-L). However, inhibitor of FAS-mediated killing FLIP was expressed at high levels at the same time point after IFA (Figure 7M), though never with AS15, suggesting that there may be negative feedback loop dampening T cell deletion after IFA but not AS15. Thus, accumulation of immune cells, vaccination with AS15 may not be accompanied by inhibition or deletion to the same extent as IFA, leading to fewer in number, but more functional immune cells.

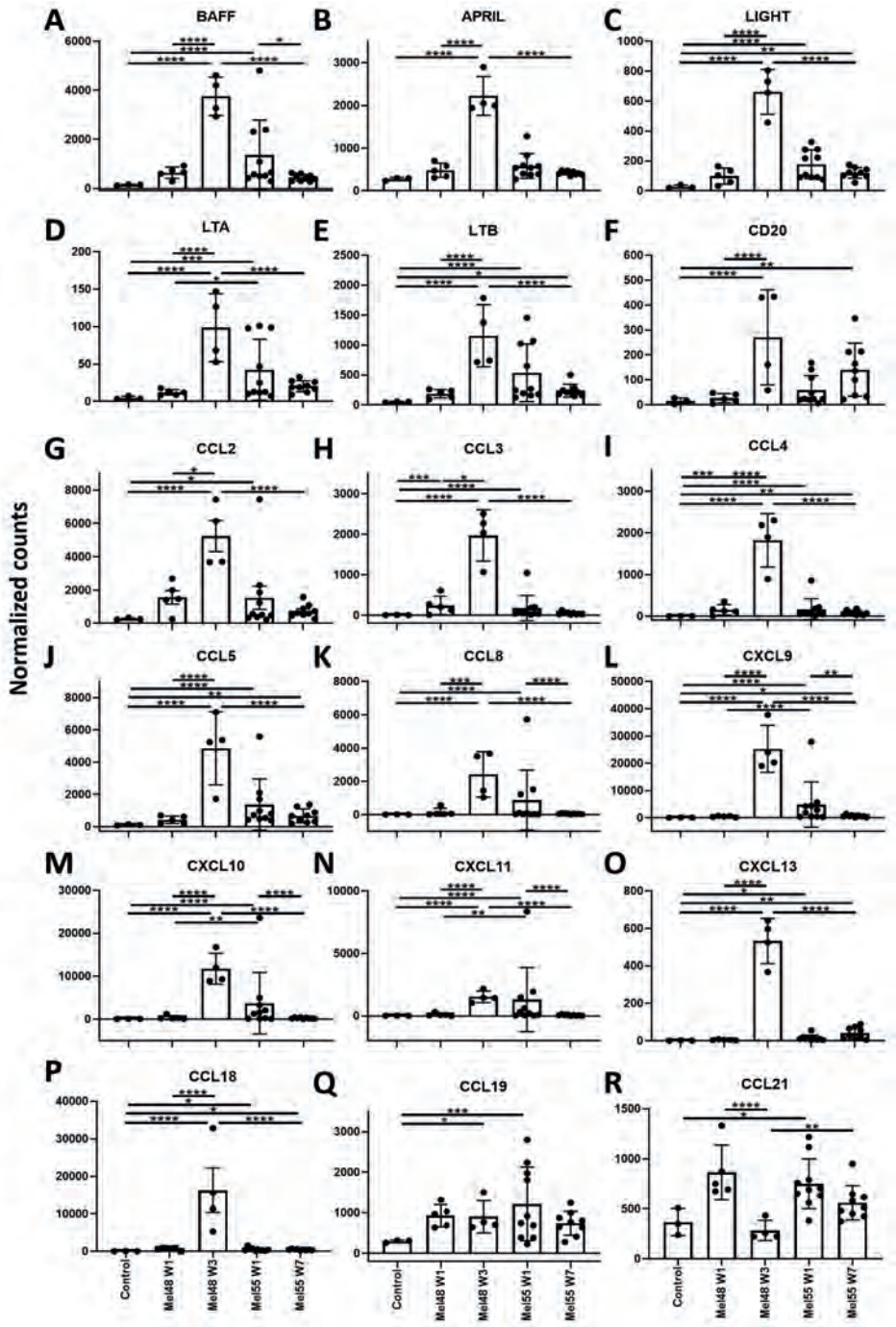

Figure 6. Individual gene expression of eighteen genes that have been previously associated with TLS formation: **(A)** BAFF, **(B)** APRIL, **(C)** LIGHT, **(D)** Lymphotoxin alpha, **(E)** Lymphotoxin beta, **(F)** CD20, **(G)** CCL2, **(H)** CCL3, **(I)** CCL4, **(J)** CCL5, **(K)** CCL8, **(L)** CXCL9,

(M) CXCL10 **(N)** CXCL11, **(O)** CXCL13 **(P)** CCL18, **(Q)** CCL19, **(R)** CCL21. Expression data was obtained from vaccine site biopsies of patients treated with IFA (MEL48) or AS15 (MEL55), as well as normal tissue obtained pre-vaccination for control purposes (n=3). For patients treated with IFA, gene expression is shown at week (w) 1 (n=5), and week 3 (n=4), following initial vaccination at a site separate from the biopsied tissue. For patients treated with AS15, gene expression is shown at week 1 (n=10) and week 7 (n=9) , following initial vaccination at a distant site. For factors of significance: * p <0.05, ** p < 0.01, *** p < 0.001, **** p < 0.0001; derived from differential gene expression.

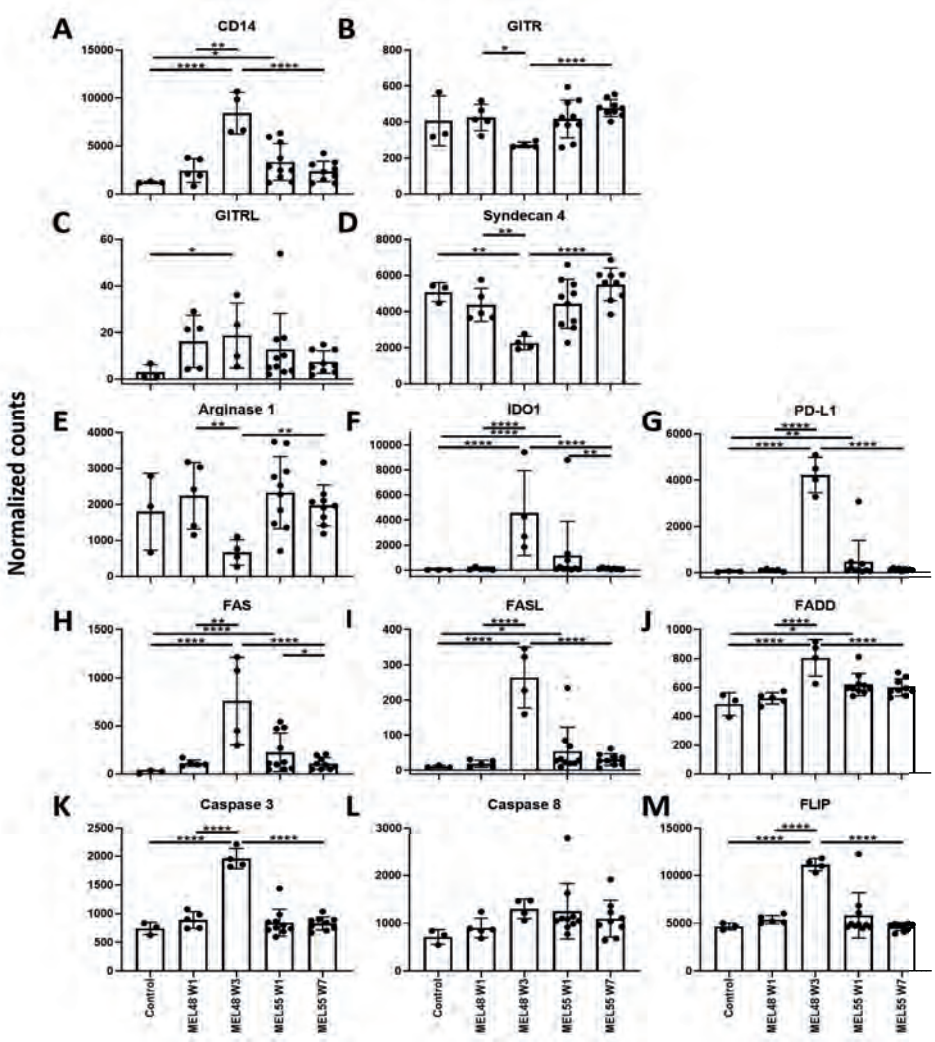

Figure 7. Individual gene expression of MDSC-related genes **(A-D)**, inhibitory molecule genes **(E-G)** and genes involved in FAS-mediated apoptosis **(H-M)**. Expression data was obtained from vaccine site biopsies of patients treated with IFA (MEL48) or AS15 (MEL55), as well as normal tissue obtained pre-vaccination for control purposes (n=3). For patients

treated with IFA, gene expression is shown at week (w) 1 (n=5), and week 3 (n=4), following initial vaccination at a site separate from the biopsied tissue. For patients treated with AS15, gene expression is shown at week 1 (n=10) and week 7 (n=9) , following initial vaccination at a distant site. For factors of significance: * $p < 0.05$, ** $p < 0.01$, *** $p < 0.001$, **** $p < 0.0001$; derived from differential gene expression.

DISCUSSION

In this study, we have analyzed the VSME following immunization with a MAGE-A3/AS-15 vaccine at two time points and compared findings to similar time points from a separate clinical trial using IFA as an adjuvant. There were significant differences in the VSME between the two immunotherapeutic approaches. The findings support our hypothesis that a vaccine containing AS15 would induce less accumulation of innate and adaptive immune cells, as well as $FoxP3^+$ cells, at the VSME than a vaccine incorporating IFA. Lymphocyte accumulation differed significantly between the two groups, with $CD8^+$ T cells, B cells, and $FoxP3^+$ cells all accumulating within the VSME in significantly higher numbers by week 7 in Mel48 samples than Mel55. While the increase in $FoxP3^+$ cells within the IFA-induced VSME at week 7 could suggest a transition to a more suppressive environment over time, it is also important to recognize that more regulatory T cells are expected in an inflammatory environment, as CCL22 production by activated CD8 T cells effectively recruits these cells. Additionally, despite the greater accumulation of immune cells at the VSME with IFA, expression of DC- and T cell-related genes was induced with AS15 compared to normal skin. Furthermore, in addition to greater $FoxP3^+$ cell accumulation, CD8 T cell inhibitory pathways, including PD-L1 and IDO, were also increased with IFA, compared to AS15, though both adjuvants induced PD-L1 and IDO over normal skin. Neither induced MDSC suppressive pathways. These results suggest that AS15 induces a less suppressive environment than IFA, but this is accompanied with low levels of immune cell accumulation. Future analysis will have to determine whether the suppressive and inhibitory mechanisms at the VSME are a direct result of the increased inflammation and whether this inflammation and accumulation of immune cells is beneficial or harmful to the induction and/or maintenance of the systemic response.

Regardless of the density of lymphocytes at the vaccine site, there appears to be a Th2-dominant phenotype, both in Mel48 and Mel55 at weeks 1 and 7. The Th2 cytokine IL-5 can induce eosinophils; thus, additional evidence for Th2 dominance in the VSME after IFA included a marked accumulation of eosinophils identified at week 7 for the Mel48 patients(21, 41); however, this was not seen in the Mel55 trial with AS15 (Figure 3C), suggesting that the slight GATA3 dominance in Mel55 was not sufficient to enhance eosinophils in the VSME, and that the much higher GATA3/Tbet ratio early in IFA-injected sites may have a greater biologic effect.

We have previously reported that $CD8^+$ T cells retained at vaccine sites have increased expression of the retention integrins α1β1, α2β1, and αEβ7, which may explain a mechanism for their retention in the peripheral tissues(20). Here we find that gene expression for integrin subunits α1and β1 are significantly induced by vaccination with IFA, suggesting an increase in infiltration of cells expressing the α1β1 integrin. T cells expressing α1β1 (VLA-1, CD49a) have been identified as long-lived resident-memory T cells in peripheral tissues(42-44); so, their presence in vaccine sites may be favorable, and is not entirely consistent with the findings in murine studies where T cells recruited to vaccine sites do not survive there long-term(12).

The enhanced accumulation of B cells in the Mel48 trial patients may reflect TLS development, as B cell clusters are critical components of TLS. TLS accommodate recruitment and activation of naïve T cells, are observed in chronically inflamed tissues, and can support antigen-specific T cell responses(45-48); so, the formation of these structures could potentially enhance T cell reactivity of vaccines. We have previously demonstrated that IFA-containing vaccines can induce formation of TLS in the VSME, including ($DC\text{-}LAMP^+$ $CD83^+$) DC in 12/18 patients(23). Upon single vaccination with IFA alone, TLS formation was somewhat disorganized, peaked within 1 week following injection, and dissipated after about 2 weeks(23). However, repeated vaccination with IFA, together with melanoma peptides, induced more prominent and organized TLS formation, including organized B and T cells areas as well as expression of lymphoid-associated chemokines, including CXCL13 and CCL21(23). In the present study, we observed the changing expression of TLS-associated genes over time, following both single and repeat vaccination with IFA or AS15. Our data support and expand upon our previous findings. One week following one vaccine with IFA, a modest increase in TLS-associated gene expression was observed compared to normal tissue. Repeat vaccination with IFA appears to augment this response, as demonstrated by the dramatic increase in gene expression seen when comparing the effects of 1 versus 3 vaccinations.

The immune cell infiltration data suggest that IFA enhances infiltration of immature and mature DC. Classically, inflammation in the skin induces maturation of Langerhans cells and dermal DC, and those maturing DC migrate to the draining nodes within hours to a few days(49-51). Thus, the greater accumulation of mature ($CD83^+$) DC in the IFA group suggests that this adjuvant either slows DC migration to the draining nodes or supports DC maturation on a continuing basis after vaccine administration. It is possible that many of the adaptive immune cells present in the VSME at week 7 in Mel48 samples may be residing in TLS, potentially serving as sites of further, long-term antigen-specific immune cell activation in situ. It may follow then that the accumulation of DC in the VSME upon vaccination with IFA can be explained, at least in part, by retention of DC in TLS in the VSME, where they may be able to support presentation of antigen locally.

While our data also support the ability of AS15 to induce TLS formation, the extent, composition, and timeline for development appear to differ from that of IFA. Specifically, single vaccination with AS15 induced TLS-associated gene expression to a stronger degree than that of single vaccination with IFA. However, despite the increased gene expression, AS15-treated biopsy sites had lesser accumulation of $CD83^+$ DC, compared to IFA-treated sites at a similar time point. Furthermore, unlike the augmented response seen upon repeated vaccination with IFA, TLS-associated gene expression either declined or remained stable following repeat vaccination with AS15. PNAd staining and immune cell infiltration data corroborate this finding, as the number of $PNAd^+$ biopsy sites did not increase with repeated AS15 vaccination (Figure 5). Similarly, the accumulation of immune cells remained stable between the two vaccination time points. Thus, it appears that while single vaccination with AS15 induces TLS-gene expression to a greater degree than IFA after 1 week, the latter agent may induce secondary effects that evolve over time but support stronger, more durable TLS formation. Previous studies have found that the structure and formation of TLS's vary depending upon certain variables, including anatomical site and tumor type(38). In light of our findings, it seems plausible that vaccination composition may also affect the formation and possibly even the function of TLS.

A limitation of the comparisons between the two studies is that, in addition to differences in the adjuvants, there were differences in the antigen used between the trials: AS15 was combined with recombinant MAGE-A3 protein, whereas IFA was combined with 12 short melanoma peptides. Protein antigens and peptide are different in that protein must be processed by professional APCs, whereas peptides may bind directly to cell surface MHC. However, both vaccines have induced both CD8 and CD4 T cell responses(5, 18, 20). Also, the peptide vaccine included a MAGE-A3 peptide and three other MAGE-A antigens(20, 52); so, there is some antigenic similarity with the MAGE-A3 protein. We have previously found that immune cell infiltrates and gene expression changes induced locally at the VSME appear to be attributable to the adjuvant more than to the antigen(21, 39). Thus, we anticipate that differences at the VSME between these studies are likely to be driven primarily by the adjuvant, though we acknowledge potential impact of the antigen on the cellular and gene expression changes. Another limitation of the present study is that biopsies were evaluated at limited time points after vaccination, whereas VSME infiltrates evolve over time. IFA-based emulsions create a long-term antigen-depot, but aqueous vaccines like the MAGE-A3/AS15 vaccines likely dissipate over hours to days, which coincides with clinical resolution of initial redness and inflammation. Since biopsies were taken 7 days after vaccine administration, there may well have been strong effects on T cell activation within those 7 days, which are missed by the time of biopsy. Thus, evaluation 1-2 days after AS15 vaccines may reveal greater inflammatory cell infiltrates than those one week after the vaccine. Our results from week 7 are also limited by differences in vaccine schedules. because the number of vaccines before week 7 differ. However, the VSME evaluations at week 1 are comparable. In summary, our data highlight effects of vaccine adjuvants AS15 and IFA on the

VSME. We found less accumulation of innate and adaptive immune cells within the AS15-induced VSME, compared to that of IFA. Though AS15 still induced T cell- and DC-related genes compared to normal skin. The AS15-induced VSME featured a lower number of inflammatory cells, as well as less accumulation of $FoxP3^+$ cells, while IFA induced increases in $FoxP3^+$ cells over time. Similarly, AS15 induced lower levels of CD8 inhibitory pathways PD-L1 and IDO. The CD8/FoxP3 ratio was higher with AS15 vaccines than IFA-containing vaccines, suggesting that the reduction in $FoxP3^+$ cells with AS15 is due to more than just a proportional decrease in overall immune cell infiltration. Interestingly, AS15 vaccines induced a more Th1-dominant VSME than IFA vaccines, at 1 week, but this difference did not persist with repeated vaccination based on biopsies at week 7. Evidence of TLS formation was demonstrated with both adjuvants, though $PNAd^+$ vasculature was observed in a smaller number of patients on the Mel55 trial than we have previously reported with IFA-based vaccines. Similarly, TLS-associated gene signature expression appeared to be more transient in vaccination site biopsies taken from AS15 treated patients, compared to their IFA treated counterparts. Our findings represent new findings about the dynamic effects of adjuvants on the VSME and suggest the need for future studies to determine which of these effects support optimal systemic T cell responses to vaccines.

ACKNOWLEDGEMENTS

We thank the Biorepository and Tissue Research Facility (BTRF) for their help with purifying RNA from or paraffin embedding of patient tumor materials.

REFERENCES

1. Postow MA, Callahan MK, Wolchok JD (2015) Immune Checkpoint Blockade in Cancer Therapy. J Clin Oncol. 33: 1974-82. doi: 10.1200/jco.2014.59.4358
2. Nishino M, Ramaiya NH, Hatabu H, Hodi FS (2017) Monitoring immune-checkpoint blockade: response evaluation and biomarker development. Nature reviews. Clinical oncology. 14: 655-68. doi: 10.1038/nrclinonc.2017.88
3. Cheever MA, Higano CS (2011) PROVENGE (Sipuleucel-T) in prostate cancer: the first FDA-approved therapeutic cancer vaccine. Clin Cancer Res. 17: 3520-6. doi: 10.1158/1078-0432.ccr-10-3126
4. Schwartzentruber DJ, Lawson DH, Richards JM et al. (2011) gp100 peptide vaccine and interleukin-2 in patients with advanced melanoma. N. Engl. J Med. 364: 2119-27.
5. Slingluff CL, Jr., Petroni GR, Smolkin ME et al. (2010) Immunogenicity for $CD8^+$ and $CD4^+$ T cells of two formulations of an incomplete Freund's adjuvant for multipeptide melanoma vaccines. Journal of Immunotherapy. 33: 630-8. doi: 10.1097/CJI.0b013e3181e311ac
6. Gnjatic S, Sawhney NB, Bhardwaj N (2010) Toll-like receptor agonists: are they good adjuvants? Cancer J. 16: 382-91.
7. Hyer RN, Janssen RS (2019) Immunogenicity and safety of a 2-dose hepatitis B vaccine, HBsAg/CpG 1018, in persons with diabetes mellitus aged 60-70years. Vaccine. 37: 5854-61. doi: 10.1016/j.vaccine.2019.08.005
8. Sabbatini P, Tsuji T, Ferran L et al. (2012) Phase I trial of overlapping long peptides from a tumor self-antigen and poly-ICLC shows rapid induction of integrated immune response in ovarian cancer patients. Clin Cancer Res. 18: 6497-508. doi: 10.1158/1078-0432.ccr-12-2189
9. Melssen MM, Petroni GR, Chianese-Bullock KA et al. (2019) A multipeptide vaccine plus toll-like receptor agonists LPS or polyICLC in combination with incomplete Freund's adjuvant in melanoma patients. J Immunother Cancer. 7: 163. doi: 10.1186/s40425-019-0625-x
10. Baumgaertner P, Costa Nunes C, Cachot A et al. (2016) Vaccination of stage III/IV melanoma patients with long NY-ESO-1 peptide and CpG-B elicits robust CD8(+) and CD4(+) T-cell responses with multiple specificities including a novel DR7-restricted epitope. Oncoimmunology. 5: e1216290. doi: 10.1080/2162402x.2016.1216290
11. Speiser DE, Lienard D, Rufer N, Rubio-Godoy V, Rimoldi D, Lejeune F, Krieg AM, Cerottini JC, Romero P (2005) Rapid and strong human CD8+ T cell responses to vaccination with peptide, IFA, and CpG oligodeoxynucleotide 7909. Journal of Clinical Investigation. 115: 739-46.
12. Hailemichael Y, Dai Z, Jaffarzad N et al. (2013) Persistent antigen at vaccination sites induces tumor-specific CD8(+) T cell sequestration, dysfunction and deletion. Nat. Med. 19: 465-72.
13. Kruit WH, Suciu S, Dreno B et al. (2013) Selection of immunostimulant AS15 for active immunization with MAGE-A3 protein: results of a randomized phase II study of the European Organisation for Research and Treatment of Cancer Melanoma Group in Metastatic Melanoma. J Clin. Oncol. 31: 2413-20.
14. Kruit WH, Suciu S, Dreno B, al. e (2008) Immunization with recombinant MAGE-A3 protein combined with adjuvant systems AS15 or AS02B in patients with unresectable

and progressive metastatic cutaneous melanoma: A randomized open-label phase II study of the EORTC Melanoma Group (16032-18031). Journal of Clinical Oncology. 26: abstract 9065.
15. Gutzmer R, Rivoltini L, Levchenko E et al. (2016) Safety and immunogenicity of the PRAME cancer immunotherapeutic in metastatic melanoma: results of a phase I dose escalation study. ESMO open. 1: e000068. doi: 10.1136/esmoopen-2016-000068
16. Vansteenkiste JF, Cho BC, Vanakesa T et al. (2016) Efficacy of the MAGE-A3 cancer immunotherapeutic as adjuvant therapy in patients with resected MAGE-A3-positive non-small-cell lung cancer (MAGRIT): a randomised, double-blind, placebo-controlled, phase 3 trial. Lancet Oncol. 17: 822-35. doi: 10.1016/s1470-2045(16)00099-1
17. Dreno B, Thompson JF, Smithers BM et al. (2018) MAGE-A3 immunotherapeutic as adjuvant therapy for patients with resected, MAGE-A3-positive, stage III melanoma (DERMA): a double-blind, randomised, placebo-controlled, phase 3 trial. Lancet Oncol. 19: 916-29. doi: 10.1016/s1470-2045(18)30254-7
18. Slingluff CL, Jr., Petroni GR, Olson WC et al. (2015) A randomized pilot trial testing the safety and immunologic effects of a MAGE-A3 protein plus AS15 immunostimulant administered into muscle or into dermal/subcutaneous sites. Cancer Immunol Immunother. doi: 10.1007/s00262-015-1770-9
19. Hu Y, Smolkin ME, White EJ, Petroni GR, Neese PY, Slingluff CL, Jr. (2014) Inflammatory adverse events are associated with disease-free survival after vaccine therapy among patients with melanoma. Ann Surg Oncol. 21: 3978-84. doi: 10.1245/s10434-014-3794-3
20. Salerno EP, Shea SM, Olson WC, Petroni GR, Smolkin ME, McSkimming C, Chianese-Bullock KA, Slingluff CL, Jr. (2013) Activation, dysfunction and retention of T cells in vaccine sites after injection of incomplete Freund's adjuvant, with or without peptide. Cancer Immunol Immunother. 62: 1149-59. doi: 10.1007/s00262-013-1435-5
21. Schaefer JT, Patterson JW, Deacon DH, Smolkin ME, Petroni GR, Jackson EM, Slingluff CL, Jr. (2010) Dynamic changes in cellular infiltrates with repeated cutaneous vaccination: a histologic and immunophenotypic analysis. J Transl Med. 8: 79. doi: 10.1186/1479-5876-8-79
22. Slingluff CL, Jr., Petroni GR, Olson WC et al. (2016) A randomized pilot trial testing the safety and immunologic effects of a MAGE-A3 protein plus AS15 immunostimulant administered into muscle or into dermal/subcutaneous sites. Cancer Immunol Immunother. 65: 25-36. doi: 10.1007/s00262-015-1770-9
23. Harris RC, Chianese-Bullock KA, Petroni GR, Schaefer JT, Brill LB, 2nd, Molhoek KR, Deacon DH, Patterson JW, Slingluff CL, Jr. (2012) The vaccine-site microenvironment induced by injection of incomplete Freund's adjuvant, with or without melanoma peptides. J Immunother. 35: 78-88. doi: 10.1097/CJI.0b013e31823731a4
24. Patro R, Duggal G, Love MI, Irizarry RA, Kingsford C (2017) Salmon provides fast and bias-aware quantification of transcript expression. Nature methods. 14: 417-9. doi: 10.1038/nmeth.4197
25. Love MI, Huber W, Anders S (2014) Moderated estimation of fold change and dispersion for RNA-seq data with DESeq2. Genome Biol. 15: 550. doi: 10.1186/s13059-014-0550-8
26. Benjamini Y, Hochberg Y (1995) Controlling the false discovery rate: a practical and powerful approach to multiple testing. Journal of the Royal Statistical Society Series

B. 57: 289-300.
27. Luo W, Friedman MS, Shedden K, Hankenson KD, Woolf PJ (2009) GAGE: generally applicable gene set enrichment for pathway analysis. BMC Bioinformatics. 10: 161. doi: 10.1186/1471-2105-10-161
28. Erdag G, Schaefer JT, Smolkin ME, Patterson JW, Petroni GR, Slingluff CL (2010) Immunohistological Characterization of Tumor Infiltrating Immune Cells in Metastatic Melanomas. Journal of Immunotherapy. 33: 881-2.
29. Girard JP, Moussion C, Förster R (2012) HEVs, lymphatics and homeostatic immune cell trafficking in lymph nodes. Nature reviews. Immunology. 12: 762-73. doi: 10.1038/nri3298
30. Messina JL, Fenstermacher DA, Eschrich S et al. (2012) 12-Chemokine Gene Signature Identifies Lymph Node-like Structures in Melanoma: Potential for Patient Selection for Immunotherapy? Scientific reports. 2. doi: 10.1038/srep00765
31. Jonsson MV, Szodoray P, Jellestad S, Jonsson R, Skarstein K (2005) Association between circulating levels of the novel TNF family members APRIL and BAFF and lymphoid organization in primary Sjögren's syndrome. J Clin Immunol. 25: 189-201. doi: 10.1007/s10875-005-4091-5
32. Grogan JL, Ouyang W (2012) A role for Th17 cells in the regulation of tertiary lymphoid follicles. Eur J Immunol. 42: 2255-62. doi: 10.1002/eji.201242656
33. Barone F, Gardner DH, Nayar S, Steinthal N, Buckley CD, Luther SA (2016) Stromal Fibroblasts in Tertiary Lymphoid Structures: A Novel Target in Chronic Inflammation. Front Immunol. 7: 477. doi: 10.3389/fimmu.2016.00477
34. Ciccia F, Rizzo A, Maugeri R et al. (2017) Ectopic expression of CXCL13, BAFF, APRIL and LT-beta is associated with artery tertiary lymphoid organs in giant cell arteritis. Ann Rheum Dis. 76: 235-43. doi: 10.1136/annrheumdis-2016-209217
35. Pipi E, Nayar S, Gardner DH, Colafrancesco S, Smith C, Barone F (2018) Tertiary Lymphoid Structures: Autoimmunity Goes Local. Front Immunol. 9: 1952. doi: 10.3389/fimmu.2018.01952
36. Weinstein AM, Storkus WJ (2015) Therapeutic Lymphoid Organogenesis in the Tumor Microenvironment. Adv Cancer Res. 128: 197-233. doi: 10.1016/bs.acr.2015.04.003
37. Jing F, Choi EY (2016) Potential of Cells and Cytokines/Chemokines to Regulate Tertiary Lymphoid Structures in Human Diseases. Immune network. 16: 271-80. doi: 10.4110/in.2016.16.5.271
38. Engelhard VH, Rodriguez AB, Mauldin IS, Woods AN, Peske JD, Slingluff CL, Jr. (2018) Immune Cell Infiltration and Tertiary Lymphoid Structures as Determinants of Antitumor Immunity. J Immunol. 200: 432-42. doi: 10.4049/jimmunol.1701269
39. Pollack KE, Meneveau MO, Melssen MM et al. (2020) Incomplete Freund's adjuvant reduces arginase and enhances Th1 dominance, TLR signaling and CD40 ligand expression in the vaccine site microenvironment. J Immunother Cancer. 8. doi: 10.1136/jitc-2020-000544
40. Berendam SJ, Koeppel AF, Godfrey NR et al. (2019) Comparative Transcriptomic Analysis Identifies a Range of Immunologically Related Functional Elaborations of Lymph Node Associated Lymphatic and Blood Endothelial Cells. Front Immunol. 10: 816. doi: 10.3389/fimmu.2019.00816
41. Takatsu K, Nakajima H (2008) IL-5 and eosinophilia. Curr Opin Immunol. 20: 288-94. doi: 10.1016/j.coi.2008.04.001

42. Mackay LK, Stock AT, Ma JZ, Jones CM, Kent SJ, Mueller SN, Heath WR, Carbone FR, Gebhardt T (2012) Long-lived epithelial immunity by tissue-resident memory T (TRM) cells in the absence of persisting local antigen presentation. Proc. Natl. Acad. Sci. U. S. A. 109: 7037-42.
43. Haddadi S, Thanthrige-Don N, Afkhami S, Khera A, Jeyanathan M, Xing Z (2017) Expression and role of VLA-1 in resident memory CD8 T cell responses to respiratory mucosal viral-vectored immunization against tuberculosis. Scientific reports. 7: 9525. doi: 10.1038/s41598-017-09909-4
44. Mackay LK, Rahimpour A, Ma JZ et al. (2013) The developmental pathway for CD103(+)CD8+ tissue-resident memory T cells of skin. Nat. Immunol. 14: 1294-301.
45. Neyt K, Perros F, GeurtsvanKessel CH, Hammad H, Lambrecht BN (2012) Tertiary lymphoid organs in infection and autoimmunity. Trends Immunol. 33: 297-305. doi: 10.1016/j.it.2012.04.006
46. Hayasaka H, Taniguchi K, Fukai S, Miyasaka M (2010) Neogenesis and development of the high endothelial venules that mediate lymphocyte trafficking. Cancer Sci. 101: 2302-8. doi: 10.1111/j.1349-7006.2010.01687.x
47. Hiraoka N, Ino Y, Yamazaki-Itoh R (2016) Tertiary Lymphoid Organs in Cancer Tissues. Front Immunol. 7: 244. doi: 10.3389/fimmu.2016.00244
48. Dieu-Nosjean MC, Giraldo NA, Kaplon H, Germain C, Fridman WH, Sautes-Fridman C (2016) Tertiary lymphoid structures, drivers of the anti-tumor responses in human cancers. Immunol Rev. 271: 260-75. doi: 10.1111/imr.12405
49. Cumberbatch M, Kimber I (1992) Dermal tumour necrosis factor-alpha induces dendritic cell migration to draining lymph nodes, and possibly provides one stimulus for Langerhans' cell migration. Immunology. 75: 257-63.
50. Clausen BE, Kel JM (2010) Langerhans cells: critical regulators of skin immunity? Immunol Cell Biol. 88: 351-60. doi: 10.1038/icb.2010.40
51. Said A, Weindl G (2015) Regulation of Dendritic Cell Function in Inflammation. Journal of immunology research. 2015: 743169. doi: 10.1155/2015/743169
52. Slingluff CL, Jr., Petroni GR, Chianese-Bullock KA et al. (2007) Immunologic and clinical outcomes of a randomized phase II trial of two multipeptide vaccines for melanoma in the adjuvant setting. Clinical Cancer Research. 13: 6386-95. doi: 10.1158/1078-0432.CCR-07-0486

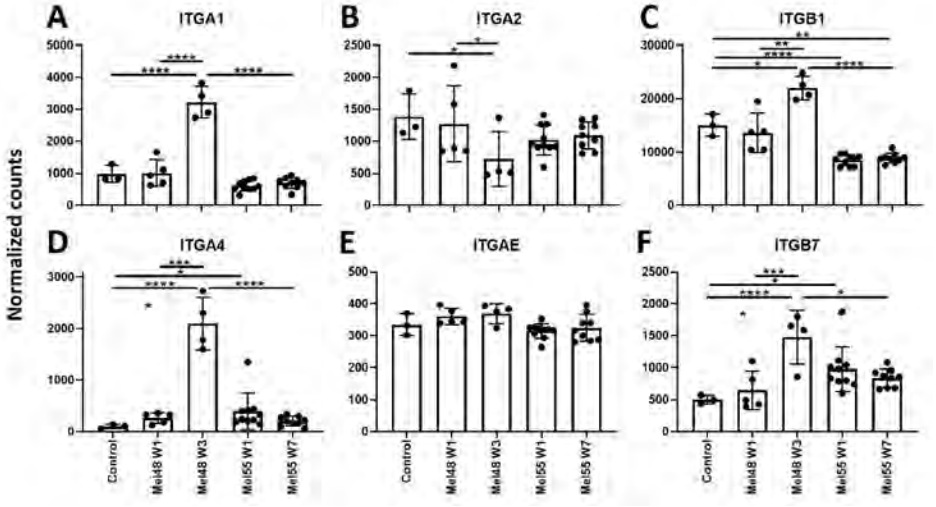

Supplemental Figure 1. Individual gene expression of integrin genes ITGA1 (CD49a) **(A),** ITGA2 (CD49b) **(B),** ITGB1 (CD29) **(C),** ITGA4 (CD49d) **(D),** ITGAE (CD103) **(E),** ITGB7 **(F).** Expression data was obtained from vaccine site biopsies of patients treated with IFA (MEL 48) or AS15 (MEL 55), as well as normal tissue obtained pre-vaccination for control purposes (n=3). For patients treated with IFA, gene expression is shown at week (w) 1 (n=3), and week 3 (n=4), following initial vaccination at a site separate from the biopsied tissue. For patients treated with AS15, gene expression is shown at week 1 (n=10) and week 7 (n=9) , following initial vaccination at a distant site. For factors of significance: * p <0.05, ** p < 0.01, *** p < 0.001, **** p < 0.0001; derived from differential gene expression.

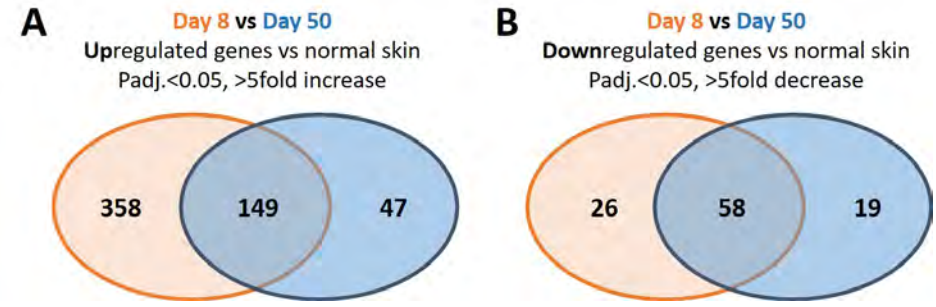

Supplemental Figure 2. Differentially upregulated **(A)** or downregulated **(B)** genes in Mel55 VSME compared to normal skin. Differential expression was determined as adjusted P value of less than 0.05 and at least 5-fold change compared to normal skin.

Supplemental Table 1. Overview of patient samples, categorized by trial, week of biopsy, and inclusion in experimental group

Patient ID	TRIAL	STAGE	AGE	SEX	WEEK	IHC	RNAseq
VMM1026	MEL 48	IIIB	59	M	0	Y	X
VMM1032	MEL 48	IIIB	60	M	0	Y	X
VMM1050	MEL 48	IV	59	M	0	Y	X
VMM1007	MEL 48	IIIC	47	M	1	X	X
VMM1021	MEL 48	IIIC	60	M	1	X	X
VMM1029	MEL 48	IIIC	51	M	1	X	X
VMM1033	MEL 48	IIIA	27	M	1	X	X
VMM1055	MEL 48	IIIC	48	F	1	X	X
VMM1036	MEL 48	IV	67	M	1	X	--
VMM1024	MEL 48	IIIB	72	M	1	X	--
VMM1045	MEL 48	IIIB	60	F	1	X	--
VMM1014	MEL 48	IIIB	62	M	1	X	--
VMM1008	MEL 48	IIIC	53	M	3	Y	X
VMM1023	MEL 48	IIIC	72	F	3	Y	X
VMM1034	MEL 48	IIIB	31	F	3	Y	X
VMM1048	MEL 48	IIIC	50	M	3	Y	X
VMM871	MEL 48	IV	37	F	7	X	--
VMM1010	MEL 48	IIB	60	M	7	X	--
VMM1018	MEL 48	IIIA	37	M	7	X	--
VMM1022	MEL 48	IIIC	56	F	7	X	--
VMM1039	MEL 48	IIIA	36	M	7	X	--
VMM1041	MEL 48	IIIB	49	F	7	X	--
VMM1044	MEL 48	IV	58	M	7	X	--
VMM1106	MEL 55	IIIB	51	F	1	X	X
VMM1106	MEL 55				7	X	--
VMM1077	MEL 55	IIIB	69.5	M	1,7	X	X
VMM1078	MEL 55	IIIB	43	M	1,7	X	X
VMM1076	MEL 55	IV	65	M	1,7	X	X
VMM1086	MEL 55	IIIC	51.8	M	1,7	X	X
VMM1089	MEL 55	IV	59.5	M	1,7	X	X
VMM1093	MEL 55	IIIB	54.6	M	1,7	X	X
VMM1095	MEL 55	IV	51.2	F	1,7	X	X
VMM1098	MEL 55	IIIB	40.7	F	1,7	X	X
VMM1112	MEL 55	IIIC	59.2	F	1,7	X	X

X = done in this study, Y = done in Scheafer et al

Supplemental Table 2. Mean gene expression in normalized counts (± Standard Deviation), categorized by gene, trial, and time point

	Control	Mel 48 Week 1	Mel 48 Week 3	Mel 55 Week 1	Mel 55 Week 7
BAFF	146.9 (± 20.15)	644.5 (±210.1)	3756.2 (±679.2)	1359 (±1433)	442.7 (±137.3)
APRIL	279 (±36.49)	483.1 (±148.1)	2222.6 (±392.3)	582.3 (±289.8)	420.1 (±45.04)
LIGHT	28.19 (±10.67)	99.3 (±48.0)	662.3 (130.0)	177.9 (±96.48)	120.3 (±35.49)
LTA	4.719 (±2.15)	12.2 (±3.4)	98.7 (±39.3)	42.48 (±40.79)	20.5 (±7.41)
LTB	51.97 (±7.26)	187.5 (±62.9)	1156.5 (±449.6)	537.8 (±482.5)	239.7 (±106.8)
CD20	14.84 (±12.22)	26.2 (±16.1)	271.0 (±165.5)	58.26 (±58.73)	140.6 (±107)
CCL2	281.2 (±57.84)	1563.5 (±797.9)	52443.5 (±1617.1)	1537 (±2195)	754.1 (±388.8)
CCL3	6.692 (±3.56)	243.8 (±201.6)	1970.6 (±548.0)	50.05 (±35.64)	177.3 (±311.7)
CCL4	5.963 (± 3.759)	154.4 (±112.8)	1821.5 (±554.6)	169.3 (± 250)	82.24 (± 54.76)
CCL5	101.5 (± 42.09)	421.6 (±203.8)	4858.5 (±1958.8)	1372 (± 1586)	668.9 (± 427.1)
CCL8	19.71 (± 11.00)	160.6 (±210.0)	2423.9 (±1179.7)	886.5 (± 1790)	62.04 (± 27.02)
CXCL9	113.5 (± 40.22)	457.4 (±215.4)	25312.3 (±7466.4)	4862 (± 8327)	681.4 (± 425.6)
CXCL10	49.35 (± 20.21)	364.1 (±424.0)	11735.9 (±3120.6)	3718 (± 7170)	225 (± 147.7)
CXCL11	19.46 (± 13.16)	108.3 (±111.9)	1530.5 (±403.6)	68.1 (± 50.13)	1321 (± 2564)
CXCL13	0.5997 (± 1.039)	4.3 (±1.8)	532.7 (±104.3)	14.08 (± 15.29)	39.87 (± 31.64)
CCL18	83.81 (± 38.26)	635.6 (±289.8)	16296.0 (±10233.5)	517.2 (± 430.1)	483 (± 159.3)
CCL19	296.5 (± 31.35)	930.4 (±247.9)	904.2 (±349.1)	1217 (± 908)	742 (± 292.9)
CCL21	367.1 (± 135.6)	865.4 (±243.9)	284.7 (±87.1)	561.2 (± 171.6)	751.2 (± 248.7)

Supplemental Table 3. Differentially expressed pathways in VSME of patients vaccined with AS15 (Mel55) at day 8 or day 50 after the first vaccine, compared to normal skin. Results were obtained through a GAGE pathway analysis. Q-values are provided for each enriched pathway at each time point.

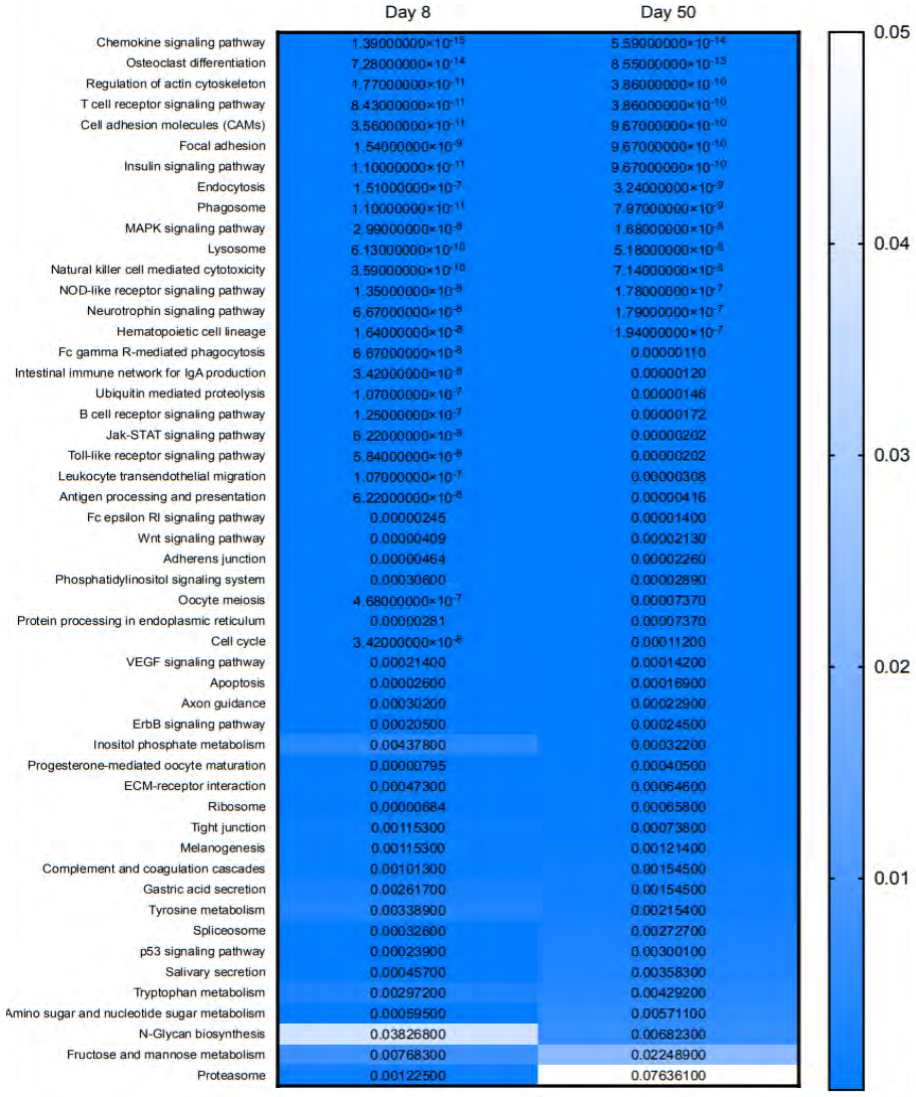

Chapter 5

Formation and phenotypic characterization of CD49a, CD49b and CD103 expressing CD8 T cell populations in human metastatic melanoma

Marit M. Melssen, Walter Olson, Nolan A. Wages, Brian J. Capaldo, Ileana S. Mauldin, Adela Mahmutovic, Ciara Hutchison, Cornelis J.M. Melief, Timothy N. Bullock, Victor H. Engelhard and Craig L. Slingluff Jr.

Oncoimmunology. 2018 Aug 6;7(10):e1490855.

ABSTRACT

Integrins α1β1 (CD49a), α2β1 (CD49b) and αEβ7 (CD103) mediate retention of lymphocytes in peripheral tissues, and their expression is upregulated on tumor infiltrating lymphocytes (TIL) compared to circulating lymphocytes. Little is known about what induces expression of these retention integrins (RI) nor whether RI define subsets in the tumor microenvironment (TME) with a specific phenotype. Human metastatic melanoma-derived CD8 TIL could be grouped into five subpopulations based on RI expression patterns: RI^{neg}, $CD49a^+$ only, $CD49a^+CD49b^+$, $CD49a^+$ $CD103^+$, or positive for all three RI. A significantly larger fraction of the $CD49a^+$ only subpopulation expressed multiple effector cytokines, whereas $CD49a^+$ $CD103^+$ and $CD49a^+CD49b^+$ cells expressed IFNγ only. RI^{neg} and $CD49a^+CD49b^+CD103^+$ CD8 TIL subsets expressed significantly less effector cytokines overall. Interestingly, however, $CD49a^+CD49b^+CD103^+$ CD8 expressed lowest CD127, and highest levels of perforin and exhaustion markers PD-1 and TIM-3, suggesting selective exhaustion rather than conversion to memory. To gain insight into RI expression induction, normal donor PBMC were cultured with T cell receptor (TCR) stimulation and/or cytokines. TCR stimulation alone induced two RI+ cell populations: CD49a single positive and $CD49a^+CD49b^+$ cells. TNFα and IL-2 each were capable of inducing these populations. Addition of TGFβ to TCR stimulation generated two additional populations; $CD49a^+CD49b^{neg}CD103^+$ and $CD49a^+CD49b^+CD103^+$. Taken together, our findings identify opportunities to modulate RI expression in the TME by cytokine therapies and to generate subsets with a specific RI repertoire in the interest of augmenting immune therapies for cancer or for modulating other immune-related diseases such as autoimmune diseases.

INTRODUCTION

Integrins are transmembrane molecules that mediate intercellular interactions as well as interactions between cells and extracellular matrix. The integrins α1 (CD49a), α2 (CD49b) and αE (CD103) bind collagen IV, collagen I and E-cadherin respectively, and are thought to retain lymphocytes in peripheral nonlymphoid tissues (1-6). These retention integrins (RI) are also highly expressed on tumor infiltrating lymphocytes (TILs) compared to circulating lymphocytes (7). $CD49a^+$ and/or $CD103^+$ T cells residing in healthy peripheral tissues have features of tissue resident memory T (TRM) cells. TRM cells remain in the tissue long term and can be rapidly induced to have effector function upon exposure to antigen (8-13). In addition, RI expression on effector T cells in inflammatory diseases, including arthritis and hypersensitivity responses, exacerbates inflammatory pathology (14). This suggests that RI directly or indirectly support effector T cell function. The presence of $CD103^+$ or $CD49a^+$ TILs in the tumor microenvironment (TME) is associated with improved survival in several types of cancer, suggesting CD49a and CD103 may support retention, survival or effector function of T cells in the TME, or that they may mark a T cell subset more effective in anti-tumor immunity (15-21). Little is known about the contribution of CD49b to T cell persistence or efficacy in the TME. RI are mainly expressed on T cells after they infiltrate peripheral tissues, suggesting that they are either lineage markers of a later differentiation stage or induced by molecules in the local tissue environment. Little is known about factors inducing RI expression. TGFβ has been shown to upregulate CD103 expression directly on activated CD8 T cells (22-25). While studies have shown a correlation with the presence of TNFα and TGFβ and $CD49a^+$ T cells in mice (26-28), the direct cause of CD49a induction remains unknown. To our knowledge, factors that induce CD49b have not been identified. Understanding the factors that induce expression of RI is crucial for continued improvements of immune therapies, as it gives perspectives on the role of the TME in retention and dissemination of T cells subsets in the tumor. In addition to the knowledge gap concerning the induction of RI expression, little is known about whether different RI expression patterns characterize specific functional subsets. We hypothesized that a subset of T cells in the TME co-express CD103 and CD49a, representing memory–like cells. Additionally, we hypothesized that terminal or exhausted effectors can be defined based on RI marker expression pattern. We sought to characterize population dynamics based on the RI expression pattern and to compare in vitro-generated RI^+ CD8 T cells to RI^+ TIL. We have focused our studies on the effects of TCR stimulation and addition of cytokines associated with antitumor immunity (TNFα, IFNs), tumor-associated immune dysfunction (TGFβ, IL-10), and T cell subsets differentiation (IL-1β, IL-2, IL-4, IL-5, IL-17), as well as chemokines associated with immune cell migration. By defining T cell subsets based on the RI expression profile, generated under different conditions in vitro or patient-derived TIL, we provide insight in the induction of RI as well as a potential link between cytokine presence and RI expressing functional CD8 T cell subsets in the TME.

MATERIALS AND METHODS

Cell culture

All studies were conducted in a laboratory that operates under Good Laboratory Practice (GLP) principles. Peripheral blood mononuclear cells (PBMC) from seven healthy donors were obtained from a leukopak (BRT Laboratories Inc.), a buffy coat (Virginia Blood Services) or volunteers through a Ficoll gradient sedimentation. Purified PBMC were cryopreserved in 90% FCS, 10% DMSO until used. The PBMC were thawed in DNAse (100U/ml; Worthington Biochemical Corp.) containing media (RPMI 1640 with 5% heat-inactivated (HI) fetal calf serum (FCS) (Gibco), washed and rested overnight in complete media (RPMI 1640 with 5% HI FCS, 1% penicillin/ streptomycin (Gibco) and 20 Cetus units (CU)/ml IL-2). Prior to use, FCS was tested for supportive capacity of cell growth and proliferation, as well as screened for mitogenicity. For assays, PBMCs were seeded in 24-well plates at 5×10^5 cells per well in complete media as described above. PBMCs were stimulated with soluble 1μg/ml purified NA/LE (non-azide, low endotoxin) mouse anti-human CD3 (clone HIT3a, BD Biosciences) and 4μg/ml LEAF (low endotoxin, azide-free) purified anti-human CD28 (clone CD28.2, Biolegend) for 24 hours. In order to prevent overstimulation, medium was replaced after 24 hours and PBMCs were cultured with IFNα (5ng/ml), IFNβ (10ng/ml), IFNγ (2ng/ml), IL-1β (1ng/ml), IL-2 (1000CU/ml), IL-4 (20ng/ml), IL-5 (10ng/ml), IL-10 (100ng/ml), IL-15 (20ng/ml), IL-17 (50ng/ml), TGFβ (5ng/ml), TNFα (50ng/ml), CCL2 (100ng/ml), CCL3 (10ng/ml), CCL4 (20ng/ml), CCL5 (10ng/ml), CXCL9 (100ng/ml), CXCL10 (50ng/ml), CXCL11 (all 10ng/ml), or CXCL12 (80ng/ml), for seven days in complete media unless indicated otherwise. All cytokines and chemokines were human recombinant proteins obtained from Peprotech. Throughout cell culture, cell numbers were determined by counting with a hemocytometer.

Patient samples

Metastatic melanoma lesions were obtained from surgical specimens with patient consent (IRB 10598). Patients ranged between age 28–87 with stage IIB-IV melanoma, and the cohort included 12 males and 7 females. Three normal donor PBMC samples were used as controls (obtained and processed as described above). Melanoma samples were made into single cell suspensions by mechanical separation and filtered through a 100 micron filter, within 4 hours of collection (median of approximately an hour). Single cells suspensions were cryopreserved in 90% FCS and 10% DMSO using a controlled rate cell freezing container. Cells were cryopreserved in liquid nitrogen ranging from 1 up to 12 years. Samples were thawed as described above for PBMC and counted on a Guava EasyCyte Plus benchtop flow cytometer (cell viability ranged between 33–78% with a median yield of 1.65E+ 07 viable cells). After thaw, cells were either directly stained for flow cytometry or sorted on an Influx Cell Sorter (BD Biosciences). Sorted cells were cultured in RPMI 1640 with 5% heat-inactivated FCS (Gibco), 1% penicillin/streptomycin (Gibco) and 20CU/ml IL-2, and stimulated with 50ng/ml PMA (Sigma-Aldrich) and 1μg/ml Ionomycin (Gibco ThermoFisher Scientific)

for 6 hours in the presence of BD Golgiplug (1:1000, BD Biosciences) prior to flow cytometry staining. Experiments included either all 19 patient samples, or a subset selected based on sample availability or cell numbers. Selection was not intentionally made based on survival or stage.

Antibodies and flow cytometry analysis

For surface staining, the following antibodies were used: PE CD49a (TS2/7, Biolegend), APC CD49b (P1H1, eBioscience), Pe-Cy7 CD103 (B-Ly7, eBioscience), PerCPCy5.5 CD3 (OKT3, Biolegend), APC-H7 CD8 (Sk1, BD Biosciences), Fitc CD45RO (UCHL1, Biolegend), BV605 CD127 (A019D5, Biolegend), v450 CD69 (FN50, BD Biosciences), FITC IFNγ (B27, BD Biosciences), v450 TNFα (Mab11, BD Biosciences), PE/Dazzle 594 Perforin (dG9, Biolegend), BV605 IL-2 (MQ1-17H12, BD Biosciences), BV650 PD1 (EH12, BD Biosciences) and BV421 TIM3 (7D3, BD Biosciences). Cells were labeled with the LIVE/DEAD® Fixable Aqua dead cell stain (Life Technologies) according to manufacturer's protocol prior to surface stain to visualize viable cells for analysis. Intracellular staining for PerCP-Cy5.5 Ki67 and BV421 Granzyme B (both BD biosciences) was performed according to instructions in the BD Cytofix/Cytoperm kit (BD Biosciences) for intracellular staining protocol. Flow cytometry data were collected on a Canto II in eight color mode (BD Biosciences) or on a Cytoflex in 14 color mode (Beckman Coulter) and analyzed using FlowJo software V10.1 (Tree Star). In FACS sorting experiments cells were stained similarly, though sorted on a BD Influx Cell Sorter (BD Biosciences). An example of the gating strategy used for these experiments is depicted in supplemental Figure 1A/B. Gating strategies for stains were set based on Fluorescence Minus One (FMO) (extracellular stains) or isotype controls (intracellular stains; Supplemental Figure 1C) with predefined background of < 1%. Raw data for all flow cytometry experiments can be provided per request.

Immunofluorescent staining

Three 4-µm thick sections were cut from each formalin fixed paraffin embedded (FFPE) specimen; a section from a small bowel melanoma metastasis previously shown to contain alpha1+ T cells by flow cytometric analysis was used as a positive control.7 Multispectral Staining was performed according to the manufacturer's protocol using the OPAL Multiplex Manual IHC kit, and antigen retrieval buffers (AR) 6 and 9 (PerkinElmer, Waltham, Massachusetts, USA). AR for the Sox10 stain was performed using Diva Decloaker (Biocare Medical, Concord, California, USA). Staining sequence, antibodies, and antigen retrieval buffers were as follows: AR9, CD8 (dilution 1:500; Dako, Santa Clara, California, USA, cat#m710301-2 clone c8) Opal540; AR9, alpha1 (1:4000, Abcam, Cambridge, United Kingdom, cat#ab181434) Opal650; DIVA, Sox10 (1:100, Cell Marque, Rocklin, CA, cat#383A-77) Opal690; and spectral DAPI (PerkinElmer, Waltham, Massachusetts, USA). Slides were mounted using prolong diamond antifade (Life Technologies, Carlsbad, California, USA) and scanned at 10x magnification using the PerkinElmer Vectra 3.0 system and Vectra software (PerkinElmer, Waltham,

Massachusetts, USA). Regions of interest were then identified in Phenochart software, and a 20x magnification images were acquired with the Vectra 3.0 system. These images were spectrally unmixed using a single stain positive controls and analyzed using the InForm software (PerkinElmer, Waltham, Massachusetts, USA).

Image analysis

Images acquired and unmixed by InForm were further analyzed with ImageJ (29) Per slide, the CD8 signal was translated into a Region Of Interest (ROI), within which alpha1 (CD49a) positive pixels were measured and depicted as a fraction of total CD8 positive pixels. Two thresholds were evaluated for both CD8 and CD49a.

Cell separation

$CD45RO^{+}$ and $CD45RO^{neg}$ cells were isolated from PBMCs directly after thawing, using MACS Anti-Mouse IgG MicroBeads (Miltenyi Biotec) according to manufacturer's protocol. Briefly, 10^7 PBMCs were labeled with Fitc CD45RO (Biolegend) for 1 hour followed by a blocking step with 2% mouse serum in PBS. Cells were washed, incubated with Anti-Mouse IgG MicroBeads and labeled cells were positively selected with a MS MACS separation column. Purity of $CD45RO^{neg}$ and $CD45RO^{+}$ populations are shown in Supplemental Figure 1D. Both positive and negative populations were stimulated with CD3 and CD28 antibodies followed by 7 days of culture in the presence of the indicated cytokines. Statistical analysis RI expression data in different conditions were compared in 3–7 healthy donors or in 19 melanoma tumor samples. The significance of changing conditions as well as marker expression by different subsets was tested with a paired T-test with Graphpad Prism software (edition 7). For multiple group comparisons, a Kruskall-Wallis test was used. Non-hierarchical clustering FCS files consisting of $CD8^{+}$ events were loaded into the R statistical programming environment using the flowCore package from Bioconductor (30,31). Data was compensated using the compensation matrix generated in FlowJo software V10.1 (Tree Star), and transformed using the inverse hyperbolic sin with a cofactor of 150, as described previously (32). The bioconductor package flowSOM was used to build a self-organizing map (SOM) with 9 grid points or clusters using CD49a, CD49b, and CD103 (33). Data and code for this analysis is available at the UVA Flow Repository.

RESULTS

Expression patterns of CD49a, CD49b and CD103 identify distinct populations of tumor infiltrating CD8 T cells

Tumor-infiltrating CD8 T cells can express CD103, CD49a or CD49b (7). However, the co-expression and functional characteristics of RI^{+} subsets have not yet

been addressed. We evaluated CD8 TIL from 19 melanoma samples from skin, small bowel and lymph node metastases. TIL from all samples contained both RI^{neg} and RI^{+} populations. Among the RI^{+} cells we identified a $CD49a^{+}CD103^{neg}$ population, a subpopulation of which also expressed CD49b. These two CD49a+ subsets were present in virtually all samples (Figure 1A). A fraction of tumors also contained a substantial $CD103^{+}$ TIL population (Figure 1A). The large majority of these $CD103^{+}$ cells co-expressed either CD49a only or both CD49a and CD49b. Based on these findings, the large majority of CD8 TIL from each patient could be grouped into five subpopulations based on RI expression patterns: RI^{neg}, $CD49a^{+}$ only, $CD49a^{+}CD49b^{+}$, $CD49a^{+}CD103^{+}$, or positive for all three RI (Figure 1B). Importantly, $CD103^{+}$ subsets were found only in a fraction of tumors, which were mainly small bowel metastases (Supplemental Figure 2A/B). These data reveal variations in RI expression patterns among tumors and raise the possibility that tissue specific factors may contribute to the generation of $CD103^{+}$ subsets. Interestingly, each RI^{+} subset expressed at least CD49a, made clear by the absence of CD49b single positive (SP), CD103 SP and CD49bCD103 double positive (DP) TIL in most tumors. When CD8 TIL from these 19 melanoma metastases were distributed in nine clusters through nonhierarchical clustering based on the frequency of RI expression, we find each of these same subsets (Figure 1C/D). However, they fall into 3 main subcategories: RI^{neg}, $CD103^{+}$ and $CD49a^{+}$ $CD103^{neg}$ subpopulations. Interestingly, these may also be correlated with expression of activation and memory markers CD45RO, CD69 and CD127 (Figure 1D) indicating they may be functionally distinct subpopulations (Figure 1D).

CD49a SP cells express the largest levels of effector activity, while triple positive (TP) cells express the least

To determine whether these five subsets are functionally distinct, they were evaluated by Fluorescence-activated Cell Sorting (FACS) (n=5, selected from 19 patients stained above) and restimulated with PMA/Ionomycin. After restimulation, IFNγ, TNFα and IL-2 expression were measured by intracellular flow cytometry. Each cytokine was expressed by a significantly larger fraction of the CD49a SP population, whereas a high fraction of the $CD49a^{+}CD49b^{+}$ and $CD49a^{+}CD103^{+}$ subsets expressed IFNγ only (Figure 2A). Fractions of RI^{neg}, and $CD49a^{+}CD49b^{+}CD103^{+}$ CD8 TIL subsets expressing any of the three effector cytokines were substantially lower (Figure 2A). These data indicated that significantly more CD49a SP cells are polyfunctional effectors, whereas $CD49a^{+}CD103^{+}$ and $CD49a^{+}CD49b^{+}$ CD8 TIL are primarily monofunctional $IFN\gamma^{+}$ effectors and the remaining two subsets are more quiescent. In contrast, cytotoxicity marker perforin was significantly more highly expressed on the subsets expressing multiple RI, compared to CD49a SP cells (Figure 2B).

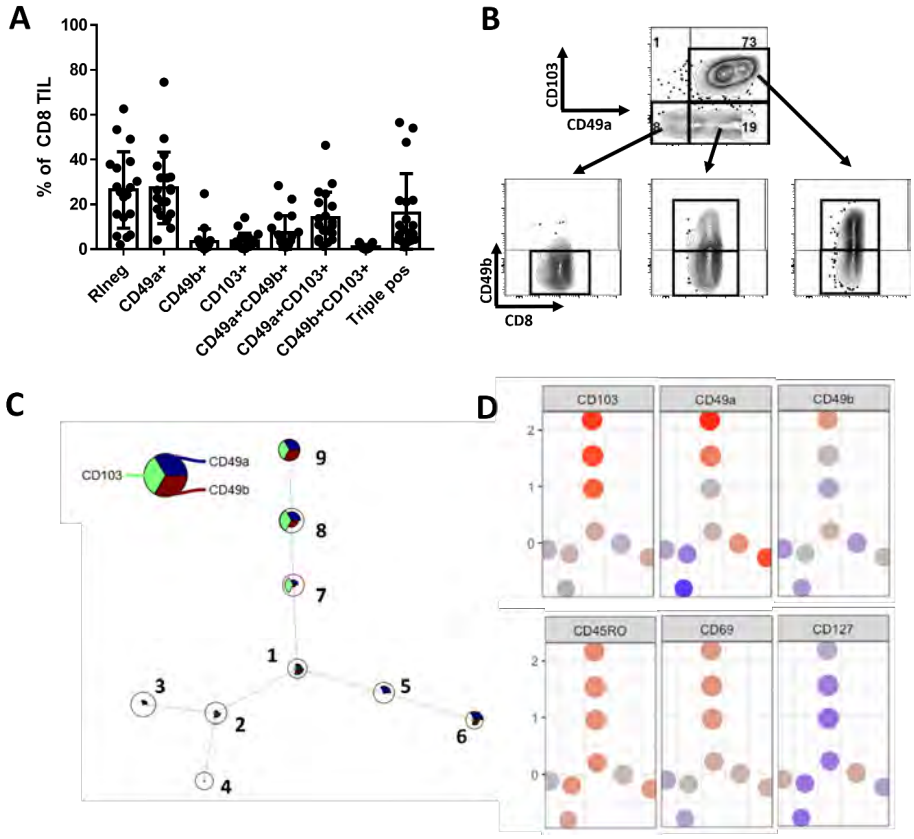

Figure 1. RI expression dynamics on human melanoma-derived CD8 TIL. A total of 19 metastatic tumors were analyzed: 7 small bowel, 5 skin and 7 tumor-involved lymph nodes. (A) Fraction of CD103, CD49a and/or CD49b expressing subsets of CD8 TIL (n = 19). (B) Example showing CD49b co-expression on CD103 and/or CD49a subsets, marking five main subpopulations. (C) Non-hierarchical clustering of CD8 T cells from same 19 patients, based on CD49a, CD49b and CD103 expression. (D) Intensity of RI, activation markers CD45RO and CD69 and memory marker CD127 on clusters as defined in Figure 1C.

Quiescence of CD49a$^+$CD49b$^+$ and CD49a$^+$CD49b$^+$CD103$^+$ CD8 TIL may be explained by high expression of exhaustion markers

At this point lower effector cytokine expression by CD49a$^+$CD49b$^+$, CD49a$^+$CD103$^+$ and CD49a$^+$CD49b$^+$CD103$^+$ CD8 TIL subsets could be explained by the gain of either a memory phenotype or an exhausted phenotype. To distinguish between these possibilities, we stained tumors for memory cell marker CD127 and exhaustion markers PD1 and TIM3. Interestingly, CD127 expression was significantly lower in all three subsets, compared to CD49a SP cells (Figure 2C). PD1 and TIM3 expression, however, were significantly higher, both measured as fraction of total subset and geometric MFI (Figure 2D/E). These results suggest

that either: CD8 TIL that express multiple retention integrins and thus remain in peripheral tissues may become quiescent/exhausted, or CD8 TIL that become exhausted in the TME also upregulate multiple RI.

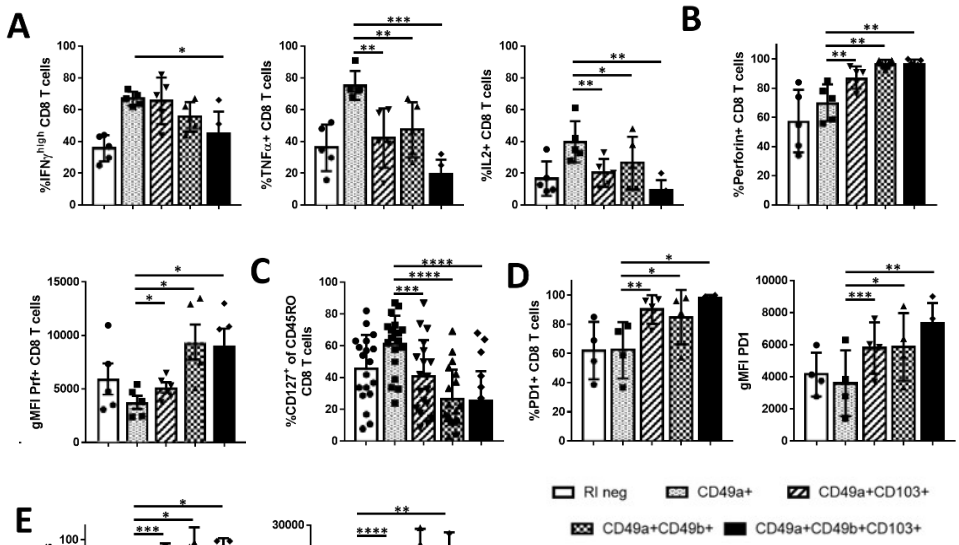

Figure 2. Functional and phenotypical characteristics of distinct RI+ CD8 TIL subsets. (A) A subset of samples (n = 5, 2 skin metastases, 2 small bowel metastases and 1 TIN), selected from the earlier analyzed 19 samples based on T cell numbers and sample availability. Displayed is the fraction of CD8 TIL in each subset expressing IFNγ HI (left), TNFα (middle) or IL-2 (right) after 6hr in vitro incubation with PMA/Ionomycin and Brefeldin A. (B) Fraction and geometric mean fluorescent intensity (gMFI) of perforin (n = 5, 1 skin metastases, 2 small bowel metastases and 2 TIN). (C) Proportion of each subset expressing CD127 (n = 19). (D/E) Fraction and intensity of PD1 (D) and TIM3 (E) expression by each RI+ CD8 TIL subpopulation (n = 4, 2 small bowel metastases and 2 TIN, selected based on sample availability). * $P < 0.05$, ** $P \leq 0.01$, *** $P \leq 0.001$, **** $P < 0.0001$.

CD49a expressing cells are trending to be more prominent in tumors with perivascular T cells, compared to diffusely infiltrated tumors

The phenotype of integrin-expressing cells is distinct among subsets; however, it is unknown whether these integrins also determine the localization of these TIL. To test this, we stained FFPE sections from tumors previously characterized as either uninfiltrated (immunotype A), perivascularly infiltrated (immunotype B) or diffusely infiltrated (immunotype C) for CD49a and CD834. The mean values were 32% (A), 62% (B) and 33% (C) when cells were evaluated with a low threshold (Supplemental Fig. 3A) and 14% (A), 36% (B) and 19% (C) with a high threshold

(Supplemental Fig. 3B). These findings provide preliminary data to suggest there may be a difference in CD49a expression depending on T cell location, in particular, associating CD49a-expressing T cells with perivascular locations.

IL-2 increased expression of both CD49a and CD49b on unstimulated T cells

Our in vivo data showed that certain populations always develop, whereas others only develop in a fraction of the tumors. This raises the possibility that immune activation or soluble immune mediators in the tumor environment may be responsible for the development of these RI$^+$ subpopulations, which is known to vary among tumors. We thus hypothesized that TCR stimulation and/or common immune stimulatory or immunosuppressive cytokines would initiate the development of CD49a$^+$ and CD49a$^+$ CD49b$^+$ subpopulations. To test this hypothesis, we initially cultured total peripheral blood CD8 T cells with CD3/CD28 antibodies (TCR stimulation) in presence or absence of IL-2. After TCR stimulation alone there were two main RI$^+$ cell populations, one that co-expressed CD49a and CD49b, and another that expressed CD49a alone (Figure 3A, top panels, Figure 3B/C). Interestingly, IL-2 by itself, increased both CD49a$^+$ and CD49b$^+$ CD8 T cell subsets in unstimulated condition resulting in a large population of CD49a$^+$ CD49b$^+$ CD8 T cells (Figure 3A, bottom panels, Figure 3B/C). This population expanded after longer periods of culture and was absent when the culture media was not supplemented with IL-2 (data not shown). In TCR stimulated conditions, IL-2 did not further enhance CD49a or CD49b expression (Figure 3A-C). The increase of CD49a and CD49b expression on unstimulated T cells by IL-2 might be explained by selective proliferation of RI$^+$ memory T cells, present among PBMCs. To test this, we separated memory and naïve T cells from PBMC, based on CD45RO expression, before adding IL-2. As expected, most CD49a$^+$ or CD49b$^+$ CD8 T cells at baseline are found among the CD45RO$^+$ subset (Figure 3D/F). However, when stimulated with IL-2 alone, only CD45RO^{neg} CD8 T cells were induced to express CD49a compared to control (Figure 3E). Thus, the increase in CD49a was caused by induction on CD45RO^{neg}, naïve T cells only, rather than selective proliferation or survival of CD49a$^+$ memory cell subsets. CD49b was induced at similar rate in both CD45RO$^+$ and CD45RO^{neg} populations, suggesting that only part of the increase in CD49b$^+$ CD8 T cells with IL-2 may be due to induced expression (Figure 3G). After characterizing the effects of TCR stimulation and IL-2 on RI expression, we tested the impact of adding cytokines and chemokines (IFNα, IFNβ, IFNγ, IL-4, IL-5, IL-10, IL-15, IL-17, CCL2-5 and CXCL9-12), commonly found in the TME. Interestingly, most of these molecules had no discernible effect on RI expression by CD8 T cells in PBMC after 8 day culture with or without TCR stimulation (Table 1, supplemental Fig. 5, and data not shown). Data in Table 1 represent geometric MFI values for each condition. IL-10 minimally increased CD49a expression, in the absence of TCR stimulation (Supplemental Fig. 6C). On the other hand, IL-4 decreased CD49a expression when combined with TCR stimulation (Supplemental Fig. 6D).

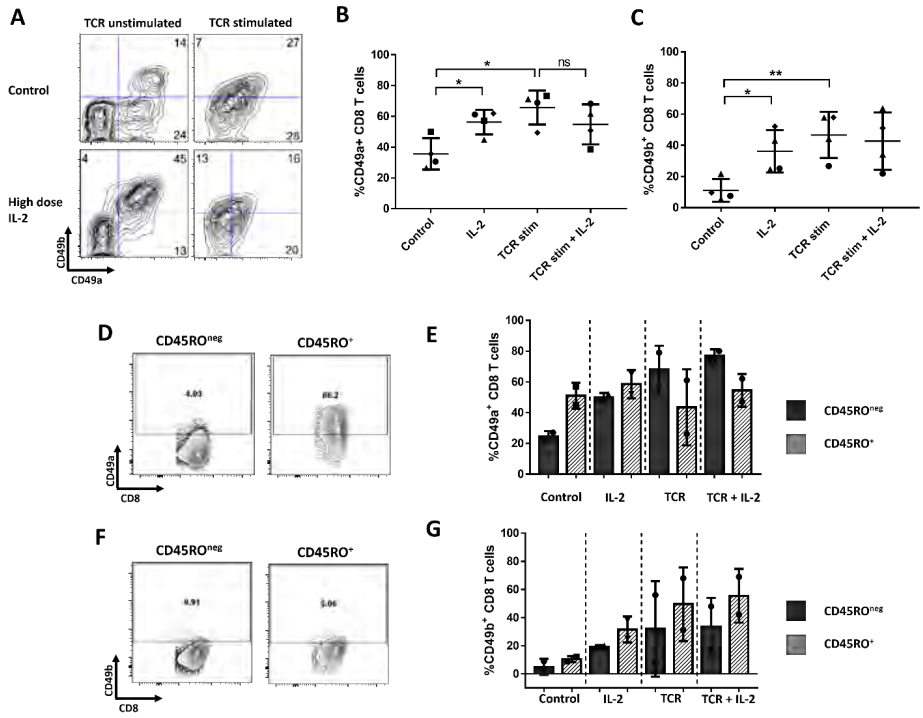

Figure 3. CD49a and CD49b expression on normal donor CD8 T cells after TCR stim and 7 days of culture with IL-2. (A) Plots for one example. (B and C) Percentage of CD8 T cells expressing CD49a or CD49b. Accumulated data for 4 different donors. (D/F). Baseline CD49a and CD49b expression on CD45RO^{neg} and CD45RO^{+} ND CD8 T cells. (E/G). CD49a and CD49b expression for either CD45RO^{neg} or CD45RO^{+} ND CD8 T cells, after TCR stim and 7 days of culture with/without IL-2. * P < 0.05, ** P ≤ 0.01, *** P ≤ 0.001, **** P < 0.0001.

Adding TGFβ after T cell activation further induced CD103 expression on both CD49a^{+} CD8 populations

While TCR stimulation and IL-2 were identified as potential factors generating CD49a^{+} and CD49a^{+} CD49b^{+} subpopulations, factors responsible for the generation of CD103^{+} subpopulation in a fraction of the tumors have yet to be identified. Previous studies have shown that CD103 and CD49a can be upregulated by TGFβ when combined with T cell receptor (TCR) stimulation (22-24,28). We thus hypothesized that TGFβ could be responsible for the generation of both CD103+ subsets (CD49a^{+}CD103^{+} and CD49a^{+}CD49b^{+}CD103^{+}). When TGFβ was added to TCR stimulation CD49b expression decreased overall (Supplemental Fig. 4B). Importantly, a significant proportion of T cells remained CD49b^{+}, which largely co-expressed CD49a and CD103 (Figure 4A, lower right panel, Figure 4B), a population we also observed among CD8 TIL. CD49a intensity was also increased by the addition of TGFβ to TCR stimulation. However, in contrast to the in vivo

findings, both CD49a^{+}CD49b^{+} and CD49a^{+}CD49b^{+}CD103^{+} populations showed a significant increase in CD49a expression intensity (Figure 4C). Importantly, the CD49a intensity increased over time (Figure 4D), indicating that CD49a is upregulated as CD8 T cells differentiate further. CD103 was upregulated by day 2 and did not significantly change over the course of 7 days. These data indicate that, despite all receiving TCR stimulation + TGFβ, CD8 T cells did not uniformly upregulate or downregulate RI. Instead, CD49a, CD49b and/or CD103 expression profiles marked subpopulations from the beginning, indicating the combination of activation followed by TGFβ could play a role in the existence of these subsets on melanoma TIL. For most of the in vitro activated RI subsets, levels of activation, effector or memory cell markers did not change as dramatically as the patient TIL, suggesting that tissue microenvironment and time may play a role in the further differentiation and specification of these subsets (Figure 4E).

Table 1. Expression intensity of each retention integrin by CD8 T cells from PBMC cultured 7d with TCR stimulation (TCR) or without TCR stimulation (TCRneg), for selected cytokines and chemokines.

	CD49a		CD49b		CD103	
	TCRneg	TCR	TCRneg	TCR	TCRneg	TCR
Control	355	375	60	64	43	170
IL-17	376	336	64	65	41	147
IL-5	350	369	54	64	38	140
IFNβ	357	355	57	71	37	163
IFNα	313	367	49	77	15	181
CXCL12	399	285	62	64	76	136
CXCL11	384	338	62	61	43	136
CXCL10	357	333	56	69	40	142
CXCL9	397	312	61	64	55	131
CCL5	367	353	57	57	45	136
CCL4	386	362	57	66	47	143
CCL3	390	348	62	67	43	144
CCL2	404	335	71	70	57	142

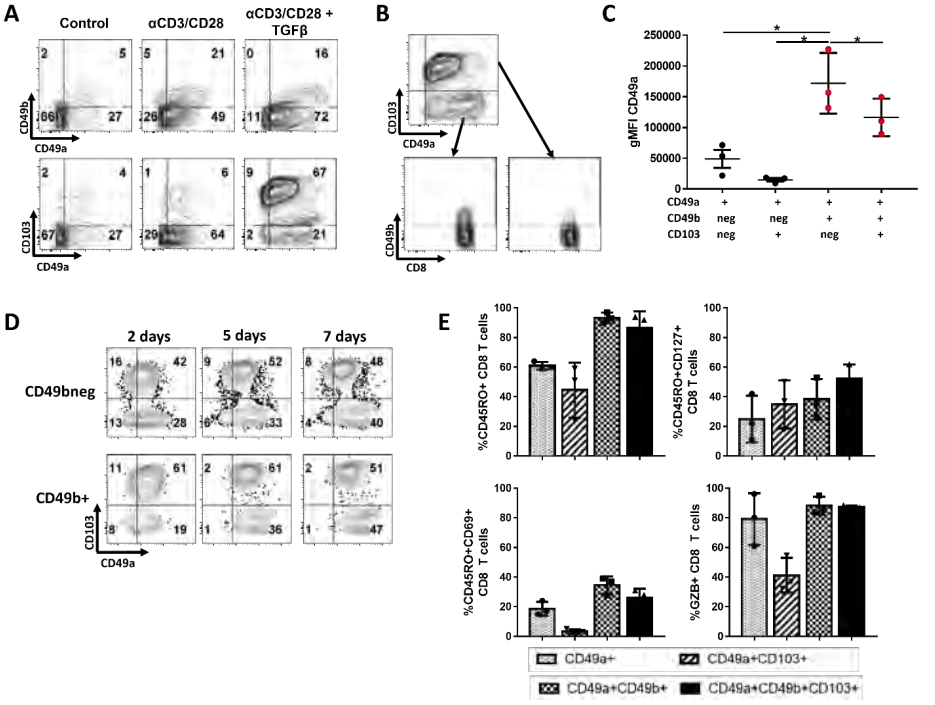

Figure 4. Normal donor PBMC were cultured with CD3 and CD28 activating antibodies (TCR stim) for 24h, after which they were grown for 2–7 days with or without TGFβ. (A) CD103, CD49a and CD49b expression percentage on CD8 T cells, with/without 24 hours of TCR stim and/or TGFβ, after 7 days of culture. (B) Visualization of CD49b co-expression on the most dominant CD49a and/or CD103 expressing CD8 T cell populations after TGFβ + TCR stimulation in vitro. (C) Intensity of CD49a expression on a per-cell basis, after TCR stim and 7 days of culture with TGFβ on each CD49a$^+$ subpopulation. *P < 0.05. (D) Induction of CD49a, CD49b and CD103 over time when culture with TGFβ, 2, 5 and 7 days after TCR stimulation. (E) Percentage of RI+ CD8 T cell subsets expressing functional markers CD45RO, CD69, Granzyme B and CD127 expression in most dominant populations, after TCR stim and 7 days of culture with TGFβ. Normal donor PBMC from three different donors were used in this experiment. * P < 0.05, ** P ≤ 0.01, *** P ≤ 0.001, **** P < 0.0001.

TNFα induces CD49a expression on CD8 T cells, though at low intensity TCR stimulation in conjunction with TGFβ induced very similar

RI$^+$ populations as the subsets found among approximately 50% of CD8 melanoma TIL (Figure 1A). However, other patients had very few CD103$^+$ TIL populations (Figure 1A), suggesting low levels of TGFβ in those microenvironments. Yet, in those tumors CD49a was expressed on a high proportion of the TIL. Thus, we hypothesized that in the tumors with low CD103 co-expression, factors other than TGFβ modulate CD49a and/or CD49b expression. Addition of TNFα to TCR

stimulation increased CD49a expression slightly, but significantly (Figure 5A/B). However, even after 7 days of culture with TNFα, the intensity of CD49a expression remained low, and the fraction expressing high intensity CD49a seen after TCR stimulation with TGFβ was not observed (Figure 5C). TNFα also decreased CD49b expression when combined with TCR stimulation (Figure 5D), but had no effect on CD103 co-expression which was virtually absent (data not shown).

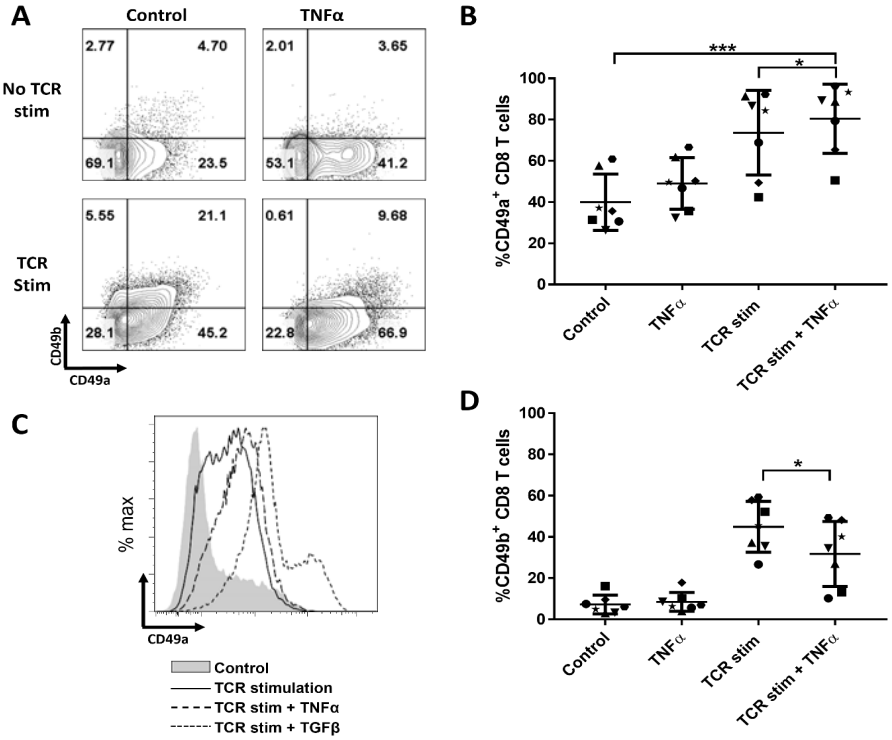

Figure 5. CD49a and CD49b expression on normal donor CD8 T cells after TCR stim and 7 days of culture with TNFα. (A) Plots for one example. (B and C) Percentage of CD8 T cells expressing CD49a or CD49b. Accumulated data for 7 different donors. (D). CD49a expression intensity histograms under different culture conditions. Examples for one donor. * $P < 0.05$, ** $P \leq 0.01$, *** $P \leq 0.001$, **** $P < 0.0001$.

Discussion

Interactions between tumors and the immune system are often characterized by the presence or absence of infiltrating T lymphocytes; however, there has been little attention paid to the processes that retain T cells in the tumor. RIs are involved in persistence of lymphocytes in healthy peripheral tissues, and their expression has been associated with increased effector function (7,15–18). In human cancers, infiltrating lymphocytes expressing RIs and CD103 have been associated with

improved patient survival (7,15). Immune therapy of melanoma and other solid tumors is more effective when infiltrating T cells are present and functional (35-37). Thus, the expression of RI may be critical to patient survival and response to immune therapy. We posit that the presence of functional tumor-reactive T cells within a cancer depends on infiltration, retention, and persistence of function. CD49a, CD49b, and CD103 can mediate retention and function of T cells, thus, failure to induce these integrins may impair T cell persistence and efficacy in the TME. Understanding conditions that enhance RI expression will facilitate the development of strategies to enhance functional antitumor immunity. In this study, we have identified several subpopulations of CD8 T cells based on their expression of retention integrins. Interestingly these populations are evident both among T cells infiltrating melanoma metastases and among PBMC induced to express RI in vitro. Our findings suggest a stepwise progression of RI expression, which may be accompanied by classical processes of T cell differentiation. In vitro, TCR stimulation alone induced $CD49a^+$ and $CD49a^+CD49b^+$ populations. We thus expect that T cells responding to antigen in lymph nodes may upregulate CD49a and/or CD49b and subsequently travel to the tumor site. In melanoma patients, these subpopulations were found among virtually all TIL and contained a heterogeneous population of naïve, effector and memory-like cells. Upon TGFβ addition to TCR stimulation in vitro, CD103 was upregulated on subsets of these cells. These data indicate that $CD103^+$ subsets require an additional signal in vivo to develop, on top of antigen stimulation, similar to what we observed in vitro. This signal is present in some tumors, but not others, and may well be TGFβ. Interestingly, $CD103^+$ CD8 TIL subsets were present at significantly higher fractions in small bowel metastases, compared to tumor involved nodes or skin metastases. Based on these findings, we hypothesize that the tumors, such as skin and TIN metastases, with small to absent $CD103^+$ CD8 TIL have little active TGFβ in the TME. Future studies will test this hypothesis. Our data confirm the hypothesis that RI expression on CD8 T cells marks functionally and phenotypically distinct subpopulations. Importantly, we found that CD49a SP cells not only are capable of inducing expression of multiple effector cytokines, they additionally expressed memory marker CD127. On the other hand, subsets expressing CD49b and/or CD103 in addition to CD49a were more dysfunctional and expressed high levels of exhaustion markers PD1 and TIM3. These data indicate one of two explanations; CD8 TIL that express multiple retention integrins and thus remain in the TME may become quiescent/ exhausted. Alternatively, CD8 TIL that become exhausted in the TME may also upregulate multiple retention integrins. Interestingly though, the most exhausted subsets also expressed the highest level of cytotoxicity marker perforin, suggesting that there may be a diversification in TIL subsets, some that are most polyfunctional for cytokine secretion and others with maximal cytotoxic function. The subset expressing highest perforin levels were also the most exhausted/quiescent, raising important questions about the association between exhaustion state and effector dysfunction. In vivo studies addressing the dynamics of retention integrin expression on CD8 TIL and their location may provide more insight into the relationship among RI expression, exhaustion and effector molecule expression. Regardless, these results offer important insights

for adoptive T cell therapies and may guide strategies to selectively enhance more functional T cell subsets in the TME by other immune therapies. However, our preliminary data on CD49a^{+} CD8 T cell localization showed that differences in functional state may not simply be caused by distinct differentiation state. The different integrins may also provide retention in specific locations within the TME leading to selective exposure to tumor cells. Interestingly, CD49a^{+}CD8 T cells may be associated with perivascular locations. This may be expected since the primary ligand for CD49a is collagen IV, which is highly expressed in perivascular tissues. IL-2 increases the proportion of CD49a and CD49b on CD45RO^{neg} CD8 T cells, which raises important questions about the possible advantage of having naïve T cells retained in peripheral tissues. However, we have only selected naïve T cells based on CD45RO and CD45RA expression. Thus, CD8 T cells inducing CD49a and CD49b upon IL-2 stimulation, may also be terminal effectors. If CD49a and CD49b are indeed induced on naïve T cells by IL-2, it is possible that these RI^{+} naive cells are recruited to and retained in tertiary lymphoid structures (TLS) within chronically inflamed tissues, including tumors, and subsequently get activated in situ (38). High levels of IL-2 in the TME, provided by Th1 CD4 cells, may thus be beneficial for the retention of naïve CD8 cells within TLS's and thus may increase the probability of their activation by DCs presenting tumor antigen. Heterogeneity of neoantigens has been identified among different metastases in the same tumor (39); so, there may be an advantage to retaining naïve T cells that could recognize new antigens locally. Further experiments regarding naïve T cells based on CD45RA as well as CCR7 and CD62L will have to be done to confirm our conclusions. Since chemokines can recruit T cells to peripheral tissues, and some are critical for activating homing receptors on T cell, we suspected that chemokines may also support their retention in those tissues (40-42). However, none of the 7 chemokines we tested had any impact on induction of these RI. We cannot rule out effects of other chemokines, or effects of chemokines on cytokine mediated induction of RI, but thus far our data suggest that the process of T cell retention in the TME through integrins is controlled separately from the process of homing to tumor. The molecular mechanisms by which cytokines upregulate RI are not completely understood. Because CD49a (VLA-1) and CD49b (VLA-2) are induced fully over several days, we suspect the effect of antigen stimulation and/or TGFβ is indirect; so future work should identify key intermediate proteins or signaling pathways. From a clinical perspective, the present report raises the possibility that RI can be upregulated in the TME by changing the cytokine milieu. Manipulations of this sort may enable selective induction of functional rather than dysfunctional T cell subpopulations. Intratumoral or tumor-targeted therapies to support CD49a-mediated T cell retention in the TME may improve the efficacy of current immune therapies by increasing retention and function of long-lived tumor-reactive T cells. We are currently testing whether the present findings can be replicated in vivo in murine models, and whether myeloid cells, stromal cells, or tumor cells themselves may modulate or support RI expression and function of RI^{+} T cells among both murine and human TIL. Such studies will provide further guidance toward clinical manipulation of RI expression for support of antitumor immunity or for modulation of autoimmune diseases.

References

1. Cepek KL, Shaw SK, Parker CM, Russell GJ, Morrow JS, Rimm DL, Brenner MB. Adhesion between epithelial cells and T lymphocytes mediated by E-cadherin and the alpha E beta 7 integrin. Nature. 1994;372:190–193. doi:10.1038/372190a0.
2. Roberts AI, Brolin RE, Ebert EC. Integrin alpha1beta1 (VLA-1) mediates adhesion of activated intraepithelial lymphocytes to collagen. Immunology. 1999;97:679–685.
3. Kim SK, Schluns KS, Lefrancois L. Induction and visualization of mucosal memory CD8 T cells following systemic virus infection. J Immunol. 1999;163:4125–4132.
4. Cepek KL, Parker CM, Madara JL, Brenner MB. Integrin alpha E beta 7 mediates adhesion of T lymphocytes to epithelial cells. J Immunol. 1993;150:3459–3470.
5. Wakim LM, Woodward-Davis A, Bevan MJ. Memory T cells persisting within the brain after local infection show functional adaptations to their tissue of residence. Proc Natl Acad Sci U S A. 2010;107:17872–17879. doi:10.1073/pnas.1010201107.
6. El-Asady R, Yuan R, Liu K, Wang D, Gress RE, Lucas PJ, Drachenberg CB, Hadley GA. TGF-{beta}-dependent CD103 expression by CD8(+) T cells promotes selective destruction of the host intestinal epithelium during graft-versus-host disease. J Exp Med. 2005;201:1647–1657. doi:10.1084/jem.20041044.
7. Salerno EP, Olson WC, McSkimming C, Shea S, Slingluff CL Jr. T cells in the human metastatic melanoma microenvironment express site-specific homing receptors and retention integrins. Int J Cancer J Int Du Cancer. 2014;134:563–574. doi:10.1002/ijc.28391.
8. Piet B, De Bree GJ, Smids-Dierdorp BS, Van Der Loos CM, Remmerswaal EB, Von Der Thusen JH, Van Haarst JMW, Eerenberg JP, Ten Brinke A, Van Der Bij W, et al. CD8(+) T cells with an intraepithelial phenotype upregulate cytotoxic function upon influenza infection in human lung. J Clin Invest. 2011;121:2254–2263. doi:10.1172/JCI44675.
9. Franciszkiewicz K, Le Floc'h A, Jalil A, Vigant F, Robert T, Vergnon I, Mackiewicz A, Benihoud K, Validire P, Chouaib S, et al. Intratumoral induction of CD103 triggers tumor-specific CTL function and CCR5-dependent T-cell retention. Cancer Res. 2009;69:6249–6255. doi:10.1158/0008-5472.CAN-08-3571.
10. Boisvert M, Gendron S, Chetoui N, Aoudjit F. Alpha2 beta1 integrin signaling augments T cell receptor-dependent production of interferon-gamma in human T cells. Mol Immunol. 2007;44:3732–3740. doi:10.1016/j.molimm.2007.04.003.
11. Richter MV, Topham DJ. The alpha1beta1 integrin and TNF receptor II protect airway CD8+ effector T cells from apoptosis during influenza infection. J Immunol. 2007;179:5054–5063. doi:10.4049/ jimmunol.179.8.5054.
12. Mackay LK, Rahimpour A, Ma JZ, Collins N, Stock AT, Hafon ML, Vega-Ramos J, Lauzurica P, Mueller SN, Stefanovic T, et al. The developmental pathway for CD103(+) CD8+ tissue-resident memory T cells of skin. Nat Immunol. 2013;14:1294–1301. doi:10.1038/ni.2744.
13. Gebhardt T, Lm W, Eidsmo L, Pc R, Wr H, Carbone FR. Memory T cells in nonlymphoid tissue that provide enhanced local immunity during infection with herpes simplex virus. Nat Immunol. 2009;10:524–530. doi:10.1038/ni.1718.
14. De Fougerolles AR, Sprague AG, Nickerson-Nutter CL, Chi-Rosso G, Rennert PD, Gardner H, Gotwals PJ, Lobb RR, Koteliansky VE. Regulation of inflammation by collagen-binding integrins alpha1- beta1 and alpha2beta1 in models of hypersensitivity

and arthritis. J Clin Invest. 2000;105:721–729. doi:10.1172/JCI7911.
15. Webb JR, Wick DA, Nielsen JS, Tran E, Milne K, McMurtrie E, Nelson BH. Profound elevation of CD8+ T cells expressing the intraepithelial lymphocyte marker CD103 (alphaE/beta7 Integrin) in high-grade serous ovarian cancer. Gynecol Oncol. 2010;118:228– 236. doi:10.1016/j.ygyno.2010.05.016.
16. Webb JR, Milne K, Watson P, Deleeuw RJ, Nelson BH. Tumorinfiltrating lymphocytes expressing the tissue resident memory marker CD103 are associated with increased survival in highgrade serous ovarian cancer. Clinical Cancer Res. 2014;20:434– 444. doi:10.1158/1078-0432.CCR-13-1877.
17. Cresswell J, Robertson H, Neal DE, Griffiths TR, Kirby JA. Distribution of lymphocytes of the alpha(E)beta(7) phenotype and E-cadherin in normal human urothelium and bladder carcinomas. Clin Exp Immunol. 2001;126:397–402.
18. Djenidi F, Adam J, Goubar A, Durgeau A, Meurice G, De Montpreville V, Validire P, Besse B, Mami-Chouaib F. CD8+CD103+ tumor-infiltrating lymphocytes are tumor-specific tissue-resident memory T cells and a prognostic factor for survival in lung cancer patients. J Immunol. 2015;194:3475–3486.
19. Workel HH, Komdeur FL, Wouters MC, Plat A, Klip HG, Eggink FA, Wisman GBA, Arts HJG, Oonk MHM, Mourits MJE, et al. CD103 defines intraepithelial CD8+ PD1+ tumour-infiltrating lymphocytes of prognostic significance in endometrial adenocarcinoma. Eur J Cancer. 2016;60:1–11.
20. Wang ZQ, Milne K, Derocher H, Webb JR, Nelson BH, Watson PH. CD103 and intratumoral immune response in breast cancer. Clinical Cancer Res. 2016;22:6290–6297. doi:10.1158/1078-0432. CCR-16-0732.
21. Murray T, Fuertes Marraco SA, Baumgaertner P, Bordry N, Cagnon L, Donda A, Romero P, Verdeil G, Speiser DE. Very late antigen-1 marks functional tumor-resident CD8 T cells and correlates with survival of melanoma patients. Front Immunol. 2016;7:573. doi:10.3389/fimmu.2016.00573.
22. Rihs S, Walker C, Virchow JC Jr., Boer C, Kroegel C, Giri SN, Braun RK. Differential expression of alpha E beta 7 integrins on bronchoalveolar lavage T lymphocyte subsets: regulation by alpha 4 beta 1- integrin crosslinking and TGF-beta. Am J Respir Cell Mol Biol. 1996;15:600–610. doi:10.1165/ajrcmb.15.5.8918367.
23. Kilshaw PJ, Murant SJ. A new surface antigen on intraepithelial lymphocytes in the intestine. Eur J Immunol. 1990;20:2201–2207. doi:10.1002/eji.1830201008.
24. Kilshaw PJ, Murant SJ. Expression and regulation of beta 7(beta p) integrins on mouse lymphocytes: relevance to the mucosal immune system. Eu J Immunol. 1991;21:2591–2597. doi:10.1002/ eji.1830211041.
25. Sheridan BS, Lefrancois L. Regional and mucosal memory T cells. Nat Immunol. 2011;12:485–491.
26. Goldstein I, Ben-Horin S, Koltakov A, Chermoshnuk H, Polevoy V, Berkun Y, Amariglio N, Bank I. alpha1beta1 Integrin+ and regulatory Foxp3+ T cells constitute two functionally distinct human CD4+ T cell subsets oppositely modulated by TNFalpha blockade. J Immunol. 2007;178:201–210. doi:10.4049/jimmunol.178.1.201.
27. Ben-Horin S, Goldstein I, Koltakov A, Langevitz P, Ehrenfeld M, Rosenthal E, Gur H, Bank I. The effect of blockade of tumor necrosis factor alpha on VLA-1+ T-cells in rheumatoid arthritis patients. J Clin Immunol. 2007;27:580–588. doi:10.1007/ s10875- 007-9119-6.

28. Zhang N, Bevan MJ. Transforming growth factor-beta signaling controls the formation and maintenance of gut-resident memory T cells by regulating migration and retention. Immunity. 2013;39:687–696. doi:10.1016/j.immuni.2013.08.019.
29. Schindelin J, Arganda-Carreras I, Frise E, Kaynig V, Longair M, Pietzsch T, Preibisch S, Rueden C, Saalfeld S, Schmid B, et al. Fiji: an open-source platform for biological-image analysis. Nat Methods. 2012;9:676–682. doi:10.1038/nmeth.2019.
30. Ellis B, Haaland P, Hahne F, Le Meur N, Gopalakrishnan N, Spidlen J, Jiang M. flowCore: Basic structures for flow cytometry data. R package version 1.44.0. 2017. doi:10.18129/B9.bioc. flowCore

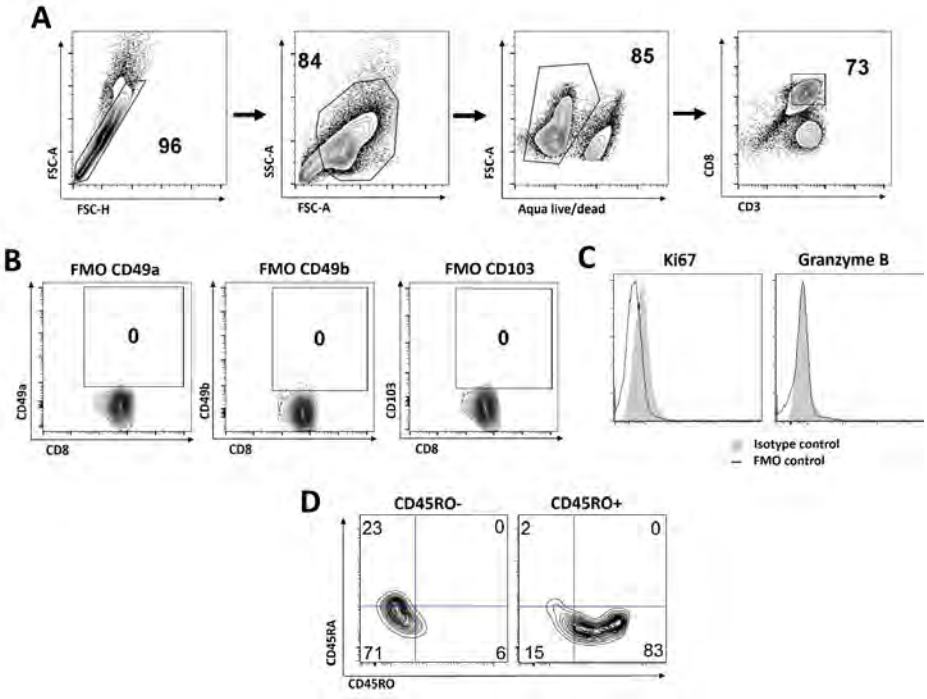

Supplemental Figure 1. (A) Gating strategy used to analyze flow cytometry data. **(B)** FMO controls to establish positive expression of RI. **(C)** Isotype controls for Ki67 and Granzyme B. **(D)** Assessment of CD45RO and CD45RA expression after CD45RO enrichment.

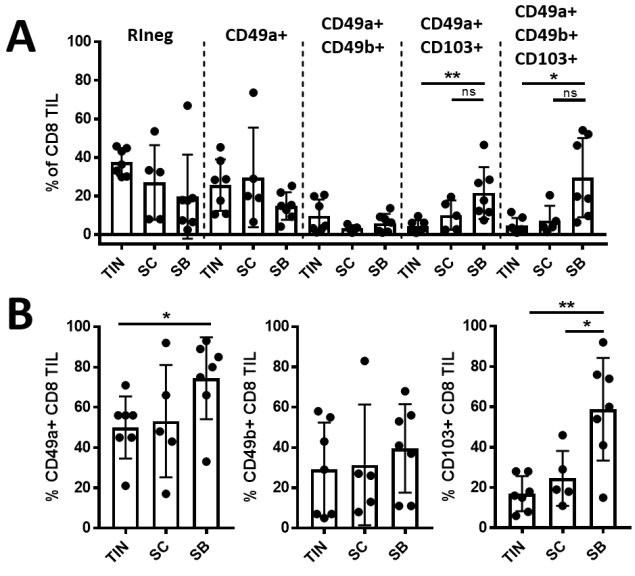

Supplemental Figure 2. Fraction of RI-expressing subsets on human melanoma-derived CD8 TIL per tissue origin (n=19; 7 small bowel, 5 skin and 7 tumor-involved lymph nodes (TIN)). Subsets are displayed as defined in Figure 1B **(A)** or as total integrin+ fraction for CD49a, CD49b or CD103 separately **(B)**. * P<0.05, ** P≤0.01, *** P≤0.001, **** P<0.0001.

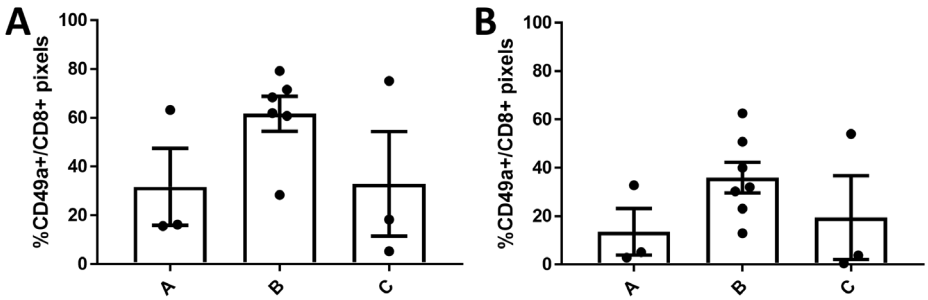

Supplemental Figure 3. CD49a expression on CD8 TIL may depend on localization within the tumor microenvironment. **(A/B).** Average fraction of CD49a^{+} pixels per total CD8^{+} pixels depicted for each FFPE tumor section. Tumors were previously characterized for localization of immune cells (immune absent/ immunotype A, perivascular/immunotype B or diffusely/immunotype C). Per section a minimum of 3 and a maximum of 10 20x images were analyzed. Positive pixels were determined with either a low threshold **(A)** or a high threshold **(B)** to ensure accuracy.

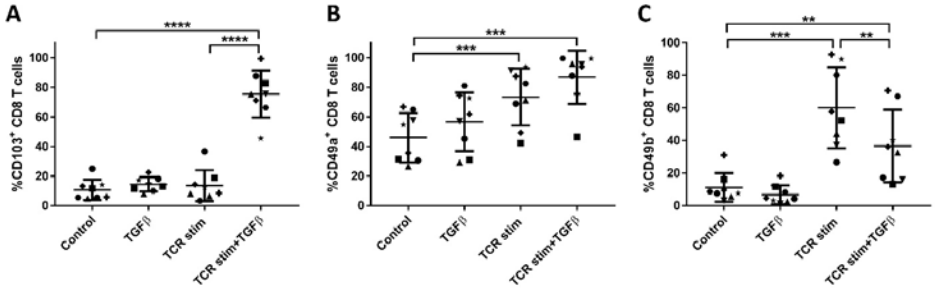

Supplemental Figure 4. Normal donor PBMC were cultured with CD3 and CD28 activating antibodies (TCR stim) for 24h, after which they were grown for 7 days with or without TGFβ. Accumulated data for fraction of CD103 **(A)**, CD49a **(B)** and CD49b **(C)** expressing CD8 T cells after 8 days of culture, with/without TCR stim and/or TGFβ. * P<0.05, ** P≤0.01, *** P≤0.001, **** P<0.0001.

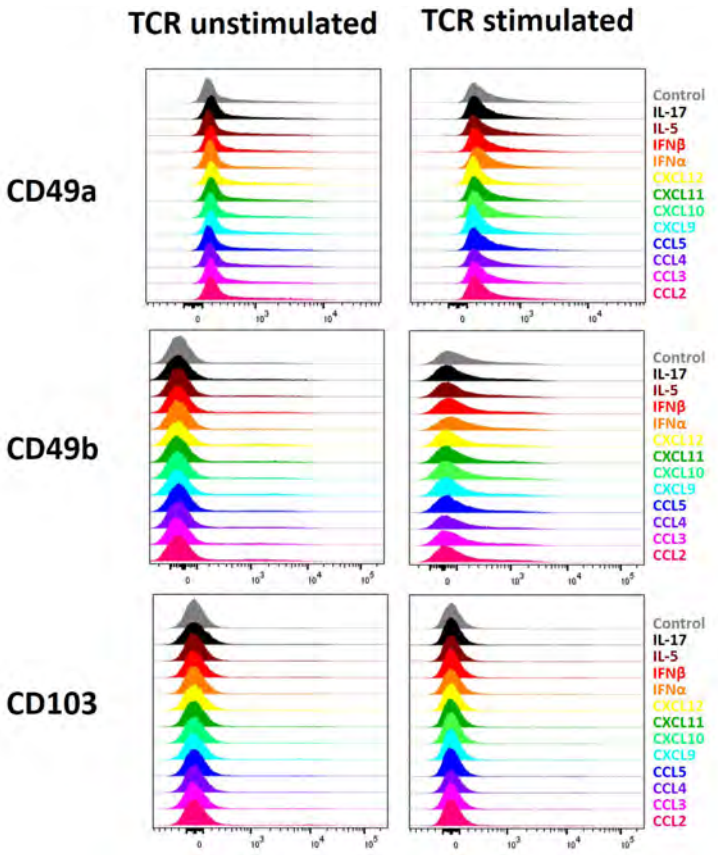

Supplemental Figure 5. Histograms for CD49a, CD49b and CD103 expression after addition of cytokines or chemokines IL-17, IL-5, IFNβ, IFNα, CXCL9-12, CCL2-5, with or without TCR stimulation.

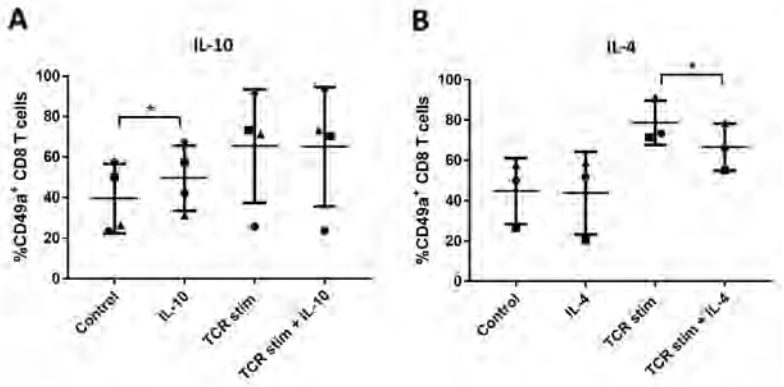

Supplemental Figure 6. Fraction of CD49a expressing CD8 T cells after TCR stimulation and/or 7 days of culture with IL-10 **(A)** or IL-4 **(B)**. * P<0.05, ** P≤0.01, *** P≤0.001, **** P<0.0001.

Chapter 6

Differential expression of CD49a and CD49b determines localization and function of tumor infiltrating CD8 T-cells

Marit M. Melssen, Robin S. Lindsay, Katarzyna Stasiak, Anthony B. Rodriguez, Amanda M. Briegel, Salwador Cyranowski, Melanie Rutkowski, Mark R. Conaway, Cornelis J.M. Melief, Sjoerd H. van der Burg, Ukpong Eyo, Craig L. Slingluff, Jr and Victor H. Engelhar

Submitted

ABSTRACT

CD8 T-cell infiltration and effector activity in solid tumors are correlated with better overall survival of patients suggesting that the ability of T-cells to enter and to remain in contact with tumor cells supports tumor control. CD8 T-cells are known to express the collagen-binding integrins CD49a and CD49b, although little is known about the function of these integrins or how their expression is regulated in the tumor microenvironment (TME). Here, we found that tumor-infiltrating CD8 T-cells initially express CD49b, gain CD49a, and then lose the expression of CD49b over the course of tumor outgrowth. This differentiation sequence is driven by antigen-independent elements in the TME, although T-cell receptor stimulation further increased CD49a expression. On intratumoral CD49a-expressing CD8 T-cells, CD69 was upregulated in the absence of T-cell receptor signaling, consistent with both the establishment of a tissue resident memory-like T-cell phenotype, and a lack of productive antigen engagement. Imaging T-cells in live tumor slices revealed that CD49a increases their motility, especially of those in close proximity to tumor cells. Thus, CD49a may block the interaction of T-cells with tumor cells by not allowing productive engagement. Together, our results illuminate a new mechanism of CD8 T-cell dysfunction in tumors, which is driven by and dependent upon antigen-independent elements in the TME.

INTRODUCTION

Survival of cancer patients is prolonged in those whose tumors are robustly infiltrated by T-cells (1–3). The extent of T-cell representation in tumors depends on several factors (4), including their capacity to utilize homing mechanisms as well as their ability to survive and to be retained in the tumor microenvironment (TME). Homing mechanisms used by tumor-infiltrating T-cells depend on expression of homing receptor ligands VCAM-1, ICAM-1, E-selectin, and CXCR3-binding chemokines on tumor-associated vasculature (5–7). However, the processes of T-cell retention and localization in tumors are less well-studied and likely depend on antigen recognition, interaction with extracellular matrix (ECM) proteins, and expression of molecules that mediate tissue egress into lymphatics (8–15). Specifically, interaction with ECM could either retain T-cells in tumor tissue generally or sequester T-cells in ECM-rich areas, preventing them from engaging with tumor cells (16,17). T-cell interactions with ECM proteins, including collagens, can be mediated by integrins such as a1b1 (CD49a) and a2b1 (CD49b) (18). CD49a and CD49b predominantly bind to collagen type IV and type I, respectively (5,18–21). Blocking CD49a interaction with collagen *in vivo* has been shown to decrease the number of intraepithelial CD8 T-cells in the gut under homeostatic conditions and to decrease total T-cell numbers in mucosal tumors (22,23). Furthermore, CD49a signaling is associated with increased T-cell motility in tissues (24–26). Together, these findings suggest that interactions between ECM collagens and T-cell integrins in tumors could determine overall T-cell numbers and localization, and also their ability to engage with target cells productively. Importantly, whether these processes are supported or impaired by CD49a and CD49b equally and how each specifically impacts T-cell function in tumors remains to be elucidated.

CD49b is expressed on a fraction of effector T-cells in the context of arthritis, influenza or LCMV infection and in tumors, while CD49a expression is limited to a fraction of effector cells specifically localized to peripheral tissue sites in these models (18,21,27,28). CD49a is also expressed on tissue resident memory T-cells (T_{RM}) in lung, skin and mucosal sites (29). Neither CD49a or CD49b are expressed on naïve or circulating memory T-cells (18,30,31). T-cell receptor (TCR)-mediated activation is thus likely required for the expression of these integrins, while CD49a may additionally require stimulation provided by an element in the peripheral tissue microenvironment. We previously observed increased expression of CD49a and CD49b on human CD8 T cells after *in vitro* TCR stimulation, and expression was further enhanced by TGFβ, TNFα, and IL-2 (31). Others have found that the presence of CD49a$^+$ T_{RM} cells in mice depends on TGFβ and Notch signaling (32,33). However, it is not known whether any of these are dominant mediators of CD49a and CD49b expression during an immune response *in vivo*, or in chronic inflammatory environments or tumors. Thus, in addition to understanding their direct role in T-cell function, it is important to further understand the regulation and expression dynamics of collagen-binding integrins CD49a and CD49b *in vivo*. Based on known expression patterns as described above, we hypothesized that

CD49a and CD49b expression on CD8 T-cells is tightly regulated during antigen-driven differentiation, as well as by anatomical residence of the activated T-cell. To address this, we determined the dynamics of CD49a and CD49b integrin expression on CD8 T-cells during vaccine-induced and anti-tumor immune responses. Furthermore, we utilized adoptive transfer of specific integrin-expressing T-cell populations to track their differentiation over time in tumor-bearing hosts. We established separate roles of antigen-driven differentiation and elements in the TME in controlling the expression of CD49a and CD49b by CD8 T-cells. We also hypothesized that CD49a and CD49b play distinct roles in T-cell function by affecting T-cell location and motility. Therefore, we determined how expression of either integrin affects CD8 T-cell functional capacity in tumors and how expression correlated with the generation of exhausted and T_{RM} phenotypes. Our studies revealed a potentially important role for CD49a in T-cell motility and ability to engage with tumor cells.

METHODS

Mice

C57BL/6 mice were from Charles River/NCI. CD2-dsRed (kindly provided by Jordan Jacobelli at the University of Colorado, Anschutz Medical Campus), Nur77-GFP reporter (C57BL/6-Tg(Nr4a1-EGFP/cre)820Khog/J) (34), OT-I transgenic (C57BL/6-Tg(TcraTcrb)1100Mjb/J), and Thy1.1 congenic mice (B6.PL-Thy1a/CyJ) (Jackson Laboratories) were bred in-house in a pathogen-free facility. For tumor studies, male and female mice between 6-12 weeks of age were used. All procedures were approved by the University of Virginia Animal Care and Use Committee in accordance with the NIH Guide for Care and Use of Laboratory Animals.

Tumor lines and injections

BRPKp110 breast carcinoma cells (expressing GFP) were provided by Jose Conejo-Garcia and Melanie Rutkowski (35). B16-F1 cells were obtained from the American Type Culture Collection and transfected with cytoplasmic ovalbumin (OVA) as described(36). Cells ($4x10^5$) were injected subcutaneously (SC) in the neck scruff in 200ml Phosphate-Buffered Saline (PBS). All cell lines used for tumor injections were cultured a within 2-8 passages post thaw and testing for mycoplasma contamination.

In vitro T-cell activation and culture

Single cell suspension of spleens from OT-IxThy1.1 or C57BL/6 mice were filtered through 70m mesh (Miltenyi) and treated with red blood cell (RBC) lysis buffer (Sigma). CD8 T-cells were enriched with magnetic beads (Miltenyi) according to the manufacturer's protocol, and cultured at $1x10^6$ cells/ml in RPMI1640 with 10%

Fetal Bovine Serum (FBS) (Sigma), 15mM Hepes, 2mM L-glutamine, 10mM sodium pyruvate, 1X essential and non-essential amino-acids, 1mg/ml gentamicin (all from Gibco), 0.05mM β-mercaptoethanol (Sigma), 120 IU/ml human recombinant IL-2 and 10ng/ml murine recombinant IL-7 (Peprotech). CD3/CD28 T activator beads (Gibco) were added for the first 48h, after which they were magnetically removed. Cells were split to $1x10^6$ cells/ml with fresh medium every 2-3 days.

Tumor lysates for addition to OT-I cell cultures were generated from day 28 BRPKp110 tumors. Tumors were harvested, cut into small pieces, resuspended in H_2O for 20 min, and sonicated on ice for 20 min (30 sec on, 30 sec off throughout) with a Sonic Dismembrator Model 500 (Fisher Scientific), amplitude of 37%. Lysates were centrifuged at 10,000 x g for 20 min at 4°C. Supernatants were collected, filtered through a 0.2m filter and supplemented with PBS containing 10% FBS (Sigma), 15mM Hepes, 2mM L-glutamine, 10mM sodium pyruvate, non-essential amino-acids, essential amino-acids, 1mg/ml gentamicin (all from Gibco) and 0.05mM β-mercaptoethanol (Sigma).

Vaccination and adoptive cell transfer

Single cell suspension of spleens from OT-IxThy1.1 mice were filtered through 70m mesh (Miltenyi), treated with RBC lysis buffer (Sigma), washed in PBS, and injected intravenously (IV) ($5x10^4$ cells) into naïve Thy1.2$^+$ C57BL/6 mice. The next day, mice were injected IV with 500mg ovalbumin (Sigma), 50mg anti-CD40 (BioXcell) and 100mg polyIC (InvivoGen). Five days post vaccination, filtered and RBC lysed single cell suspensions of spleens were depleted of CD49a$^+$ cells and subsequently enriched for CD49b$^+$ cells. Cells were incubated with biotinylated CD49a (Miltenyi) or CD49b (clone HMa2, Biolegend) specific antibodies for 15 min, washed in PBS supplemented with 0.5% BSA, 2mM EDTA, 2mM L-glutamine, 10mM sodium pyruvate, 1X essential and non-essential amino acids, and (concentration) dextrose, and incubated with anti-biotin microbeads (Miltenyi) for 15 min. Cells were then depleted (CD49a) or enriched (CD49b) with magnetic separation columns (Miltenyi). The fraction of Thy1.1$^+$ OT-I cells was quantitated and $1x10^6$ Thy1.1$^+$ cells were injected IV into tumor bearing mice in 200ml PBS supplemented with 15,000U/ml IL2.

In vivo checkpoint inhibitor blockade

Mice were treated intraperitoneally with anti-PD-1 (clone RMP1, BioXCell), anti-LAG-3 (clone C9B7W, BioXCell), and anti-TIM-3 (clone RMT2-23, BioXCell) or matching IgG isotype controls (clones HRPN and 2A3, BioXCell) (250mg/mouse for each antibody) 48h prior to tumor harvest.

Tumor harvest

At indicated time points, tumors were harvested in RPMI-1640 supplemented with 2% FBS (Sigma), 15mM HEPES, 2mM L-glutamine, 10mM sodium pyruvate, 1X

essential and non-essential amino acids (all Gibco), 0.05mM b-mercaptoethanol (Sigma), 1mg/ml gentamicin (Gibco), 76mg/ml liberase TM (Roche) and 40mg/ml DNAse (Sigma). Tumors were digested for 15 min at 37°C and homogenized to a single cell suspension. The CD45 fraction was enriched with magnetic beads (Miltenyi) and the Miltenyi Automacs system.

Flow cytometry

Cells were Fc blocked (BioXcell), stained with Aqua Live/Dead dye and stained with fluorescently labeled antibodies (Supplemental Table 1). The BD Cytofix/Cytoperm and BD Transcription Factor Staining kits were used for fixation/permeabilization in intracellular and intranuclear stains, respectively. Cells were analyzed on Cytoflex (Beckman Coulter) or Attune (BD Biosciences) flow cytometers and analyzed with FlowJo software.

Live tumor slice imaging

Tumors were harvested and directly embedded in 2% low-melting point agarose. Tissue was cut into 100-200µm slices and placed in RPMI1640 without phenol red (Gibco). From each tumor, 3 slices were cut and either left untreated, treated with 10µg/ml purified CD49a antibodies (clone Ha/31, BD Biosciences) or 10µg/ml purified CD49b antibodies (clone HMa2, BD Biosciences) for 2h at room temperature. Slices were mounted and stabilized in an imaging chamber under the microscope objective lens. Imaging was conducted using an in-line heating chamber with circulating media maintained in oxygenated RPMI1640 without phenol red (Gibco) at a flow rate of ~2ml/min. Cells were imaged using a two-photon microscope (Leica TCS SP8) with a Coherent Chameleon laser tuned to 880 nm with a 25X water-immersion lens (0.9NA). Fluorescence was detected using three photomultiplier tubes in whole-field detection mode and a 565nm dichroic mirror with 450/50nm (blue channel) 525/50nm (green channel) and 620/60nm (red channel) emission filters. The laser power was maintained at 25mW or below. We imaged cells between 78-84µm from the slice surface. Images were collected for at least 30 minutes. Typically, consecutive z-stack images were collected at 3µm intervals every minute. Movies were generated and processed using with Imaris software for analysis.

Statistical analysis

In flow cytometry experiments, when comparing integrin-expressing subpopulations, a Repeated-Measures one-way ANOVA with Tukey's multiple comparisons test was performed. When different time points, or treatment groups were tested, a Welch's corrected T-test was used. For imaging analyses of T-cell motility and distance to collagen or tumor cells, all T-cell spots for the slices evaluated were combined and compared amongst groups with an ordinary one-way ANOVA with Tukey's multiple comparisons test. Trends were confirmed by comparing groups with the same test for T-cell spots per tumor.

RESULTS

Identification of CD49a and CD49b expressing subpopulations of CD8 T cells in murine B16 melanoma and BRPKp110 breast tumor models

We previously showed that CD49a and CD49b integrins are expressed on CD8 tumor infiltrating lymphocytes (TIL) from human melanomas, but they are almost completely absent on CD8 T cells from normal donor PBMC or tumor-free lymph nodes from patients (31,37). Additionally, we showed that expression of these integrins identified human CD8 TIL subpopulations that varied in levels of perforin, CD127, PD-1, LAG-3 and TIM-3. To further elucidate the origin and evolution of these tumor-associated subpopulations, we utilized two implantable murine tumor models: collagen-rich breast cancer BRPKp110 and collagen-poor melanoma B16-F1 (38). In both models, we observed CD49aCD49b double negative (DN), CD49b single positive (SP), CD49aCD49b double positive (DP) and CD49a SP populations (Fig. 1B). Collagen-rich BRPKp110 contained proportionally more CD49a- and CD49b-expressing cells than collagen-poor B16-F1 (Fig. 1B). Although the CD49b SP subpopulation was more abundant in both murine models than in human TIL, the same subpopulations of retention integrin expressing cells were present in both mouse and human TIL, allowing us to further understand their characteristics.

CD49b- and CD49a-expressing CD8 T-cells appear sequentially after immunization and in the tumor microenvironment

To understand the regulation of CD49a and CD49b expression during an immune response, we evaluated ovalbumin-specific OT-I cells after ovalbumin (OVA) immunization. Early after activation (day 3), expression of CD49a and CD49b remained low and comparable to that of resting OT-I cells (Fig. 1C). By day 5, the fraction of OT-I cells expressing CD49b increased markedly, while the fraction expressing CD49a did not increase until day 9 (Fig. 1C, Supplemental Fig. 2A). By day 14, an overall decline in cells expressing CD49b was observed (Fig. 1C). Next, we quantitated CD49a and CD49b expressing subpopulations among CD8 TIL over the course of BRPKp110 tumor outgrowth. All 4 subpopulations were evident 14 and 23 days after tumor implantation (Fig. 1D). However, the fraction of CD49b SP cells was higher on day 14, while the fractions of CD49a SP cells and DP cells were increased at the later timepoint (Fig. 1E,F). These transitions in integrin-expressing subpopulations were accompanied by an early increase in the absolute number of CD49b SP and DP cells, followed by a decline in the CD49b SP cells and an increase in the absolute number of CD49a SP cells later in tumor development (day 23) (Fig. 1F). The absolute number of DN cells remained low and constant throughout. Collectively, these results establish that the four subpopulations identified in tumors are not stable, but arise sequentially during the course of an immune response.

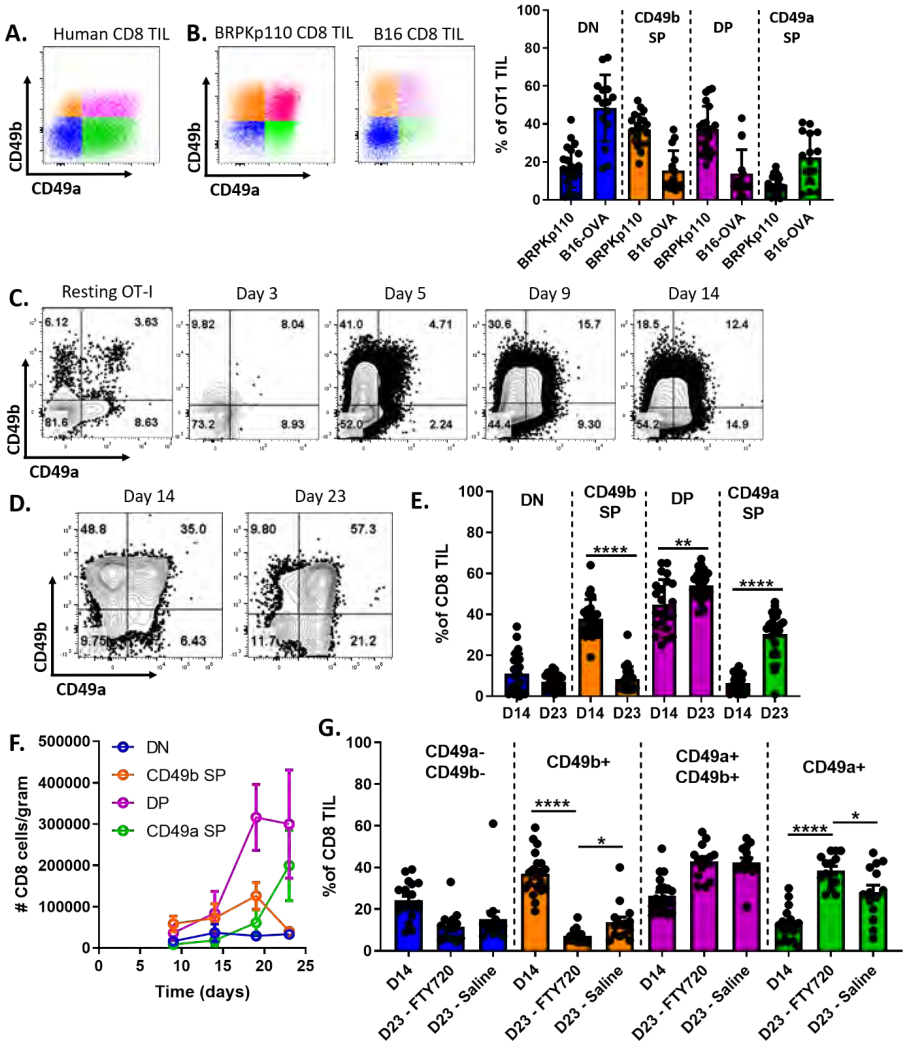

Figure 1: CD49b and CD49a expressing CD8 T-cells arise sequentially during immune responses induced by vaccination or tumor. (A) Single cell suspensions of human metastatic melanoma lesions were analyzed for CD49a and CD49b expression on $CD3^+$ $CD8^+$ cells. (B) C57BL/6 mice were implanted SC with BRPKp110 breast carcinoma (n=21, 4 independent experiments) and murine B16-OVA melanoma (n=15, 3 independent experiments) samples. Tumors were harvested on day 14, single cell suspensions were prepared and enriched $CD45^+$ cells were analyzed for CD49a and CD49b expression on $CD3^+$ $CD8^+$ cells. (C) $Thy1.1^+$ OT-I splenocytes were transferred IV into C57BL/6 mice, which were subsequently immunized with OVA, polyIC, and anti-CD40. Baseline OT-I spleens (pre-transfer) or spleens harvested on the indicated days post transfer and vaccination (n=3 per time point) were analyzed for CD49a and CD49b expression on $Thy1.1^+$ $CD3^+$ $CD8^+$ cells by flow cytometry. (D-G) Subcutaneous BRPKp110 tumors were harvested on the

indicated days, and the $CD45^+$ enriched fraction was analyzed for CD49a and CD49b expression on $CD3^+$ $CD8^+$ cells. (E) n=23-24, 5 independent experiments. Day 14 (D14) and day 23 (D23) were compared within each subset with a Welch's corrected T-test. (F) n=6-8 per time point from 2 independent experiments. (G) Groups of BRPKp110-bearing mice received daily IP injections with either saline or FTY720, starting on day 14 to block migration of additional T-cells from secondary lymphoid organs to the tumor. N=14-20 mice per group from 3 independent experiments. Groups were compared within subsets with a Welch's corrected T-test.

Change in integrin expression occurs specifically in the TME

Our results suggest either that CD49b and CD49a are sequentially expressed on CD8 TIL over the course of tumor outgrowth, or that separate subpopulations of CD8 T-cells with distinct integrin expression patterns are sequentially generated during vaccine-induced and anti-tumor immune responses. To test the latter hypothesis, we utilized FTY720 to block new T-cell infiltration from the periphery, starting on day 14 after tumor implantation. Despite that blockade, the proportion of CD49a SP cells still increased between day 14 and 23 (Fig. 1G). Interestingly, this increase was also significantly greater after FTY720 treatment compared to the saline control (Fig. 1G), potentially because the entry of new CD49b SP cells was also blocked. Together, these data suggest that CD49b SP cells differentiate into CD49a SP cells in the TME over time, with DP cells as a likely intermediate.

CD49a is upregulated on CD49b SP CD8 T-cells after they enter the TME

To interrogate if the TME drives upregulation of CD49a on CD49b SP cells independent of cognate antigen, we transferred CD49b SP cells into mice bearing OVA-negative tumors. First, mice that had been adoptively transferred with OT-I cells were immunized with OVA, leading to upregulation of CD49b on a substantial fraction of the OT-I cells (Fig. 1C). Five days post immunization, we purified CD49b SP OT-I cells from spleens and transferred them into either naïve, tumor-free or established (day 14), OVA-negative BRPKp110 tumor-bearing mice (Fig. 2A). Seven days post transfer, CD49b SP OT-I cells transferred into non-tumor bearing mice failed to upregulate CD49a and had significantly diminished expression of CD49b (Fig. 2B). This contrasts with the behavior of these cells in the original immunized mice, in which CD49a was upregulated over time (Fig. 1C). CD49b SP OT-I cells transferred into mice with BRPKp110 tumors trafficked to tumors consistently and numerously, despite the lack of OVA expression (Fig. 2C). CD49a was expressed on 50-60% of the intratumoral OT-I cells within 24h and virtually all cells expressed CD49a after 7 days (Fig. 2D). At early time points most of the cells were DP, but a CD49a SP subpopulation was evident after 7 days, suggesting DP OT-I cells lose CD49b over time (Fig. 2D). Importantly, transferred CD49b SP OT-I cells isolated from the spleens of these tumor-bearing mice never upregulated CD49a, and showed a significantly lower CD49b expression (Fig. 2E,F), similar to the behavior seen in non-tumor bearing mice (Fig. 2B).

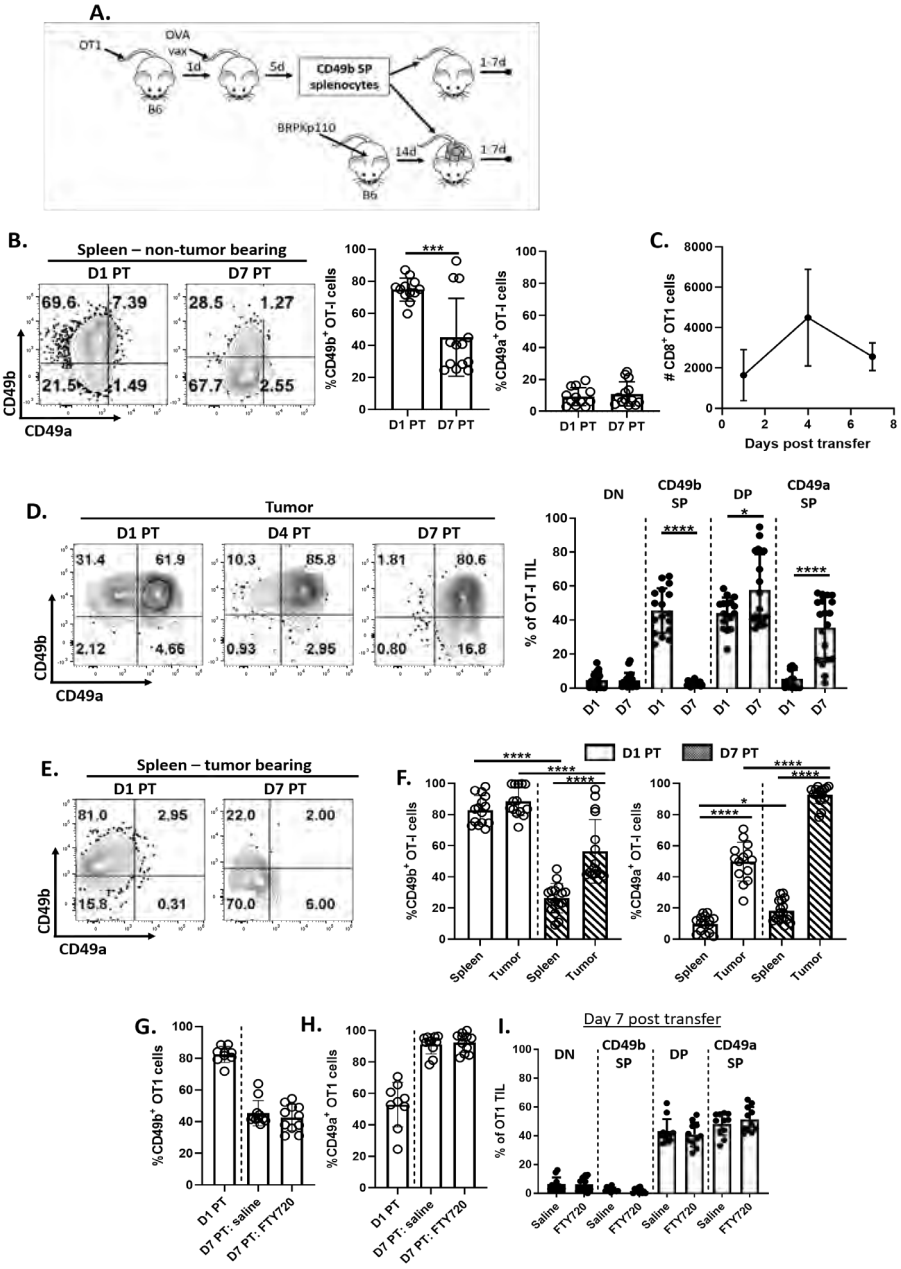

Figure 2: CD8 T-cell differentiate in a stepwise manner from a CD49b SP to DP to CD49a SP in the TME. (A) Schematic of experimental immunization and adoptive transfer model. Details are in Methods and Results. (B) Spleens from tumor-free mice were harvested 1 or 7 days post transfer (PT) of CD49b SP Thy1.1$^+$ OT-I effectors and analyzed for CD49a and CD49b expression on Thy1.1$^+$ CD3$^+$ CD8$^+$ cells by flow cytometry (n=12-13 from 4 independent

experiments, groups were compared with a Welch's corrected T-test). (C-I) Tumors or spleens from BRPKp110 tumor-bearing mice were harvested on the indicated days post transfer (PT) of CD49b SP Thy1.1$^+$ OT-I effectors. Tumor suspensions were enriched for CD45$^+$ cells and the number of accumulated Thy1.1$^+$ CD3$^+$ CD8$^+$ cells (C, n=6 per time point, 2 independent experiments) and CD49b and CD49a expression on accumulated Thy1.1$^+$ CD3$^+$ CD8$^+$ cells (D, F, G, H, I; n=17-19 per time point from 4 independent experiments) was evaluated by flow cytometry. Time points in (D) were compared in each subpopulation with a Welch's corrected T-test. Splenocytes were analyzed for CD49a and CD49b expression on Thy1.1$^+$ CD3$^+$ CD8$^+$ cells by flow cytometry (E, F). Comparisons in (E) were done with an ordinary one-way ANOVA. (G-I) Thy1.1$^+$ OT-I splenocytes were activated and transferred IV into BRPKp110-bearing C57BL/6 mice, as described in (A). Mice received daily IP injections FTY720 or saline control starting at day 1 PT, to block migration of additional T-cells from secondary lymphoid organs to the tumor. Tumors were harvested on day 7 post transfer and enriched CD45$^+$ fractions were analyzed for CD49b and CD49a expression on Thy1.1$^+$ CD3$^+$ CD8$^+$ cells (n=9-11 per group from 2 independent experiments).

These data did not exclude the possibility that OT-I cells upregulated CD49a elsewhere in the animal, and then infiltrated the tumor. To test this latter possibility, we transferred CD49b SP activated OT-I cells into BRPKp110 tumor-bearing mice and treated them with FTY720 starting 1 day post transfer. Despite reducing CD8 T-cell numbers in the blood (Supplemental Fig. 3A), FTY720 had no impact on the number of tumor-infiltrating OT-I cells (Supplemental Fig. 3B). Additionally, FTY720 treatment did not change the reduction in CD49b expression (Fig. 2G) and the induction of CD49a expression on OT-I TIL (Fig. 2H), or the overall proportions of SP and DP OT-I cells in the spleen or tumor (Fig. 2I, Supplemental Fig. 3C). This demonstrates that CD49a is upregulated on CD49b SP cells after they enter the tumor. Overall, our data indicate that activation-induced differentiation of CD8 T-cells is insufficient to induce CD49a, and that this is instead dependent on an environmental factor, present both in spleens of immunized mice and the TME, that upregulates CD49a independent of antigen-stimulation.

A soluble factor in the TME upregulates CD49a expression on CD8 T-cells

We hypothesized that the mediator(s) responsible for CD49a upregulation might be intrinsic to the tumors. To test this, we cultured *in vitro* activated OT-I cells with lysates from 28-day old BRPKp110 tumors. The lysate upregulated CD49a on most of these cells within 24h, independent of CD49b status, and without apparent change in CD49b expression (Fig. 3A). Since CD49a is upregulated on activated human CD8 T-cells *in vitro* by TGFβ(31), *in vitro* activated OT-I cells were cultured with BRPKp110 tumor lysates in the presence of TGFβ1-3 blocking antibodies. However, there was no difference in CD49a upregulation (Fig. 3B). Blocking TGFβ1-3 with the same antibodies during BRPKp110 tumor outgrowth *in vivo* only modestly diminished the fraction of CD49a$^+$ CD8 TIL (Supplemental Fig. 4A). Additionally, culturing *in vitro* activated OT-I cells with recombinant TGFβ1 did not induce CD49a expression, although it did diminish CD49b expression (Fig.

3B, Supplemental Fig. 4B). Thus, a soluble factor other than TGFβ that is present in tumor lysates upregulates CD49a expression on CD8 T-cells *in vitro* and is likely responsible for induction of CD49a on CD8 TIL *in vivo*.

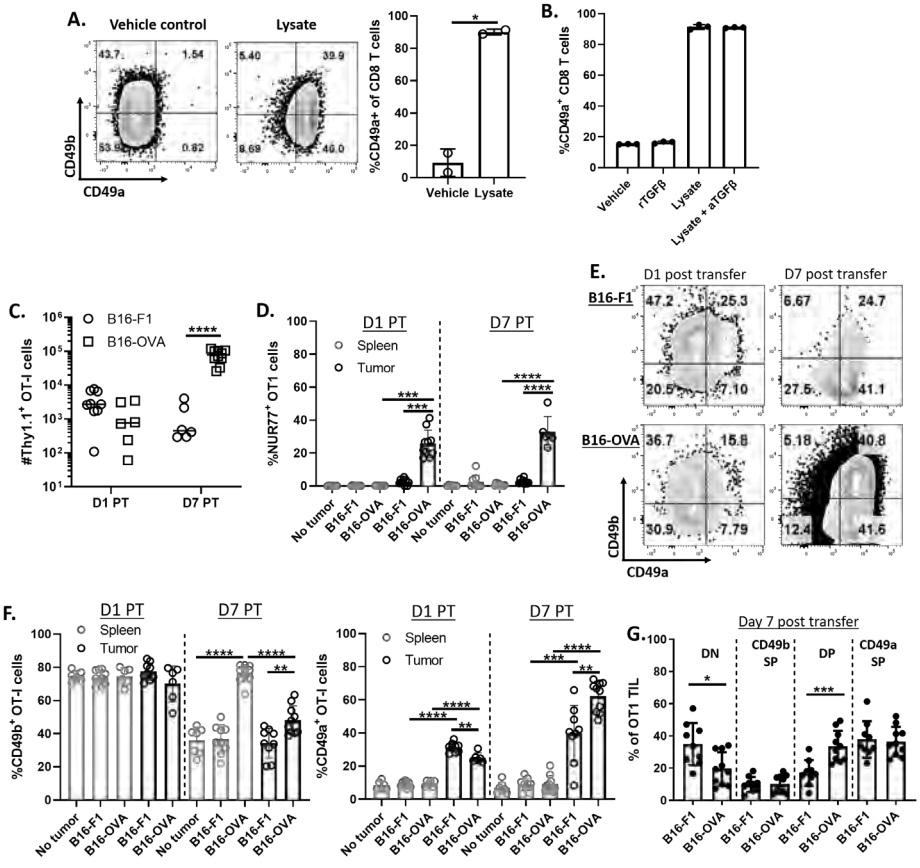

Figure 3: Soluble tumor-derived factors are responsible for upregulation of CD49a. (A, B) Thy1.1⁺ CD8⁺ OT-I cells were activated with CD3/CD28 activation beads, cultured in presence of IL-2 and IL-7, and then cultured for 24h with BRPKp110-derived tumor lysate (A) or recombinant human TGFβ1, BRPKp110 tumor lysate, or tumor lysate with added TGFβ blocking antibody (B). Cells were evaluated for CD49a expression by flow cytometry. (C-G) Thy1.1⁺ OT-I Nur77-GFP reporter splenocytes were transferred into C57BL/6 mice that were subsequently immunized with OVA, polyIC, and anti-CD40, and CD49b SP Thy1.1⁺ OT-I effectors isolated and transferred into B16-F1 or B16-OVA tumor-bearing or tumor-free mice as in Figure 2A. Tumors or spleens from tumor-bearing mice were harvested 1 or 7 days post transfer and the number of accumulated Thy1.1⁺ CD3⁺ CD8⁺ cells (C), and Nur77-GFP expression (D) and CD49b and CD49a expression (E-G) on accumulated Thy1.1⁺ CD3⁺ CD8⁺ cells evaluated by flow cytometry. Each time point and group contained n=6-10 from 2 independent experiments and direct comparisons between groups within a time point were tested with a Welch's corrected T-tests.

Antigen stimulation augments environmentally-induced expression of CD49a

We next addressed the impact of TCR stimulation on the expression of CD49a and CD49b integrins, beyond the early TCR-induced upregulation of CD49b. BRPKp110 expresses very low levels of MHC-I molecules, and BRPKp110 transfected with OVA is very poorly recognized by OT-I cells *in vitro* and *in vivo* (not shown). Consequently, activated CD49b SP OT-I cells were transferred into mice bearing B16-F1 melanomas, either non-transfected or transfected to express OVA (B16-F1 and B16-OVA, respectively). These OT-I cells came from Nur77-GFP reporter mice, enabling us to measure TCR signaling in the transferred population. OT-I cells trafficked into both types of tumors, but their number was substantially increased over 7 days when tumors expressed OVA (Fig. 3C). A significant fraction of cells transferred into B16-OVA tumor-bearing mice upregulated Nur77, indicating local activation by antigen, whereas no Nur77 was expressed in OT-I cells isolated from spleens of B16-OVA bearing-mice or in spleens and tumors of B16-F1 bearing-mice (Fig. 3D). In B16-F1 tumor-bearing mice, OT-I cells lost CD49b in spleen and tumor comparably (Fig. 3E,F). Thus, in contrast to the BRPKp110 TME (Fig. 2D), the B16-F1 TME does not support CD49b maintenance. In B16-OVA tumor-bearing mice, CD49b was maintained on OT-I cells in the spleen, and lost in the TME, although not to the same extend as in B16-F1 tumors (Fig. 3E,F). These results suggest that TCR stimulation not only upregulates CD49b, but also maintains its expression. However, aspects of the TME, such as TGFβ1 or continuous antigen exposure, may diminish CD49b expression. As was observed in BRPKp110 tumors, CD49a was upregulated on CD49b SP OT-I cells in B16 tumors but not spleens of tumor-bearing mice, and this occurred regardless of antigen (Fig. 3F,G). However, the upregulation was significantly greater by day 7 in B16-OVA than B16-F1 tumors. Although it is possible that B16-OVA could support the selective proliferation of CD49a-expressing subpopulations, a more likely explanation is that antigen stimulation augments the TME-dependent upregulation of CD49a expression.

Expression of exhaustion markers is not linked to differential expression of CD49b and CD49a

CD8 TIL become exhausted over time due to chronic antigen stimulation(39). Since both the TME and antigen stimulation drove CD49a upregulation, we determined how CD49a expression and expression of exhaustion markers PD-1, LAG-3 and TIM-3 were associated. Due to the low numbers of transferred cells recovered from BRPKp110 and B16-F1 tumors, it was not possible to evaluate this association as driven by the TME in the absence of antigen. However, we did evaluate integrin-expressing subpopulations arising after transfer of CD49b SP OT-I cells into B16-OVA tumor bearing mice. At the time of transfer, CD49b SP OT-I cells adoptively transferred into tumor-free or B16-OVA tumor-bearing mice expressed PD-1 uniformly, but expressed low levels of LAG-3 and TIM-3, consistent with an effector T-cell phenotype (Fig. 4A). Seven days after transfer into tumor-free mice, a fraction of OT-I cells in the spleen had lost PD-1 expression

and the gMFI on the remaining PD-1^{+} OT-I cells was substantially lower (Fig. 4B). Expression of LAG-3 and TIM-3 on OT-I, though already low at time of transfer, was decreased further. In B16-OVA tumor-bearing mice, exhaustion marker expression on splenic OT-I cells 7 days after transfer was similar to that of tumor-free mice (Fig. 4C). In contrast, PD-1 expression was maintained on all OT-I cells that infiltrated B16-OVA tumors while the MFI was also substantially increased. They also upregulated LAG-3 and TIM-3. These results establish that adoptively transferred CD49b SP OT-I cells acquire an exhausted phenotype based on residency in an antigen-expressing TME. To test whether the upregulation of CD49a was associated with generation of an exhausted phenotype, we evaluate PD-1, LAG-3 and TIM-3 expression on each integrin-expressing OT-I subpopulation, 7 days post transfer. Compared to CD49b SP OT-I phenotype at the time of transfer, PD-1 remained expressed on essentially all cells in all 4 subpopulations, and TME-induced upregulation of the level of expression was also consistent (Fig. 5A). The percentage of DP cells expressing LAG-3 and TIM-3 was very slightly but significantly higher than that of CD49b SP and DN cells, but there was no further increase in the CD49a SP population (Fig. 5A). Similarly, when naïve OT-I cells were transferred prior to B16-OVA implantation and thus activated *in vivo* by tumor-derived OVA, these exhaustion markers were not differentially expressed among integrin-expressing subpopulations (Supplemental Fig. 5). These results suggest that acquisition of an exhausted phenotype is largely independent of CD49a expression.

We also examined the endogenous CD8 T-cells from the same B16-OVA tumors analyzed above, as well as endogenous CD8 T-cells from BRPKp110 and B16-F1 tumors. In contrast to the results above, the fractions of endogenous DP and CD49a SP subpopulations expressing PD-1, LAG-3, Tigit and/or TIM-3 in B16-OVA and BRPKp110 tumors were significantly higher than that of the CD49b SP cells, as was the gMFI of PD-1 (Fig. 5B,C). These same trends were observed in B16-F1 tumors, although the fractions of the subpopulations expressing PD-1 were not different (Fig. 5D). However, the CD49a SP subpopulation only significantly differed from the DP population in B16-OVA tumors, and only in relation to expression of PD-1 and LAG-3. Thus, there is an association between the gain of an exhausted-like phenotype and CD49a expression on endogenous CD8 TIL. As described earlier (Fig. 1G), endogenous T-cells are likely infiltrating into tumors continuously, in contrast to transferred OT-I cells. Endogenous CD49b SP cells are therefore “newer” on average and for that reason, less exhausted. This suggests that the association between integrin differentiation and an exhausted phenotype on endogenous CD8 TIL is temporal, but not mechanistically linked.

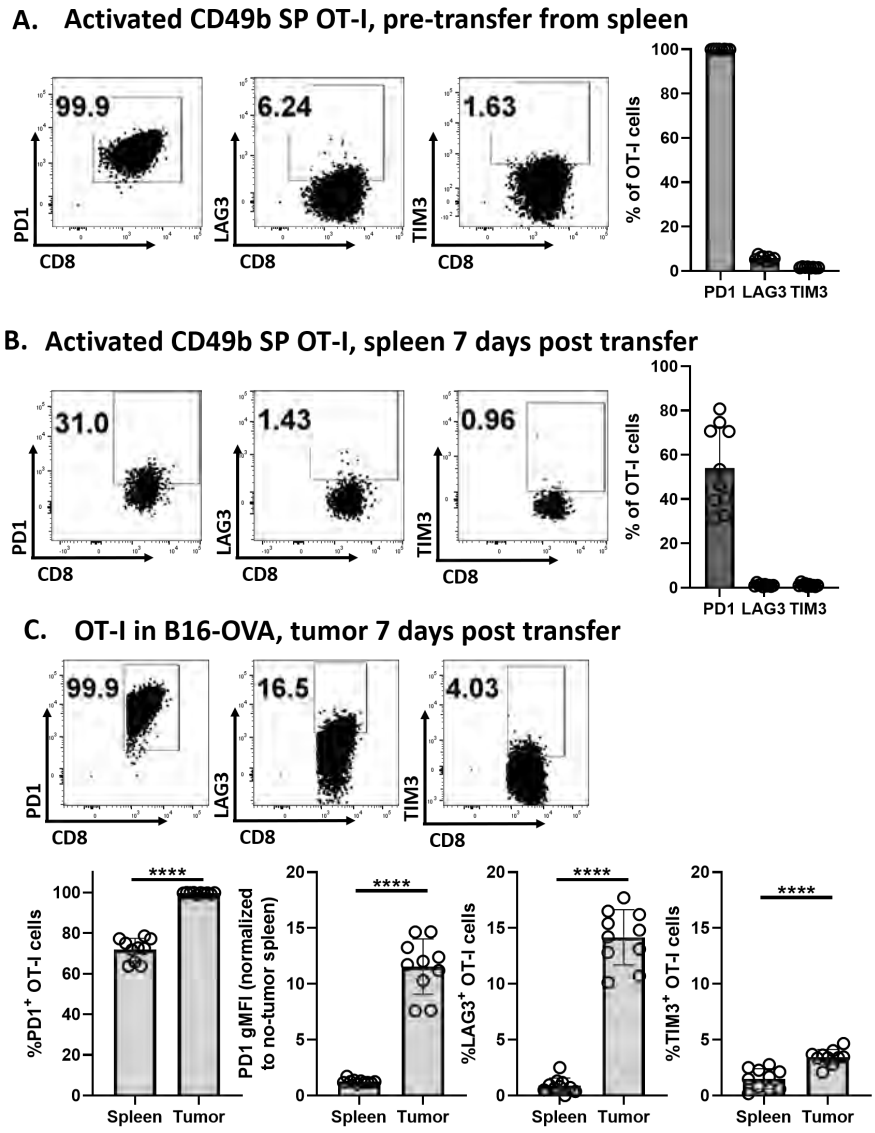

Figure 4. Exhaustion marker expression is driven by environment and antigen-driven differentiation. Experiments were set up as in Figure 2A. Expression of PD-1, LAG-3, TIM-3 and Tigit on isolated CD49b SP Thy1.1$^+$ OT-I cells were determined by flow cytometry. (A) 5 days after vaccination, and prior to transfer. (B) Seven days after transfer into tumor-free mice. (C) Seven days after transfer into B16-OVA tumor-bearing mice (n=10 from 2 independent experiments). Exhaustion marker expression between spleens and tumors were compared with a Paired T-test.

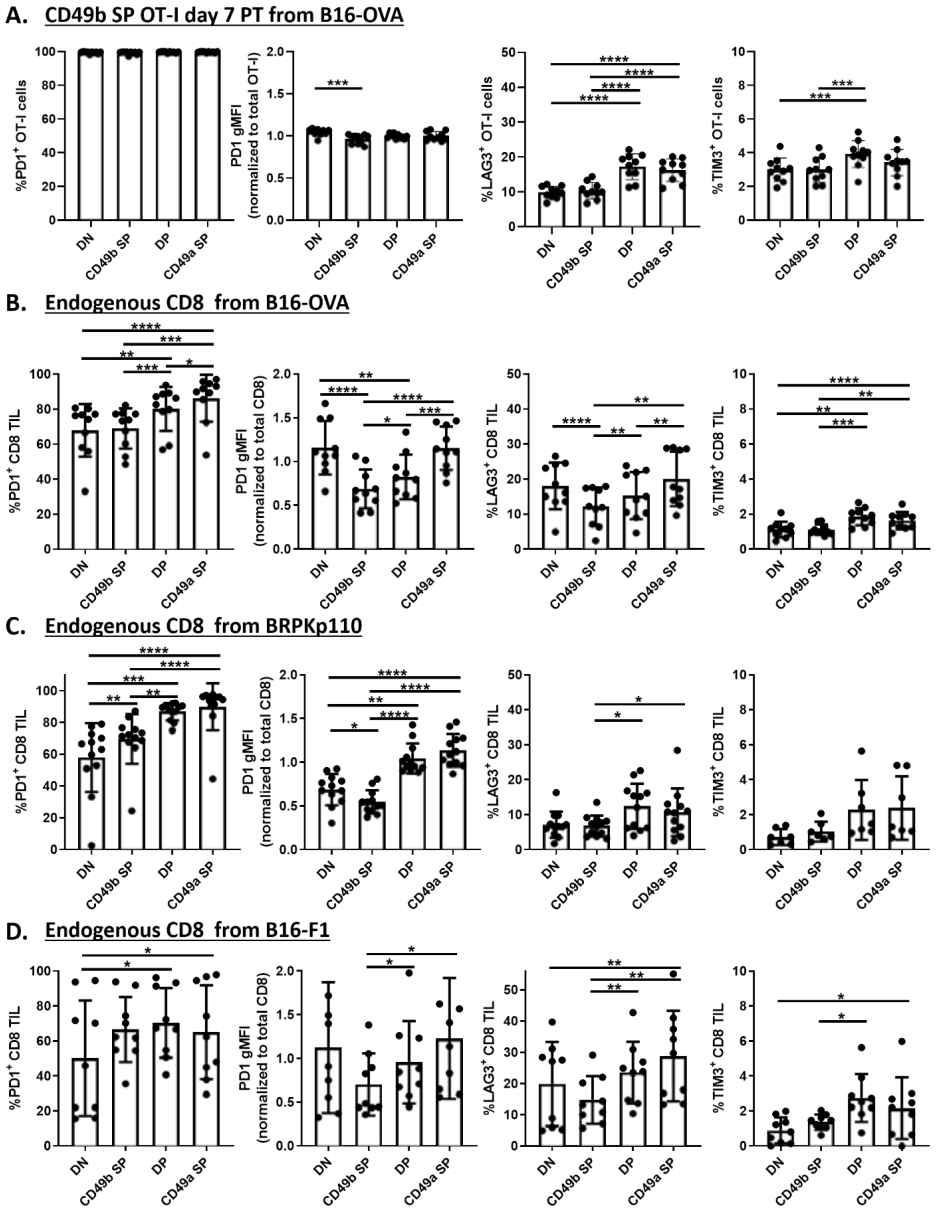

Figure 5: Progression of integrin expression is linked to gain of exhaustion phenotype on endogenous CD8 T-cells. Experimental details were as in Figure 2A. The indicated exhaustion markers were evaluated on either Thy1.1^{+} OT-I cells isolated from B16-OVA tumors seven days after transfer (A), or endogenous Thy1.1^{neg} CD3^{+} CD8^{+} cells isolated from the same B16-OVA (B; n=10), B16-F1 (C; n=9) and BRPKp110 (D; n=12) tumors evaluated in Fig. 4C-E. Marker expression between subpopulations was compared with a Repeated Measures one-way ANOVA and Tukey's multiple comparisons test.

CD49b SP cells can engage with antigen, whereas TCR signaling is low or absent in DP and CD49a SP cells

Based on the elevated expression of exhaustion markers on endogenous CD49a$^+$ CD8 T-cells, we hypothesized that these cells would be less functional *in vivo*. To test this, BRPKp110 tumors were implanted into Nur77-GFP reporter mice. As hypothesized, DP and CD49a SP subpopulations showed significantly less TCR signaling than CD49b SP cells, as measured by Nur77 expression (Fig. 6A, Supplemental Fig. 6A). In fact, Nur77 expression in the CD49a SP cells was not higher than the baseline expression in CD8 T-cells from non-draining lymph nodes. Irrespective of CD49a or CD49b expression, no CD8 TIL expressed IFNg or TNFa directly *ex vivo* after *in vivo* brefeldin A treatment 4-6h prior to harvest (Fig. 6B). However, significant fractions expressed IFNγ, TNFα and surface CD107a after *in vitro* restimulation for 4-6h with anti-CD3/CD28, demonstrating that they are active outside the context of a tumor (Fig. 6C, Supplemental Fig. 6B). Interestingly, IFNg, CD107a and TNFa were expressed on larger fractions of DP cells than either SP subpopulation. Importantly, all subpopulations upregulated Nur77 equivalently upon re-stimulation for 12 hours with anti-CD3/CD28 *in vitro* (Fig. 6D). These data demonstrate that, while all subpopulations are suppressed downstream of Nur77 *in vivo*, CD49b SP cells are able to engage with antigen and express Nur77, whereas CD49a SP cells are not. This suggest that either these subpopulations are suppressed by different mechanisms or that CD49a SP T-cells are not actively engaged with antigen.

As CD49a SP and DP T-cells expressed higher levels of exhaustion markers, we hypothesized that these inhibitory pathways suppressed TCR signaling more in these subpopulations. To test this, we treated established BRPKp110 tumors with a cocktail of checkpoint blockade inhibitors for 48h. Due to the short nature of treatment, tumor weight, CD8 T-cell infiltration, and CD49a and CD49b expression were unaltered (Supplemental Fig. 6C). However, neither Nur77 expression (Fig. 6E) nor effector cytokine expression was changed (Fig. 6F), indicating that blockade of inhibitory signaling via PD-1, LAG-3, or TIM-3 could not rescue effector activity or Nur77 expression of CD49a SP and DP T-cells in BRPKp110 tumors.

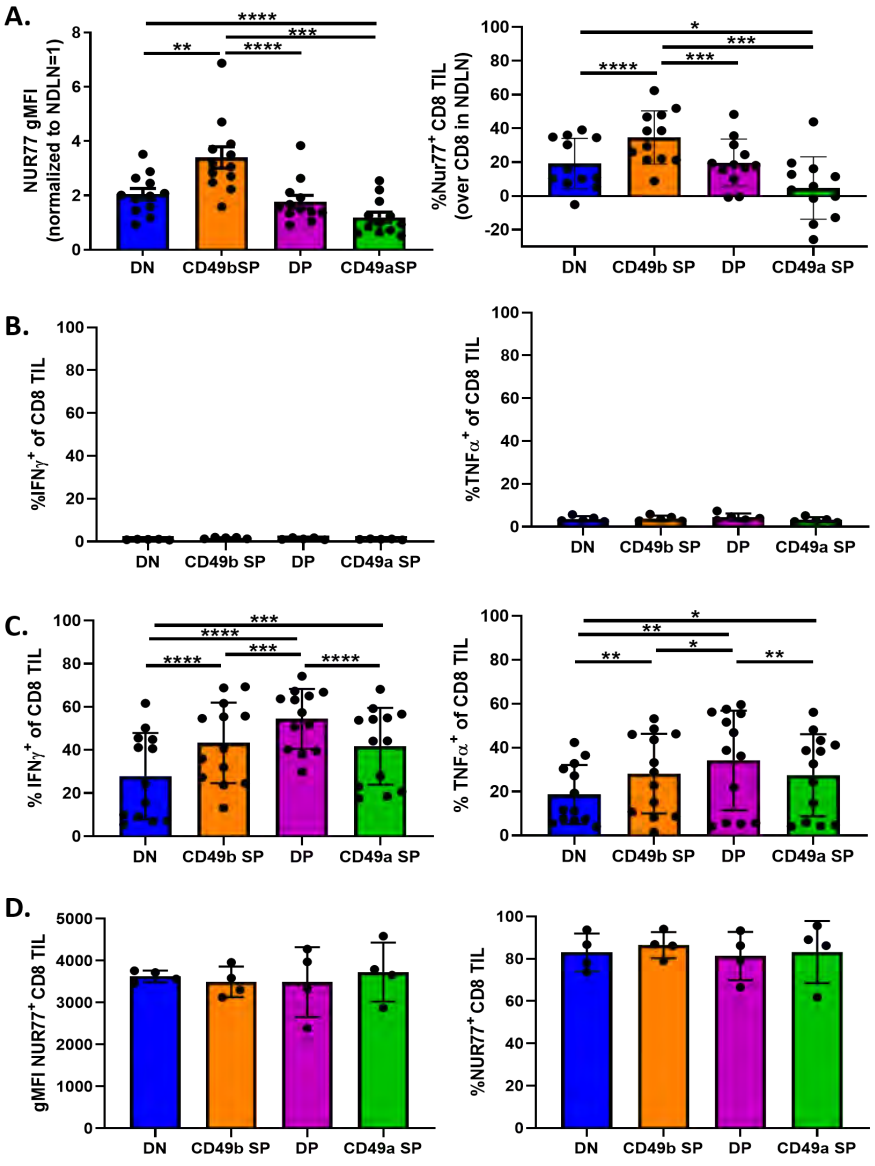

Figure 6. CD49a-expressing subpopulation are not inhibited by PD-1, LAG-3 or TIM-3, instead they display a TRM-like phenotype. (A) Nur77-GFP reporter mice were implanted SC with BRPKp110 (n=12 from 3 independent experiments). Tumors were harvested on day 14, single cell suspensions were prepared and enriched CD45 fraction was analyzed for Nur77-GFP, CD49a and CD49b expression on $CD3^+$ $CD8^+$ cells. Nur77 gMFI was normalized to CD8 T-cells in non-draining lymph nodes (NDLN) and Nur77% on CD8 T-cells from NDLN (ranging between 17.1-41.8%) was subtracted from the fraction on CD8 TIL subpopulations. Subpopulations were compared with a Repeated-Measures

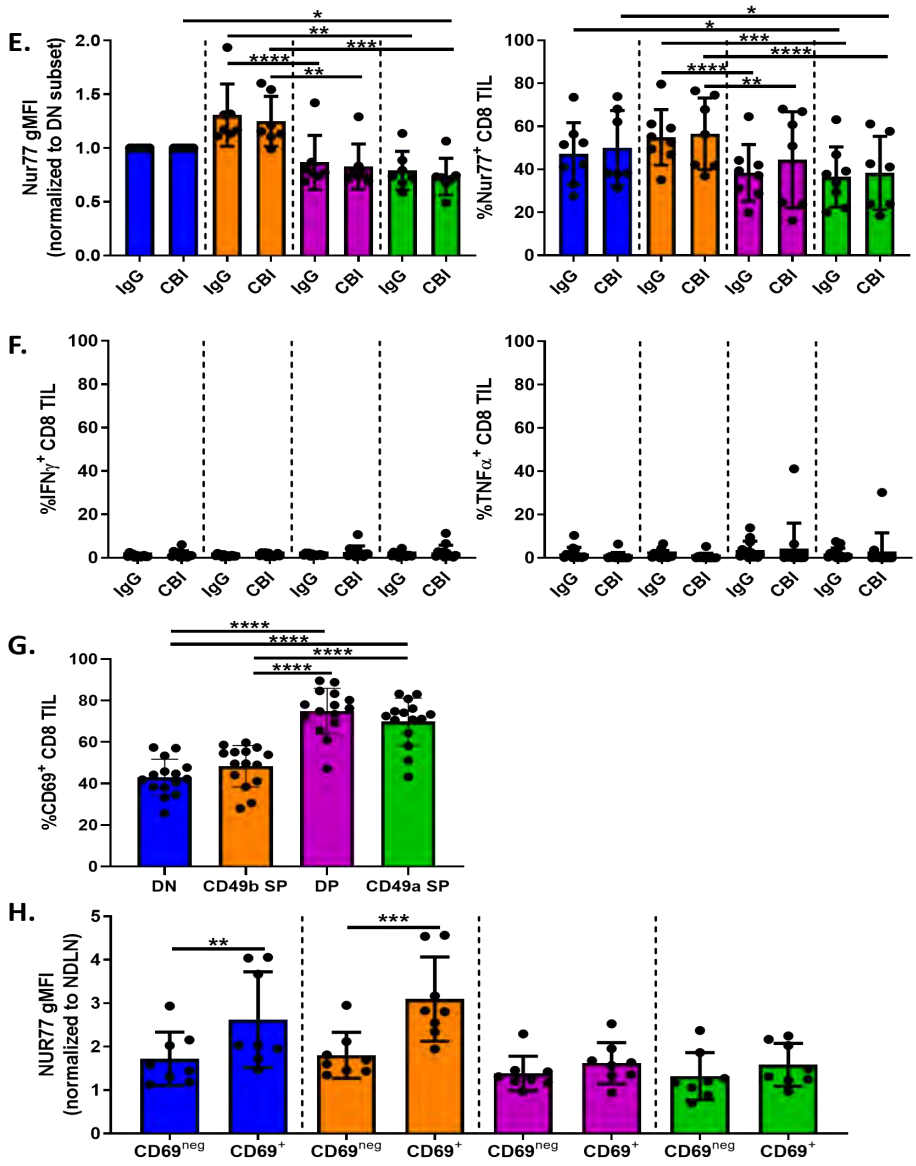

ANOVA. (B) C57BL/6 mice were implanted SC with BRPKp110 tumors (n=5). Tumors were harvested on day 14, 4-6h after IV injection of Brefeldin A. Single cell suspensions were prepared and enriched CD45 fraction was analyzed for CD49a, CD49b, IFNγ and TNFα expression on $CD3^+$ $CD8^+$. (C) C57BL/6 mice were implanted SC with BRPKp110 (n=13 from 2 independent experiments). Tumors were harvested on day 14, single cell suspensions were prepared and enriched $CD8^+$ cells were cultured with CD3/CD28 beads for 4-6h in presence of Brefeldin A. Cells were analyzed for expression CD49a, CD49b, IFNγ and TNFα expression on $CD3^+$ $CD8^+$. Expression between subpopulations was compared with a Repeated-Measures one-way ANOVA and Tukey's multiple comparisons test. (D)

Nur77-GFP reporter mice were implanted SC with BRPKp110 breast carcinoma (n=4). Tumors were harvested on day 14, single cell suspensions were prepared and enriched $CD8^+$ cells were cultured with CD3/CD28 beads for 12h and analyzed for Nur77-GFP, CD49a and CD49b expression $CD3^+$ $CD8^+$ cells. Expression between subpopulations was compared with a Repeated-Measures one-way ANOVA and Tukey's multiple comparisons test. (E/F) Nur77-GFP reporter mice were implanted SC with BRPKp110 (n=7 per group, 2 independent experiments). Mice were IP injected 48h prior to harvest with a checkpoint blockade inhibitor (CBI) cocktail including anti-PD-1, anti-LAG-3 and anti-TIM-3. Tumors were harvested, single-cell suspensions were prepared and enriched CD45 fraction was analyzed for Nur77-GFP, CD49a, CD49b, IFNγ and TNFα expression on $CD3^+$ $CD8^+$ cells. (G) C57BL/6 mice were implanted SC with BRPKp110 (n=15 from 3 independent experiments). Tumors were harvested on day 14, single cell suspensions were prepared and enriched $CD45^+$ cells were analyzed for CD69, CD49a and CD49b expression on $CD3^+$ $CD8^+$ cells. Expression between subpopulations were statistically compared as in (A) and differences between groups within a subpopulation were tested with a Welch's corrected T-test. (H) Nur77-GFP reporter mice were implanted SC with BRPKp110 breast carcinoma (n=8 per group, 2 independent experiments). Tumors were harvested on day 14, single cell suspensions were prepared and enriched $CD45^+$ cells were analyzed for Nur77, CD69, CD49a and CD49b expression on $CD3^+$ $CD8^+$ cells. $CD69^+$ and $CD69^{neg}$ subsets within the integrin-expressing subpopulations were compared with a Paired T-test.

CD49a-expressing subpopulations express elevated levels of CD69 in an antigen-independent manner

While extrinsic suppression mechanisms, such as myeloid-derived suppressor cells or regulatory T-cells, could be responsible for the selective inhibition of TCR signaling in CD49a-expressing subpopulations, this would require that these cell types be differentially localized in proximity to one another. This led us to consider a more straightforward possibility: that CD49a-expressing subpopulations were localized away from antigen-expressing cells in the tumor and thereby able to functionally resemble a T_{RM}-like T-cell population. CD49a has been described as a marker of T_{RM} cells, along with PD-1 and CD69 (40,41). Consequently, we evaluated CD69 expression on integrin-expressing subpopulations in conjunction with their expression of Nur77. All integrin-expressing subpopulations expressed CD69, though the fraction of $CD69^+$ cells was elevated in DP and CD49a SP subpopulations (Fig. 6G). In CD49b SP and DN subpopulations, these $CD69^+$ cells expressed elevated levels of Nur77, tying CD69 expression to TCR stimulation (Fig. 6H). However, in DP and CD49a SP subpopulations, there was no difference in Nur77 expression between CD69 positive and negative cells. This TCR-stimulation independent expression of CD69 is consistent with the antigen-independent expression of CD69 in T_{RM} cells, and further consistent with the possibility that CD49a SP and DP cells are not in contact with antigen-expressing cells in the tumor

CD49a, but not CD49b, ligation alters T-cell localization and interaction with tumor cells resulting in high motility

The results above led us to consider that the engagement of CD49a with collagen reduced the ability of CD8 T-cells to engage with antigens expressed on tumor cells. To test this hypothesis, we implanted GFP-expressing BRPKp110 cells into CD2-dsRed (labeling all T-cells) transgenic mice. The resulting tumors were cut into 100-200μm thick live tumor slices, and tumor cells, $CD2^+$ T-cells, and collagen fibers identified by second harmonic generation (SHG) were imaged with 2-photon microscopy for 30 minutes at 37°C. Separate slices from the same tumors were incubated with blocking antibodies against CD49a or CD49b prior to imaging. Under control conditions, T-cells displayed a wide range of speeds and relatively few were slow-moving (<1μm/min) (Fig. 7A,B, Supplemental Fig. 7A, Supplemental Video 1-3). Only 5% of T-cells were <10 mm from a collagen fiber (Fig. 7C). However, SHG enables visualization only of well-structured collagen fibers (42,43). Immunofluorescent staining of day 21 BRPKp110 sections for collagen type I or IV confirmed a more pervasive presence of collagen molecules compared to that observed by SHG (Supplemental Fig. 7B), suggesting our live-imaging underestimates the true fraction of collagen-engaged cells. Nonetheless, those few cells in close proximity to visible collagen fibers moved significantly slower (Fig. 7D). In untreated tumors, about 22% of T-cells were <10mm from a tumor cell (Fig. 7E). However, no difference in speed was observed when comparing these T-cells to those located further away from collagen fibers (Fig. 7F, Supplemental Fig. 7E). These characteristics are consistent with a low level of productive tumor cell engagement (44,45). When CD49b was blocked, significantly more cells were located in closer proximity to tumor cells (Fig. 7E), but their track speed remained the same as T-cells at a distance, suggesting no change in their interaction (Fig. 7F, Supplemental Fig. 7C). Also, neither proximity nor track speed, overall or in relation to well-structured collagen fibers, was altered (Fig. 7A-D, Supplemental Fig. 7A, Supplemental Video 1-3). In contrast, CD49a blockade resulted in a significant decline in average T-cell motility (Fig. 7A,B, Supplemental Fig. 7A, Supplemental Video 1-3). Curiously, a significantly larger fraction of T-cells was in close proximity to well-structured collagen fibers but not to tumor cells (Fig. 7A-C). However, in contrast to control slices, the CD49a blocked T-cells in close proximity to tumor cells were moving significantly slower than those at a distance (Fig. 7F, Supplemental Fig. 7C), suggesting that their engagement was enhanced. This decrease in speed was not due to a larger fraction of T-cells interacting with both collagen and tumor cells simultaneously (Supplemental Fig. 7D): only T-cells close to tumor cells, and not those close to collagen fibers, showed significantly decreased speed when CD49a was blocked (Supplemental Fig. 7E). These data suggest that CD49a on T-cells either increases motility, which diminishes productive engagement with tumor cells. Alternatively, CD49a may diminish the ability of T-cells to productively engage with tumor cells, resulting in an increased T cell motility. Regardless, they point to a mechanism in which CD49a inhibits T-cell function by blocking the engagement with tumor cells.

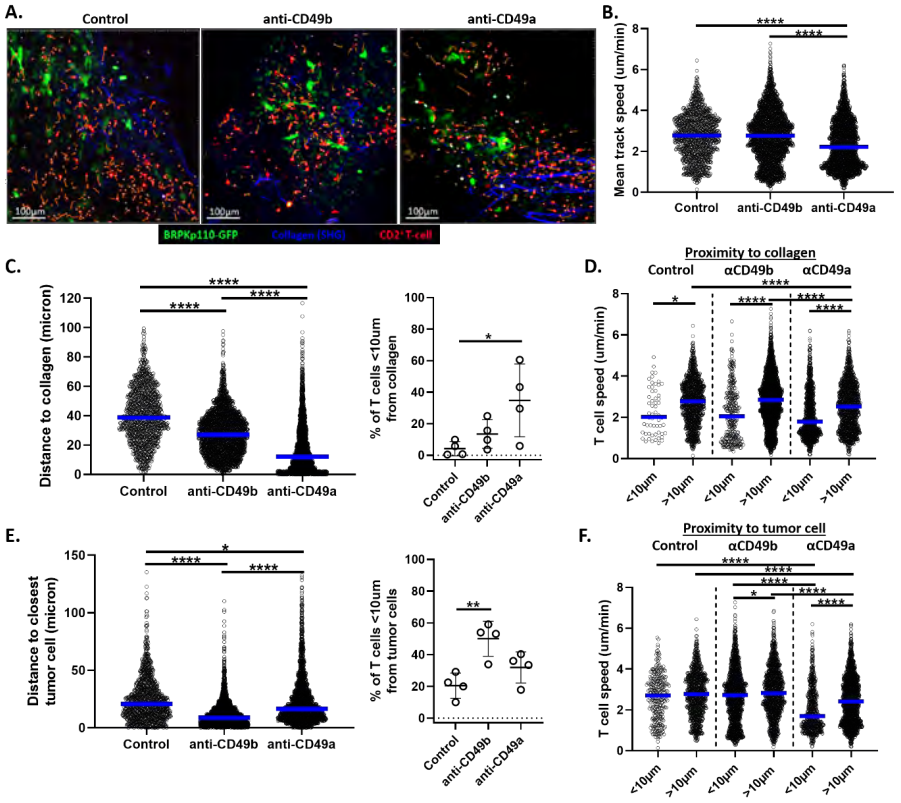

Figure 7. CD49a affects localization and motility of T-cells in the tumor. CD2-dsRed mice were implanted SC with BRPKp110-GFP tumors. Tumors were harvested on day 21/22, embedded in agarose and cut into thick slices of approximately 100-200µicrons. Slices were incubated with anti-CD49a or anti-CD49b blocking antibodies for 2h and assessed forCD2$^+$T-cells, GFP$^+$ BRPKp110 cells and collagen fibers with second harmonics generation (SHG) on a 2-photon microscope. 30-minute videos of 2 fields per slice were made while maintaining oxygenation and 37°C with warm flowing media. For each figure, groups were compared with an ordinary one-way ANOVA and Tukey's multiple comparisons test. (A) Composite image examples. Orange tracks represent CD2$^+$ T-cell movement for the last 10 minutes. (B) Mean track speed of the CD2$^+$ T-cells. (C) Average distance of CD2$^+$ T-cells to closest SHG collagen fiber (left). Fraction of CD2$^+$ T-cells <10µm to closest SHG collagen fiber (right), fraction displayed per analyzed field. (D) Mean track speed of the CD2$^+$ T-cells, stratified by distance to SHG collagen fibers. Close proximity: <10µm, large distance: >10µm. (E) Average distance of CD2$^+$ T-cells to closest GFP$^+$ BRPKp110 tumor cell (left). Fraction of CD2$^+$ T-cells <10µm to closest GFP$^+$ BRPKp110 tumor cell (right), fraction displayed per analyzed field. (F) Mean track speed of the CD2$^+$ T-cells, stratified by distance to GFP$^+$ BRPKp110 tumor cells. Close proximity: <10µm, large distance: >10µm.

DISCUSSION

Successful anti-tumor immune responses depend on robust T-cell infiltration in the tumor. Retention mechanisms may be involved in defining the extent of the T-cell infiltrate. The collagen-binding integrins CD49a and CD49b are considered to be involved in the retention of T-cells in peripheral tissues, including tumors (31). Thus, their regulation and function on T-cells in the TME may impact tumor control. Here, we found that CD8 T-cells express CD49b early after infiltration into tumors and then, over the course of tumor outgrowth, gain CD49a, and subsequently lose CD49b. This differentiation sequence is driven by antigen-independent elements in the TME, but antigen stimulation further enhances CD49a expression. CD49a-expressing CD8 TIL also expressed higher levels of PD-1, LAG-3, TIM-3 and Tigit, but these exhaustion markers were also upregulated on CD49a^{neg} CD8 TIL. Our work suggests that exhaustion markers and CD49a are associated temporally, but not mechanistically. On the other hand, CD49a-expressing CD8 TIL expressed CD69 in the absence of TCR signaling while its expression on CD49b populations was TCR signaling-associated. Co-expression of CD69 and CD49a is characteristic of T_{RM} cells; thus, upregulation of CD49a may be associated with establishment of T_{RM}-like TIL that are not actively engaging with antigen. Unexpectedly, imaging T-cells in live tumor slices revealed that CD49a enhances T-cell motility, especially in close proximity to tumor cells, suggesting that it may interfere with T-cell recognition of tumor cells by distracting them from productive engagement. Together, our results illuminate a new mechanism of CD8 TIL dysfunction that is induced by and dependent upon antigen-independent aspects of the TME.

It has been previously shown that CD49b is expressed on only a subset of specific effector CD8 T-cells in mouse models of arthritis and influenza or LCMV infection (18,21,27), and our work extends this observation to immunization with antigen in adjuvant. Thus, it is likely that a second signal or a specifically preprogrammed naïve T-cell subset is responsible for the initial upregulation of CD49b. However, we also showed that expression is maintained by elements in immunized mice and in the TME of BRPKp110, but not B16-F1 tumors. The B16-F1 TME may either lack these maintenance elements, or they may be antagonized by additional suppressive elements, such as TGFβ, which downregulated CD49b on activated OT-I cells *in vitro*. Surprisingly, CD49b was maintained fully on OT-I cells in the spleens of B16-OVA tumor bearing mice, and to a lesser extent on OT-I TIL, although this level was still higher than on TIL from B16-F1 tumors. We interpret this to suggest that TCR stimulation can also promote the expression of CD49b in both spleens and tumors of mice bearing B16-OVA, but continual stimulation or environmental factors in the TME ultimately lead to diminished expression. Future experiments will directly address which elements of the tumor lysate are responsible for CD49b maintenance or downregulation on CD8 T-cells.

Our results also establish that CD49a is upregulated on CD8 T-cells by elements in the TME that are present in both BRPKp110 and B16 tumors and in the splenic

environment of immunized but not naïve mice. Others have observed CD49a expression on influenza-specific T-cells after localization in airways and lungs, and also on T_{RM} T-cells, but not circulating memory T-cells (18,29,30). Together this suggests that peripheral tissue microenvironments contain element(s) that upregulate CD49a, such as TGFβ, IL-2, IL-7, or IL-15, which can upregulate CD49a directly (31,46–48). However, TGFβ does not play a significant role in controlling expression of CD49a on CD8 T-cells in BRPKp110 tumors. Future experiments will directly address which elements of the tumor lysate are responsible for CD49a upregulation or maintenance on CD8 T-cells.

We observed that expression of CD69 on CD49b SP cells was tightly associated with TCR signaling, but its expression on CD49a$^+$ cells was entirely independent, and indeed, there was little evident TCR signaling in this population. Antigen-independent expression of CD69, together with PD-1, are cardinal markers of T_{RM} cells (41), and others have shown that the environment plays a role in the generation of T_{RM} cells in the skin, pointing to an antigen-independent regulation of CD49a (49,50). The overall upregulation of CD49a, CD69, and PD-1 could thus also be explained by a differentiation of CD49a$^+$ CD8 TIL towards a T_{RM}-like phenotype.

The selective lack of TCR signaling evident in CD49a SP cells in the TME of BRPKp110 tumors was particularly striking, in that signaling was not restored by blockade of inhibitory pathways, and these cells were fully TCR responsive *in vitro*. This strongly suggested that CD49a SP cells are not making productive contacts with antigen-expressing cells. While we hypothesized that CD49a binding to collagens would trap T-cells in dense stromal areas well-separated from tumor cells, our tumor slice imaging showed that CD49a promotes increased motility, specifically in those T-cell residing in close proximity to tumor cells. Consistent with this, CD49a binding to collagen increases motility of T-cells *in vitro* and in lung tissue (25,26). Our imaging does not show clear motility of cells along ordered collagen bundles visualized by SHG. However, antibody staining of tumor sections for collagen type IV and type I, and work performed by others, demonstrates that SHG does not enable visualization of less well-ordered collagen(48). In addition, CD49a binds predominantly collagen type IV but also collagen type I (18,20). Together with the lack of TCR signaling, these data suggest that by driving motility, CD49a engagement distracts T-cells from productive engagement with tumor cells. This points to an intriguing role for CD49a in T-cell retention, not by “trapping” the cells in collagen structures but by promoting cells to rapidly move along collagen fibers, scanning the whole tissue. This role of CD49a may be especially important in T_{RM} T-cells, as their function is to remain in the tissue long-term, while scanning the tissue for re-exposure (30,52,53). However, in tumors, this mechanism may distract the T-cells from engaging effectively with their antigen and thus point to a new mechanism of immune evasion. This suggests that CD49a blockade may be an important therapeutic strategy to ensure that T-cells in tumors are able to engage with and eradicate tumors cells efficiently when co-administered with agents that overcome immune suppression in the TME.

ACKNOWLEDGEMENTS

We thank all members of the Rutkowski, Bullock, Slingluff and Engelhard laboratories for their help and constant input in this project. Special thanks go to Claire Rosean for sharing their knowledge regarding the BRPKp110 model. Lastly, we thank Andrew Dudley for input and help with tumor slicing and Jordan Jacobelli from the University of Colorado, Anschutz Medical Campus for sharing the CD2-dsRed mice.

REFERENCES

1. Erdag G, Schaefer JT, Smolkin ME, Deacon DH, Shea SM, Dengel LT, et al. Immunotype and immunohistologic characteristics of tumor-infiltrating immune cells are associated with clinical outcome in metastatic melanoma. Cancer Res. 2012;72:1070–80.
2. Aaltomaa S, Lipponen P, Eskelinen M, Kosma V-M, Marin S, Alhava E, et al. Lymphocyte infiltrates as a prognostic variable in female breast cancer. Eur J Cancer. 1992;28:859–64.
3. Liu S, Lachapelle J, Leung S, Gao D, Foulkes WD, Nielsen TO. CD8+ lymphocyte infiltration is an independent favorable prognostic indicator in basal-like breast cancer. Breast Cancer Res. 2012;14:R48.
4. Chen DS, Mellman I. Oncology Meets Immunology: The Cancer-Immunity Cycle. Immunity. Elsevier; 2013;39:1–10.
5. Ley K, Laudanna C, Cybulsky MI, Nourshargh S. Getting to the site of inflammation: the leukocyte adhesion cascade updated. Nat Rev Immunol. 2007;7:678–89.
6. Ferguson AR, Engelhard VH. CD8 T cells activated in distinct lymphoid organs differentially express adhesion proteins and coexpress multiple chemokine receptors. J Immunol Baltim Md 1950. 2010;184:4079–86.
7. Woods AN, Wilson AL, Srivinisan N, Zeng J, Dutta AB, Peske JD, et al. Differential expression of homing receptor ligands on tumor associated vasculature that control CD8 effector T cell entry. Cancer Immunol Res [Internet]. 2017 [cited 2020 Feb 24]; Available from: https://cancerimmunolres.aacrjournals.org/content/early/2017/11/01/2326-6066.cir-17-0190
8. Matheu MP, Teijaro JR, Walsh KB, Greenberg ML, Marsolais D, Parker I, et al. Three Phases of CD8 T Cell Response in the Lung Following H1N1 Influenza Infection and Sphingosine 1 Phosphate Agonist Therapy. von Herrath MG, editor. PLoS ONE. 2013;8:e58033.
9. Honda T, Egen JG, Lämmermann T, Kastenmüller W, Torabi-Parizi P, Germain RN. Tuning of Antigen Sensitivity by T Cell Receptor-Dependent Negative Feedback Controls T Cell Effector Function in Inflamed Tissues. Immunity. 2014;40:235–47.
10. Benechet AP, Menon M, Khanna KM. Visualizing T Cell Migration in situ. Front Immunol [Internet]. Frontiers; 2014 [cited 2020 Mar 30];5. Available from: https://www.frontiersin.org/articles/10.3389/fimmu.2014.00363/full
11. Espinosa-Carrasco G, Le Saout C, Fontanaud P, Michau A, Mollard P, Hernandez J, et al. Integrin β1 Optimizes Diabetogenic T Cell Migration and Function in the Pancreas. Front Immunol [Internet]. Frontiers; 2018 [cited 2020 Mar 30];9. Available from: https://www.frontiersin.org/articles/10.3389/fimmu.2018.01156/full
12. Debes GF, Arnold CN, Young AJ, Krautwald S, Lipp M, Hay JB, et al. Chemokine receptor CCR7 required for T lymphocyte exit from peripheral tissues. Nat Immunol. Nature Publishing Group; 2005;6:889–94.
13. Brown MN, Fintushel SR, Lee MH, Jennrich S, Geherin SA, Hay JB, et al. Chemoattractant receptors and lymphocyte egress from extralymphoid tissue: changing requirements during the course of inflammation. J Immunol Baltim Md 1950. 2010;185:4873–82.
14. Torcellan T, Hampton HR, Bailey J, Tomura M, Brink R, Chtanova T. In vivo photolabeling of tumor-infiltrating cells reveals highly regulated egress of T-cell subsets from tumors. Proc Natl Acad Sci. 2017;201618446.

15. Steele MM, Churchill MJ, Breazeale AP, Lane RS, Nelson NA, Lund AW. Quantifying Leukocyte Egress via Lymphatic Vessels from Murine Skin and Tumors. J Vis Exp JoVE. 2019;
16. Salmon H, Franciszkiewicz K, Damotte D, Dieu-Nosjean M-C, Validire P, Trautmann A, et al. Matrix architecture defines the preferential localization and migration of T cells into the stroma of human lung tumors. J Clin Invest. American Society for Clinical Investigation; 2012;122:899–910.
17. Bougherara H, Mansuet-Lupo A, Alifano M, Ngô C, Damotte D, Le Frère-Belda M-A, et al. Real-Time Imaging of Resident T Cells in Human Lung and Ovarian Carcinomas Reveals How Different Tumor Microenvironments Control T Lymphocyte Migration. Front Immunol [Internet]. Frontiers; 2015 [cited 2020 May 1];6. Available from: https://www.frontiersin.org/articles/10.3389/fimmu.2015.00500/full
18. Richter M, Ray SJ, Chapman TJ, Austin SJ, Rebhahn J, Mosmann TR, et al. Collagen distribution and expression of collagen-binding alpha1beta1 (VLA-1) and alpha2beta1 (VLA-2) integrins on CD4 and CD8 T cells during influenza infection. J Immunol Baltim Md 1950. 2007;178:4506–16.
19. Goldman R, Harvey J, Hogg N. VLA-2 is the integrin used as a collagen receptor by leukocytes. Eur J Immunol. 1992;22:1109–14.
20. Hemler ME. VLA Proteins in the Integrin Family: Structures, Functions, and Their Role on Leukocytes. Annu Rev Immunol. 1990;8:365–400.
21. Fougerolles AR de, Sprague AG, Nickerson-Nutter CL, Chi-Rosso G, Rennert PD, Gardner H, et al. Regulation of inflammation by collagen-binding integrins α1β1 and α2β1 in models of hypersensitivity and arthritis. J Clin Invest. American Society for Clinical Investigation; 2000;105:721–9.
22. Meharra EJ, Schön M, Hassett D, Parker C, Havran W, Gardner H. Reduced gut intraepithelial lymphocytes in VLA1 null mice. Cell Immunol. 2000;201:1–5.
23. Sandoval F, Terme M, Nizard M, Badoual C, Bureau M-F, Freyburger L, et al. Mucosal Imprinting of Vaccine-Induced CD8+ T Cells Is Crucial to Inhibit the Growth of Mucosal Tumors. Sci Transl Med. American Association for the Advancement of Science; 2013;5:172ra20-172ra20.
24. Richter MV, Topham DJ. The α1β1 Integrin and TNF Receptor II Protect Airway CD8+ Effector T Cells from Apoptosis during Influenza Infection. J Immunol. American Association of Immunologists; 2007;179:5054–63.
25. Conrad C, Boyman O, Tonel G, Tun-Kyi A, Laggner U, de Fougerolles A, et al. α 1 β 1 integrin is crucial for accumulation of epidermal T cells and the development of psoriasis. Nat Med. Nature Publishing Group; 2007;13:836–42.
26. Reilly EC, Emo KL, Buckley PM, Reilly NS, Chaves FA, Yang H, et al. TRM Integrins CD103 and CD49a Differentially Support Adherence and Motility After Resolution of Influenza Virus Infection. bioRxiv. Cold Spring Harbor Laboratory; 2020;2020.02.14.947986.
27. Andreasen SØ, Thomsen AR, Koteliansky VE, Novobrantseva TI, Sprague AG, Fougerolles AR de, et al. Expression and Functional Importance of Collagen-Binding Integrins, α1β1 and α2β1, on Virus-Activated T Cells. J Immunol. American Association of Immunologists; 2003;171:2804–11.
28. Murray T, Fuertes Marraco SA, Baumgaertner P, Bordry N, Cagnon L, Donda A, et al. Very Late Antigen-1 Marks Functional Tumor-Resident CD8 T Cells and Correlates

with Survival of Melanoma Patients. Front Immunol [Internet]. 2016 [cited 2020 Feb 24];7. Available from: https://www.ncbi.nlm.nih.gov/pmc/articles/PMC5150229/
29. Topham DJ, Reilly EC. Tissue-Resident Memory CD8+ T Cells: From Phenotype to Function. Front Immunol. 2018;9:515.
30. Cheuk S, Schlums H, Gallais Sérézal I, Martini E, Chiang SC, Marquardt N, et al. CD49a Expression Defines Tissue-Resident CD8+ T Cells Poised for Cytotoxic Function in Human Skin. Immunity. 2017;46:287–300.
31. Melssen MM, Olson W, Wages NA, Capaldo BJ, Mauldin IS, Mahmutovic A, et al. Formation and phenotypic characterization of CD49a, CD49b and CD103 expressing CD8 T cell populations in human metastatic melanoma. OncoImmunology. 2018;7:e1490855.
32. Hombrink P, Helbig C, Backer RA, Piet B, Oja AE, Stark R, et al. Programs for the persistence, vigilance and control of human CD8 + lung-resident memory T cells. Nat Immunol. Nature Publishing Group; 2016;17:1467–78.
33. Zhang N, Bevan MJ. Transforming Growth Factor-β Signaling Controls the Formation and Maintenance of Gut-Resident Memory T Cells by Regulating Migration and Retention. Immunity. Elsevier; 2013;39:687–96.
34. Moran AE, Holzapfel KL, Xing Y, Cunningham NR, Maltzman JS, Punt J, et al. T cell receptor signal strength in Treg and iNKT cell development demonstrated by a novel fluorescent reporter mouse. J Exp Med. 2011;208:1279–89.
35. Allegrezza MJ, Rutkowski MR, Stephen TL, Svoronos N, Perales-Puchalt A, Nguyen JM, et al. Trametinib Drives T-cell–Dependent Control of KRAS-Mutated Tumors by Inhibiting Pathological Myelopoiesis. Cancer Res. American Association for Cancer Research; 2016;76:6253–65.
36. Hargadon KM, Brinkman CC, Sheasley-O'Neill SL, Nichols LA, Bullock TNJ, Engelhard VH. Incomplete Differentiation of Antigen-Specific CD8 T Cells in Tumor-Draining Lymph Nodes. J Immunol. American Association of Immunologists; 2006;177:6081–90.
37. Salerno EP, Olson WC, McSkimming C, Shea S, Slingluff Jr. CL. T cells in the human metastatic melanoma microenvironment express site-specific homing receptors and retention integrins. Int J Cancer. 2014;134:563–74.
38. Rosean CB, Bostic RR, Ferey JCM, Feng T-Y, Azar FN, Tung KS, et al. Preexisting Commensal Dysbiosis Is a Host-Intrinsic Regulator of Tissue Inflammation and Tumor Cell Dissemination in Hormone Receptor–Positive Breast Cancer. Cancer Res. American Association for Cancer Research; 2019;79:3662–75.
39. Hashimoto M, Kamphorst AO, Im SJ, Kissick HT, Pillai RN, Ramalingam SS, et al. CD8 T Cell Exhaustion in Chronic Infection and Cancer: Opportunities for Interventions. Annu Rev Med. Annual Reviews; 2018;69:301–18.
40. Jiang X, Clark RA, Liu L, Wagers AJ, Fuhlbrigge RC, Kupper TS. Skin infection generates non-migratory memory CD8 + T RM cells providing global skin immunity. Nature. Nature Publishing Group; 2012;483:227–31.
41. Kumar BV, Ma W, Miron M, Granot T, Guyer RS, Carpenter DJ, et al. Human tissue-resident memory T cells are defined by core transcriptional and functional signatures in lymphoid and mucosal sites. Cell Rep. 2017;20:2921–34.
42. Chen X, Nadiarynkh O, Plotnikov S, Campagnola PJ. Second harmonic generation microscopy for quantitative analysis of collagen fibrillar structure. Nat Protoc.

2012;7:654–69.
43. Mostaço-Guidolin L, Rosin NL, Hackett T-L. Imaging Collagen in Scar Tissue: Developments in Second Harmonic Generation Microscopy for Biomedical Applications. Int J Mol Sci [Internet]. 2017 [cited 2020 Apr 20];18. Available from: https://www.ncbi.nlm.nih.gov/pmc/articles/PMC5578161/
44. Dustin ML, Bromley SK, Kan Z, Peterson DA, Unanue ER. Antigen receptor engagement delivers a stop signal to migrating T lymphocytes. Proc Natl Acad Sci. 1997;94:3909–13.
45. Friedman RS, Jacobelli J, Krummel MF. Mechanisms of T cell motility and arrest: Deciphering the relationship between intra- and extracellular determinants. Semin Immunol. 2005;17:387–99.
46. Gao Y, Souza-Fonseca-Guimaraes F, Bald T, Ng SS, Young A, Ngiow SF, et al. Tumor immunoevasion by the conversion of effector NK cells into type 1 innate lymphoid cells. Nat Immunol. 2017;18:1004–15.
47. Rubio MA, Sotillos M, Jochems G, Alvarez V, Corbií AL. Monocyte activation: rapid induction of α1/β1 (VLA-1) integrin expression by lipopolysaccharide and interferon-γ. Eur J Immunol. 1995;25:2701–5.
48. Ni X, Fu B, Zhang J, Sun R, Tian Z, Wei H. Cytokine-Based Generation of CD49a+Eomes−/+ Natural Killer Cell Subsets. Front Immunol [Internet]. 2018 [cited 2020 Feb 25];9. Available from: https://www.frontiersin.org/articles/10.3389/fimmu.2018.02126/full
49. Mackay LK, Rahimpour A, Ma JZ, Collins N, Stock AT, Hafon M-L, et al. The developmental pathway for CD103 + CD8 + tissue-resident memory T cells of skin. Nat Immunol. Nature Publishing Group; 2013;14:1294–301.
50. Adachi T, Kobayashi T, Sugihara E, Yamada T, Ikuta K, Pittaluga S, et al. Hair follicle-derived IL-7 and IL-15 mediate skin-resident memory T cell homeostasis and lymphoma. Nat Med. 2015;21:1272–9.
51. Pena A-M, Boulesteix T, Dartigalongue T, Schanne-Klein M-C. Chiroptical Effects in the Second Harmonic Signal of Collagens I and IV. J Am Chem Soc. American Chemical Society; 2005;127:10314–22.
52. Ariotti S, Hogenbirk MA, Dijkgraaf FE, Visser LL, Hoekstra ME, Song J-Y, et al. Skin-resident memory CD8+ T cells trigger a state of tissue-wide pathogen alert. Science. American Association for the Advancement of Science; 2014;346:101–5.
53. Masopust D, Soerens AG. Tissue-Resident T Cells and Other Resident Leukocytes. Annu Rev Immunol. 2019;37:521–46.

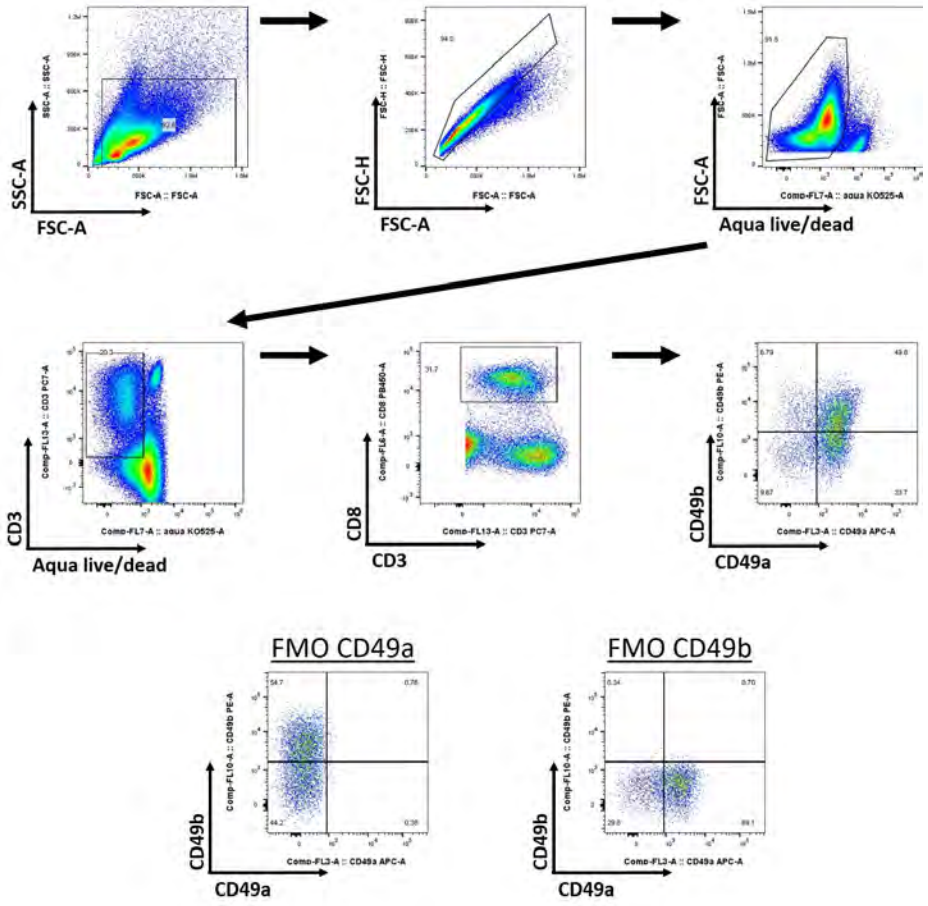

Supplemental Figure 1. Gating strategy for flow cytometry experiments. Debris, doublets and dead cells were excluded (top panels), $CD3^+$ and $CD8^+$ T cells were selected and CD49a and CD49b positivity was determined based on their respective fluorescence minus one (FMO) control samples.

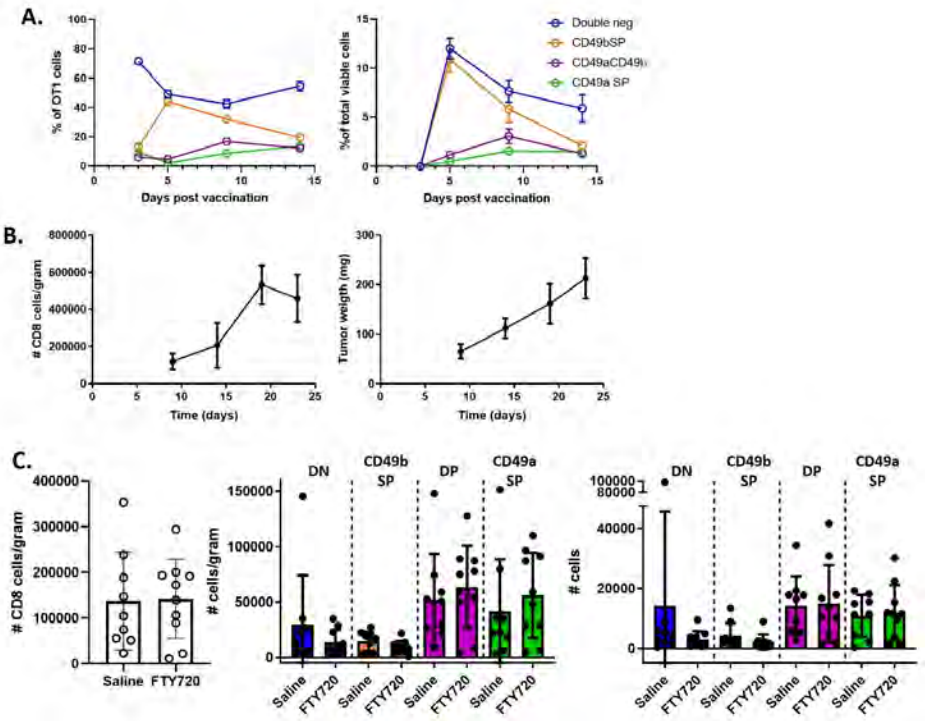

Supplemental Figure 2. (A) 5x10^6 Thy1.1$^+$ OT-I splenocytes were transferred IV into C57BL/6 mice. 1 day post transfer, mice were vaccinated IV with ovalbumin, polyIC and anti-CD40. Spleens of vaccinated mice were harvested 3, 5, 9 and 14 days post vaccination and analyzed for CD49a and CD49b expression on Thy1.1$^+$ CD3$^+$ CD8$^+$ cells by flow cytometry. (B) C57BL/6 mice were implanted SC with BRPKp110 breast carcinoma tumors. Tumors were harvested on day 9, 14, 19 or 23 (as indicated), single cell suspensions were prepared and enriched for CD45$^+$ cells. CD3$^+$CD8$^+$ cells/gram of tumor were quantified with flow cytometry. (C) C57BL/6 mice were implanted SC with BRPKp110 breast carcinoma tumors. Baseline tumors were harvested on day 14 and processed for flow cytometry as in (B). Other BRPKp110-bearing animals received daily IP injections with FTY720 or saline control. Treated tumors were harvested on day 23 and processed for flow cytometry.

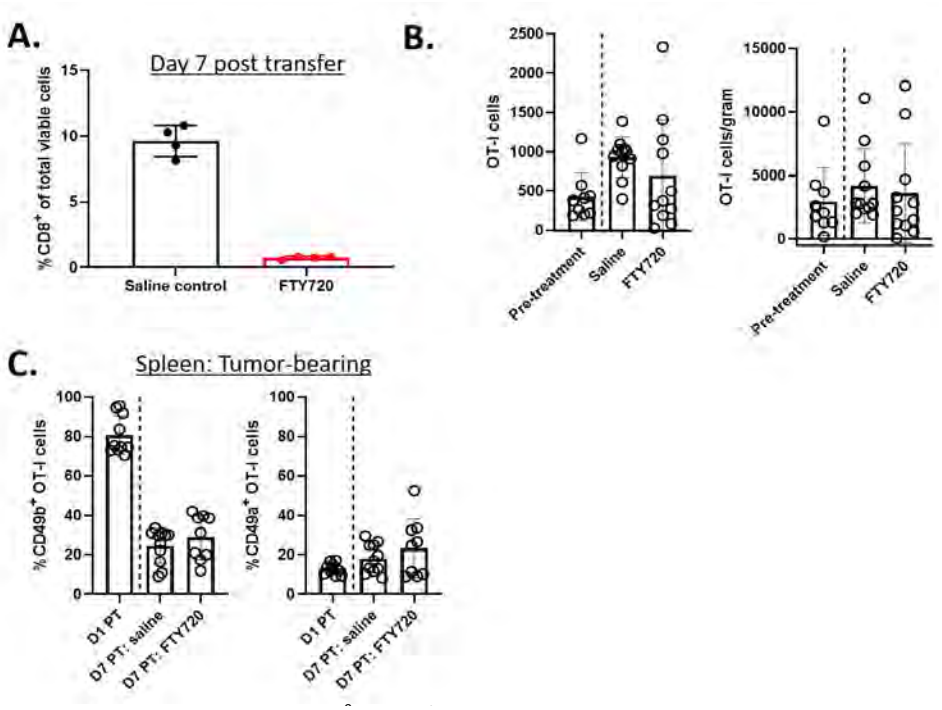

Supplemental Figure 3. (A/B) 5x10^6 Thy1.1$^+$ OT-I splenocytes were transferred IV into C57BL/6 mice. 1 day post transfer, mice were vaccinated IV with ovalbumin, polyIC and anti-CD40. 5 days post vaccination splenocytes were depleted for CD49a$^+$ cells and subsequently enriched for CD49b$^+$ cells. Enriched cells were evaluated for Thy1.1$^+$ fraction to ensure adoptive transfer of 1x10^6 CD49b SP Thy1.1$^+$ OT-I effectors. Cells were transferred IV into BRPKp110 tumor-bearing-mice. Baseline tumors were harvested on day 1 post transfer and processed for flow cytometry. Other animals received daily IP injections with FTY720 or saline control and blood samples and tumors were harvested on day 7 post transfer. (A) Blood samples were analyzed for CD3$^+$ CD8$^+$ cells by flow cytometry. (B) Tumor were processed into single-cell suspensions, enriched for CD45$^+$ and analyzed for CD49b and CD49a expression on Thy1.1$^+$ CD3$^+$ CD8$^+$ cells. (C) Spleens were processed into single-cell suspensions and analyzed for CD49b and CD49a expression on Thy1.1$^+$ CD3$^+$ CD8$^+$ cells.

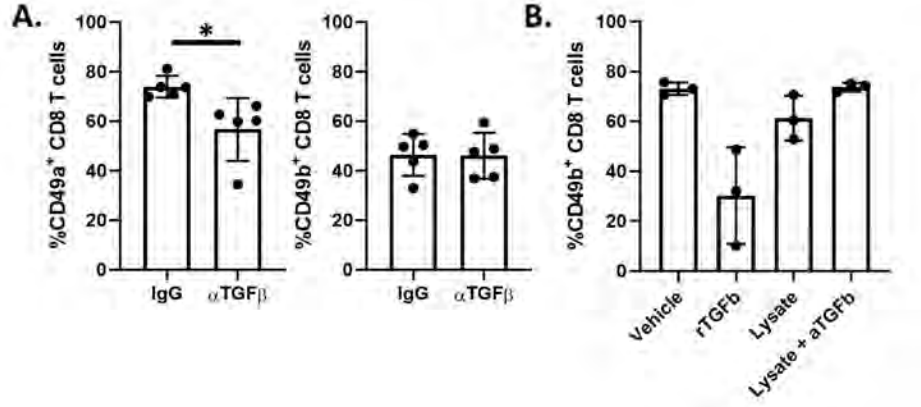

Supplemental Figure 4. (A) C57BL/6 mice were implanted SC with BRPKp110 breast carcinoma tumors. Mice were injected IP with anti-TGFβ1/2/3 or IgG control every 3 days between day 8-19 post tumor implantation. Tumors were harvested and single-cell suspensions were enriched for CD45$^+$ cells. CD45 fractions were analyzed for CD49a and CD49b expression on CD3$^+$ CD8$^+$ cells. (B) Thy1.1$^+$ OT-I splenocytes were enriched for CD8$^+$ cells by magnetic bead enrichment. Cells were activated for 48 hours with CD3/CD28 activation beads and cultured for an additional 3 days in presence of IL-2 and IL-7. Next, OT-I cells were cultured for 24 hours with recombinant human TGFβ1, BRPKp110-derived tumor lysate or lysate with anti-TGFβ blocking antibodies. Cells evaluated for CD49b expression by flow cytometry.

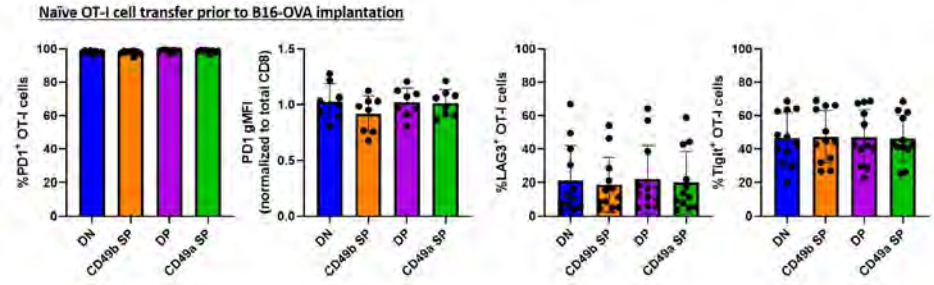

Supplemental Figure 5. 5x10^6 Thy1.1$^+$ OT-I splenocytes were transferred IV into C57BL/6 mice. 1 day post transfer, mice were subcutaneously injected with B16-OVA tumor cells. Tumors were harvested on day 19 and processed for flow cytometry evaluation.

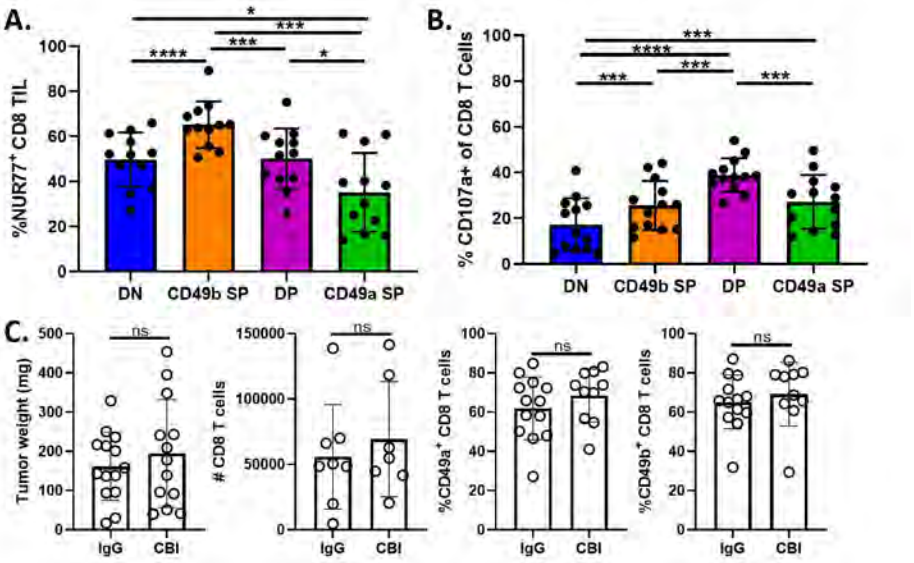

Supplemental Figure 6. (A) Nur77-GFP reporter mice were implanted SC with BRPKp110 breast carcinoma. Tumors were harvested on day 14, single cell suspensions were prepared and enriched for $CD45^+$ cells. CD45 fraction was analyzed for Nur77-GFP, CD49a and CD49b expression on $CD3^+$ $CD8^+$ cells. (B) C57BL/6 mice were implanted SC with BRPKp110 breast carcinoma. Tumors were harvested on day 14, single cell suspensions were prepared and enriched for $CD8^+$ cells. Cells were cultured with CD3/CD28 stimulation beads for 4-6 hours in presence of Brefeldin A and CD107a antibody. Cells were analyzed for expression CD49a, CD49b and CD107a expression on $CD3^+$ $CD8^+$ cells with intracellular staining for flow cytometry. (C) Nur77-GFP reporter mice were implanted SC with BRPKp110 breast carcinoma. Mice were IP injected 48 hours prior to harvest with a checkpoint blockade inhibitor (CBI) cocktail including anti-PD1, anti-LAG3 and anti-TIM3. Tumors were harvested, single-cell suspensions were prepared and enriched for $CD45^+$ cells. CD45 fraction was analyzed for CD49a and CD49b expression on $CD3^+$ $CD8^+$ cells by flow cytometry.

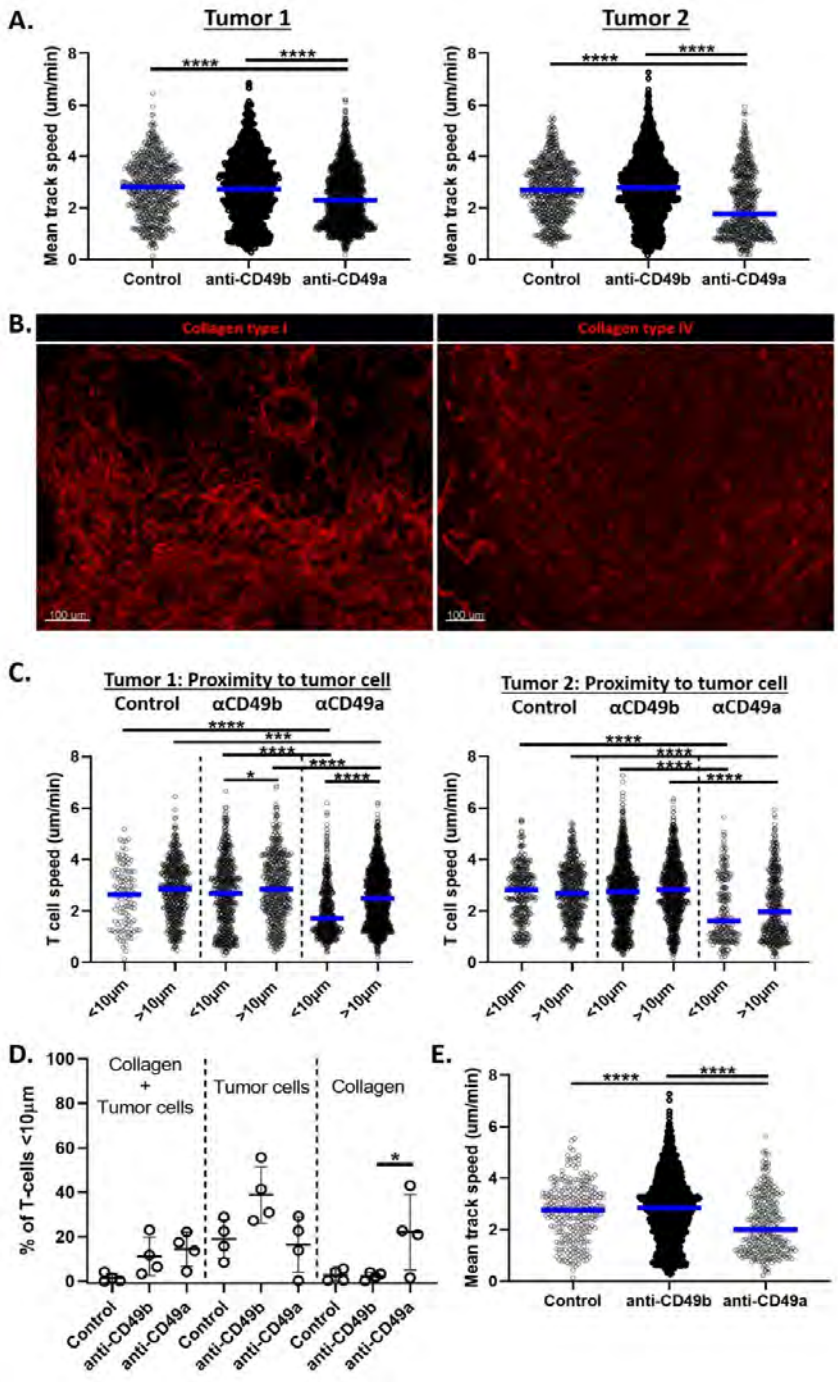

Supplemental Figure 7. CD2-dsRed mice were implanted SC with BRPKp110-GFP tumors. Tumors were harvested on day 21/22, embedded in agarose and cut into thick slices of

approximately 100-200µicrons. Slices were incubated with anti-CD49a or anti-CD49b blocking antibodies for 2 hours and assessed for $CD2^+$ T-cells, GFP^+ BRPKp110 cells and collagen fibers with second harmonics generation (SHG) on a 2-photon microscope. 30-minute videos of 2 fields per slice were made while maintaining oxygenation and 37°C with warm flowing media. (A) Mean track speed of the $CD2^+$ T-cells in each tumor evaluated. Treatment groups were compared with an ordinary one-way ANOVA and Tukey's multiple comparisons test. (B) C57BL/6 mice were implanted with BRPKp110 tumors. Day 21 tumors were harvested, fixed and thin sections were cut and stained with collagen type I or collagen type IV antibodies. (C) Mean track speed of the $CD2^+$ T-cells, stratified by distance to GFP^+ BRPKp110 tumor cells for tumor 1 (left) and tumor 2 (right). Close proximity: <10µm, large distance: >10µm. Groups were compared with an ordinary one-way ANOVA and Tukey's multiple comparisons test. (D) Live tumor slices were prepared and imaged by 2-photon microscopy as described in (A). Fraction of $CD2^+$ T-cells are displayed per field: fraction of cells <10µm to closest GFP^+ BRPKp110 tumor cell, <10µm to closest SHG-collagen fiber or <10µm to tumor cell and collagen (left). (E) Mean track speed of those $CD2^+$ T-cells located <10µm to tumor cells and >10µm from SHG-collagen.

Chapter 7

Discussion

The interplay between cancer and the immune system is an intricate balance, and several immune evasion strategies are used by tumors when they progress. Ideally, a type I immune response is generated, leading to effective eradication of tumor cells by effector T cells. As described in **Chapter 1**, cancer impairs type I T cell responses by impeding the priming, trafficking, infiltration and/or function of T cells. Currently approved immune therapies aim to reinvigorate effector responses, by targeting mechanisms that inhibit T cell function in the tumor. These therapies have shown great potential in cancers with pre-existing T cell infiltrates. However, the failure in a large fraction of patients also stresses the need for therapies targeting other mechanisms of immune evasion. Our incomplete understanding of immune evasion mechanisms utilized by different cancer types impairs the development of novel therapies for all patients. Especially mechanisms that diminish T cell priming and infiltration require attention, as tackling these hurdles would potentiate the presence of a more robust T cell pool in tumors. Cancer vaccines are a promising treatment to overcome suboptimal T cell priming. Vaccines utilize the administration of tumor-specific antigens in combination with immune stimulatory agents, named adjuvants[1], to generate new effector T cells and to boost existing memory T cell populations. For optimal effector T cell function, priming requires antigen-presentation by fully matured, professional antigen-presenting cells (APCs), such as dendritic cells (DCs), as well as CD4 T cell help. With proper CD4 help, mature APCs are able to generate signals 1 to 3 required for appropriate T cell activation: T cell receptor (TCR) engagement, co-stimulation and cytokine signaling[2]. Vaccine adjuvants thus have to support tumor-specific antigen presentation (signal 1) by inducing both signals 2 and 3. We have a good understanding of the important factors required for full DC maturation and T cell help through studies on viral infections **(Chapter 2**). Vaccine strategies and adjuvants to protect against viral infections have thus been well established. It is unclear which of the currently available adjuvants are the most capable to support vaccine-induced responses in the context of cancer; and thus, which strategy can generate the most full-blown and durable systemic type 1 T cell response. In this thesis, we have studied the effects of different adjuvants on local and systemic immune responses, in patients with metastatic melanoma (**Chapter 3 and 4**). Once tumor-specific T cells are primed, tumors can still escape from this immune response by preventing T cells to enter the tumor and find their target. Barriers installed by tumors, preventing proper T cell infiltration and functional engagement with tumor cells, remain poorly understood. Although, these barriers likely involve manipulation of extracellular matrix (ECM) proteins in the tumor microenvironment and adhesion receptors on T cells, including integrins. In **Chapters 5 and 6** we aimed to unravel the dynamics and regulation of integrin expression on T cells, as well as their individual role in T cell adherence to ECM and tumor cells.

A need for a better mechanistic understanding of vaccine adjuvants.

In recent years, a large number of clinical trials evaluated peptide-based vaccine strategies as a treatment for solid tumors, including melanoma and breast cancer[3].

Results for these trials are primarily documented by evaluating either: IFNγ production by circulating T cells, upon stimulation with antigen through enzyme-linked immunospot assays (ELIspot); level of CD4 and CD8 T cell infiltrates in the tumor; or antigen-specific antibodies in serum[3]. These assays can provide very valuable information on the overall systemic effects of different vaccination strategies, but they fail to provide mechanistic understanding of the beneficial or detrimental effects of vaccine adjuvants. As described in **Chapter 1**, inflammation at the vaccine site, and the resulting level of DC maturation, are crucial for adjuvants to properly induce antigen-specific T cells. By contrast, in mice, certain adjuvants, or lack thereof, can reportedly support a suppressive vaccine site, in which T cells get sequestered and deleted[4,5]. With the current assays to evaluate T cell responses in patients, we fail to address how the composition of the response at the vaccine site affects the systemic response. If a systemic response is lacking: is that due to failure in DC maturation, CD4 help, induction of tolerance or suppressive mechanisms at the vaccine site? In order to address this question, we aimed to go beyond these "standard" peptide vaccine evaluations and compared systemic T cell responses to local inflammation and immune cell accumulation at the vaccine site (**Chapter 4**)[6,7].

So, what did we learn from our trials? **Chapter 4** showed that the depot-forming adjuvant IFA induces more robust and durable local immune cell accumulation at the vaccine site than TLR agonist cocktail AS15. Additionally, **Chapter 3** revealed that IFA administered with TLR agonists generates a better systemic immune response than TLR agonists alone. The robust local immune response supported by IFA likely further augments the systemic tumor-specific T cell response. The increase in early accumulation of innate immune cells, especially DCs **(Chapter 4)**, and constant supply of antigen to these innate immune cells[4], may contribute to robust and lasting inflammation, driving APC maturation and ultimately longer-lasting and effective T cell activation. The combination of TLR agonists and IFA leads to a systemic, type I immune response in melanoma patients, with circulating tumor-specific effector T cells (**Chapter 3**). This suggests that the addition of TLR agonists to IFA induced even more robust DC maturation at the vaccine site, followed by improved T cell activation in the draining lymph nodes.

In mice, peptide vaccination in large amounts of IFA was shown to result in excessive accumulation of activated T cells at the vaccine site[4,5]. Is a robust response at the vaccine site, therefore, a good or a bad thing? In the murine studies, T cells were properly activated, but then sequestered away from circulation and tumor into the vaccine site, leading to dysfunction and eventual deletion of tumor-specific T cells. However, when instead of short – exact MHC class I fitting - peptides, mice were vaccinated with longer peptides in IFA, the systemic T cell response was more durable[4]. Long peptides, in contrast to short peptides, have to be ingested and processed by APCs in order to be presented in the context of MHC class I molecules, whereas short peptides can be presented by any cell displaying MHC class I, including cells that can induce tolerance. It is speculated that by combining short peptides and IFA, surrounding, non-immunogenic cells at the

vaccine site continuously present the peptides to T cells, ultimately sequestering and silencing them. The deletion and suppression appears to be mostly mediated by FAS-induced apoptosis and myeloid-derived suppressor cells (MDSC)-induced suppression[5]. Alternatively, because antigen processing is not required with short peptides, T cell activation in the lymph node can be driven by APCs other than mature DCs[8]. These APCs are more likely to induce a tolerogenic response.

These opposing results between our trial and the murine studies can be explained in several ways:

1. Humans and mice may simply respond differently to the use of depot-forming IFA in combination with short peptides. In mice vaccinated with short peptide in IFA, MDSCs infiltrated and suppressed sequestered T cells at the vaccine site[5]. Our analysis in **Chapter 4** did not show increased expression of MDSC gene signatures at vaccine sites of melanoma patients vaccinated with short peptides in IFA[7]. It is thus possible that the presentation of short peptides by surrounding cells, induces less tolerance or suppression in humans, compared to mice.
2. In the clinical trial showing systemic benefit of IFA as adjuvant, it was always given together with either TLR agonist LPS or polyICLC. Furthermore, these vaccine regimens include a tetanus peptide to induce a CD4 helper response. Despite being non-specific to tumor antigen, this CD4 activation is envisioned to provide CD40 co-stimulation and cytokines to optimize CD8 T cell activation. CD4 help is crucial to induce a cytotoxic CD8 T cell response with neo-epitope vaccination strategies[9]. Importantly, in mice, TLR stimulants and/or CD4 help abolished the negative local effects of IFA[4]. The absence of CD4 help or TLR stimulation in the Overwijk study[5] could thus have caused the lack of a systemic CD8 response. By adding these components to our vaccine adjuvant regimen, the antigen depot effect of IFA may be optimally utilized, without the induction of suppressive mechanisms.
3. Our analysis in **Chapter 3** compared the amount of IFA used to administer normalized to average weight of mice and human. This showed that the murine studies used significantly larger amounts than our patient trial. This suggests there is likely a tipping point in the use of IFA: enough to create a proper depot for continuous antigen release and resulting circulating tumor-specific T cells; but not so much it leads to complete sequestration of these tumor-specific T cells at the activation site, through peptide presentation on suppressive surrounding cells.
4. In **Chapter 4,** we found that IFA induced robust expression of tertiary lymphoid structure (TLS) related genes. In humans, local accumulation of adaptive immune cells may therefore be caused by recruitment into newly formed lymphoid structures, which can lead to *in situ* activation of naïve T cells[10,11]. By creating TLS, IFA in humans could contribute to the systemic antigen-specific T cell pool from a local perspective, instead of sequestering T cells away from the circulation.

5. If the correct volume is given to patients, IFA addition to short peptides and TLR agonists LPS or polyICLC, induced responses of higher magnitude and greater durability than TLR agonists alone **(Chapter 3)** and we would recommend it as a vaccine adjuvant for melanoma patients. However, whether the beneficial systemic effects of IFA are due to or in spite of the accumulation of adaptive immune cells at the vaccine site needs to be elucidated in future experiments. For example, it will be important to link accumulation of the different immune cell subsets at the vaccine site directly to the magnitude of the systemic response, as well as patient survival. Additionally, the specific composition and balance of inflammatory versus suppressive immune cell subsets should be evaluated in relation to systemic response and patient survival. In doing so, the beneficial or detrimental effects of the local immune response, in the resulting magnitude and quality of the vaccine-induced immune response, can be determined.

How can vaccination strategies affect the quality of the response?

Irrespective of how many circulating effector T cells a vaccine generates, reaching the desired anti-tumor effect depends upon the ability of these cells to infiltrate tumors and find their target. The route of vaccine administration and strength of activation signals 1-3 play an important role in the homing and chemokine receptor repertoire expressed by a T cell[12–16]. In melanoma patients, vaccination with IFA, but not TLR agonist combination AS15, led to the expression of homing receptor on T cells (**Chapter 4**)[6], suggesting the use of IFA as a vaccine adjuvant does support T cell homing and infiltration. In addition to homing and chemokines receptors, **Chapter 5 and 6** showed that expression of collagen-binding integrins CD49a and CD49b and E-cadherin binding integrin CD103, also depends on activation signals and environmental cues. Increased CD49a expression was observed in vaccine sites of patients vaccinated with melanoma peptides and IFA, compared to control skin (**Chapter 4**)[6]. This suggests that collagen-binding CD49a is induced by currently explored vaccination strategies. The integrins CD49b and CD103 were not induced at the vaccine site by either IFA or AS15 adjuvants over control skin. However, a different study did observe IFA-driven CD103 expression on T cells at the vaccine site at a later time point[6]. Combined, our data indicate that expression of homing, collagen-binding and E-cadherin binding receptors depend on T cell activation signals and/or environmental cues; and thus, vaccination strategy and choice of adjuvant.

Current peptide-based vaccine trials largely evaluate either the magnitude of antigen-specific T cells in the blood or T cell accumulation in tumors to determine the effectiveness of the vaccine. These assessments do not allow for studying the homing and adhesion receptor repertoire, and thus their capacity to enter tumors and eradicate tumor cells. We propose that a comprehensive phenotypic analysis of T cells at the vaccine site, the circulation and in tumors after different vaccine adjuvant strategies, is required to further understand their full impact on T cell activation. This can be achieved by comparing the phenotype and functional

capacity of tetramer-positive T cells from each location, by flow cytometry. Furthermore, single cell RNA sequencing could provide a more unbiased analysis of T cell status. These assays would measure both the magnitude of the immune response at different sites, as well as the expression of homing and adhesion receptors after different vaccine approaches. The differential induction of homing and adhesion receptors can subsequently be analyzed in relation to T cell localization and engagement with tumor cells, through immunofluorescent staining of vaccine-induced T cells in tumors.

What is the individual role of CD49a, CD49b and CD103 in T cell function?

Prior studies have speculated that integrins CD49a, CD49b and CD103 are adhesion molecules, important for retaining T cells in peripheral tissues with abundant collagen or E-cadherin expression[17]. Blocking CD49a or CD49b *in vivo* diminished overall T cell numbers in models for rheumatoid arthritis, influenza or tumors[17–19]. Similarly, CD103 binding to E-cadherin is important for the presence of tissue resident memory-like populations in peripheral tissues or tumors[20,21]. More generally, however, integrins have been described either to provide strong adhesion or to drive cell motility and migration[22]. Integrin-mediated "retention" is thus likely obtained through one of two mechanisms; it can encompass durable adhesion to molecules or cells and thereby establish long-term residence in a tissue. Alternatively, ligand binding drives motility, leading to confined cell migration within the specific tissue or area that contains abundant ligand. The combination of integrin repertoire, ligand availability/organization and resulting integrin signaling pathways may then ultimately determine whether and how a T cell remains in a tissue.

The impact of CD103 signaling on T cell motility and adhesion has been studied *in vitro* and during *in vivo* influenza infection of murine lungs[23]. In this work, CD103 binding to E-cadherin *in vitro* specifically caused T cell arrest. Knocking out or blocking CD103 *in vivo* directly increased velocity of influenza-specific effector CD8 T cells in the lung. In addition to providing adhesion to E-cadherin^{+} cells, CD103/E-cadherin interactions cause active F-actin remodeling and polarization of cytolytic granules, thereby supporting degranulation and TCR-mediated target cell killing[24,25]. CD103 plays an important and very direct role in both T cell adhesion to target cells and subsequent killing.

CD49b signaling in the context of T cell motility is less well-studied. CD49b can mediate migration of other immune cell subsets[26], but in primary T cells CD49b expression has only been correlated with accumulation in collagen-rich matrices or tissues[27]. In line with these findings, we observed that T cell motility was not affected by blocking CD49b-collagen interactions in collagen-rich tumor slices **(Chapter 6)**, but T cell localization was altered and allowed them to reside closer to tumor cells. CD49b binding to collagen may thus provide adhesion, not active migration, similar to CD103. Although, in contrast to CD103, this interaction does not lead to long-term arrest, because blocking CD49b did not increase

overall migration. Other reports have shown a direct role for CD49b signaling in the protection of T cells against FAS- or drug-induced apoptosis[28,29]. Together, this evidence points to a role for CD49b-collagen binding in short-term T cell adhesion and survival, not migration.

On the other hand, collagen-binding integrin CD49a signaling has been directly linked to increased T cell motility of primary T cells both *in vitro* and in epithelial tissues *in vivo*, including lungs and tumors[23] (**Chapter 6**). *In vitro* CD49a binding to collagen increased T cell migration, suggesting that T cells utilize collagen-CD49a interactions to move within a collagen-rich tissue. It can be envisioned that CD49a provides a mechanism for T cells to scan tissues for cognate antigen.

How do the opposing functions of CD49a, CD49b and CD103 differentially guide T cell subset movement in peripheral tissues?

Elegant imaging work in a subcutaneous lung tumor model has shown that antigen-specific T cells either engage with tumor cells in long-term firm contact or establish sequential short-term interactions[30]. During optimal tumor eradication in regressing tumors, long-lasting interactions dominate. Multiple tumor and infection models confirm the importance of these durable interactions to induce target cell killing[30–32]. Additionally, antigen-specific effector T cells displayed higher velocity than non-specific cells, suggesting antigen-specific T cells move rapidly between target cells. For optimal "serial killing" of tumor cells, a complementary role for CD49a, CD49b and CD103 in migration and arrest can thus be envisioned to mediate both effective and rapid scanning for new target cells, as well as efficient adhesion and eradication once the target cell is spotted.
The complementary roles of integrins CD49a, CD49b and CD103 fit with the envisioned movement of different T cell subsets that express them. Effector cells can express CD49a and CD49b, but generally not CD103 (**Chapter 5**). In acute infections, scanning tissues for antigen is mediated by CD49a, and the addition of inflammatory signals from innate immune cells, such monocytes and macrophages, then likely direct the T cells to target cells[33,34]. At the same time, CD49b provides survival signals to effector cells[28,29], by generating short-term contacts with collagen while the cells are moving through the tissue. Contrastingly, tissue resident memory (TRM) T cells generally express both CD49a and CD103, but not CD49b. TRM T cells remain in tissues long after acute infections have dissipated, therefore inflammation and infection are normally absent[35]. In this case, CD49a can allow for rapid movement and scanning through collagen-structured tissues. While scanning, CD103 can bind to E-cadherin expressing cells, cause T cell arrest and create the opportunity to sample the cell for its antigen[23,25]. Together this would provide rapid migration, with intermittent stops to efficiently sample all cells in the tissue for potential re-infection.

In tumors, ligand availability and organization are not as straightforward as other peripheral tissues: collagen matrix is disorganized and E-cadherin is often downregulated on tumor cells, as a part of epithelial-mesenchymal transition

(EMT)[36]. In this context, tumor infiltrating CD8 T cells often express collagen- and E-cadherin-binding integrins CD49a, CD49b and/or CD103 (**Chapter 5 and 6**). Thus, we can envision a few possible scenarios. 1) If collagen is expressed as a mesh among tumors cells, and these tumor cells express E-cadherin, T cells utilize CD49a and CD103 to scan for and adhere to tumor cells, similar to how TRM may utilize these mechanisms. In this situation, because collagen is dispersed in the tumor microenvironment, CD49b may also allow for short-term adhesion and arrest among tumors cells to either complement or replace CD103. 2) When collagen is localized only outside of tumor cell nests, T cells are confined within the stromal regions mediated by CD49a and/or CD49b, unable to find and engage tumor cells. Here, it is irrelevant whether E-cadherin and CD103 are expressed. Interaction of CD49b, CD49a and/or other collagen-binding integrins with collagen needs to be blocked for T cells to reach and engage with tumor cells. 3) Lastly, if tumor cells don't express sufficient levels of E-cadherin, T cells may find and recognize tumors cells, but the cue for long-term arrest and adherence through CD103 is absent. In this situation, subsequent cytotoxic target cell killing will be impaired. When collagen is dispersed among tumor cells, CD49b may be able to replace the CD103-induced long-term arrest to a certain degree. However, whether short-term CD49b adherence to collagen is able to support a durable engagement with the tumor cell, as required for killing[30,31], is unclear and should be further investigated.

In any of these three scenarios, CD49b-mediated survival signals are of course beneficial for ultimate T cell numbers and the overall capacity to eradicate tumor cells. However, even then, when cells are only protected from apoptosis in dense stromal regions, as described in scenario 2, they continue to migrate within this region alone. T cells remain unable to find their target and T cell-mediated tumor cell killing will be suboptimal. Despite this, T cells confined in stromal regions could contribute by producing inflammatory cytokines, if in contact with APCs. This is supported by the notion that, patients who only have T cell infiltration outside of tumor cell regions still have a better prognosis than patients with no T cells at all[37]. An important remaining question is whether CD49b-mediated adhesion in tumors with dense stromal regions (and their lacking ability to interact with tumor cells), outweighs the positive effects that CD49b signaling has on T cell survival; especially if the T cells in stromal regions contribute with inflammatory cytokines. In summary, we propose that CD49a, CD49b and CD103 expression affect tumor control either positively or negatively, depending on the exact tumor-specific context. Under "normal" inflammatory conditions, with nicely organized ECM, blocking β1 integrins (which include CD49a and CD49b) impairs T cell motility and target cell killing[38,39]. This suggest that indeed, in normal ECM structures, integrin signaling benefits effector function. Therefore, understanding the specifics of ECM disorganization and E-cadherin expression in tumors, is crucial in regulating T cell motility and adhesion through integrins. We hypothesize that reorganization of the ECM to resemble normal epithelial tissues will optimize integrin signaling and subsequent T cell migration and function. Later in this chapter we will delve deeper into the different types of collagen organization that

can be found in tumors and how we could aim to normalize the distribution and nature of the ECM to facility better T cell motility.

How does collagen organization in tumors affect T cell motility and function?

A diffuse, mesh-like ECM distribution will have a vastly different effect on T cell motility and function than dense localized ECM. In general it is known that overall presence, collagen fiber thickness, rigidity and organization are all crucial for direction and speed of T cell motility[40]. Most normal epithelial tissues are in a tensional homeostatic state, which leads to a relaxed meshwork of collagens. However, as was described in **Chapter 1**, tumors often display increased collagen deposition, cross-linking and distorted organization[41,42]. Additionally, high levels of matrix metalloproteinases (MMPs) cause increased remodeling of collagen fibers in tumors[43]. Thus overall, collagen alignment, length, width, density and straightness is altered in tumors compared to adjacent normal tissue[44] and the level of disorganization is highly variable between tumors. Due to the high variability, the exact specifics of the collagen organization and structure within a tumor, likely determine the ultimate effect the ECM has on T cell motility and function. Few comprehensive analyses have been done to understand the role of differential collagen organization on T cell function in tumors. One major problem is that no standardized visualization method exists to characterize collagen organization[44]. Currently used methods range from conventional to sophisticated microscopic techniques visualizing collagen structures with ranging sensitivity, making it very difficult to compare between studies. Regardless, anecdotal studies, combined with the findings in this thesis, can teach us about different collagen structures and how they may affect T cell localization, motility and function.

A common collagen organization in stromal-rich tumors involves dense, aligned collagen fibers outside of tumor cell clusters. In these tumors, T cells are often confined within these collagen-dense regions and are unable to interact with tumor cells[45]. T cells can be liberated by collagenase treatment but not integrin blockade, suggesting that in this type of ECM organization, the collagen fibers form a physical barrier. Other collagen-rich tumors, including the breast carcinoma model described in **Chapter 6,** have collagen deposited more evenly throughout the tumor. Although, even when among tumor cells, these fibers are often still dense, linear and highly aligned. T cells, similar to many other cell types, have been shown to use these aligned collagen fibers as highways to migrate along[41,46]. **Chapter 6** and other research showed that CD49a may be involved in promoting this motility in epithelial tissues and tumors[23]. To successfully kill a tumor cell, a T cell has to arrest and engage for an extended time period[34]. When trafficking along collagen fibers at high velocity, it can be envisioned that the T cell is unable to engage as efficient and durable. Thus, tumors can have distinct forms of collagen deposition and create either structural barriers, preventing T cell from leaving stromal regions, or collagen-highways within tumor regions that distract T cells from engaging with target cells. Both forms of collagen deposition

can be mechanisms to hijack the ECM in the tumor microenvironment to prevent optimal T cell recognition, albeit in contrasting ways. Interestingly, treatment with recombinant Hyaluronan And Proteoglycan Link Protein 1 (HAPLN1) in a melanoma model, promoted a more "basket-weave" ECM structure, closer resembling normal epithelial tissue[47]. This correlated with improved T cell infiltration; however, whether it ultimately led to more frequent interactions with tumor cells is unknown.

Since we hypothesize that CD49a, CD49b and possibly other ECM-binding integrins play a role in the movement or adhesion of T cells along collagen fibers **(Chapter 6)**, the availability of the peptide sequence for integrin binding itself could also play a role. Rigid, dense collagen fibers may have structurally blocked the binding sequences, whereas smaller, loose collagen structure could allow for better T cell interactions via integrins. Importantly, MMP-mediated degradation of collagen generates small fragments that have chemotactic properties[48,49]. Binding sites on these fragments are likely more available than on complete collagen fibers. In this scenario, there is no collagen meshwork, as there would be in normal epithelial tissues. However, the small collagen fragments may still drive T cell motility in tumors by signaling through CD49a, but likely without directionality. MMP inhibitors have been shown to increase T cell function in a tumor model, suggesting that presence of collagen fragments can indeed be detrimental[48]. However, whether this is due to CD49a or CD49b signaling remains to be elucidated. Interestingly though, collagen fragments have been shown to antagonize CD49b function *in vitro* in sarcoma cells. The fragments bind to CD49b, but in contrast to full collagen fibers fail to elicit a signaling response[50]. An important question arising from this observation: do collagen fragments antagonize integrin signaling *in vivo*, and is this beneficial or detrimental for T cell function in tumors. We hypothesize that the answer of these questions, depends on the collagen organization of the tumor and changes thereof after MMP inhibition.

Taken together, comprehensive analyses should be conducted to characterize ECM matrix organization in relation to T cell function both in infections of epithelial tissues and different cancer types. Subsequently, novel and existing treatment strategies, altering either collagen deposition and/or organization or the integrin phenotype of T cells, can be deployed to successfully target this barrier to T cell function in tumors.

Regulation of integrin expression on human and murine T cells

Optimal T cell migration in tumors likely is obtained when ECM is organized in a relaxed, meshwork, resembling epithelial tissues. In addition to ECM organization, optimal T cell migration will require an integrin repertoire, that can mediate the desired migration pattern of the T cell. Therefore, it is important to fully understand how integrin expression is regulated on T cells. **Chapter 5 and 6** showed that CD49b is upregulated on a fraction of both human and murine

CD8 T cells after TCR-mediated activation *in vivo* and *in vitro*. However, only a fraction of the antigen-specific T cells upregulated CD49b, in any of these circumstances. This suggests that only a specific lineage of naïve CD8 T cells is capable of upregulating CD49b. With that in mind, we hypothesize that the correct epigenetic and transcriptional state of a naïve T cell is likely essential to support CD49b upregulation. Alternatively, components of the signals required for proper T cell activation, such as CD4 help, may be crucial for CD49b upregulation and are missing for a fraction of the cells. This latter explanation is deemed unlikely due to the existence of a relatively large CD49b^{neg} fraction after *in vitro* activation with CD3/CD28 activating antibodies **(Chapter 5)**. CD3/CD28 stimulation should provide signals for T cell activation equally to the all cultured T cells. In melanoma patients, vaccination either with peptides in IFA or protein in AS15 (adjuvant containing TLR agonists) alone did not increase CD49b expression on accumulated cells at the vaccine site, suggesting the lineage capable of inducing CD49b may not be targeted by these vaccine strategies **(Chapter 4)**. However, antigen-specific T cells in the blood and tumor will have to be evaluated to establish whether CD49b upregulation was absent completely with this vaccination strategy or whether CD49b^{+} T cells selectively do not accumulate at the vaccine site. Alternatively, CD49b may also be rapidly downregulated at the vaccine site. Future analyses of the epigenetic state and gene expression patterns, in relation to CD49b expression, both after *in vitro* activation and in the circulation and vaccine site of vaccinated patients, can illuminate which signaling pathways are crucial for CD49b expression. Furthermore, these analyses can establish the functional capacity of CD49b^{+} and CD49b^{neg} cells under different conditions.

In contrast to CD49b, upregulation of CD103 on human CD8 T cells requires an additional signal in the form of immune suppressive cytokine TGFβ[51] (**Chapter 5**). This finding has been corroborated by *in vivo* murine models for TRM formation[20,52] and CD103 is specifically upregulated within the TGFβ-rich tissue[53]. The availability of TGFβ during different stages of an immune response and in the target tissue itself thus likely determine whether TRM and tumor-infiltrating CD8 T cells ultimately express CD103[54]. It is not surprising that the inflammatory environment of vaccine sites after vaccination with IFA or TLR agonist AS15 did not increase CD103 expression, as TGFβ levels are likely low **(Chapter 4)**. CD103 is induced at the vaccine site, 7 weeks post vaccination with peptide in IFA[6], suggesting that TGFβ is eventually expressed at the vaccine site driven by IFA, likely to dampen the immune response. Future studies can determine whether these CD103^{+} T cells are specifically retained at the vaccine site and whether blocking TGFβ locally could improve T cell dissemination from vaccine site to circulation. In tumors, TGFβ determines what fraction of the T cells express CD103 and can utilize this to improve adhesion and effector function. However, T cells expressing CD103 have also been subject to TGFβ-driven suppression of effector function[51,55]. Therefore, even though CD103 promotes T cell adhesion and killing of tumor cells, the expression of the molecule itself suggests suppressed effector capacity by TGFβ. Future experiments can determine whether blocking TGFβ signaling in tumors relieves the suppression, while retaining the beneficial effects

of CD103 mediated adhesion. Potentially a regulated balance in TGFβ levels is required: enough to upregulate CD103, but not enough to induce high levels of suppression.

Lastly, CD49a regulation is the most complicated of these three integrins and is distinctly regulated between different subsets of human and murine lymphocytes, including T cells. Vaccination in IFA, increased expression of CD49a, but not CD49b and CD103 at the vaccine sites, when compared to normal skin **(Chapter 4)**. *In vitro* cultured human T cells upregulated CD49a on a fraction of cells after TCR-mediated activation. Further upregulation of CD49a, both in fraction and intensity, required additional signals from TGFβ or TNFα in these human CD8 T cells (**Chapter 5)**. IL-2 can induce CD49a expression independent of TCR signaling. Contrasting these findings in human T cells, *in vivo* activation of murine T cells in vaccination or tumor models showed that TCR-mediated activation alone is not sufficient. In this murine tumor model, TGFβ is also not responsible for the upregulation of CD49a on tumor infiltrating T cells **(Chapter 6)**. Other soluble factor(s) in the tumor microenvironment, and likely the vaccine site, induced CD49a in these mouse models. TGFβ does seem to play a role in CD49a expression on murine intestinal TRM[56] and TGFβ, in combination with IL-15, is also responsible for CD49a expression on murine innate lymphocyte cells (ILCs)[57,58]. The distinct regulation of CD49a between different subsets, suggests that CD49a induction by environmental and TCR signals is highly influenced by epigenetic state or cytokine receptor repertoire of the individual cell. Furthermore, our findings and current literature point to a regulation of CD49a expression through multiple pathways and thus suggests importance for CD49a in lymphocyte function under many different circumstances. More detailed studies are to be conducted to understand the relationship between epigenetic status and the signaling pathways required for the upregulation of CD49a. This creates an opportunity for therapeutic modulation of CD49a expression on various T cell subsets and thus regulating their motility in different situations.

The different ways of upregulating these integrins is linked to the functional CD8 T cell subsets expressing them. Under normal circumstances, CD103 is expressed on TRM, whose development is driven in part by TGFβ. Tumors also often contain high levels of TGFβ in the environment, explaining why TIL express CD103, even though they are not classical TRM. CD49b is predominantly expressed on a fraction of effector CD8 T cells both in infections and tumors, but generally not on memory subsets (**Chapter 6)**. This corresponds with the dependence on TCR activation for its expression, and the likely downregulation of CD49b when TCR signal is lost. Then lastly, CD49a induction appears to be driven by several different factors, depending on both the environment and the differentiation state of the cell. The discrepancy observed between CD49a-expressing human and murine CD8 TIL, and their phenotype and function in tumors (**Chapter 5 and 6**), can therefore be explained by the difference in environment and timing of the tumor-specific immune response. CD49a may simply be a sensor of the environment, similar to cytokine-driven expression of CD69 and subsequent downregulation of

T cell trafficking molecule S1P1[59]. By being a sensor of the environment, CD49a could function as a tool for the T cell to upregulate under conditions that require high motility, independent of what the phenotype or functional capacity of that particular cell is.

What other beneficial effects could targeting ECM or integrins have in tumors?

Collagen-binding integrins CD49a and CD49b are expressed on many other cell types, in addition to T cells. These include immune cell populations such as myeloid cells and neutrophils, but also endothelial cells and even tumor cells in some cases[60]. In **Chapter 6** we have shown that CD49a specifically drives T cell motility. In tumor cells and myeloid cells, CD49a also supports migration upon binding with collagens[61,62]. Targeting CD49a in tumors may not only revert T cell dysfunction by increasing arrest and engagement with tumor cells, but also directly address tumor cell migration and metastasis via collagen. It may decrease motility of suppressive myeloid populations and their capacity to inhibit T cell function throughout the tumor. In contrast, utilization of MMP inhibitors or other strategies to normalize the ECM structure could lead to increased and better guided migration of tumor cells and tumor-promoting myeloid cells. It would be important to evaluate the metastatic capacity of tumor cells in the context of these potential therapies to ensure safety in this regard.

Alternatively, there are ECM-binding integrins on T cells in addition to those described in **Chapter 5 and 6** of this thesis. Similar to CD49a and CD49b, these integrins may alter their motility/adhesion in reference to their ligands and affect engagement with tumor cells and ultimate T cell function. For example in a murine model for skin inflammation, integrins αVβ1 and αVβ3 mediated CD4 T cell migration along collagen fibers, visualized with second harmonics generation[38]. T cells can express also ECM-binding integrins α3β1, α4β1, α5β1, α6β1 and αXβ2[63], although much less is known about their regulation during an immune response or their role in T cell migration in different tissues. Given the important individual roles for CD49a, CD49b and CD103 **(Chapter 6)**[23,38,39]**,** we propose that reorganizing the ECM could allow for optimal utilization of these other ECM-binding integrins as well. Therefore, the comprehensive analysis of ECM organization and structure in relation to T cell function should include the specific ligands for each ECM-binding integrin expressed by T cells.

Overall, which potential therapeutic targets have been highlighted to improve T cell function in tumors?

Activation and environmental factors determine integrin expression pattern on CD8 T cells **(Chapter 4-6)**. These integrins can affect T cell infiltration, motility and engagement with tumor cells. A deeper understanding of the exact contributors to induction of individual integrins is necessary, and would create opportunities to adjust vaccination and adoptive transfer strategies to activate T cells with a

favorable integrin and homing receptor repertoire. In doing so, activated T cells are not simply capable of responding to their antigens, but able to arrive in target tissue and engage with target cells. Future clinical trials, in which different T cell activation conditions are evaluated, such as vaccination and adoptive T cell transfer, should assess the effect of activation conditions on T cell phenotype. Activation conditions should then be adjusted for those phenotypes that drive optimal homing to tumors and target recognition.

Separately, elements in the tumor microenvironment can be blocked or enhanced to shape the integrin repertoire for most optimal T cell motility and tumor cell engagement. **Chapter 5** stressed that cytokines TNFα, IL-2 and TGFβ may be involved in the upregulation of CD49a expression on human CD8 T cells. However, in our breast carcinoma model (**Chapter 6)**, TGFβ is not responsible for the expression of CD49a on CD8 TIL. A more comprehensive analysis of cytokines, chemokines, growth factors and other elements of the tumor microenvironment and vaccine site should be conducted, to establish the exact mechanism of CD49a expression. Understanding this mechanism would create the opportunity to block CD49a upregulation, by limiting the signaling of that particular factor. Because CD49a may be directly involved in T cell dysfunction in tumors (**Chapter 6),** blocking its upregulation could negate this mechanism of dysfunction directly. Furthermore, we observed that CD49a often coincides with expression of exhaustion markers, suggesting that blocking the upregulation of CD49a may also result in less inhibitory signals and thus possibly target another mechanism of T cell dysfunction. Inhibition of CD49a signaling through small molecule inhibitors or blocking antibodies could also tackle T cell dysfunction in tumors.

Finally, the ECM matrix in tumors itself can be targeted and reorganized to structurally resemble healthy tissue. This would allow T cells to optimally utilize their integrin repertoire and efficiently find and interact with tumor cells. **Chapter 6** lays the groundwork for understanding the role of activation and environment on integrin repertoire on T cells, as well as how this affects their ability to move and interact with tumor cells. However, comprehensive knowledge of the different ECM components and organization in tumors has to be established. Furthermore, strategies to target ECM organization are emerging, for example, as described above through MMP inhibitors and treatment with recombinant HAPLN1. Therefore, in addition to mapping the ECM in different tumors, the effect of these treatments in each ECM "phenotype" will have to be established to determine the most optimal strategy to normalize ECM structure and thus normalize T cell motility and localization within this structure.

Summary

A type I immune response is crucial for adequate tumor eradication by the immune system. However, tumors often gain evasion mechanisms that create barriers to the generation or effectiveness of a type I immune response. Among

these barriers is the suppression of effective T cell priming and the inhibition of proper T cell infiltration and function in tumors. At present, the only therapies to target these barriers are focused on direct inhibition of T cell function by the tumor, through checkpoint molecules. These therapies are thus dependent on an existing type I response, and are generally not successful when tumors have insufficient T cells primed or infiltrated. This thesis has revealed ways to improve T cell priming and the infiltration of T cells in tumors. The priming of new anti-tumor T cells with melanoma peptides can induce systemic CD8 T cells, capable of responding to antigen. As described in **Chapter 1**, the circumstances during which these T cells get activated ultimately determine their functional capacity in the tumor. The use of IFA as an adjuvant generates both local and systemic immune responses (**Chapter 3 and 4**). IFA induced higher accumulation of activated DCs and CD4 helper T cells at the vaccine site compared to a TLR agonist as adjuvant, suggesting IFA promotes CD8 T cell activation signals efficiently. Combination of IFA with TLR agonists led to an even higher systemic tumor-specific CD8 T cell response. Together, these data highlight important findings to optimize treatment for patients that have no pre-existing T cell response.

Additionally, this thesis focused on the adhesion and retention capabilities of tumor infiltrating CD8 T cells. These CD8 T cells displayed increased expression of integrins CD49a, CD49b and CD103 in human melanoma tumors, compared to circulating CD8 T cells from normal donors (**Chapter 5**). This suggests that T cells may need these integrins in order to stay in the tumor. However, human cancer studies do not provide the opportunity to interrogate T cell dynamics, hence it is impossible to determine whether T cells lacking expression of these integrins are not retained in the tumor or whether they never arose in the first place. We found that elements in the tumor microenvironment are responsible for the upregulation of CD49a and likely CD103. Therefore, the tumor itself can modulate the adhesion capabilities of T cells. The *in vivo* analyses also revealed a more complicated function of these integrins than simply "retention". CD49a drives T cell motility and thereby distracts T cells from engaging with tumor cells, essentially creating retention and T cell dysfunction simultaneously (**Chapter 6**). CD49b did not drive T cell motility or block engagement with tumor cells, suggesting a different role for CD49b ligation to collagen ligands. Other reports showed that CD103 mediated arrest and lasting engagement with E-cadherin expressing cells in lung infections[23], however, whether it serves a similar function in tumors remains to be determined. Nonetheless, these integrins serve different purposes that involve adhesion or adhesion-driven motility, with opposite results in terms of T cell function. Due to environmentally driven expression, tumors can alter the cues required for differential integrin expression, to favor integrin-driven T cell dysfunction. By therapeutically addressing these environmental cues or integrin function directly, overall T cell function in tumors and thus tumor control will be improved.

REFERENCES

1. Kwak, M., Leick, K. M., Melssen, M. M. & Slingluff, C. L. Vaccine Strategy in Melanoma. *Surg. Oncol. Clin. N. Am.* **28**, 337–351 (2019).
2. Borst, J., Ahrends, T., Bąbała, N., Melief, C. J. M. & Kastenmüller, W. CD4(+) T cell help in cancer immunology and immunotherapy. *Nat. Rev. Immunol.* **18**, 635–647 (2018).
3. Bezu, L. *et al.* Trial watch: Peptide-based vaccines in anticancer therapy. *Oncoimmunology* **7**, e1511506–e1511506 (2018).
4. Bijker, M. S. *et al.* CD8+ CTL priming by exact peptide epitopes in incomplete Freund's adjuvant induces a vanishing CTL response, whereas long peptides induce sustained CTL reactivity. *J. Immunol.* **179**, 5033–5040 (2007).
5. Hailemichael, Y. *et al.* Persistent antigen at vaccination sites induces tumor-specific $CD8^+$ T cell sequestration, dysfunction and deletion. *Nat. Med.* **19**, 465–472 (2013).
6. Salerno, E. P. *et al.* Activation, dysfunction and retention of T cells in vaccine sites after injection of incomplete Freund's adjuvant, with or without peptide. *Cancer Immunol. Immunother.* **62**, 1149–1159 (2013).
7. Pollack, K. E. *et al.* Incomplete Freund's adjuvant reduces arginase and enhances Th1 dominance, TLR signaling and CD40 ligand expression in the vaccine site microenvironment. *J. Immunother. cancer* **8**, (2020).
8. Bijker, M. S. *et al.* Superior induction of anti-tumor CTL immunity by extended peptide vaccines involves prolonged, DC-focused antigen presentation. *Eur. J. Immunol.* **38**, 1033–1042 (2008).
9. Alspach, E. *et al.* MHC-II neoantigens shape tumour immunity and response to immunotherapy. *Nature* **574**, 696–701 (2019).
10. Peske, J. D. *et al.* Effector lymphocyte-induced lymph node-like vasculature enables naive T-cell entry into tumours and enhanced anti-tumour immunity. *Nat. Commun.* **6**, 7114 (2015).
11. Luo, S. *et al.* Chronic Inflammation: A Common Promoter in Tertiary Lymphoid Organ Neogenesis. *Front. Immunol.* **10**, 2938 (2019).
12. Woods, A. N. *et al.* Differential Expression of Homing Receptor Ligands on Tumor-Associated Vasculature that Control CD8 Effector T-cell Entry. *Cancer Immunol. Res.* **5**, 1062 LP – 1073 (2017).
13. Clancy-Thompson, E. *et al.* Peptide vaccination in Montanide adjuvant induces and GM-CSF increases CXCR3 and cutaneous lymphocyte antigen expression by tumor antigen-specific CD8 T cells. *Cancer Immunol. Res.* **1**, 332–339 (2013).
14. Brinkman, C., Peske, J. & Engelhard, V. Peripheral Tissue Homing Receptor Control of Naïve, Effector, and Memory CD8 T Cell Localization in Lymphoid and Non-Lymphoid Tissues. *Front. Immunol.* **4**, 241 (2013).
15. Slingluff, C. L. J. *et al.* A randomized pilot trial testing the safety and immunologic effects of a MAGE-A3 protein plus AS15 immunostimulant administered into muscle or into dermal/subcutaneous sites. *Cancer Immunol. Immunother.* **65**, 25–36 (2016).
16. Maeng, H. M. & Berzofsky, J. A. Strategies for developing and optimizing cancer vaccines. *F1000Research* **8**, F1000 Faculty Rev-654 (2019).
17. Richter, M. *et al.* Collagen distribution and expression of collagen-binding alpha1beta1 (VLA-1) and alpha2beta1 (VLA-2) integrins on CD4 and CD8 T cells during influenza infection. *J. Immunol.* **178**, 4506–4516 (2007).

18. de Fougerolles, A. R. *et al.* Regulation of inflammation by collagen-binding integrins alpha1beta1 and alpha2beta1 in models of hypersensitivity and arthritis. *J. Clin. Invest.* **105**, 721–729 (2000).
19. Andreasen, S. Ø. *et al.* Expression and functional importance of collagen-binding integrins, alpha 1 beta 1 and alpha 2 beta 1, on virus-activated T cells. *J. Immunol.* **171**, 2804–2811 (2003).
20. Mackay, L. K. *et al.* The developmental pathway for CD103(+)CD8+ tissue-resident memory T cells of skin. *Nat. Immunol.* **14**, 1294–1301 (2013).
21. Sheridan, B. S. *et al.* Oral infection drives a distinct population of intestinal resident memory CD8(+) T cells with enhanced protective function. *Immunity* **40**, 747–757 (2014).
22. Campbell, I. D. & Humphries, M. J. Integrin structure, activation, and interactions. *Cold Spring Harb. Perspect. Biol.* **3**, (2011).
23. Reilly, E. C. *et al.* T(RM) integrins CD103 and CD49a differentially support adherence and motility after resolution of influenza virus infection. *Proc. Natl. Acad. Sci. U. S. A.* (2020) doi:10.1073/pnas.1915681117.
24. Le Floc'h, A. *et al.* Minimal engagement of CD103 on cytotoxic T lymphocytes with an E-cadherin-Fc molecule triggers lytic granule polarization via a phospholipase Cgamma-dependent pathway. *Cancer Res.* **71**, 328–338 (2011).
25. Franciszkiewicz, K. *et al.* CD103 or LFA-1 engagement at the immune synapse between cytotoxic T cells and tumor cells promotes maturation and regulates T-cell effector functions. *Cancer Res.* **73**, 617–628 (2013).
26. Werr, J. *et al.* Integrin alpha(2)beta(1) (VLA-2) is a principal receptor used by neutrophils for locomotion in extravascular tissue. *Blood* **95**, 1804–1809 (2000).
27. Yan, X., Johnson, B. D. & Orentas, R. J. Induction of a VLA-2 (CD49b)-expressing effector T cell population by a cell-based neuroblastoma vaccine expressing CD137L. *J. Immunol.* **181**, 4621–4631 (2008).
28. Gendron, S., Couture, J. & Aoudjit, F. Integrin α2β1 Inhibits Fas-mediated Apoptosis in T Lymphocytes by Protein Phosphatase 2A-dependent Activation of the MAPK/ERK Pathway. *J. Biol. Chem.* **278**, 48633–48643 (2003).
29. Abderrazak, A., El Azreq, M.-A., Naci, D., Fortin, P. R. & Aoudjit, F. Alpha2beta1 Integrin (VLA-2) Protects Activated Human Effector T Cells From Methotrexate-Induced Apoptosis. *Front. Immunol.* **9**, 2269 (2018).
30. Mrass, P. *et al.* Random migration precedes stable target cell interactions of tumor-infiltrating T cells. *J. Exp. Med.* **203**, 2749–2761 (2006).
31. Boissonnas, A., Fetler, L., Zeelenberg, I. S., Hugues, S. & Amigorena, S. In vivo imaging of cytotoxic T cell infiltration and elimination of a solid tumor. *J. Exp. Med.* **204**, 345–356 (2007).
32. Schaeffer, M. *et al.* Dynamic imaging of T cell-parasite interactions in the brains of mice chronically infected with Toxoplasma gondii. *J. Immunol.* **182**, 6379–6393 (2009).
33. Dangaj, D. *et al.* Cooperation between Constitutive and Inducible Chemokines Enables T Cell Engraftment and Immune Attack in Solid Tumors. *Cancer Cell* **35**, 885-900.e10 (2019).
34. Ariotti, S. *et al.* Subtle CXCR3-Dependent Chemotaxis of CTLs within Infected Tissue Allows Efficient Target Localization. *J. Immunol.* **195**, 5285 LP – 5295 (2015).

35. Topham, D. J. & Reilly, E. C. Tissue-Resident Memory CD8+ T Cells: From Phenotype to Function. *Front. Immunol.* **9**, 515 (2018).
36. Huang, R. Y.-J., Guilford, P. & Thiery, J. P. Early events in cell adhesion and polarity during epithelial-mesenchymal transition. *J. Cell Sci.* **125**, 4417–4422 (2012).
37. Erdag, G. *et al.* Immunotype and Immunohistologic Characteristics of Tumor-Infiltrating Immune Cells Are Associated with Clinical Outcome in Metastatic Melanoma. *Cancer Res.* **72**, 1070 LP – 1080 (2012).
38. Overstreet, M. G. *et al.* Inflammation-induced interstitial migration of effector $CD4^+$ T cells is dependent on integrin αV. *Nat. Immunol.* **14**, 949–958 (2013).
39. Espinosa-Carrasco, G. *et al.* Integrin β1 Optimizes Diabetogenic T Cell Migration and Function in the Pancreas. *Front. Immunol.* **9**, 1156 (2018).
40. Bougherara, H. *et al.* Real-Time Imaging of Resident T Cells in Human Lung and Ovarian Carcinomas Reveals How Different Tumor Microenvironments Control T Lymphocyte Migration. *Front. Immunol.* **6**, 500 (2015).
41. Egeblad, M., Rasch, M. G. & Weaver, V. M. Dynamic interplay between the collagen scaffold and tumor evolution. *Curr. Opin. Cell Biol.* **22**, 697–706 (2010).
42. Henke, E., Nandigama, R. & Ergün, S. Extracellular Matrix in the Tumor Microenvironment and Its Impact on Cancer Therapy. *Front. Mol. Biosci.* **6**, 160 (2020).
43. Nissen, N. I., Karsdal, M. & Willumsen, N. Collagens and Cancer associated fibroblasts in the reactive stroma and its relation to Cancer biology. *J. Exp. Clin. Cancer Res.* **38**, 115 (2019).
44. Zunder, S. M., Gelderblom, H., Tollenaar, R. A. & Mesker, W. E. The significance of stromal collagen organization in cancer tissue: An in-depth discussion of literature. *Crit. Rev. Oncol. Hematol.* **151**, 102907 (2020).
45. Salmon, H. *et al.* Matrix architecture defines the preferential localization and migration of T cells into the stroma of human lung tumors. *J. Clin. Invest.* **122**, 899–910 (2012).
46. Pruitt, H. C. *et al.* Collagen fiber structure guides 3D motility of cytotoxic T lymphocytes. *Matrix Biol.* **85–86**, 147–159 (2020).
47. Kaur, A. *et al.* Remodeling of the Collagen Matrix in Aging Skin Promotes Melanoma Metastasis and Affects Immune Cell Motility. *Cancer Discov.* **9**, 64 LP – 81 (2019).
48. Juric, V. *et al.* MMP-9 inhibition promotes anti-tumor immunity through disruption of biochemical and physical barriers to T-cell trafficking to tumors. *PLoS One* **13**, e0207255 (2018).
49. Fields, G. B. The Rebirth of Matrix Metalloproteinase Inhibitors: Moving Beyond the Dogma. *Cells* **8**, (2019).
50. Messent, A. J. *et al.* Effects of collagenase-cleavage of type I collagen on alpha2beta1 integrin-mediated cell adhesion. *J. Cell Sci.* **111**, 1127 LP – 1135 (1998).
51. Flavell, R. A., Sanjabi, S., Wrzesinski, S. H. & Licona-Limón, P. The polarization of immune cells in the tumour environment by TGFbeta. *Nat. Rev. Immunol.* **10**, 554–567 (2010).
52. Mackay, L. K. *et al.* T-box Transcription Factors Combine with the Cytokines TGF-β and IL-15 to Control Tissue-Resident Memory T Cell Fate. *Immunity* **43**, 1101–1111 (2015).
53. El-Asady, R. *et al.* TGF-{beta}-dependent CD103 expression by CD8(+) T cells promotes selective destruction of the host intestinal epithelium during graft-versus-host disease. *J. Exp. Med.* **201**, 1647–1657 (2005).

54. Thompson, E. A. *et al.* Monocytes Acquire the Ability to Prime Tissue-Resident T Cells via IL-10-Mediated TGF-β Release. *Cell Rep.* **28**, 1127-1135.e4 (2019).
55. Thomas, D. A. & Massagué, J. TGF-beta directly targets cytotoxic T cell functions during tumor evasion of immune surveillance. *Cancer Cell* **8**, 369–380 (2005).
56. Zhang, N. & Bevan, M. J. Transforming Growth Factor-β Signaling Controls the Formation and Maintenance of Gut-Resident Memory T Cells by Regulating Migration and Retention. *Immunity* **39**, 687–696 (2013).
57. Gao, Y. *et al.* Tumor immunoevasion by the conversion of effector NK cells into type 1 innate lymphoid cells. *Nat. Immunol.* **18**, 1004–1015 (2017).
58. Hawke, L. G., Mitchell, B. Z. & Ormiston, M. L. TGF-β and IL-15 Synergize through MAPK Pathways to Drive the Conversion of Human NK Cells to an Innate Lymphoid Cell 1-like Phenotype. *J. Immunol.* **204**, 3171–3181 (2020).
59. Mackay, L. K. *et al.* Cutting Edge: CD69 Interference with Sphingosine-1-Phosphate Receptor Function Regulates Peripheral T Cell Retention. *J. Immunol.* **194**, 2059 LP – 2063 (2015).
60. Martrus, G. *et al.* CD49a Expression Identifies a Subset of Intrahepatic Macrophages in Humans. *Front. Immunol.* **10**, 1247 (2019).
61. Lochter, A., Navre, M., Werb, Z. & Bissell, M. J. alpha1 and alpha2 integrins mediate invasive activity of mouse mammary carcinoma cells through regulation of stromelysin-1 expression. *Mol. Biol. Cell* **10**, 271–282 (1999).
62. Yang, C. *et al.* Integrin alpha1beta1 and alpha2beta1 are the key regulators of hepatocarcinoma cell invasion across the fibrotic matrix microenvironment. *Cancer Res.* **63**, 8312–8317 (2003).
63. Hogg, N., Laschinger, M., Giles, K. & McDowall, A. T-cell integrins: more than just sticking points. *J. Cell Sci.* **116**, 4695 LP – 4705 (2003).

Chapter 8

Nederlandse samenvatting

Acknowledgements

List of Publications

About the author

NEDERLANDSE SAMENVATTING

Het immuunsysteem is onze afweer tegen lichaamsvreemde, meestal schadelijke, micro-organismen. Daarnaast beschermt het ons tegen tumoren. Tumorcellen zijn namelijk zo anders dan gezonde cellen dat ze lichaamsvreemde peptiden, ofwel antigenen, tot expressie brengen. Het immuunsysteem kan deze antigenen herkennen om de tumorcellen daarna te vernietigen. Het immuunsysteem bestaat uit verschillende afweercellen, die samenwerken om de bescherming tot stand te brengen. Zo zijn er onder andere de myeloide cellen, zoals macrofagen en dendritische cellen, maar ook de lymfocyten, zoals B en T cellen. Tijdens een immuunreactie tegen de tumor werken beiden samen om de tumorcellen aan te vallen. Zo nemen dendritische cellen tumor antigenen op tijdens het opruimen van dode tumorcellen. Tijdens dit proces moeten dendritische cellen worden geactiveerd door signalen die aangeven dat er iets mis is, ook wel “Damage-Associated Molecular Patterns” ofwel DAMPs genoemd. Deze signalen zorgen voor een verhoogde activatie van het antigeen-presentatie mechanisme en de expressie van co-stimulatie moleculen. Geactiveerde dendritische cellen reizen vervolgens vanuit het tumorweefsel naar de lymfeklier, waar ze de opgenomen antigenen presenteren aan T cellen. Als een CD8 T cel het gepresenteerde antigen herkent, wordt zij geactiveerd en begint de expansiefase. Het niveau van dendritische cel activatie is hierbij cruciaal; hoe meer geactiveerd, hoe meer co-stimulatie en “hulp” van de tweede groep T cellen, ofwel CD4 helper T cellen, er zal plaatsvinden (Hoofdstuk 1, Fig. 1). Uiteindelijk bepalen deze co-stimulatie en helper signalen of een CD8 T cel optimaal wordt geactiveerd, wat de latere functionaliteit en accumulatie van deze cellen in de tumor sterk beïnvloedt. Geactiveerde CD8 T cellen reizen vervolgens via de bloedcirculatie naar de tumor. Hier aangekomen zullen ze onder begeleiding van receptoren en chemokines het bloedvat verlaten en het weefsel bereiken. Tumorweefsel is, in tegenstelling tot gezond weefsel, zeer ongeorganiseerd. Extracellulaire moleculen, zoals collageen, zijn vaak ongestructureerd en bevinden zich op de verkeerde plekken. Doordat receptoren op het membraan van een T cel aan collageenmoleculen kunnen binden, is het mogelijk dat de T cellen daardoor moeite hebben met het daadwerkelijk bereiken van de tumorcellen (Hoofdstuk 1, Fig. 1). Als de T cellen eenmaal de tumorcellen hebben bereikt, kunnen ze de tumorcel herkennen en hun beschermende functie uitoefenen. In het geval van tumor immuniteit is vooral de activatie van cytotoxische, CD8 T cellen van belang om tumorcellen te vernietigen. Deze T cellen produceren de toxische stoffen granzymes en perforines, waarmee ze tumorcellen instrueren om dood te gaan (Hoofdstuk 1, Fig. 1).

Om aanvallen van het immuunsysteem te vermijden, ontwikkelen tumoren allerlei ontwijkingsmechanismen. Zij doen dit bijvoorbeeld door moleculen tot expressie te brengen die antigeenpresentatie of T cel toxiciteit remmen. Zoals in de vorige paragraaf al is benoemd, kunnen tumoren het T cellen ook lastiger maken om de tumorcellen te bereiken, door middel van collageen disorganisatie. Echter iedere tumor ontwikkelt zijn eigen ontwijkingsmechanisme(s), waardoor de infiltratie van afweercellen in tumoren en de functionaliteit van de immuunreactie verschilt

van patiënt tot patiënt. Therapieën die ontwijkingsmechanismen blokkeren, zoals bijvoorbeeld anti-PD1 therapie, zijn daarom niet effectief in alle patiënten. Het is dus van cruciaal belang dat we de verschillende ontwijkingsmechanismen beter leren begrijpen. Op basis van de specifieke afweercelcompositie en ontwijkingsmechanismen in de tumor van een patiënt kan mogelijk een gepersonaliseerde therapie worden toegepast.

In dit proefschrift gaan we dieper in op twee verschillende ontwijkingsmechanismen van de tumor en de mogelijke therapeutische behandeling hiervan, namelijk 1) T cel activatie en 2) de locatie/beweging van T cellen in het tumorweefsel.

Om T cel activatie te verbeteren, is tumor-specifieke vaccinatie een veelbelovende behandeling. Hierbij worden tumor-specifieke antigenen, in de vorm van peptiden, in combinatie met immuunstimulerende stoffen (adjuvanten) toegediend aan de patiënt. Deze adjuvanten zijn cruciaal voor het genereren van volledig geactiveerde, professionele dendritische cellen en daarmee T cel stimulatie. Vaccinatie strategieën en bijbehorende adjuvanten voor bescherming tegen virale infecties zijn reeds goed bestudeerd, waardoor we weten hoe dendritische cellen en CD4 T cellen in deze context worden geactiveerd. Echter, het is onduidelijk of de adjuvanten die werken voor virale vaccinaties ook de immuunreactie tegen tumoren optimaal ondersteunen. In dit proefschrift hebben we daarom verschillende adjuvanten toegevoegd aan een peptide-vaccin voor melanoom patiënten. We hebben aangetoond dat vooral directe stimulatie van dendritische cellen in combinatie met een antigeen-depot, waaruit antigenen zeer langzaam aan het weefsel worden afgegeven, een functionele CD8 T cel-reactie in het bloed van melanoom patiënten kunnen opwekken. Daarnaast hebben we het effect van adjuvanten op de samenstelling van de afweercellen op de plaats van de vaccinatie zelf geanalyseerd. Hierbij hebben we gevonden dat een “antigeen-depot” meer dendritische cellen en T cellen naar de plaats van vaccinatie rekruteert, dan wanneer enkel dendritische cellen worden geactiveerd. Door de constante afgifte van antigenen, en het rekruteren van dendritische cellen in de vaccinatieplaats, zorgt een dergelijk depot voor een belangrijke ondersteuning van de T cel reactie in het bloed. We denken dan ook dat de combinatie van deze adjuvant gemedieerde effecten tot een nog grotere accumulatie en activatie van dendritische cellen en T cellen op de plaats van vaccinatie leidt. Echter, toekomstig onderzoek zal moeten uitwijzen of en hoe de lokale afweerreactie op plaats van vaccinatie uiteindelijk tot een groter aantal tumor-specifieke T cellen in de tumor leidt.

Als tumor-specifieke CD8 T cellen zijn geactiveerd moeten deze vervolgens de juiste receptoren bezitten om de tumor te kunnen infiltreren. Hierbij zijn receptoren betrokken die ervoor zorgen dat de cellen door de bloedvatwand kunnen migreren en zo de bloedcirculatie kunnen verlaten. Daarnaast zijn er receptoren die de migratie in het tumorweefsel bepalen. Ten slotte zijn er specifieke moleculen betrokken bij de adhesie van T cellen aan tumorcellen. Zonder dit hele proces kan een T cel de tumor niet efficiënt aanvallen. Over de migratie van T

cellen door de bloedvatwand is al redelijk veel beschreven en daarom focust dit proefschrift zich met name op de laatste twee processen. We hebben het belang van drie receptoren onderzocht: de twee collageen-specifieke integrines CD49a en CD49b, en het E-cadherine-specifieke integrine CD103. Doordat deze drie integrines collageen of E-cadherine binden, wordt gespeculeerd dat ze betrokken zijn in de lokalisatie, retentie en tumorcel adhesie van T cellen. In dit proefschrift hebben we aangetoond dat CD49a, CD49b en CD103 significant meer aanwezig zijn op tumor-infiltrerende CD8 T cellen in melanoom patiënten dan op T cellen in het bloed van gezonde donoren. Daarnaast hebben we in een muismodel voor borstkanker gedemonstreerd dat CD49a de bewegingssnelheid van T cellen ondersteund. CD49b speelt geen rol in de bewegingssnelheid van T cellen maar lijkt een rol te spelen in de lokalisatie van T cellen in relatie tot tumorcellen. Dit suggereert dat CD49a een bewegingsreceptor is, terwijl CD49b voor adhesie zorgt. Het zal dus sterk van de collageenorganisatie in de specifieke tumor afhangen, hoe de T cel functie wordt beïnvloed door CD49a en CD49b. Wij hebben CD103 niet in deze context kunnen bestuderen, maar andere onderzoeken hebben aangetoond dat CD103 belangrijk is voor de vertraging van T cel migratie en langdurende interactie met E-cadherine op target cellen in longinfecties. CD103 is dus, evenals CD49b, wellicht een adhesiereceptor, al vergt die functie in tumoren nog verder onderzoek. Niettemin, ons onderzoek wijst uit dat deze receptoren verschillende functies hebben in adhesie en bewegingssnelheid van T cellen, en dat dit tegenovergestelde effecten kan hebben op T cel functie. Omdat elementen in het tumorweefsel de expressie van de receptoren beïnvloedt, kan een tumor dus het receptor repertoire aanpassen om zo de impact van T cellen te onderdrukken. Therapeutisch behandelen van dit ontwijkingsmechanisme, zou T cel functie en tumorcontrole in patiënten kunnen verbeteren.

Tezamen openen onze studies nieuwe mogelijkheden voor toekomstige klinische trials en fundamenteel onderzoek in T cel activatie, functie en gedrag in tumoren, met als doel het verbeteren van de immuunreactie wat resulteert in een verbeterde overlevingskans voor de patiënt.

Acknowledgements

First and foremost, Craig, thank you for taking a chance on me 6 years ago, and allowing me to explore different angles, before committing to what eventually became this PhD project. I truly admire your commitment to science, as well as being a good person and mentor.

Vic, your eye for detail, constant commitment to push us one step forward, to get the best out of ourselves, has encouraged me to be the scientist I am today. You taught me to have the courage to speak up, ask critical and important questions and feel confident in the knowledge base backing me up.

Kees and Sjoerd, thank you for being my mentors on the other side of the ocean. It has been such a pleasure building this bridge with you. Your support and help throughout this experience gave me the opportunity to get the best of both worlds.

My deepest appreciation goes to all the people I have had the pleasure of working with over the last 5 years. First of all, Donna, Kara and Walt, for being the rocks of support and guidance in a sea of possibilities. Amber, for being the best neighbor (office and lab!). All lab members: Ileana, Kelly, Nadia, Caroline, Adela, Joseph, Alex, Karlyn, Min, Sam, Kevin, Max, Ashley, Stella, Mirna, Anthony and of course, honorary lab member Claire. Surrounding professors: Melanie, Amy, Janet, Young, Sarah, Ulrika, Tim (Bender), Tim (Bullock), Mike, Loren, Drew and Tom. The environment each and every one of you helped create made work a wonderful place. Special thanks to the best students I was allowed to mentor: Salwador and Amanda (Briegel).

Katie, my coffee buddy. Thanks for giving me different perspectives, both in science and in life.

Kasia and Amanda (Lulu), long and rough days were always a bit easier with you around. I am grateful we have been able to translate shared hardship into a beautiful friendship.

Sara, Jareth and Kay, thank you for teaching me the actual important things in life. You have become part of my family, especially while the Dutch one was so far away.

Also, many thanks to the entire Charlottesville roller derby group, having an outlet outside of work was so important. Special props go to Whitney for keeping me sane, you are the nicest person I know. Jacki, Meg, Charlotte, Emily and Abby, thanks for the thousands of coffees, beers, dinners, boardgame nights, walks etc, it means so much to me. And Camie, of course, for all the support throughout.
Sydna: thank you for the beautiful cover design and with that, completing the book in a wonderful way.

Kristen and Lee, thanks for the wonderful friendship. Our wines and whines evenings were the highlight of many weeks.

Voor mijn lieve vriendjes in Nederland; Masterminds: Annemieke, Eivind, Gido, Joris, Marjolein en Ruben. Beaufort: Anita, Berit, Kyra, Marloes, Simone, Willemijn en Winke. Bedankt voor alle gezellige middagen en avondjes als ik weer even in een wervelwind langskwam in Leiden. En voor jullie oneindige steun en vriendschap. Tijdens mijn studie was dit zo onmisbaar, en zelfs terwijl ik aan de andere kant van de wereld was, is dat altijd zo gebleven. And of course, Anita, Hussain, Willemijn and Jurre, for always giving me a place to crash in Leiden.

Anne en Pauline, van spelen in de zandbak, naar traggelospernums stokken in de kas, verder naar gezelligheid over zoom in 3 verschillende landen. En dan nu paranimf op je CV! Ik hoef er eigenlijk niet veel meer over te zeggen, we weten alledrie hoe mooi dat is. Ik ben zo blij dat ik jullie heb.

Mama, Papa, Miel en Kim, Renie en Noortje en lieve familie. Wat een fijne basis hebben jullie mij altijd gegeven. Onafhankelijkheid en eindeloze mogelijkheden waren altijd de drijfveer in mijn opvoeding. Dit is iets wat ik altijd heb kunnen meenemen in mijn keuzes en zonder dit was ik nooit zo zelfverzekerd gekomen waar ik nu ben.

Last, but not least of course, there is Robin. I met you because of this PhD and even though I am proud of all the work, meeting you will always be the infinite best thing to have come out of this process. You make my life whole and the adventures worth pursuing. I can't wait for what the future brings.

LIST OF PUBLICATIONS

Melssen MM, Lindsay RS, Stasiak K, Rodriguez AB, Briegel AM, Cyranowski S, Rutkowski M, Conaway MR, Melief CJM, van der Burg SH, Eyo U, Slingluff Jr CL, Engelhard VH, *Differential expression of CD49a and CD49b determines localization and function of tumor infiltrating CD8 T-cells.* Submitted

Melssen MM, Pollack KE, Meneveau MO, Smolkin ME, Pinczewski J, Koeppel AF, Turner SD, Sol-Church K, Hickman A, Deacon DH, Petroni GR, Slingluff Jr CL, *Characterization and comparison of innate and adaptive immune responses at vaccine sites in melanoma vaccine clinical trials*. Submitted

Rodriguez AB, Peske JD, Woods AN, Leick KM, Mauldin IS, Young SJ, Lindsay RS, **Melssen MM**, Cyranowski S, Parriott G, Meneveau MO, Conaway MR, Fu Y, Slingluff CL Jr, Engelhard VH, *Immune Mechanisms Orchestrate Tertiary Lymphoid Structures in Tumors Via Cancer-Associated Fibroblasts*. IMMUNITY-D-20-00341. Available at SSRN: https://ssrn.com/abstract=3575119 or http://dx.doi.org/10.2139/ssrn.3575119

Pollack KE, Meneveau MO, **Melssen MM,** Lynch KT, Koeppel AF, Young SJ, Turner S, Kumar P, Sol-Church K, Mauldin IS, Slingluff CL Jr, *Incomplete Freund's adjuvant reduces arginase and enhances Th1 dominance, TLR signaling and CD40 ligand expression in the vaccine site microenvironment*, J Immunother Cancer. 2020 Apr;8(1). pii: e000544.

Leick KM, Rodriguez AB, **Melssen MM,** Benamar M, Lindsay RS, Eki R, Du KP, Parlak M, Abbas T, Engelhard VH, Slingluff CL Jr, *The barrier molecules junction plakoglobin, fillagrin, and dystonin play roles in melanoma growth and angiogenesis*, Ann Surg. 2019 Oct;270(4):712-722.

Kwak M, Leick KM, **Melssen MM**, Slingluff Jr, CL *Vaccine strategy in melanoma*, Surg Oncol Clin N Am. 2019 Jul;28(3):337-351.

Melssen MM, Petroni GR, Chianese-Bullock KA, Wages NA, Grosh WW, Varhegyi N, Smolkin ME, Smith KT, Galeassi NV, Deacon DH, Gaughan EM, Slingluff Jr CL *A multipeptide vaccine plus toll-like receptor agonists LPS or polyICLC in combination with incomplete Freund's adjuvant in melanoma patients*, J Immunother Cancer. 2019 Jun 27;7(1):163.

Melssen MM, Olson W, Wages NA, Capaldo BJ, Mauldin IS, Mahmutovic A, Hutchison C, Melief CJM, Bullock TN, Engelhard VH, Slingluff CL Jr, *Formation and phenotypic characterization of CD49a, CD49b and CD103 expressing CD8 T cell populations in human metastatic melanoma*, Oncoimmunology. 2018 Aug 6;7(10):e1490855.

Melssen MM, Slingluff CL Jr, *Vaccines targeting helper T cells for cancer immunotherapy*, Curr Opin Immunol. 2017 Aug;47:85-92.

ABOUT THE AUTHOR

Marit Melssen was born on November 15th, 1990 in Helmond, Netherlands. After growing up in the countryside of Limburg and finishing secondary school at the Peelland College in Deurne in 2009, she moved to Leiden to start the Biomedical Sciences program at the Leiden University Medical Center (LUMC). During the Bachelor's and Master's program she performed research in the laboratories of Prof. Dr. Alfred Vertegaal at the LUMC and Prof. Dr. Wilbert Zwart at the Netherlands Cancer Institute (NKI). During the time at the NKI, her interest for tumor immunology research was spiked and therefore, her final research project was done at the University of Virginia, USA under supervision of Prof. Dr. Craig Slingluff Jr. The project focused on understanding the regulation of integrin expression on T cells in melanoma tumors, which eventually resulted in a collaborative PhD project between the University of Virginia and the LUMC. The main research was supervised by Prof. Dr. Craig Slingluff Jr and Prof. Dr. Victor Engelhard at the University of Virginia, with support from Prof. Dr. Cornelis Melief and Prof. Dr. Sjoerd van der Burg at the LUMC. Results of this work are described in this thesis. Currently, Marit is working as a postdoctoral researcher at the Karolinska Institute, Sweden under supervision of Mikael Karlsson. Here she is continuing to study the important and complex interactions between immune and tumor cells.